Middle Rio Grande Bernalillo Report:

Morpho-dynamic Processes and Silvery Minnow Habitat from Hwy 550 Bridge to Montaño Road Bridge

Chelsey Radobenko
Brianna Corsi
Tristen Anderson
Dr. Pierre Julien

Final: April 2023
Final report prepared for the
United States Bureau of Reclamation

Colorado State University
Engineering Research Center
Department of Civil and
Environmental Engineering
Fort Collins, Colorado 80523

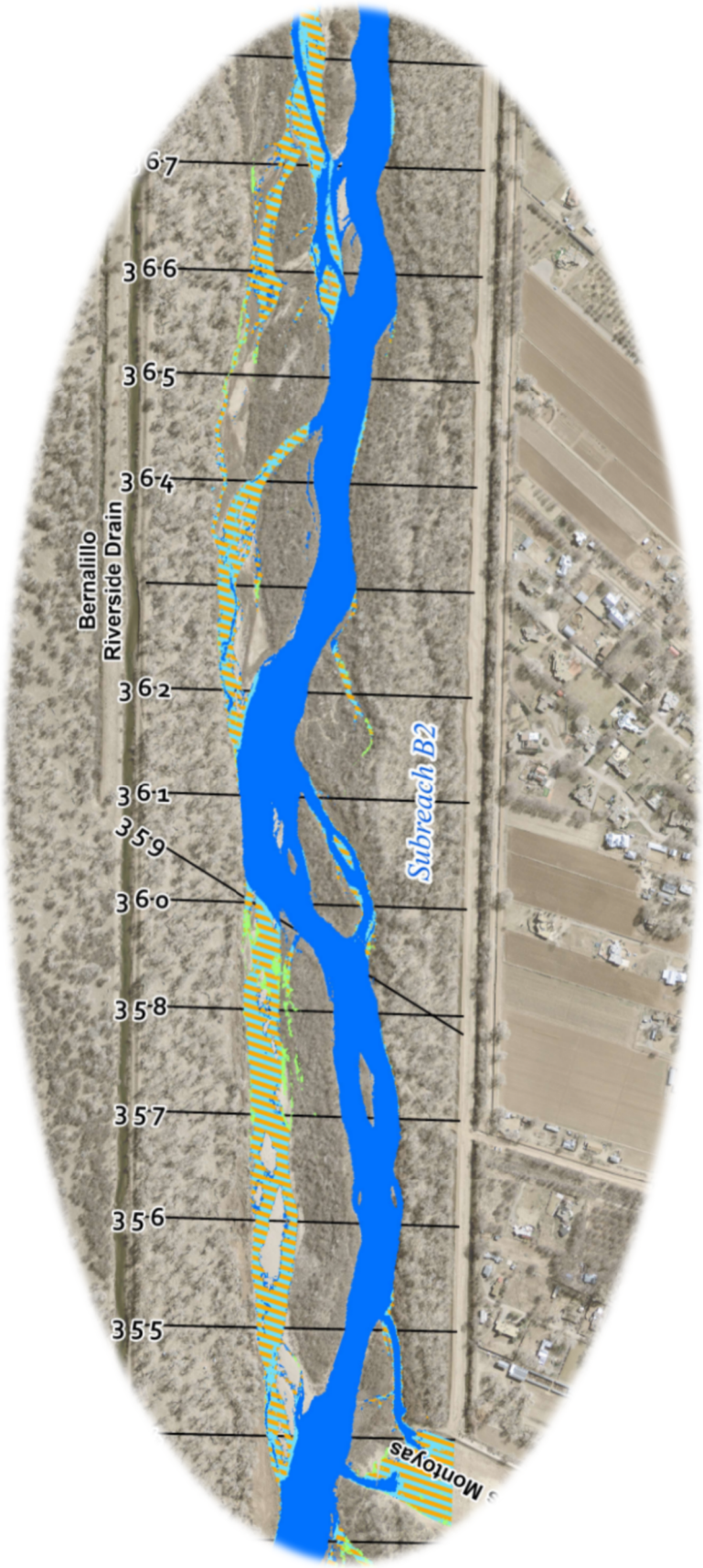

Executive Summary

The Bernalillo Reach spans approximately 16 miles of the Middle Rio Grande (MRG), from the Highway 550 Bridge to the Montaño Bridge crossing in Albuquerque, New Mexico. This reach report, prepared for the United States Bureau of Reclamation (USBR), presents a summary of the morpho-dynamic processes within the Bernalillo Reach. The MRG is a dynamic river that is still responding to anthropogenic impacts over the last century. The Bernalillo Reach is split into four subreaches (B1, B2, B3, and B4). Analysis of these four subreaches illustrates spatial and temporal trends of the channel geometry and morphology.

Discharge and sediment data from the United States Geological Survey are used to identify the time and magnitude of peak discharge and sediment load in the reach. Spring snowmelt typically supplies the greatest water and sediment discharge volumes, and the monsoonal thunderstorms often transport the greatest concentration of suspended sediment for shorter periods of time.

Georeferenced linen maps from 1918 and aerial photographs dating back to 1935 were analyzed with GIS (geographic information system) to evaluate the changes in channel width, sinuosity, and planform. Anthropogenic impacts, and droughts caused the average channel width to narrow from 1,166 feet in 1918 to 290 feet in 2019. The sinuosity of the Bernalillo Reach has remained low (slightly above 1) for most sub-reaches. The river began to shift from a braided planform to a single-threaded slightly sinuous planform between 1970 and 1990 as a result of constricting the channel from levee construction, channelization, and reduction in sediment supply causing incision. The additional channel narrowing is a function of peak reductions and longer duration of low flows.

Changes to bed elevation were observed using cross-section geometry files provided by the USBR. The Bernalillo Reach has had periods of degradation and aggradation. Between 1962 and 1972, the Bernalillo reach was in the process of aggrading, with the greatest degree of aggradation (~1 to 2 feet) occurring in Subreaches B1 and B2. This aggradation led to an increase in bed elevation and steepening in channel slope during this decade. The channel began to incise following the completion of the Cochiti dam in 1973, with the most significant channel bed degradation (~3 to 8 feet) occurring in Subreaches B1 and B2. In recent years, several grade controls are active throughout the reach. The Corrales Siphon, located near at Rio Rancho Bosque Preserve (downstream end of Subreach B1), is exposed and is potentially creating backwater effects and holding grade (pers. comm. from Ari Posner, 2023). The Albuquerque Metropolitan Area Flood Control Authority (AMAFCA) North Diversion Channel outfall, located at the downstream end of B2, provided increased sediment loads and acts a grade control by helping maintain channel width and control the aggradation/degradation trends. The Albuquerque Bernalillo County Water Utility Authority (ABCWUA) Adjustable Height Dam can also act as a temporary grade control where the channel bed responds to changes in the dam height.

The application of the Massong et al. (2010) geomorphic conceptual model aided in interpreting the planform change over time in the Bernalillo Reach. An overall trend of the channel degrading and progressing towards a single thread meandering (M) planform, indicates that this reach has excess transport capacity. The reach as a whole follows a similar trend whereby the channel classifies as Stage 1 (i.e. wide and braided) throughout the early- to mid-1900s and transitions towards Stages M4/M5 (i.e. narrow, straight, and single-threaded) in the 1990s and 2000s. This planform shift from braided to single-threaded is likely driven by changes to the sediment loads and peak flow events caused by anthropogenic factors such as the constriction of the channel from levee construction and channelization, upstream dam and reservoir construction, and changes to channel maintenance activities.

One-dimensional hydraulic models, developed with Hydrologic Engineering Center's River Analysis System (HEC-RAS) software, estimated habitat availability for the endangered Rio Grande Silvery Minnow (RGSM) within the Bernalillo Reach. A previously developed width-slice method in HEC-RAS was applied to calculate the hydraulically suitable RGSM habitat based on flow velocity and depth criteria for the larval, juvenile, and adult stages at various discharges. Calculations for a wide range of discharges were conducted for five historical river conditions (1962, 1972, 1992, 2002, and 2012) over a span of 50 years. Our findings suggest that the Bernalillo reach has lower potential for habitat availability compared with other reaches, such as the Bosque del Apache Reach (Scheid et al. 2022). Subreaches B2 and B3 show more potential habitat for the juvenile and adult life stages, while Subreaches B1 and B2 may be slightly more suitable for larvae. Detailed mapping for year 2012 was performed based on detailed LiDAR data provided by USBR to illustrate the RGSM habitat areas within the Bernalillo Reach. Due to the nature of the 1D modeling procedure used to create the habitat maps, there are areas within the floodplain that show habitat that is disconnected from the main channel. These areas may be ideal locations for future restoration projects to reconnect portions of the floodplain with the channel.

Acknowledgement

This final report has been prepared for the United States Bureau of Reclamation under Award Number R17AC00064. The authors gratefully acknowledge the numerous constructive comments and thoughtful suggestions to improve a draft version of this report. We are particularly thankful to Ari Posner, Drew Baird, Nathan Holste and Nate Bradley at Reclamation. The detailed discussions contributed to key improvements including the addition of a synthesis section, a review of HEC-RAS files, and fine-tuning of multiple graphics and calculation procedures.

These reports have been prepared in collaboration with the University of New Mexico (UNM) and the American Southwest Ichthyological Researchers (ASIR). We specifically treasure our collaboration with Tom Turner, Steven Platania, Robert Dudley and Jake Mortensen whose aquatic habitat expertise on the Rio Grande Silvery Minnow (RGSM) provided an underlying framework for this reach report.

Table of Contents

Executive Summary i
Acknowledgement iii
List of Appendix A Figures and Tables xi
List of Appendix B Figures and Tables xi
List of Appendix C Figures and Tables xi
List of Appendix D Figures and Tables xii
List of Appendix E Figures and Tables xii
List of Appendix F Figures and Tables xii
List of Appendix G Figures and Tables xii
1 Introduction 1
1.1 Site Description 2
1.2 Aggradation/Degradation Lines and Rangelines 3
1.3 Subreach Delineation 4
2 Precipitation, Flow, and Sediment Discharge Analysis 11
2.1 Precipitation 11
2.2 River Flow 13
2.2.1 USGS Gage Data 13
2.2.2 Raster Hydrographs 15
2.2.3 Yearly Peak Flow Events 17
2.2.4 Cumulative Discharge Curves 19
2.2.5 Flow Duration 24
2.2.6 Days of Flow 26
2.3 Suspended Sediment Load 27
2.3.1 Single Mass Curve 27
2.3.2 Double Mass Curve 30
2.3.3 Monthly Sediment Variation 31
2.3.4 Additional Jemez River Analysis 36
3 River Geomorphology 40
3.1 Wetted Top Width 40
3.2 Width (Defined by Vegetation) 46
3.3 Bed Elevation and Slope 48
3.4 Bed Material 51
3.5 Sinuosity 53

3.6 Hydraulic Geometry 54
3.7 Number of Channels 57
3.8 Channel Response Models 60
3.9 Geomorphic Conceptual Model 62
4 HEC-RAS Modeling for Silvery Minnow Habitat 73
4.1 Modeling Data and Background 73
4.1.1 Levee and Ineffective Flow Analysis 73
4.2 Width Slices Methodology 74
4.3 Width Slices Habitat Results 75
4.4 RAS-Mapper Methodology 79
4.5 RAS-Mapper Habitat Results in 2012 79
4.6 Disconnected Areas 82
5 Bernalillo Reach Synthesis 84
5.1 Hydrology 84
5.2 Sediment Load 84
5.3 Channel Morphology 85
5.4 Massong Classification Summary 88
5.5 Habitat 89
6 Conclusions 90
7 Bibliography 91

Appendix A A-1
Appendix B B-1
Appendix C C-1
Appendix D D-1
Appendix E E-1
Appendix F F-1
Appendix G G-1

List of Tables

Table 1-1: Bernalillo Subreach Delineation 4
Table 2-1. List of Relevant Gages 13
Table 2-2 Probabilities of daily exceedance 24
Table 3-1. Channel bed slope by subreach 51
Table 3-2 Julien-Wargadalam channel width prediction for 5,000 cfs 60
Table 4-1 Rio Grande Silvery Minnow habitat velocity and depth range requirements (from Mortensen et al., 2019) 73
Table 5-1 Geomorphic Trends Over Time by Subreach 87

List of Figures

Figure 1-1: Map with the Middle Rio Grande outlined in blue. The Bernalillo Reach is highlighted in lime green. (Google Earth) 1
Figure 1-2 Timeline of Significant Events for the Middle Rio Grande River (Makar 2006) 3
Figure 1-3 Bernalillo Subreach Delineation Overview Map (base map source: ESRI) 5
Figure 1-4 Subreach delineation with 2012 USBR ortho aerial imagery of Bernalillo Reach (B1) (turquoise line denotes the channel centerline, dark blue lines denote subreach boundaries, and black lines denote agg/deg cross-sections) 6
Figure 1-5 Subreach delineation with 2012 USBR ortho aerial imagery of Bernalillo Reach (B1 & B2) (turquoise line denotes the channel centerline, dark blue lines denote subreach boundaries, and black lines denote agg/deg cross-sections) 7
Figure 1-6 Subreach delineation with 2012 USBR ortho aerial imagery of Bernalillo Reach (B2 & B3) (turquoise line denotes the channel centerline, dark blue lines denote subreach boundaries, and black lines denote agg/deg cross-sections) 8
Figure 1-7 Subreach delineation with 2012 USBR ortho aerial imagery of Bernalillo Reach (B3 & B4) (turquoise line denotes the channel centerline, dark blue lines denote subreach boundaries, and black lines denote agg/deg cross-sections) 9
Figure 1-8 Subreach delineation with 2012 USBR ortho aerial imagery of Bernalillo Reach (B4) (turquoise line denotes the channel centerline, dark blue lines denote subreach boundaries, and black lines denote agg/deg cross-sections) 10
Figure 2-1 BEMP data collection sites (figures source: http://bemp.org) 11
Figure 2-2 Monthly precipitation at four gages near the Bernalillo and Montaño reaches 12
Figure 2-3 Cumulative precipitation at four gages near the Bernalillo and Montaño reaches 12

Figure 2-4. USGS gage data overview map (base map source: ESRI) 14
Figure 2-5 Raster hydrograph of daily discharge at USGS Station 08319000 at San Felipe (top) and USGS Station 08330000 at Albuquerque (bottom). (Source: https://waterwatch.usgs.gov) 16
Figure 2-6 Raster hydrograph of daily discharge at historical USGS Station 08329000 (top) and USGS Station 0832950 (bottom) below the Jemez Dam. (Source: https://waterwatch.usgs.gov). 17
Figure 2-7 Yearly peak flow events for the Rio Grande before Cochiti Dam at USGS Gages 08314500, 08319000, and 08330000 from 1926-1970 18
Figure 2-8 Yearly peak flow events for the Rio Grande after Cochiti Dam at USGS Gages 08317400, 08319000, and 08330000 from (1970-present). 18
Figure 2-9 Yearly peak flow events for the Jemez River 19
Figure 2-10 Discharge single mass curve at historical USGS gage 8314500 (Cochiti) before dam construction. 20
Figure 2-11 Discharge single mass curve at USGS gage 08317400 (below Cochiti Dam) after dam construction 21
Figure 2-12 Discharge single mass curve at USGS gage 08319000 (San Felipe) before dam construction. 21
Figure 2-13 Discharge single mass curve at USGS gage 08319000 (San Felipe) after dam construction. 22
Figure 2-14 Discharge single mass curve at USGS gage 08330000 (Albuquerque). 22
Figure 2-15 Discharge single mass curve at historical USGS gage 08329000 (Jemez) before dam construction in 1953. 23
Figure 2-16 Discharge single mass curve at historical USGS gage 08329000 and USGS gage 08328950 (Jemez) after dam construction in 1953 23
Figure 2-17 Flow duration curves for the Rio Grande gages before and after dam construction. 25
Figure 2-18 Flow duration curves for the Jemez River gages before and after dam construction in 1953. 25
Figure 2-19 Number of days greater than an identified discharge at the San Felipe gage before (left) and after (right) dam construction. 26
Figure 2-20 Number of days over an identified discharge at the Jemez gages before (left) and after (right) dam construction in 1953. 26
Figure 2-21 Suspended sediment discharge single mass curve for USGS gage 08329000 at Jemez River Below Jemez Canyon Dam, NM 28
Figure 2-22 Suspended sediment discharge single mass curve for USGS gage 08317400 at Rio Grande Below Cochiti Dam, NM 28

Figure 2-23 Suspended sediment discharge single mass curve for USGS gage 08329500 at Rio Grande Near Bernalillo, NM 29
Figure 2-24 Suspended sediment discharge single mass curve for USGS gage 08330000 at Rio Grande at Albq, NM 29
Figure 2-25 Double mass curve for USGS gage 08329500 at Rio Grande Near Bernalillo, NM 30
Figure 2-26 Cumulative suspended sediment (data from the Rio Grande at Albuquerque (USGS 08330000) gage) versus cumulative precipitation at the Alameda gage. 31
Figure 2-27 Monthly average suspended sediment and water discharge at USGS gage 08329000 at Jemez River Below Jemez Canyon Dam, NM 32
Figure 2-28 Monthly average suspended sediment concentration and water discharge at USGS gage 08329000 at Jemez River Below Jemez Canyon Dam, NM 32
Figure 2-29 Monthly average suspended sediment and water discharge at USGS gage 08317400 at Rio Grande Below Cochiti Dam, NM 33
Figure 2-30 Monthly average suspended sediment concentration and water discharge at USGS gage 08317400 at Rio Grande Below Cochiti Dam, NM 33
Figure 2-31 Monthly average suspended sediment and water discharge at USGS gage 08329500 at Rio Grande Near Bernalillo, NM 34
Figure 2-32 Monthly average suspended sediment concentration and water discharge at USGS gage 08329500 at Rio Grande Near Bernalillo, NM 34
Figure 2-33 Monthly average suspended sediment and water discharge at USGS gage 08330000 at Rio Grande at Albq, NM 35
Figure 2-34 Monthly average suspended sediment concentration and water discharge at USGS gage 08330000 at Rio Grande at Albq, NM 35
Figure 2-35 Suspended sediment discharge single mass curve for USGS gage 08329000 at Jemez River Below Jemez Canyon Dam, NM – Pre-Dam Modification 36
Figure 2-36 Suspended sediment discharge single mass curve for USGS gage 08329000 at Jemez River Below Jemez Canyon Dam, NM – Post-Dam Modification 36
Figure 2-37 Flow Budget through the years between 1944 and 2021 (left) and total flow percentage between 2014 and 2021 (right) for the Jemez River at the Outlet and Rio Grande at Bernalillo and Albuquerque. 37
Figure 2-38 Sediment budgets pre-, at-, and post- Jemez Dam modification 38
Figure 2-39 Average sediment budget comparison – before Cochiti Dam construction (left) and after Jemez Dam modification (right) 39

Figure 2-40 Total sediment volume2.53 budget in million tons at the USGS Gage 08330000 at Rio Grande at Albuquerque, NM from 2014 to 2021 39
Figure 3-1 Moving cross-sectional average of the wetted top width at a discharge of 1,000 cfs. 41
Figure 3-2 Moving cross-sectional average of the wetted top width at a discharge of 3,000 cfs. 42
Figure 3-3 Moving cross-sectional average of the wetted top width at a discharge of 5,000 cfs. 43
Figure 3-4 Cumulative top width at a discharge of 1,000 cfs. 44
Figure 3-5 Cumulative top width at a discharge of 3,000 cfs. 44
Figure 3-6 Cumulative top width at a discharge of 5,000 cfs. 45
Figure 3-7 Average top width for B1 (top left), B2 (top right), B3 (bottom left), and B4 (bottom right) at discharges 500 to 5,000 cfs. 46
Figure 3-8 Averaged active channel width by subreach from historical imagery (defined by vegetation) 47
Figure 3-9 Channel in 1992 (left image, green bank lines) compared with channel in 2019 (right image, red bank lines) 48
Figure 3-10 Longitudinal bed elevation profile. 49
Figure 3-11 Aggradation and degradation by subreach 50
Figure 3-12 Water surface slope at 500 cfs (left) and channel bed slope (right). 51
Figure 3-13 Median grain diameter size of samples taken throughout the Bernalillo Reach 52
Figure 3-14 D50 change over time by subreach 53
Figure 3-15 Average sinuosity by subreach 54
Figure 3-16 HEC-RAS Wetted top width of channel at 1,000 cfs (top left), 3,000 cfs (top right), and 5,000 cfs (bottom middle) 55
Figure 3-17 HEC-RAS Hydraulic depth at 1,000 cfs (top left), 3,000 cfs (top right), and 5,000 cfs(bottom) 56
Figure 3-18 HEC-RAS Main Channel Wetted Perimeter at 1,000 cfs (top left), 3,000 cfs (top right), and 5,000 cfs (bottom middle). 57
Figure 3-19 Average number of mid-channel bars and islands by subreach 58
Figure 3-20 Percentage of agg/deg lines with multiple channels, by year, segregated by number of channels between 1 and 5. 59
Figure 3-21 Aerial photograph showing evolution of vegetated bars and islands at Agg/Deg 398 in 1972 (left), 2002 (center) and 2019 (right). 59
Figure 3-22 Julien and Wargadalam predicted widths and observed widths of the channel for 5,000 cfs 61

Figure 3-23 Julien and Wargadalam predicted widths versus observed widths with 1:1 line for 5,000 cfs.....61
Figure 3-24 Planform evolution model from Massong et al. (2010). The river undergoes stages 1-3 first and then continues to Stages A4-A6 or stages M4-M8 depending on the sediment transport capacity.....63
Figure 3-25 Planform evolution model from Massong et al. (2010) applied to channel cross sectional view left to right looking downstream (modified by Brianna Corsi, 2022).....64
Figure 3-26 Subreach B1: Channel evolution of representative cross section Agg/Deg 318. Significant channel degradation and narrowing occurred between 1972 and 2012.....65
Figure 3-27 Subreach B1: Massong et al. (2010) classification (left), historical cross section profiles (center) and corresponding aerial images with channel centerline shown in blue (right) at Agg/Deg 318.....66
Figure 3-28 Subreach B2: Channel evolution of representative cross section Agg/Deg 368. Significant channel degradation and narrowing occurred between 1972 and 2012. Note: it appears that the side channel thalweg at station 100 ft was missed in the 2002 survey.....67
Figure 3-29 Subreach B2: Massong et al. (2010) classification (left), historical cross section profiles (center) and corresponding aerial images with channel centerline shown in blue (right) at Agg/Deg 368.....68
Figure 3-30 Subreach B3: Channel evolution of representative cross section Agg/Deg 418. Note less degradation and narrowing than seen in Subreaches B1 and B2.....69
Figure 3-31 Subreach B3: Massong et al. (2010) classification (left), historical cross section profiles (center) and corresponding aerial images with channel centerline shown in blue (right) at Agg/Deg 418.....70
Figure 3-32 Subreach B4: Channel evolution of representative cross section Agg/Deg 442.....71
Figure 3-33 Subreach B4: Massong et al. (2010) classification (left), historical cross section profiles (center) and corresponding aerial images with channel centerline shown in blue (right) at Agg/Deg 442.....72
Figure 4-1 Cross-section with flow distribution from HEC-RAS with 20 vertical slices in the floodplains and 25 vertical slices in the main channel. The yellow and green slices are small enough that the discrete color changes look more like a gradient.....75
Figure 4-2 Larval RGSM habitat availability throughout the Bernalillo Reach.....76
Figure 4-3 Juvenile RGSM habitat availability throughout the Bernalillo Reach.....76
Figure 4-4 Adult RGSM habitat availability throughout the Bernalillo Reach.....77

Figure 4-5 Stacked habitat charts at different scales to display spatial variations of habitat throughout the Bernalillo Reach in 2012 78
Figure 4-6 Suitable habitat in 2012 for each life stage at 1,500 cfs at the downstream section of B2. Dark blue inundation area are not suitable for habitat at any life stage..... 80
Figure 4-7 Suitable habitat in 2012 for each life stage at 3,000 cfs at the downstream section of B2. Dark blue inundation area are not suitable for habitat at any life stage..... 81
Figure 4-8 Suitable habitat in 2012 for each life stage at 5,000 cfs at the downstream section of B2. Dark blue inundation area are not suitable for habitat at any life stage..... 81
Figure 4-9 Disconnected low-laying areas that are no longer connected to the main channel at 5,000 cfs in Subreach B2..... 82
Figure 4-10 Disconnected low-laying areas that are no longer connected to the main channel at 5,000 cfs in Subreach B3. 83
Figure 5-1 Planform evolution model from Massong et al. (2010) applied to channel cross sectional view left to right looking downstream (modified by Brianna Corsi, 2022)..... 88

List of Appendix A Figures and Tables

Bernalillo and Montaño Subreach Delineation Report……. A-1

List of Appendix B Figures and Tables

Table B-1 Years used in JW Calculations for D50……...…… B-1
Table B-2 3,000 cfs Julien-Wargadalam channel width prediction ……..……...…… B-1
Figure B-1 Julien and Wargadalam predicted widths and observed widths of the channel …… B-2

List of Appendix C Figures and Tables

Figure C-1 Wetted top width at each agg/deg line in the Bernalillo Reach at a discharge of 1,000 cfs…….……...……..….. C-2
Figure C-2 Wetted top width at each agg/deg line in the Bernalillo Reach at a discharge of 3,000 cfs…….……...……..... C-2
Figure C-3 Wetted top width at each agg/deg line in the Bernalillo Reach at a discharge of 5,000 cfs……..... C-3
Figure C-4 Example of annual habitat interpolating using the sediment rating curve and alpha technique……..……... C-4

List of Appendix D Figures and Tables

Figure D-1 RGSM habitat availability in Bernalillo Subreach, B1……..…….….. D-2
Figure D-2 RGSM habitat availability in Bernalillo Subreach, B2……..…….….. D-3
Figure D-3 RGSM habitat availability in Bernalillo Subreach, B3……..…..…. D-4
Figure D-4 RGSM habitat availability in Bernalillo Subreach, B4……..……... D-5
Figure D-5 Stacked habitat charts at different scales to display spatial variations of habitat throughout the Bernalillo Reach in 1962…….…..…. D-6
Figure D-6 Stacked habitat charts at different scales to display spatial variations of habitat throughout the Bernalillo Reach in 1972……..... D-7
Figure D-7 Stacked habitat charts at different scales to display spatial variations of habitat throughout the Bernalillo Reach in 1992…….……..…. D-8
Figure D-8 Stacked habitat charts at different scales to display spatial variations of habitat throughout the Bernalillo Reach in 2002…….……... D-9
Figure D-9 Stacked habitat charts at different scales to display spatial variations of habitat throughout the Bernalillo Reach in 2012……. D-10
Figure D-10 Life stage habitat curves for Bernalillo Subreach B1 for the years 1962 to 2012…....…. D-12
Figure D-11 Life stage habitat curves for Bernalillo Subreach B2 for the years 1962 to 2012…....…. D-14
Figure D-12 Life stage habitat curves for Bernalillo Subreach B3 for the years 1962 to 2012…..….... D-16
Figure D-13 Life stage habitat curves for Bernalillo Subreach B4 for the years 1962 to 2012…....….. D-18

List of Appendix E Figures and Tables

Rio Grande Habitat Maps at 1,500 cfs, 3,000 cfs, and 5,000 cfs..……E-1

List of Appendix F Figures and Tables

Subreach B1 Agg/Deg 318 Geomorphic Habitat Linkage Quad ..……F-1
Subreach B2 Agg/Deg 368 Geomorphic Habitat Linkage Quad ..……F-2
Subreach B3 Agg/Deg 418 Geomorphic Habitat Linkage Quad ..……F-3
Subreach B4 Agg/Deg 442 Geomorphic Habitat Linkage Quad ..……F-4

List of Appendix G Figures and Tables

Table G-1 HEC-RAS files used during analyses .....…….G-2
Table G-2 Full list of HEC-RAS files .....…….G-3

1 Introduction

The purpose of this reach report is to evaluate the morpho-dynamic conditions of the Middle Rio Grande (MRG) which extends from the Cochiti Dam to the Narrows in Elephant Butte Reservoir. This report focuses on the Bernallilo Reach, which begins at the Highway 550 Bridge crossing in Bernalillo, New Mexico and ends Montaño Road Bridge crossing in Albuquerque, New Mexico. See **Figure 1-1** for a reach location map.

This report is part of a series of reports commissioned by the United State Bureau of Reclamation (USBR), which includes morpho-dynamic reach reports, reports on the biological-habitat conditions for the Rio Grande Silvery Minnow (RSGM), and process linkage reports. The process linkage reports will ultimately connect morpho-dynamic conditions with the required biological-habitat conditions. This report focuses on understanding the trends of physical conditions of the Bernalillo Reach. Specific objectives include:

- Delineate the reach into subreaches based on shared geomorphic characteristics and/or urban features.
- Summarize the flow and sediment discharge conditions and trends for the period of record available from United States Geological Survey (USGS) gages.
- Analyze geomorphic characteristics at a subreach level (sinuosity, width, bed elevation, bed material, bed slope, and other hydraulic parameters).
- Link changes in the river geomorphology with shifts in sediment and flow trends; and
- Classify subreaches using a geomorphic conceptual model.

Finally, in preparation for a future process linkage report, depth and velocity suitability characterized fish habitat throughout the Bernalillo Reach. These methods were based on HEC-RAS one-dimensional hydraulic models, which were used to understand and predict the conditions on the MRG. This series of reports will support Reclamation's mission to improve habitat for species listed by the Endangered Species Act and to support channel sustainability on the MRG while continuing to provide effective water delivery (U.S. Bureau of Reclamation, 2012).

Figure 1-1: Map with the Middle Rio Grande outlined in blue. The Bernalillo Reach is highlighted in lime green. (Google Earth)

1.1 Site Description

The Rio Grande begins in the San Juan Mountain Range of Colorado and continues into New Mexico. It travels along the Texas-Mexico border before reaching the Gulf of Mexico. The Middle Rio Grande (MRG) stretches from Cochiti Dam to Elephant Butte Reservoir. The MRG has historically been affected by periods of drought and large spring flooding events due to snowmelt. Monsoons have caused some of the largest peak flows the river has seen. These floods often caused large scale shifts in the course of the river and rapid aggradation (Massong et al., 2010). Floods helped maintain aquatic ecosystems by enabling connection of water between the main channel and the floodplains (Scurlock, 1998), but consequently threatened human establishments that were built near the Rio Grande. Agricultural development in the San Luis Valley diverts a significant portion of the Rio Grande before it even gets to New Mexico. Beginning in the 1930s, levees were installed to prevent flooding. Beginning in the 1950s, the USBR undertook a significant channelization effort involving jetty jacks, river straightening, and other techniques. Upstream dam construction began in the 1950s and was completed in the 1970s. They were used to store and regulate flow in the river; though, they also reduced downstream sediment supply.

While these efforts enabled agriculture and large-scale human developments to thrive along the MRG, they also fundamentally changed the river, which led to reduced peak flows and sediment supply while altering the channel geometry and vegetation (Makar, 2006). In parts of the MRG, narrowing of the river continues, with channel degradation due to limited sediment supply and the formation of vegetated bars that encroach into the channel (Varyu, 2013; Massong et al., 2010). Farther downstream, closer to Elephant Butte Reservoir, aggradation and sediment plugs have been observed. These factors have created an ecologically stressed environment, as seen in the decline of species such as the Rio Grande Silvery Minnow (Mortensen et al., 2019).

The Bernalillo Reach of the Middle Rio Grande In New Mexico is a 16-mile stretch that begins at the Hwy 550 bridge crossing in Bernalillo and ends at the Montaño Bridge crossing in Albuquerque. **Figure 1-2** shows a timeline of hydraulically significant events that have occurred between 1870 and 2010 (Makar 2006).

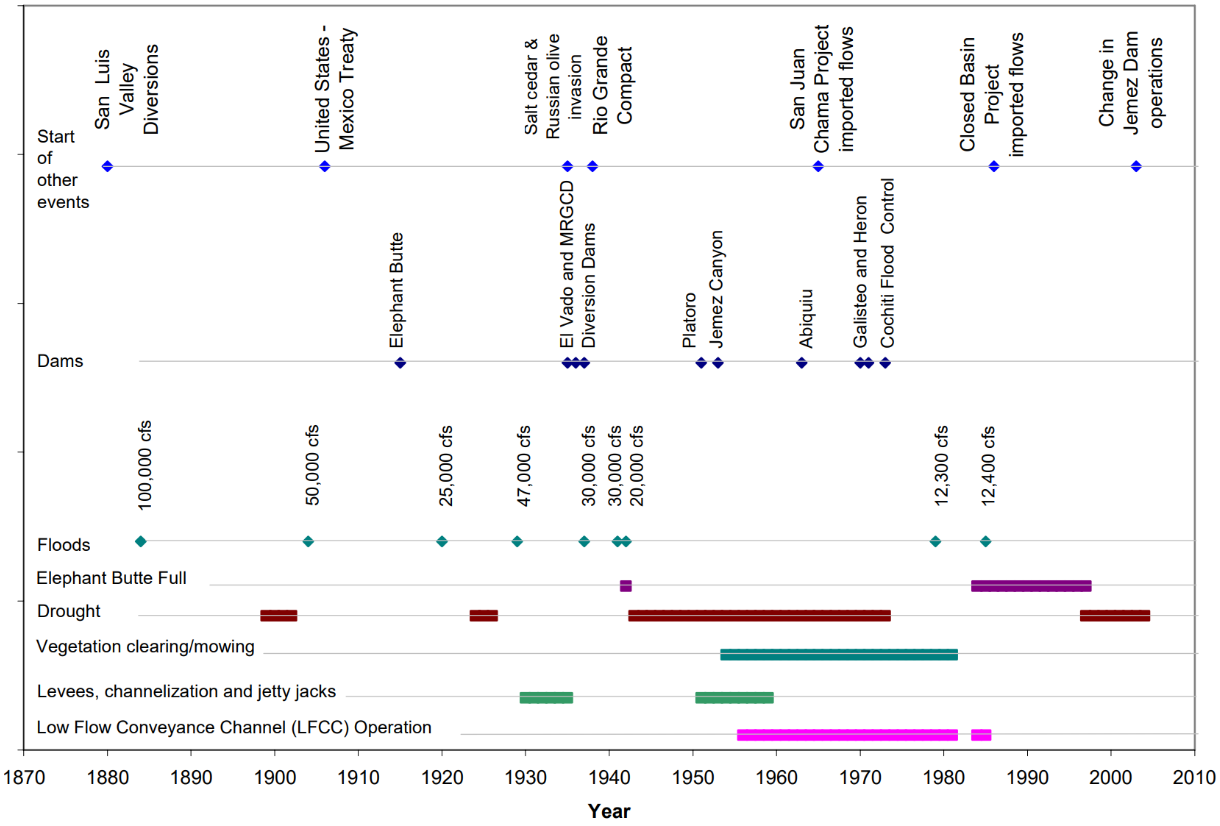

Figure 1-2 Timeline of Significant Events for the Middle Rio Grande River (Makar 2006)

1.2 Aggradation/Degradation Lines and Rangelines

Aggradation/degradation lines (agg/deg lines), spaced at approximate 500-foot intervals along the entire MRG, were established in 1962 and are used as baselines to estimate changes in sedimentation and morphological characteristics in the river channel and floodplain over time (Posner 2017). Repeat surveys are implemented along these cross-section lines as well as the collection of bed material samples. Each agg/deg line has been surveyed approximately every 10 years and are available for 1962, 1972, 1992, 2002 and 2012. The most recent 2012 survey was performed using LiDAR acquisition, while surveys prior to 2012 were developed using photogrammetry techniques. All GIS data and models use the North American Vertical Datum of 1988 (NAVD88). The cross-sectional geometry at each agg/deg line for all 5 years are available with-in HEC-RAS models that were developed for the MRG by the Technical Service Center (Varyu, 2013).

LiDAR and photogrammetric survey techniques do not deliver accurate ground elevation measurements underwater. For modeling purposes, it is necessary to appropriately characterize bathymetry of the channel for an accurate representation of channel conveyance. To accomplish this, an underwater prism was estimated using the measured top width, known slopes and the flow rate on the date of survey and has been incorporated within the HEC-RAS geometry files (Varyu, 2013).

In addition to agg/deg lines, rangelines were established for physical river surveys associated with geomorphic changes such as migrating bends, incision, and for design of river maintenance. Rangelines are surveyed using traditional rod and level or GPS techniques whereas Agg/Deg lines are derived from LiDAR or photogrammetry with an estimated underwater prism to define the underwater bed.

1.3 Subreach Delineation

The Bernalillo Reach spans approximately 16 miles beginning at Agg/Deg Line 298 (Hwy 550) and ending at Agg/Deg Line 463 (just upstream of the Montaño Bridge). This reach is located within an urban river corridor. For the purposes of hydraulic and geomorphic analysis, this reach was split into multiple subreaches based on notable urban and geomorphic features.

The Bernalillo Reach was delineated into four subreaches based on notable features such as the Highway 550 and Montano Bridge crossings, the Corrales Siphon crossing, the Albuquerque Metropolitan Area Flood Control Authority (AMAFCA) North Diversion Channel, and the Albuquerque Bernalillo County Water Utility Authority (ABCWUA) Adjustable Height Dam. **Table 1-1** below summarizes each subreach. **Figure 1-3** shows an overview map of the reach delineation. Close-up views of the subreach delineation with agg/deg lines and aerial imagery is given by **Figure 1-4, Figure 1-5**, **Figure 1-6**, **Figure 1-7**, and **Figure 1-8**.

The full combined subreach delineation report for the Bernalillo and Montaño reaches is provided in **Appendix A**. An analysis of the flood widths at a discharge of 3,000 cfs as well as channel widths identified by the bank stationing were considered. Other analyses performed as part of the subreach delineation report include the longitudinal profile of the reach and the particle distribution through the reach. All analyses preformed identified boundaries consistent with the subreach delineation.

Table 1-1: Bernalillo Subreach Delineation

Subreach Name	Agg/Deg Lines	Approximate Distance	Description
B-1	298 – 339	4.0 miles	Highway 550 Bridge to Rio Rancho Bosque Preserve (Corrales Siphon crossing)
B-2	339 – 398	5.6 miles	Rio Rancho Bosque Preserve (Corrales Siphon) to AMAFCA North Diversion Channel (tributary)
B-3	398 – 422	2.4 miles	AMAFCA North Diversion Channel (tributary) to ABCWUA Adjustable Height Dam
B-4	422 – 463	4.0 miles	ABCWUA Adjustable Height Dam to Montaño Bridge

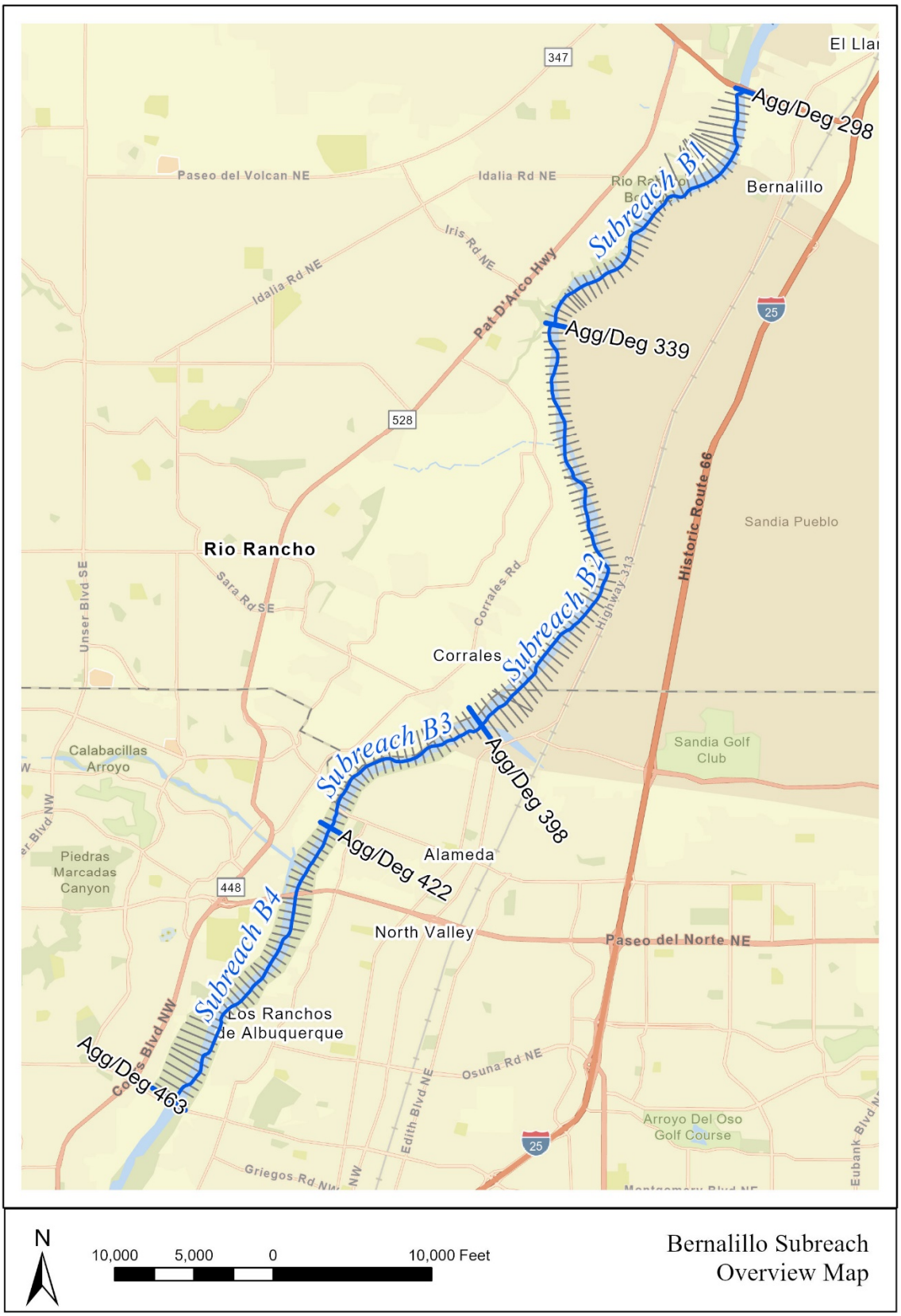

Figure 1-3 Bernalillo Subreach Delineation Overview Map (base map source: ESRI)

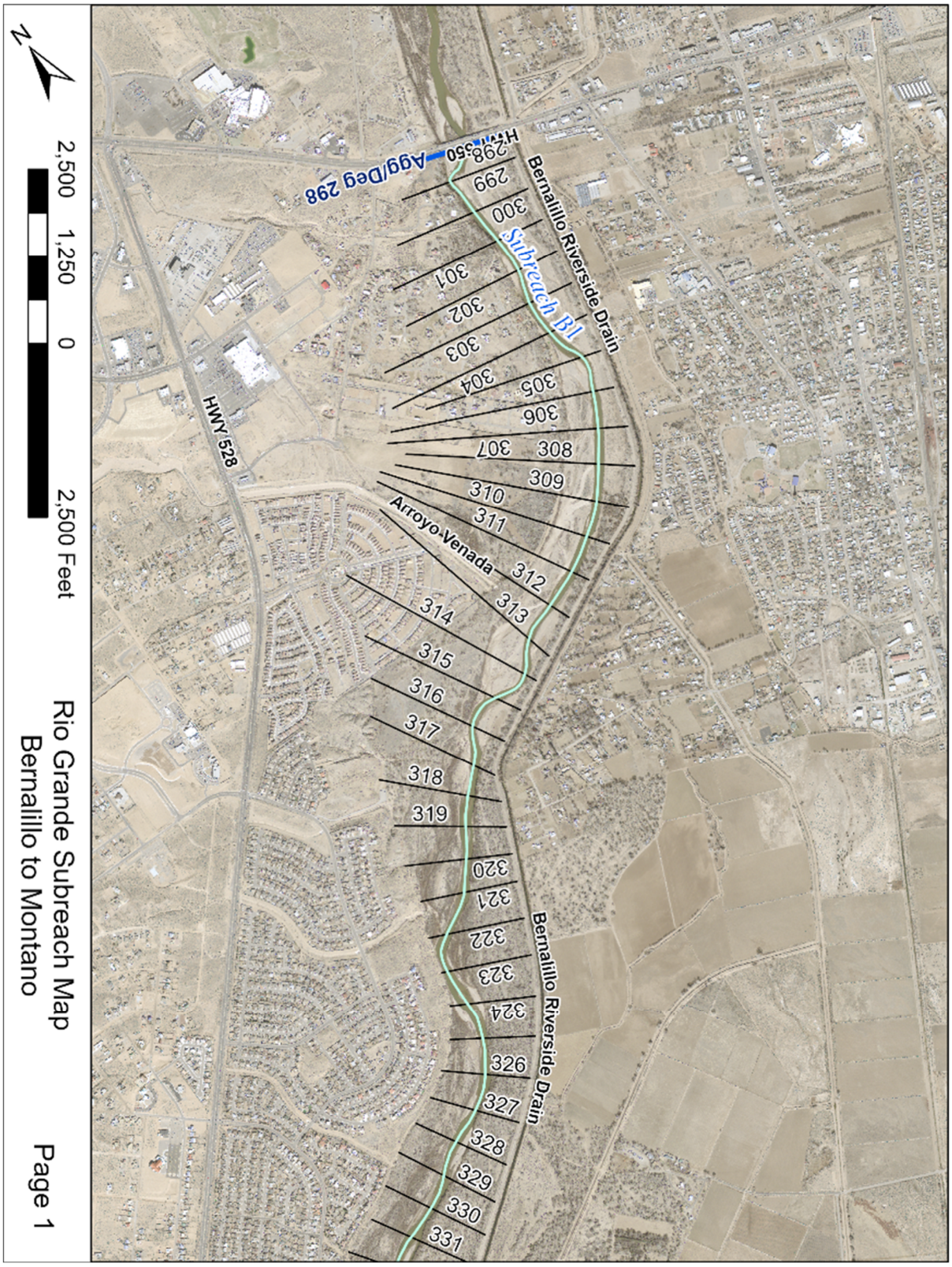

Figure 1-4 Subreach delineation with 2012 USBR ortho aerial imagery of Bernalillo Reach (B1) (turquoise line denotes the channel centerline, dark blue lines denote subreach boundaries, and black lines denote agg/deg cross-sections)

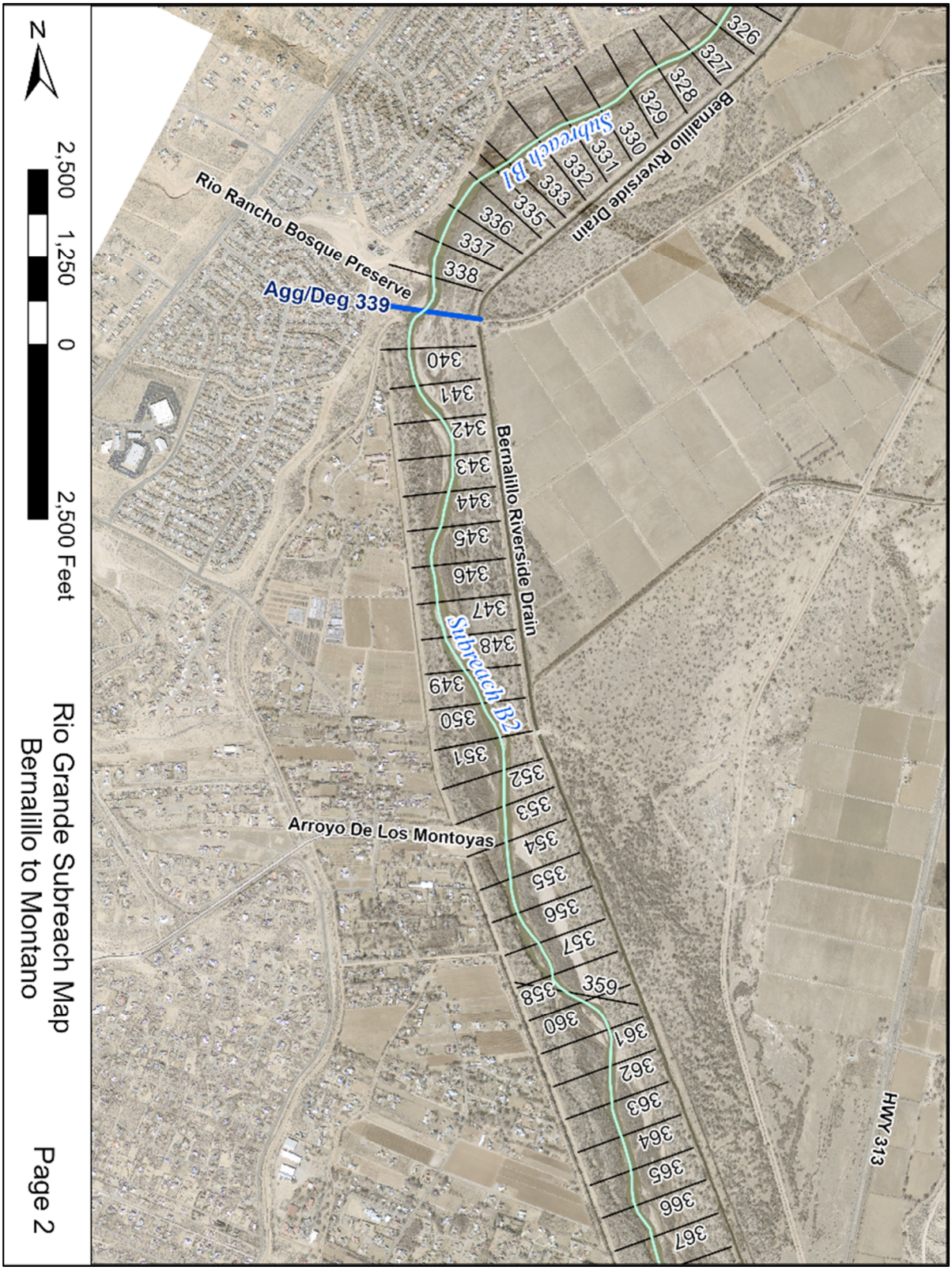

Figure 1-5 Subreach delineation with 2012 USBR ortho aerial imagery of Bernalillo Reach (B1 & B2) (turquoise line denotes the channel centerline, dark blue lines denote subreach boundaries, and black lines denote agg/deg cross-sections)

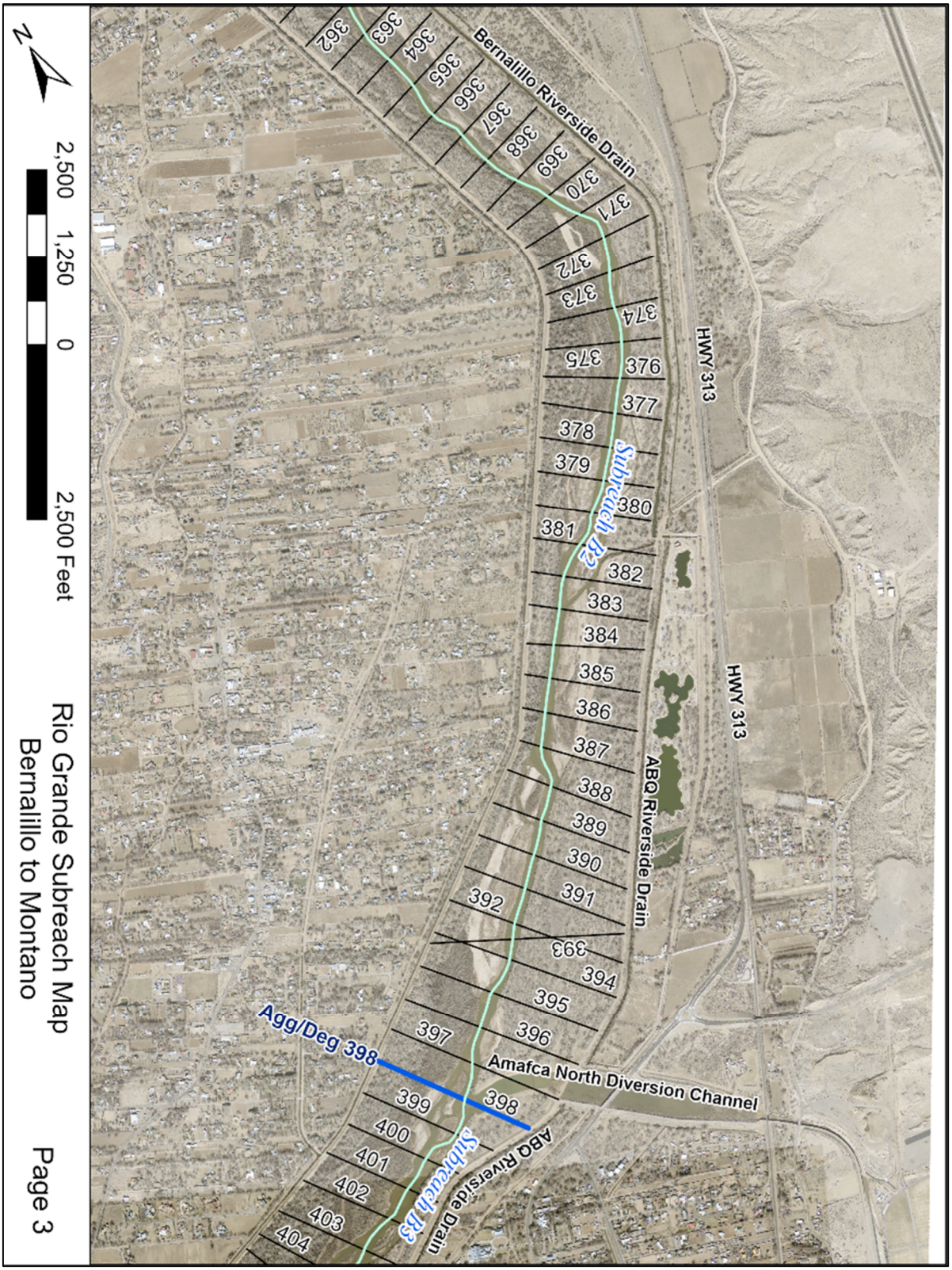

Figure 1-6 Subreach delineation with 2012 USBR ortho aerial imagery of Bernalillo Reach (B2 & B3) (turquoise line denotes the channel centerline, dark blue lines denote subreach boundaries, and black lines denote agg/deg cross-sections)

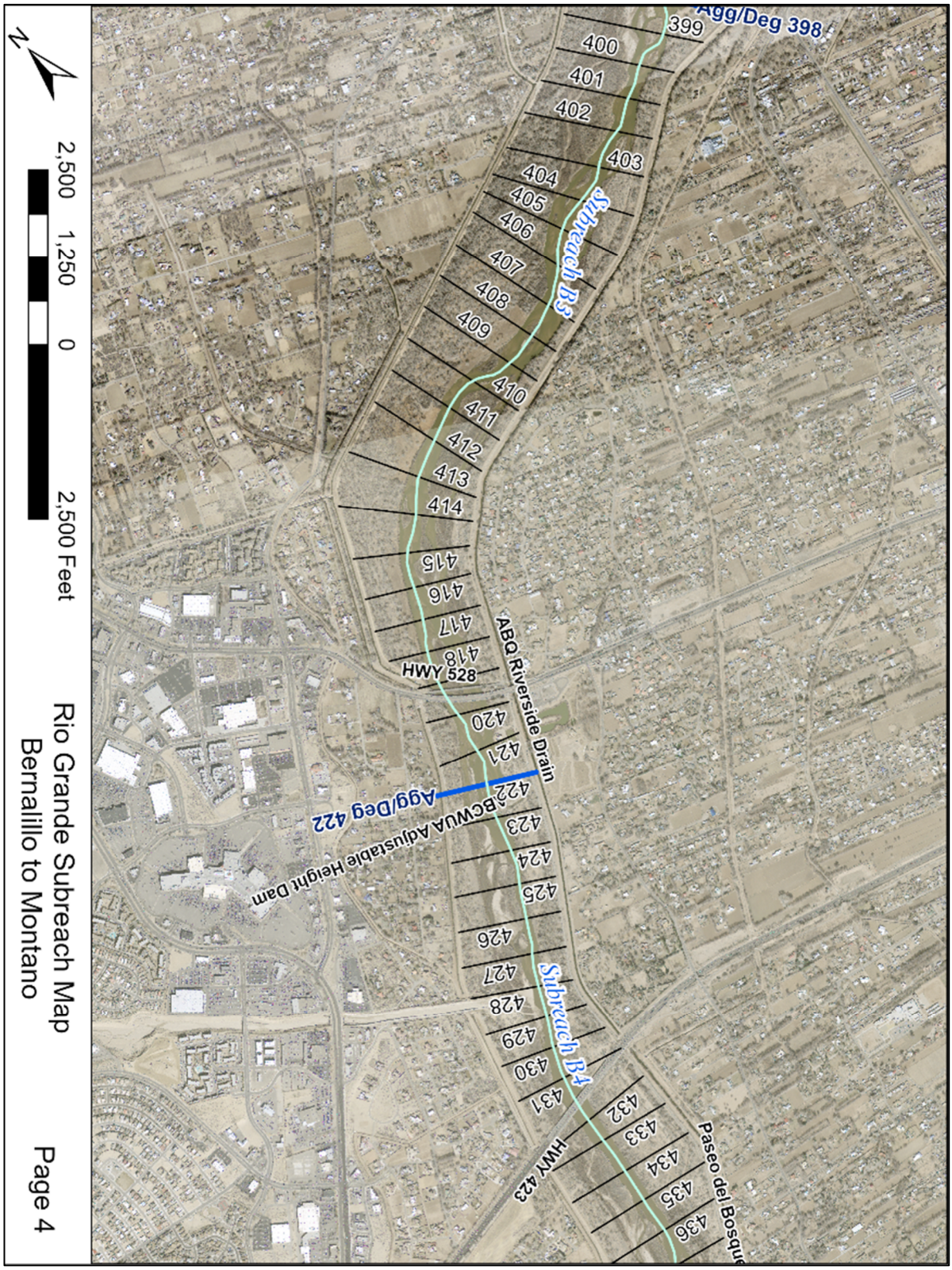

Figure 1-7 Subreach delineation with 2012 USBR ortho aerial imagery of Bernalillo Reach (B3 & B4) (turquoise line denotes the channel centerline, dark blue lines denote subreach boundaries, and black lines denote agg/deg cross-sections)

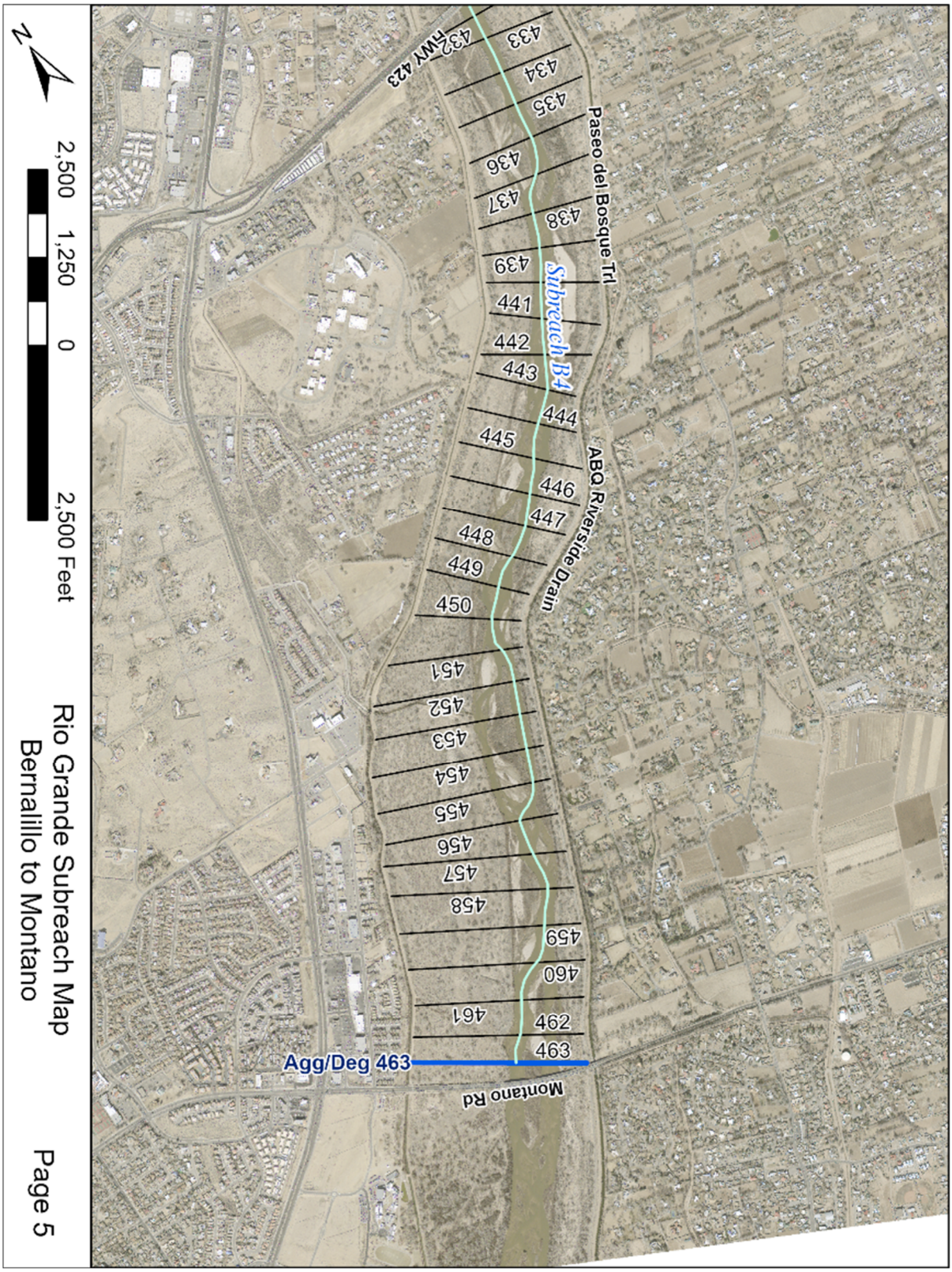

Figure 1-8 Subreach delineation with 2012 USBR ortho aerial imagery of Bernalillo Reach (B4) (turquoise line denotes the channel centerline, dark blue lines denote subreach boundaries, and black lines denote agg/deg cross-sections)

2 Precipitation, Flow, and Sediment Discharge Analysis

Due to the proximity of the reaches, a combined evaluation of precipitation, flow, and sediment characteristics was conducted for the Bernalillo and Montaño reaches.

2.1 Precipitation

Precipitation data was collected along the MRG by the Bosque Ecosystem Monitoring Program from University of New Mexico (BEMP Data, 2017). The locations of the data collection sites are shown in **Figure 2-1**. The four gage sites used in the precipitation analysis, from north to south, include Santa Ana, Alameda, Rio Grande Nature Center (RGNC), and Harrison. These sites were highlighted in the following analyses based on their proximity to the relevant river reaches and period of record. The Santa Ana gage site is just north of the upstream boundary of the Bernalillo Reach and the Harrison site is near the downstream boundary of the Montaño reach.

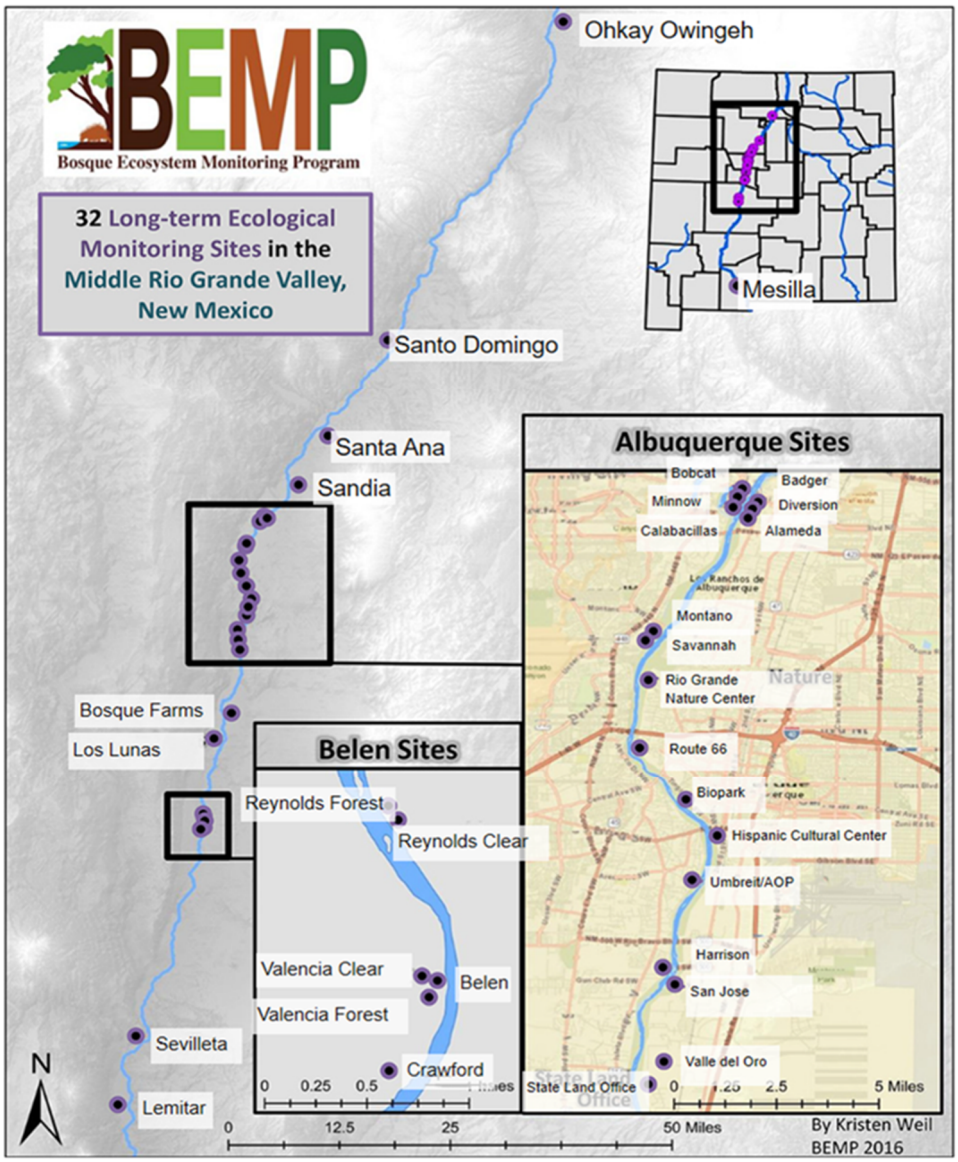

Figure 2-1 BEMP data collection sites (figures source: http://bemp.org)

The monthly precipitation data is shown in **Figure 2-2**. The highest precipitation peak, 5.7 inches of rainfall, occurred in August of 2006 at the Alameda gage. A general trend was observed with the highest precipitation values occurring during the monsoon season (late July through early September). A cumulative rainfall plot of the monthly precipitation data, **Figure 2-3**, shows that individual rain events can greatly affect the overall trend of the data. It further highlights the monsoonal rains, which create a "stepping" pattern with higher rainfall in August and September and lower levels throughout the rest of the year. The same pattern is observed across all the gage sites indicating rain patterns around the Bernalillo and Montaño reaches are spatially consistent. From the two gages with the longest period of record, Alameda, and RGNC, the cumulative rainfall pattern is similar until 2006. Since then, the Alameda gage has received slightly more precipitation (10 inches) than the RGNC gage.

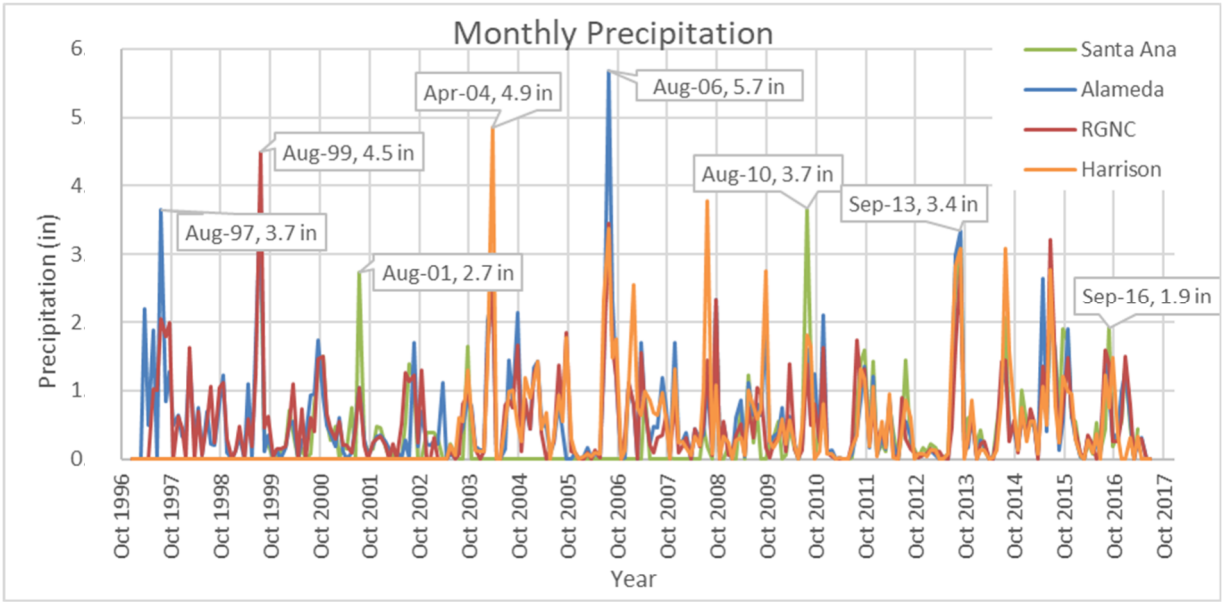

Figure 2-2 Monthly precipitation at four gages near the Bernalillo and Montaño reaches

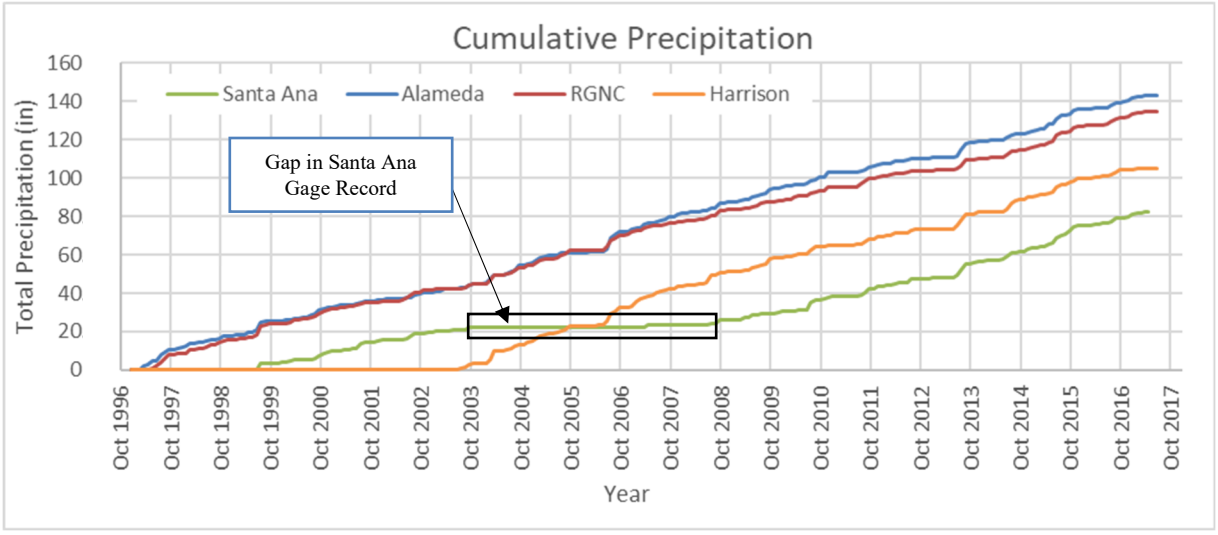

Figure 2-3 Cumulative precipitation at four gages near the Bernalillo and Montaño reaches

2.2 River Flow

2.2.1 USGS Gage Data

Information regarding river flow was gathered from the United States Geological Survey (USGS) National Water Information System. The gages relevant to the study area are included in **Table 2-1**

Table 2-1, and gage locations are shown in **Figure 2-4**. The gages highlighted in purple were chosen for closer analysis due to their location, longer period of record, and/or sediment data record.

Table 2-1. List of Relevant Gages

Reach	Station Name	Station #	Mean Daily Discharge	Suspended Sediment
Upstream	Rio Grande at Otowi Bridge, NM	08313000	February 2, 1895 to September 10, 2022	October 1, 1955 to September 30, 2021
	Rio Grande at Cochiti, NM (Historical)	08314500	June 1, 1926 to October 30, 1970	No Data
	Rio Grande Below Cochiti Dam, NM	08317400	October 1, 1970 to Present	July 1, 1974 to September 29, 1988
	Rio Grande At San Felipe, NM	08319000	January 1, 1927 to Present	No Data
	Jemez River Below Jemez Canyon Dam (Historical)	08329000	April 1, 1936 to September 29, 2009	November 15, 1955 to September 30, 2021
	Jemez River Outlet Below Jemez Dam, NM	08328950	September 30, 2009 to Present	No Data
Bernalillo Reach	Rio Grande Near Bernalillo, NM (Historical)	08329500	October 1, 1941 to September 29, 1969	October 1, 1955 to September 29, 1969
	Rio Grande at Alameda Bridge at Alameda, NM	08329918	July 4, 2003 to October 12-2020	No Data
	Rio Grande Nr. Alameda, NM	08329928	March 1, 1989 to October 12-2021	No Data
Montaño Reach	Rio Grande At Albuquerque, NM	08330000	October 1, 1965 to Present	October 1, 1969 to September 29, 2020
	Rio Grande At Isleta Lakes Nr. Isleta, NM	08330875	October 1, 2002 to September 18, 2021	No Data
Down-Stream	Rio Grande Near Bosque Farms, NM	08331160	March 16, 2006 to Present	No Data

**Note: Gages highlighted in purple were chosen for closer analysis due to their location, longer period of record, and/or sediment data record*

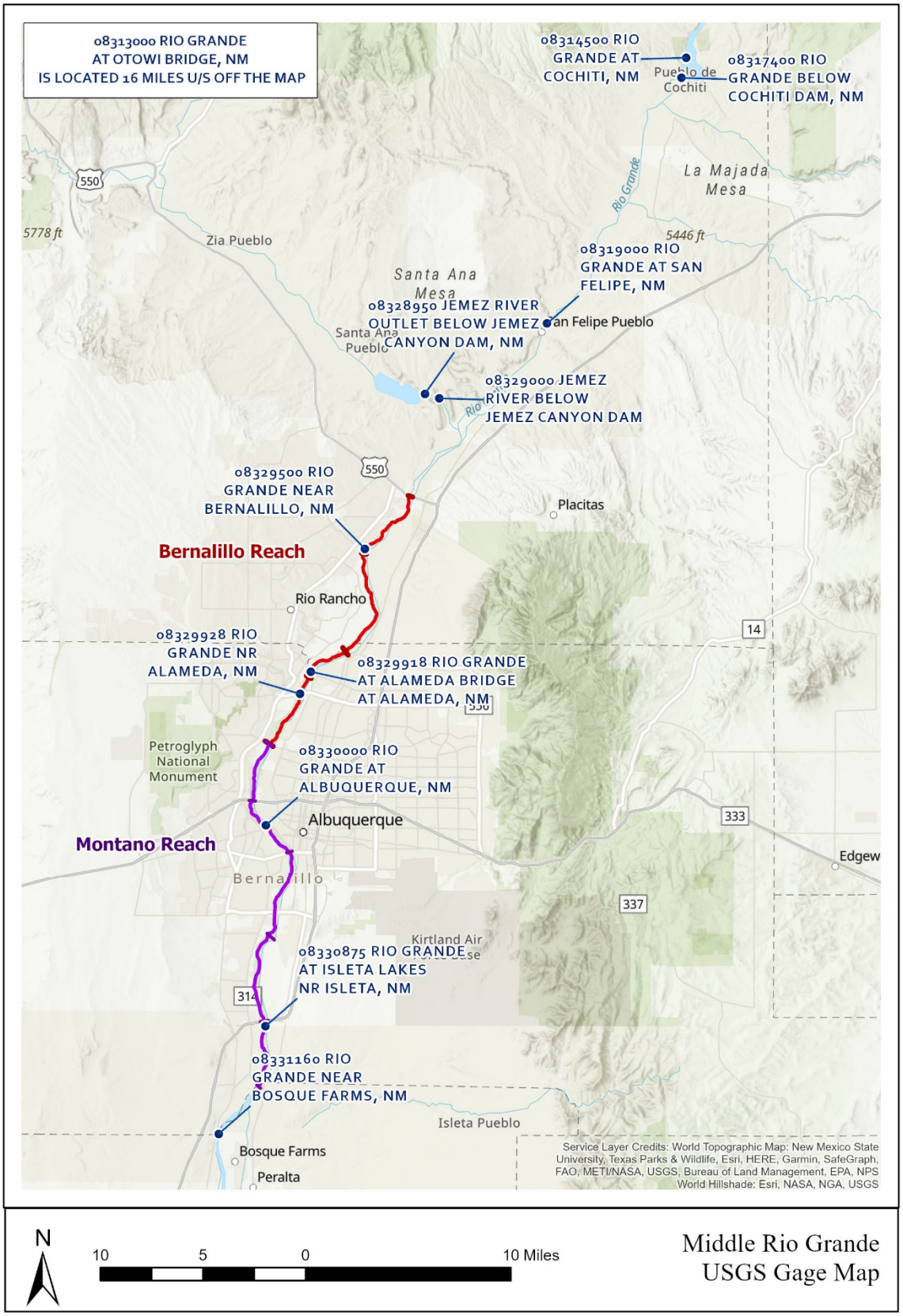

Figure 2-4. USGS gage data overview map (base map source: ESRI)

Construction of the Cochiti Dam commenced in 1965, started controlling flows in 1973, and was completed in 1975. A USGS gage (08317400) was installed in 1970 during construction of the dam. Prior to dam completion, a historical gage (08314500) with a period of record between 1926 and 1970 was located one mile upstream of the current operating gage. The current operating gage at Cochiti Dam has sediment data for a 66-year period of record between 1974 and 2021. Given the location of this gage directly downstream of the dam, it serves as a baseline for the sediment loading prior to any sediment input from tributaries or from bank and bed erosion along the Rio Grande.

Construction of the Jemez Dam was completed in 1953. A historical gage (08329000) was installed upstream of the Jemez River and Rio Grande confluence in 1936, 17 years prior to Jemez Dam construction, and has a period of record of 73-years of flow data between 1936 and 2009. This gage also has a 71-year sediment record extending between 1955 and 2021; however, the record shows 0 tons/day of suspended sediment load between 1958 and 2014, indicating that sediment was not sampled during this time. In 2009, a new gage (08328950) that is currently operational was installed 0.7 miles upstream of the historical gage. This gage only records flow data. Due to the proximity of the gages, the flow records for USGS Gage 08329000 and 08328950 were combined for this analysis. In 2014, a pass-through channel was constructed through the Jemez Dam to allow for sediment passage through the dam. At the time of this study, 7 years of sediment data are available to evaluate any effects that the additional sediment loading has had on the Bernalillo and Montaño reaches. See **Section 2.3** for additional information on the sediment loading through the Bernalillo and Montaño reaches.

The San Felipe gage (08319000) is located 10 miles upstream of the Bernalillo Reach and 7 miles upstream of the Rio Grande confluence with the Jemez River. This gage is still operational today and has a period of record of 95 years, between 1927 and 2022. This gage has a significant period of record both before and after the Cochiti Dam began controlling flows in 1973 and was used to evaluate the effects of the dam on flow characteristics within the Bernalillo and Montaño reaches. This gage does not include sediment data.

The historical gage near Bernalillo (08329500), located in Subreach B1 near Agg/Deg 337 and has 28 years of flow data between 1941 and 1969 as well as 14 years of sediment data between 1955 and 1969. Combined with the Albuquerque gage (below), this gage was useful in evaluating sediment loading within the Bernalillo and Montaño reaches.

The Albuquerque gage (08330000) has been operational from 1965 to present and has a sediment record between 1969 and 2020. It is located in Subreach M2 of the Montaño reach at Central Ave. in Albuquerque (Anderson et al. 2022). The data from this gage was helpful in evaluating sediment loading within the Bernalillo and Montaño reaches of the MRG.

2.2.2 Raster Hydrographs

The raster hydrographs of daily discharge at the gages at San Felipe (left) and Albuquerque (right) are shown in **Figure 2-5**. Both gages are operational today, with a period of record of 95 years for the San Felipe gage and 57 years for the Albuquerque gage. These raster hydrographs show seasonal flow patterns, with peak flows often occurring from snowmelt runoff in April through June, low flow throughout the rest of the summer (except for strong summer thunderstorms), and medium flow from November onwards representing the end of the irrigation season. These raster hydrographs also highlight differences in flood magnitude before and after the Cochiti dam construction in 1970. Prior to 1970, the San Felipe gage shows long duration spring flood events that are sometimes on the order of magnitude between 8,000 cfs and 20,000 cfs. Conversely, the Albuquerque gage after 1970 shows these longer duration spring floods on an order of magnitude between 4,000 cfs and 6,000 cfs.

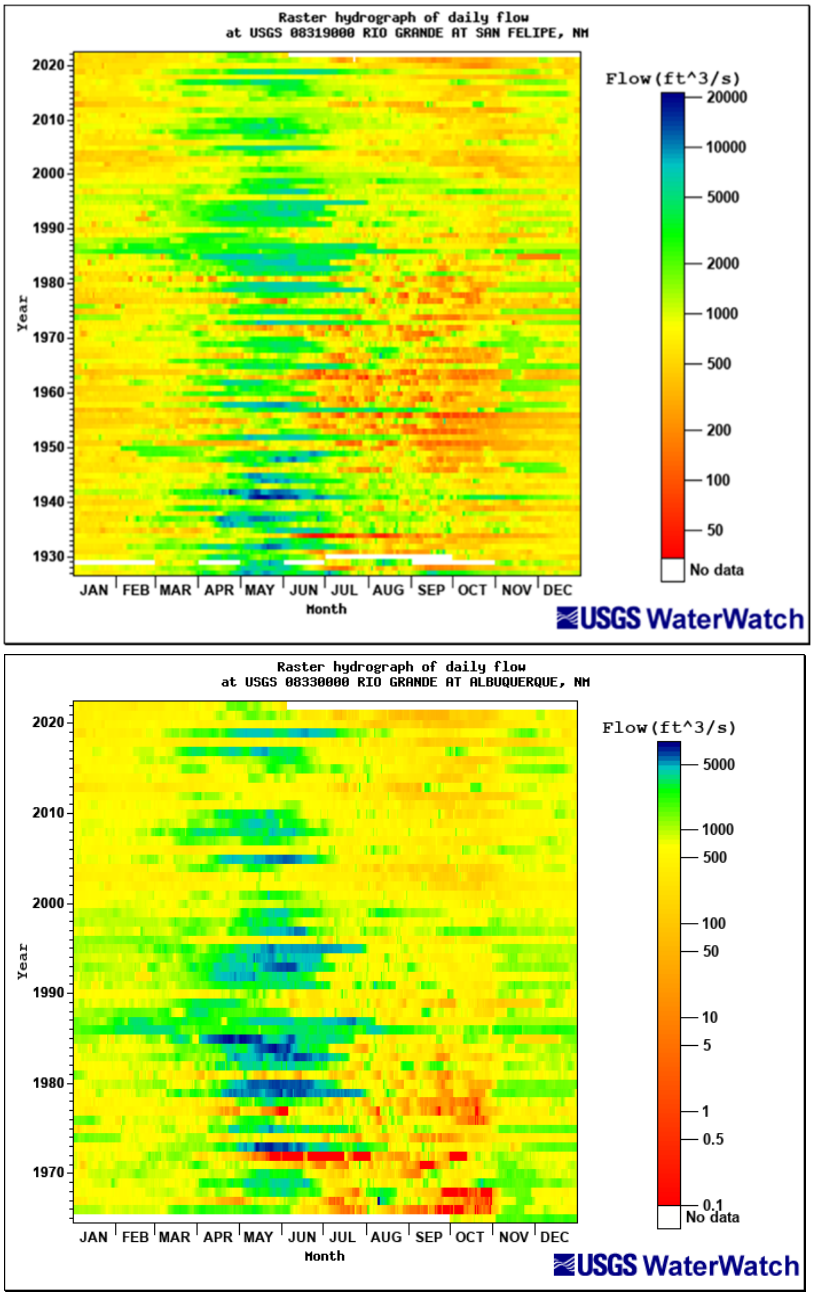

Figure 2-5 Raster hydrograph of daily discharge at USGS Station 08319000 at San Felipe (top) and USGS Station 08330000 at Albuquerque (bottom). (Source: https://waterwatch.usgs.gov)

The raster hydrographs of daily discharge at the gages located directly downstream of the Jemez Dam are shown in **Figure 2-6**. The combined period of record for these gages is 86 years between 1936 and present. The figures show seasonal flow patterns, with peak flows often occurring from snowmelt runoff in April through June, low flow throughout the rest of the summer (except for strong summer thunderstorms), and medium flow from November onwards representing the end of the irrigation season. The Rio Jemez regularly experiences very low flows (below 1 cfs) or no flow during long periods of the summer season.

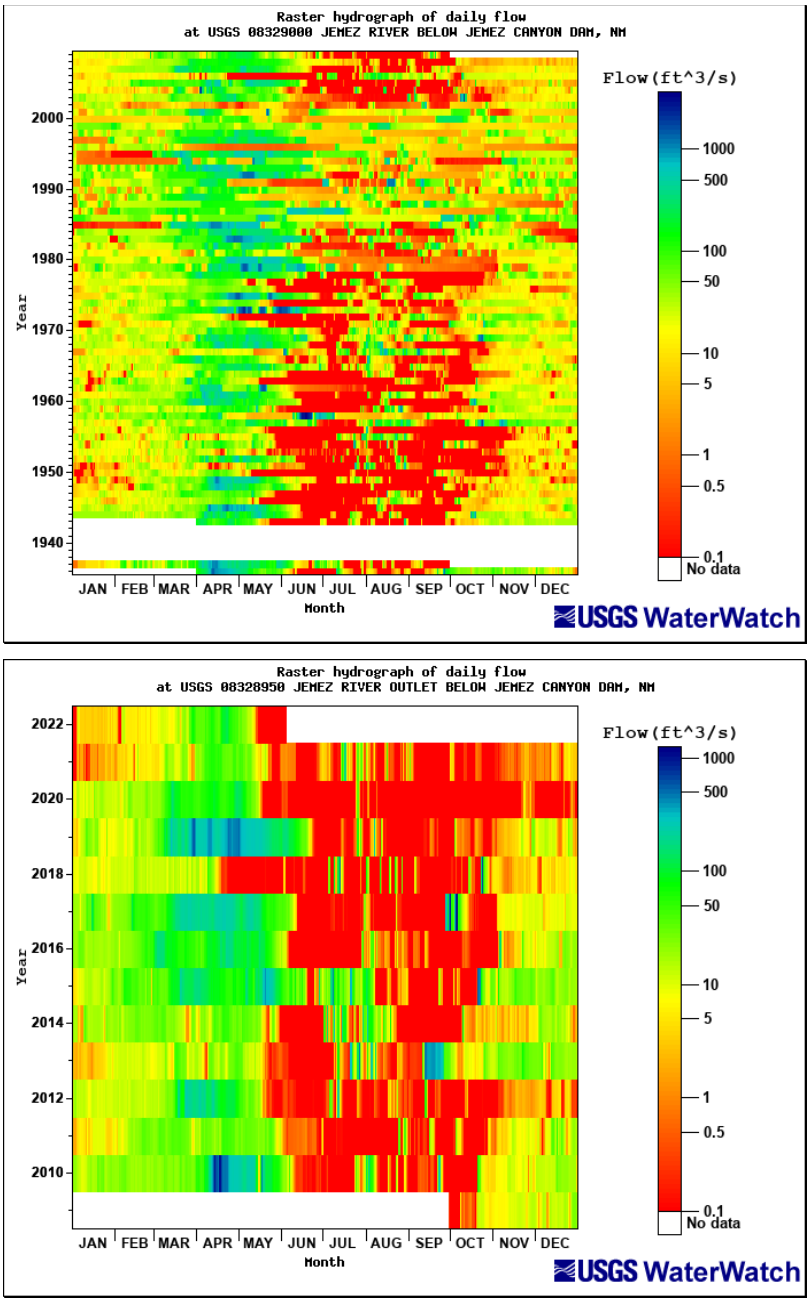

Figure 2-6 Raster hydrograph of daily discharge at historical USGS Station 08329000 (top) and USGS Station 0832950 (bottom) below the Jemez Dam. (Source: https://waterwatch.usgs.gov).

2.2.3 Yearly Peak Flow Events

Yearly peak flow events for the Cochiti, San Felipe, and Albuquerque gages are shown in **Figure 2-7** and **Figure 2-8**. These peak flow events were determined from average daily flow data. **Figure 2-7** shows the yearly peak flow events prior to the Cochiti Dam completion in 1970, while **Figure 2-8** shows the peak events after dam completion to present day. Like the raster hydrographs shown above, these graphs show a clear distinction between pre- and post-dam conditions. In the 44 years of gage record prior to Cochiti Dam completion there were 11 flood events with peak daily flows larger than 10,000 cfs. In the 52 years of gage record after dam completion, peak flows became less variable and have not peaked above 10,000 cfs.

The flood of record at the San Felipe gage occurred in June of 1937, with a peak of 27,300. Two notable flood events also occurred in series in May of 1941 and the following April of 1942, with peak flows of 22,600 cfs and 18,900 cfs, respectively, at the San Felipe gage. The 3 years between 1983 and 1985 show larger than normal spring flood events, with a peak flood at 10,200 cfs in May 1985 at the Cochiti gage. The more recent larger flood events occurred in May of 2017 and June of 2019, with peak flows of 8,180 cfs and 6,260 cfs, respectively, at the San Felipe gage.

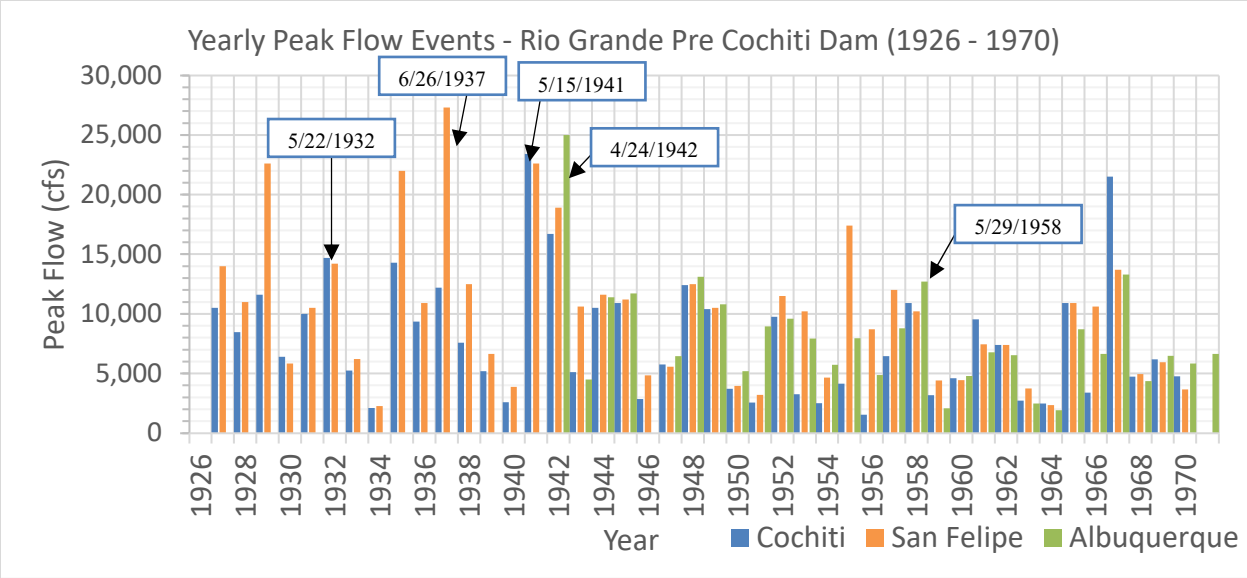

Figure 2-7 Yearly peak flow events for the Rio Grande before Cochiti Dam at USGS Gages 08314500, 08319000, and 08330000 from 1926-1970.

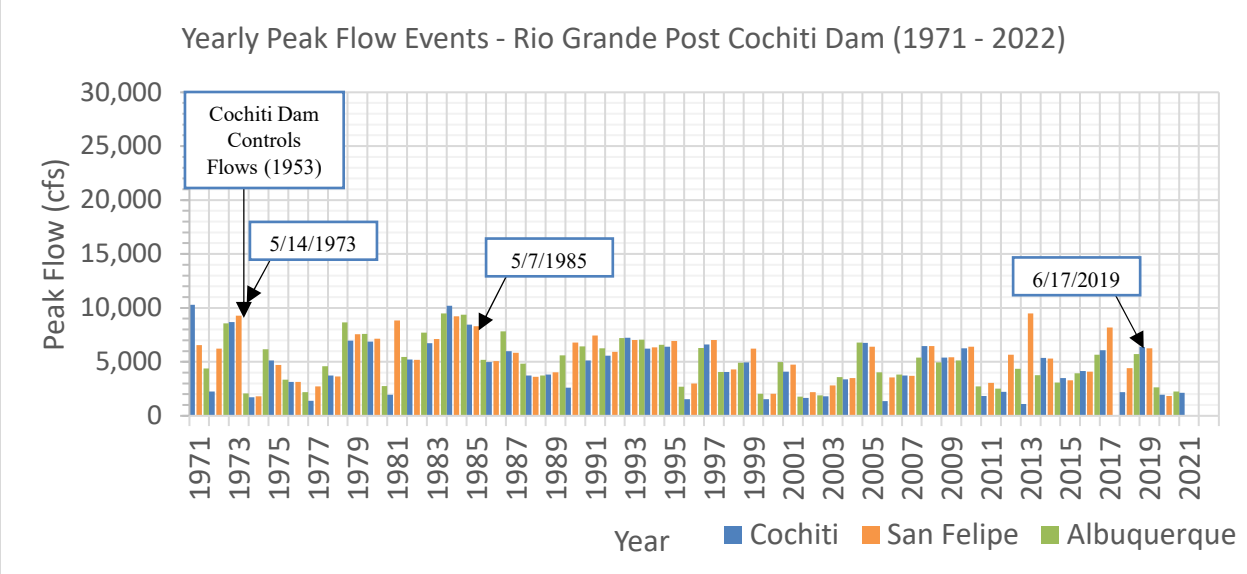

Figure 2-8 Yearly peak flow events for the Rio Grande after Cochiti Dam at USGS Gages 08317400, 08319000, and 08330000 from (1970-present).

Yearly peak flow events for the Jemez River gages are shown in **Figure 2-9**. The flow record does appear to show dam influence on peak flow rates for the Jemez River caused by completion of the Jemez Dam in 1953. The largest flood event for the period of record occurred in August of 1943, with a peak flow rate of 16,300 cfs. After the dam completion, the largest peak flow occurred in June of 1958, with a peak flow of 4,870 cfs.

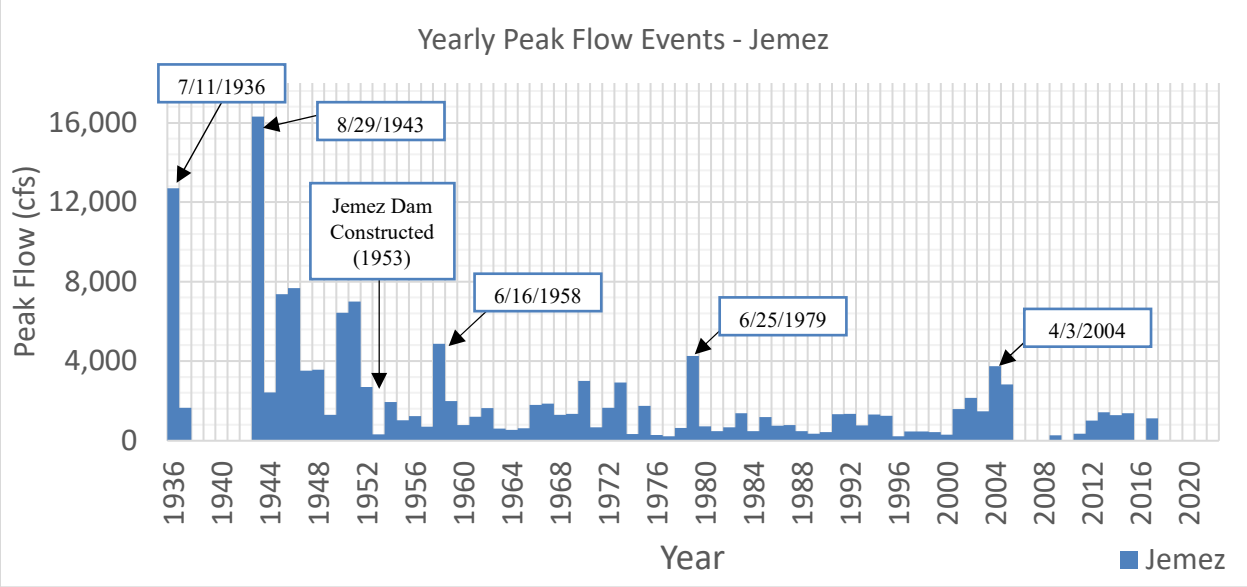

Figure 2-9 Yearly peak flow events for the Jemez River

2.2.4 Cumulative Discharge Curves

Cumulative discharge curves show changes in flow volume over a given time period. The slope of the line of the mass curve gives the mean discharge for the respective time interval, while breaks in the slope show changes in flow volume trends. **Figure 2-10** through **Figure 2-14** show the single mass curves at Cochiti, San Felipe, and Albuquerque. The gage records for Cochiti and San Felipe were split into pre- and post-dam construction, with October of 1970 chosen as the break point, because there was sufficient record before and after dam construction to compare differences in flow trends. The gage record at Albuquerque only begins 8 years before completion of the dam, and so the full gage record was shown in one graph. The single mass curves were divided into time periods of similar slopes to analyze long term patterns in discharge. While cumulative discharge plots are particularly useful for analyzing long-term trends in flows, occasionally, large flow-altering events can be identified from spikes in the curve.

The pre- and post- dam mass curves for Cochiti are shown by **Figure 2-10** and **Figure 2-11**, respectively. Between 1926 and 1941, the mean discharge was 1,375 cfs. The curve becomes steeper for a short time between spring of 1941 and fall of 1942, which corresponds to the two large flood events that occurred, as described above in **Section 2.2.3**. Between 1943 and 1970 the trend flattens out, with an average flow rate of 1,113 cfs.

In the years following dam completion until 1979 the slope of the curve flattens, giving an average flow rate of 966. Between 1979 and 1995 the slope of the curve steepens to an average flow rate of 1,714 cfs, indicating that this is a wetter than normal period. This trend can also be seen in the yearly peak flood events shown by **Figure 2-8** (previous page). Between 1995 and present day the slope of the curve again flattens, giving an average flow rate for this period of 974 cfs. Similar trends can be seen in the San Felipe and Albuquerque mass curves shown in **Figure 2-12** through **Figure 2-14**. Note that the period between

1980 and 1988 was a particularly wet period compared with other periods following construction of the dam.

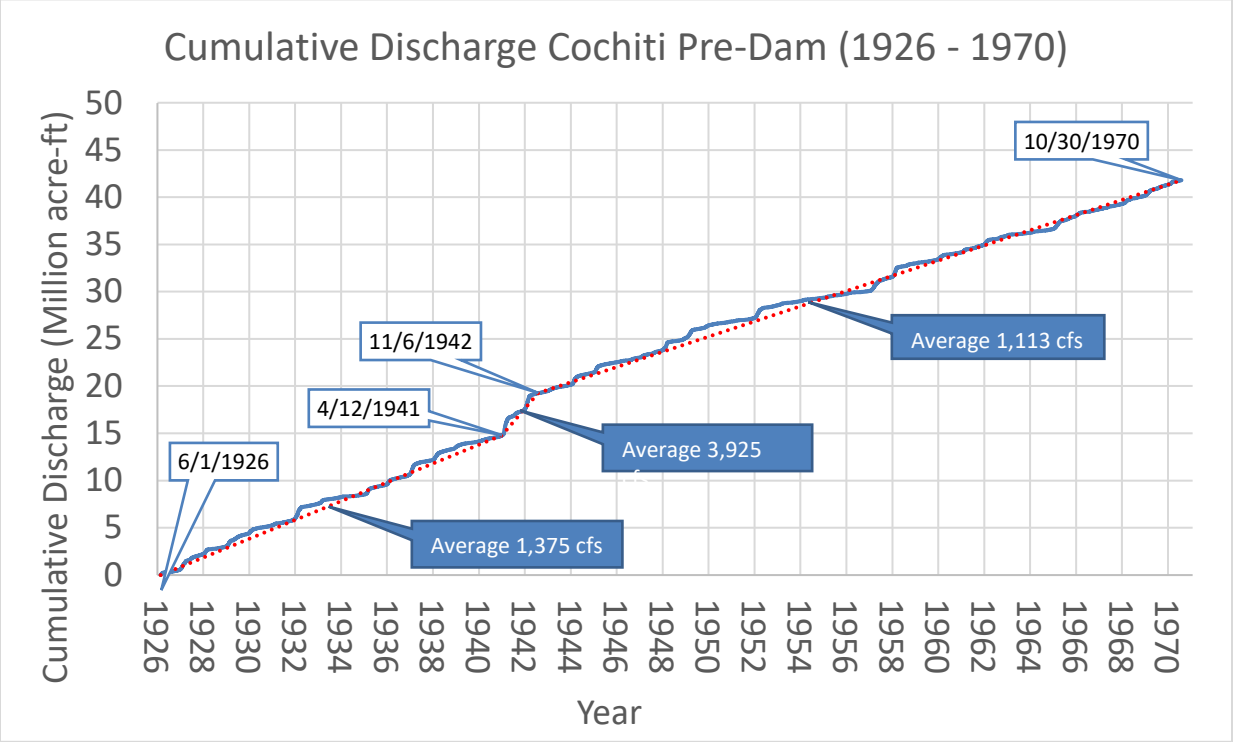

Figure 2-10 Discharge single mass curve at historical USGS gage 8314500 (Cochiti) before dam construction.

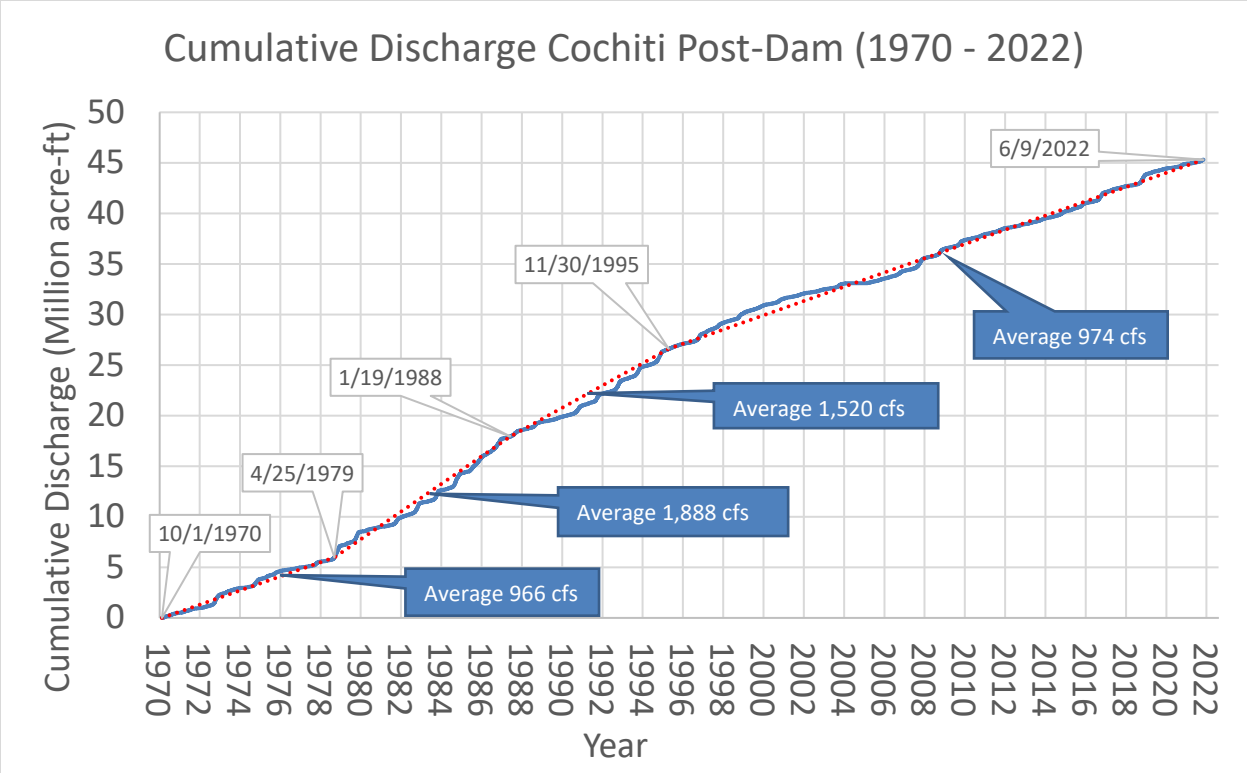

Figure 2-11 Discharge single mass curve at USGS gage 08317400 (below Cochiti Dam) after dam construction

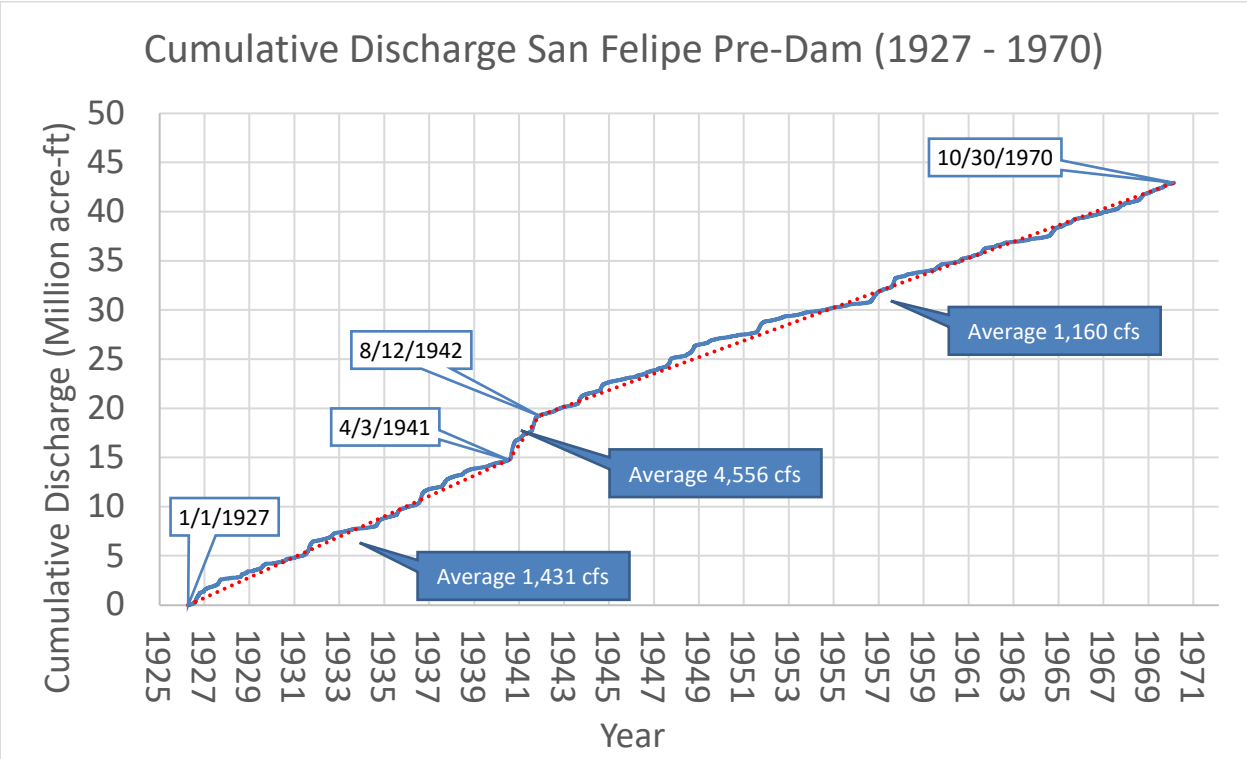

Figure 2-12 Discharge single mass curve at USGS gage 08319000 (San Felipe) before dam construction.

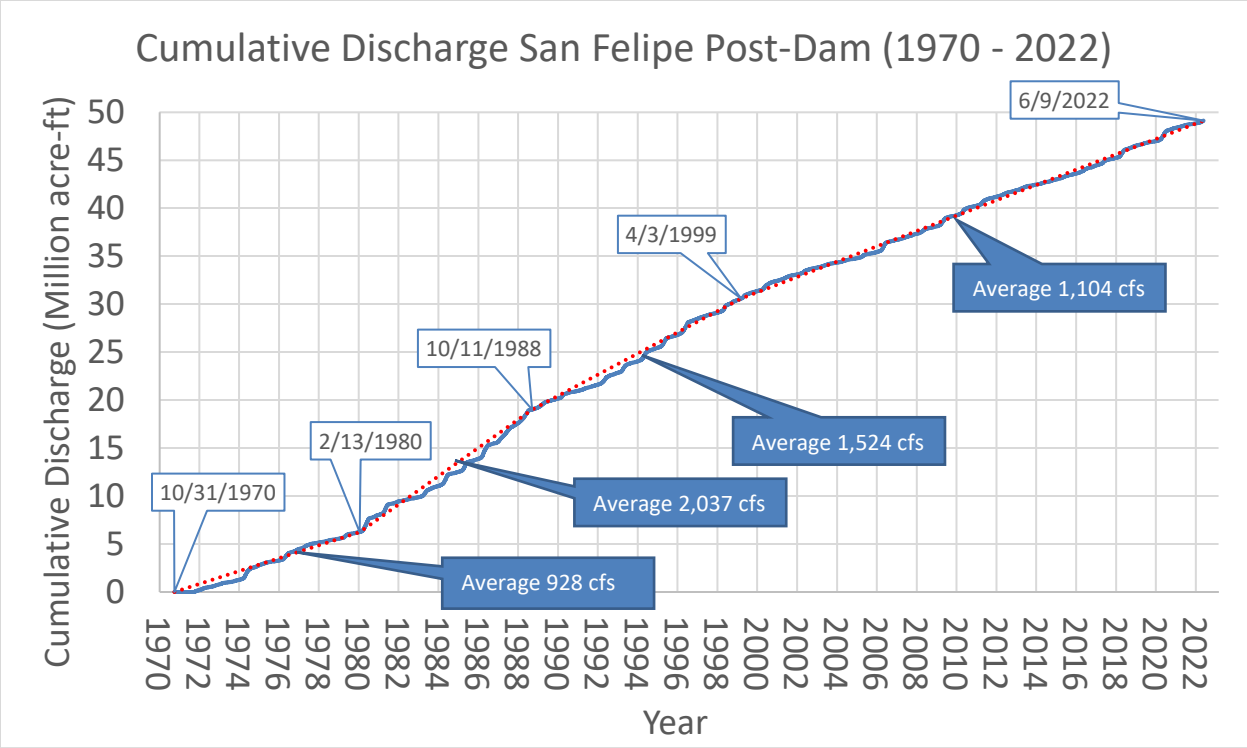

Figure 2-13 Discharge single mass curve at USGS gage 08319000 (San Felipe) after dam construction.

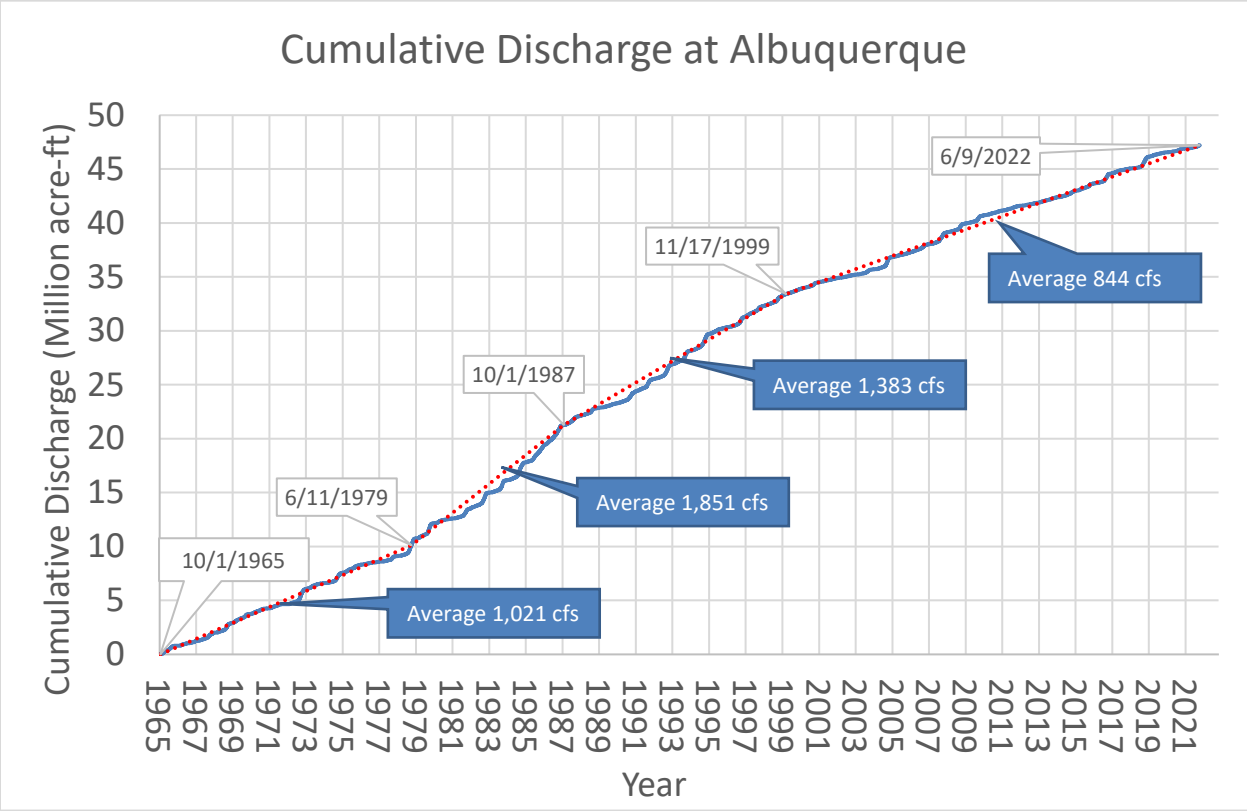

Figure 2-14 Discharge single mass curve at USGS gage 08330000 (Albuquerque).

Figure 2-15 and **Figure 2-16** show the single mass curves at the Jemez River gages. These gage records were also split into pre- and post-dam construction to compare differences in flow trends. No flow record is available between September of 1937 and March of 1943. In the two years before this gap, the average flow rate was 123 cfs. In the 10 years between 1943 and dam completion in 1953, the average flow rate was 47 cfs.

In the 26 years following completion of the dam between 1953 and 1979, the average flow rate is 54 cfs. The time period between 1979 and 1995 shows a similar trend of wetter than normal years as the Rio Grande gages, with an average flow rate increasing to 89 cfs. Between 1995 and present day the slope of the curve flattens, giving an average flow rate of 42 cfs.

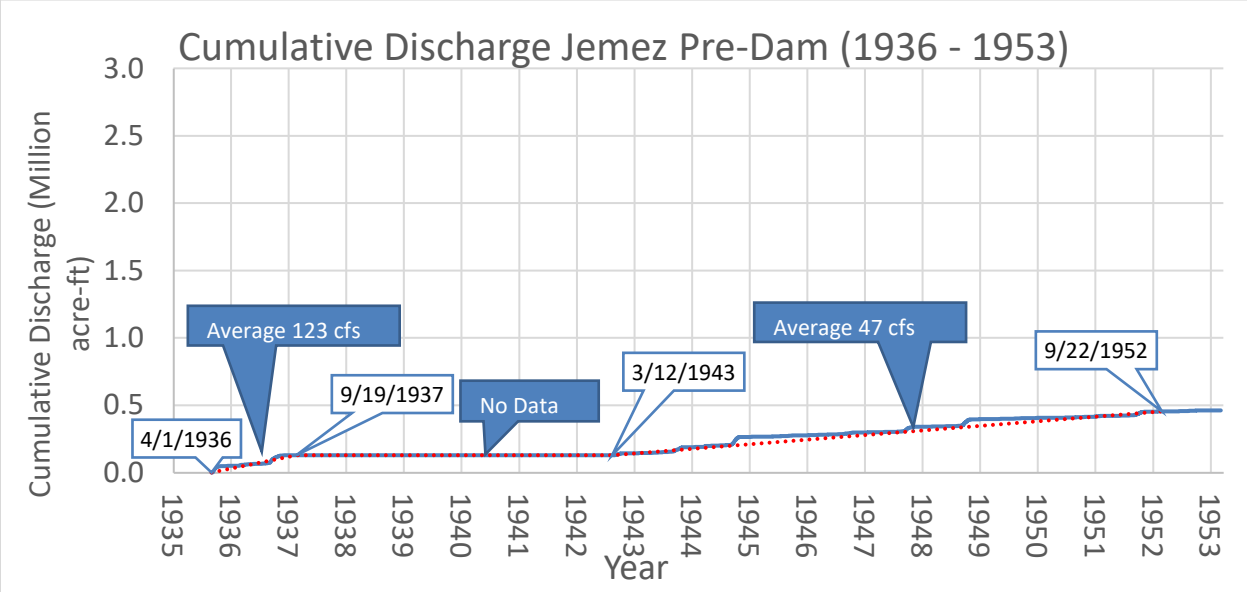

Figure 2-15 Discharge single mass curve at historical USGS gage 08329000 (Jemez) before dam construction in 1953.

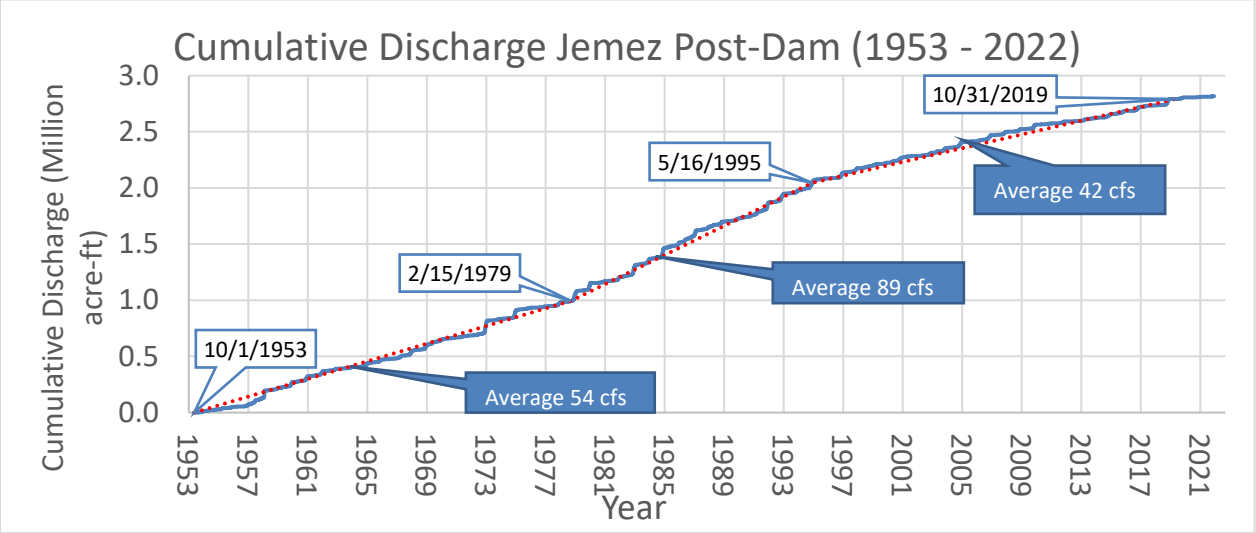

Figure 2-16 Discharge single mass curve at historical USGS gage 08329000 and USGS gage 08328950 (Jemez) after dam construction in 1953.

2.2.5 Flow Duration

Flow duration curves were developed using the mean daily discharge values for the Cochiti, San Felipe, Albuquerque, and Jemez River gages. **Table 2-2** shows the probabilities of daily exceedance values calculated from the flow duration curves for a range of exceedance probabilities. The gage records were split between pre- and post- construction of the Cochiti Dam for the Rio Grande gages. Gage records were similarly split for the Jemez River gages to account for any differences in flow conditions before and after the completion of the Jemez Dam. The curves for the Rio Grande gages are shown in **Figure 2-17**, and the curves for the Jemez River gages are shown in **Figure 2-18**.

While more frequent flood events with daily exceedance probabilities greater than 10% do not appear to be significantly impacted by the Cochiti Dam, the less frequent flood events less than 10% exceedance probability show a clear divergence between pre and post Cochiti Dam construction (**Figure 2-17**). The 1% daily exceedance probability shows a 3,000 cfs reduction in flow magnitude after completion of the dam. This does not appear to be the case for the Jemez Dam for the period of record. **Figure 2-18** shows a similar pattern in flows before and after the completion of the Jemez Dam in 1953.

Table 2-2 Probabilities of daily exceedance

	Discharge (cfs)						
	Pre Cochiti Dam (1926 to 1973)		Post Cochiti Dam (1973 – Present)			Pre Jemez Dam (1936 to 1953)	Post Jemez Dam (1953 to Present)
Daily Probability of Exceedance	8314500 Rio Grande at Cochiti, NM June 1, 1926 to September 30, 193	8319000 Rio Grande at San Felipe, NM January 1, 1927 to September 30, 1970	8317400 Rio Grande Below Cochiti Dam, NM October 1, 1973 to Present	8319000 Rio Grande At San Felipe, NM October 1, 1973 to Present	[1] 8330000 Rio Grande at Albuquerque, NM October 1, 1973 to Present	[2] 8329000 Jemez River Below Jemez Canyon Dam April 1, 1936 to September 30, 1953	[3] 8329000 & 08328950 Jemez River Below Jemez Dam October 1, 1953 to Present
1%	9,130	9,430	6,190	6,320	6,090	750	650
10%	2,840	2,980	3,010	3,120	2,980	110	143
25%	1,300	1,400	1,260	1,340	1,230	36	45
50%	730	780	812	899	702	11	16
75%	488	530	575	654	470	0	2
90%	278	325	390	470	292	0	0

Notes:
[1] The pre-Cochiti Dam gage record between 1965 and 1970 for USGS gage 8330000 at Albuquerque were omitted from this analysis for consistency.
[2] Six years of missing data between 1938 and 1943 for the USGS 8329000 Jemez River gage.
[3] USGS gage 8328950 below Jemez Dam is located approximately 0.7 miles upstream of historical USGS gage 8329000. Gage records were combined for this analysis.

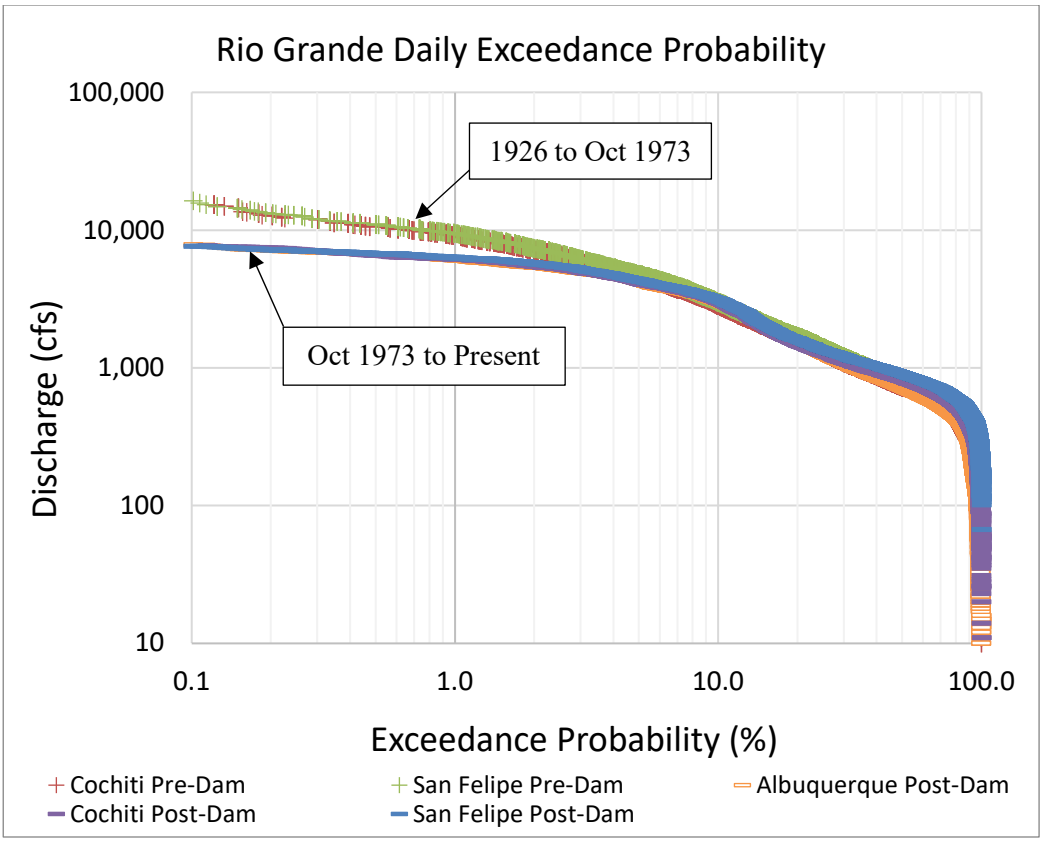

Figure 2-17 Flow duration curves for the Rio Grande gages before and after dam construction.

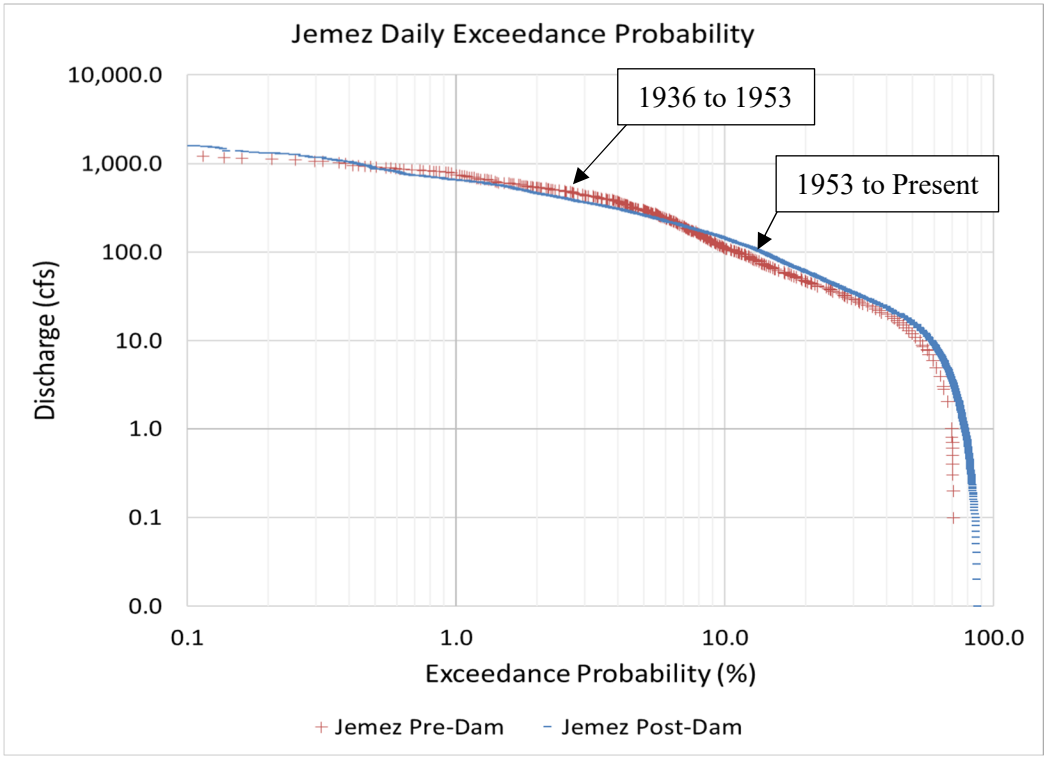

Figure 2-18 Flow duration curves for the Jemez River gages before and after dam construction in 1953.

2.2.6 Days of Flow

In addition to flow duration curves, the number of days in the water year exceeding the identified flow values at each gage were analyzed. This is purely a count of days and does not consider consecutive days. This analysis was performed for the entire record at the San Felipe and Jemez River gages shown by **Figure 2-19** and **Figure 2-20**, respectively. Like previous analyses, the gage records were split between pre and post dam construction for the purposes of comparison.

The most notable difference observed in the San Felipe graphs before and after Cochiti Dam construction is that pre-dam flow conditions saw a greater number of days above 6,000 cfs. The graphs also seem to indicate that the years between 1979 and 1999 show a greater number of days (around half of the year, on average) above 1,000 cfs. These graphs also give a good indication of dry years. For example, between 2003 and 2006, fewer than 50 days of the year saw flows greater than 1,000 cfs. In general, the larger flows become less frequent after 2001.

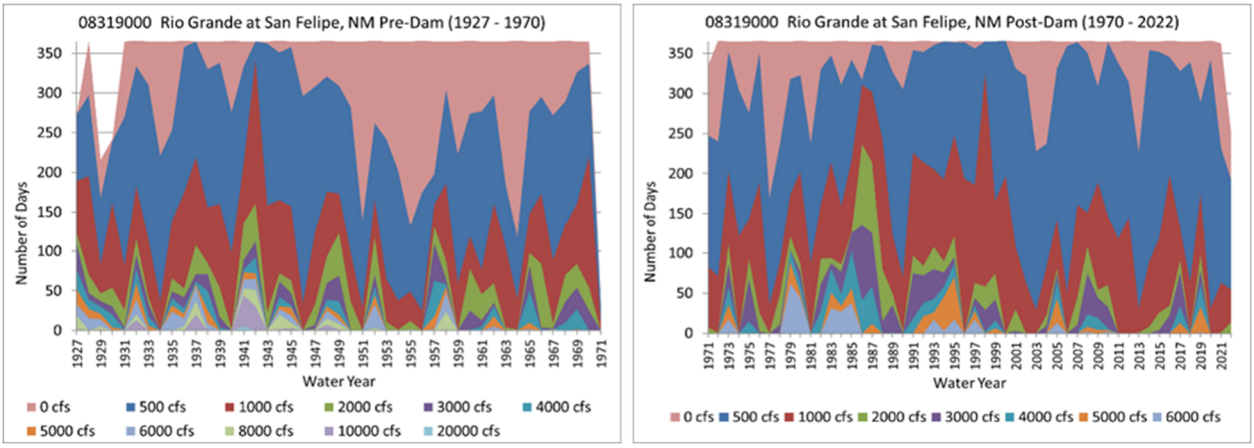

Figure 2-19 Number of days greater than an identified discharge at the San Felipe gage before (left) and after (right) dam construction.

The Jemez River is more likely to see days with no flow. Before dam construction, the river appears to have had more frequent days with no flow than after dam construction. In the years between 1999 and present day, the Jemez River has generally seen fewer than 100 days of the year with flows greater than 50 cfs.

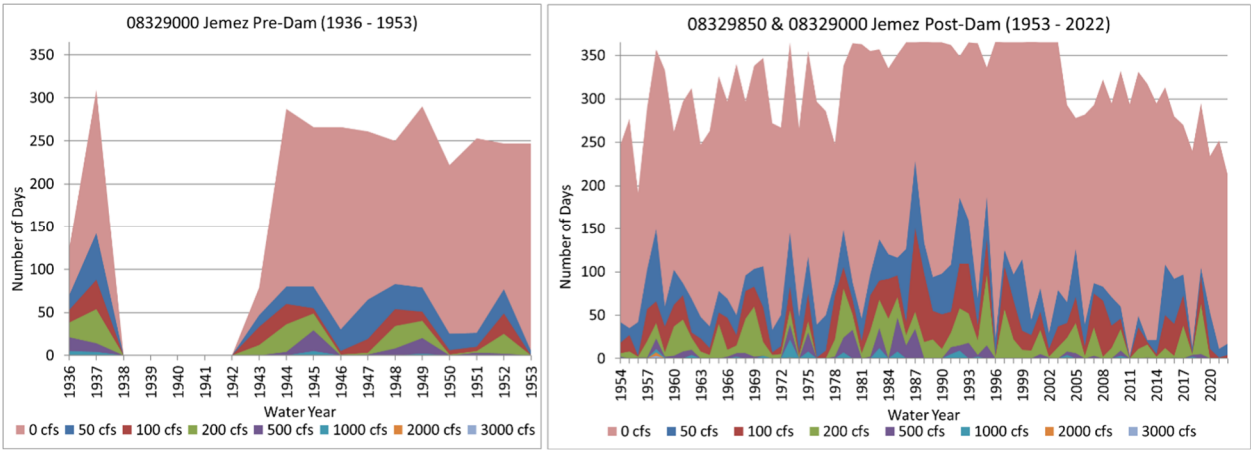

Figure 2-20 Number of days over an identified discharge at the Jemez gages before (left) and after (right) dam construction in 1953.

2.3 Suspended Sediment Load

2.3.1 Single Mass Curve

Single mass curves of cumulative suspended sediment (in millions of tons) at the Jemez River (USGS 08329000), Rio Grande Below Cochiti (USGS 08317400), Rio Grande Near Bernalillo (USGS 08329500), and Rio Grande at Albuquerque (USGS 08330000) gages are shown in **Figure 2-21** to **Figure 2-24**, respectively. These curves were created from the average daily sediment data. Additional single mass curves that show greater detail of the sediment load in the Jemez River before and after the Jemez Dam modification are found in **Section 2.3.4**.

The single mass curves show changes in daily sediment volume over a given time period. The slope of the line of the mass curve gives the mean sediment discharge, while breaks in the slope along the single mass curve show the changes in sediment flux. The Cochiti Dam began controlling flows in 1973 and was completed in 1975. Downstream of Cochiti, at the Albuquerque gage, there is a large decrease in the mean sediment discharge after 1973 and the historical Bernalillo gage data showed large mean sediment discharges before 1973. The correlation shows that the construction of Cochiti Dam had a dramatic impact on the sediment discharge going through the MRG. The mean sediment discharge at the Cochiti gage after construction is relatively low and consistent compared to other inputs to the system. The horizontal steps in **Figure 2-22** demonstrate that the water is relatively sediment free and clear between events, which indicates that a majority of the sediment upstream of Cochiti is getting stopped at the dam. There are no major tributaries that enter the MRG below Cochiti, however there are several small arroyos that enter the river and two flood-controlled channels (Towne 2007). As mentioned in **Section 1.1**, the ephemeral tributaries are the primary source of sediment input into to MRG (Fitzner 2018). Other sources of sediment include bed erosion as the channel degrades and bank erosion during channel migration.

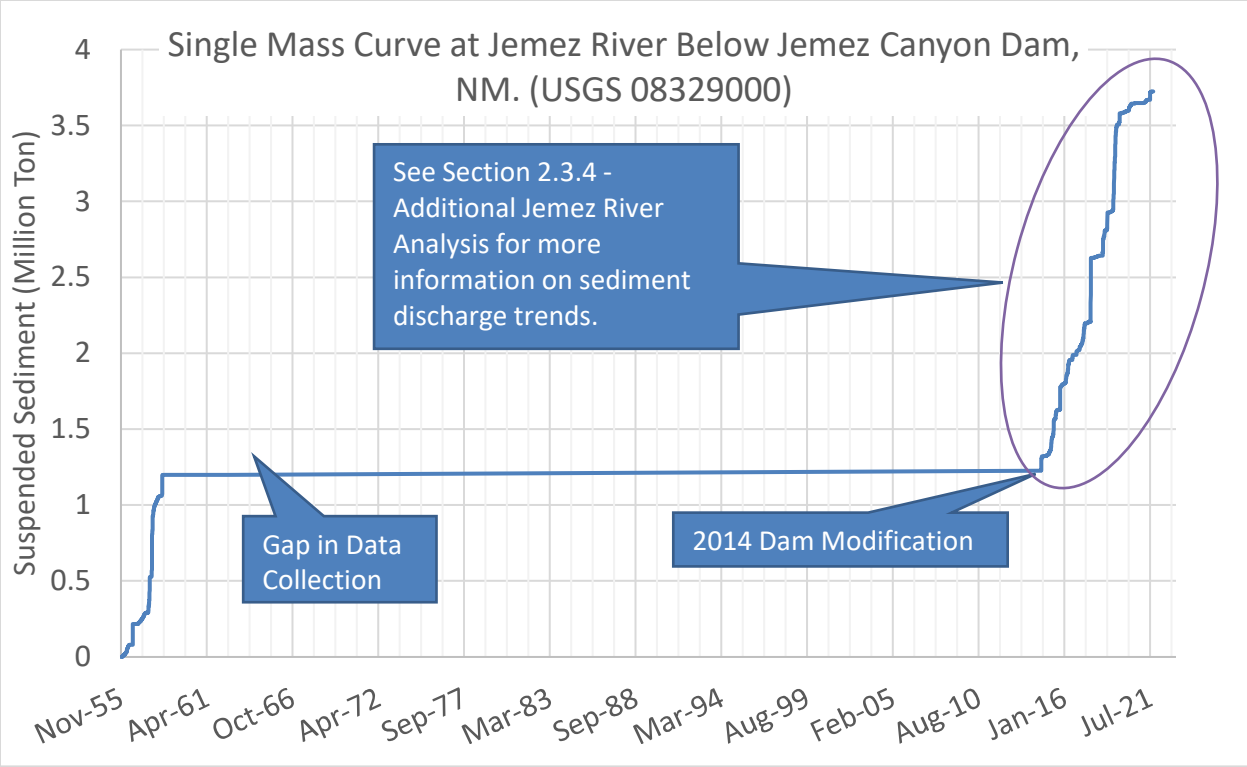

Figure 2-21 Suspended sediment discharge single mass curve for USGS gage 08329000 at Jemez River Below Jemez Canyon Dam, NM

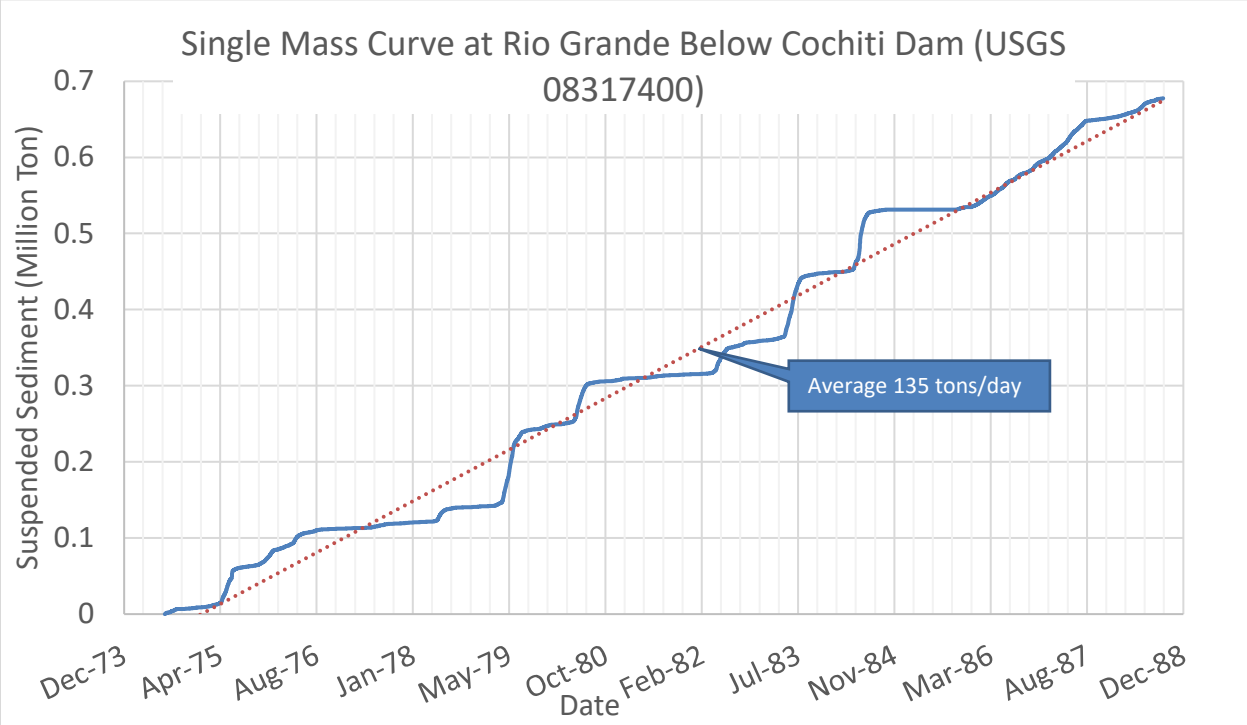

Figure 2-22 Suspended sediment discharge single mass curve for USGS gage 08317400 at Rio Grande Below Cochiti Dam, NM

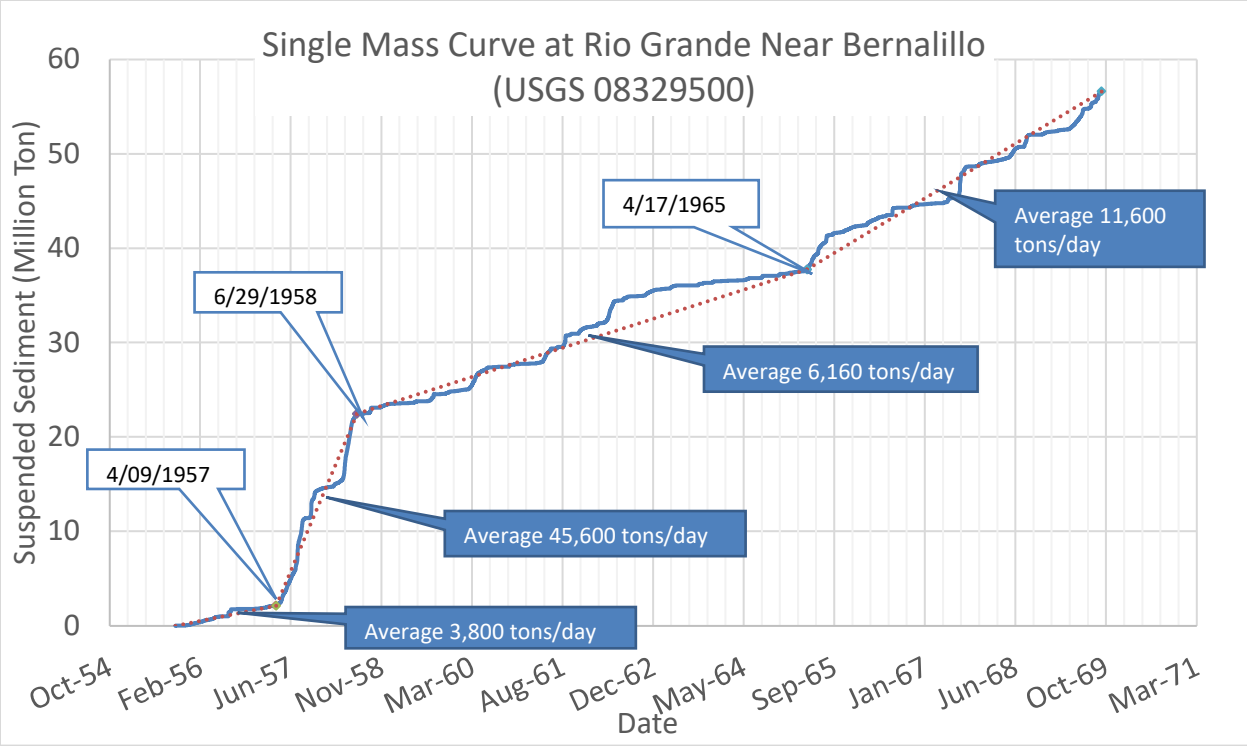

Figure 2-23 Suspended sediment discharge single mass curve for USGS gage 08329500 at Rio Grande Near Bernalillo, NM

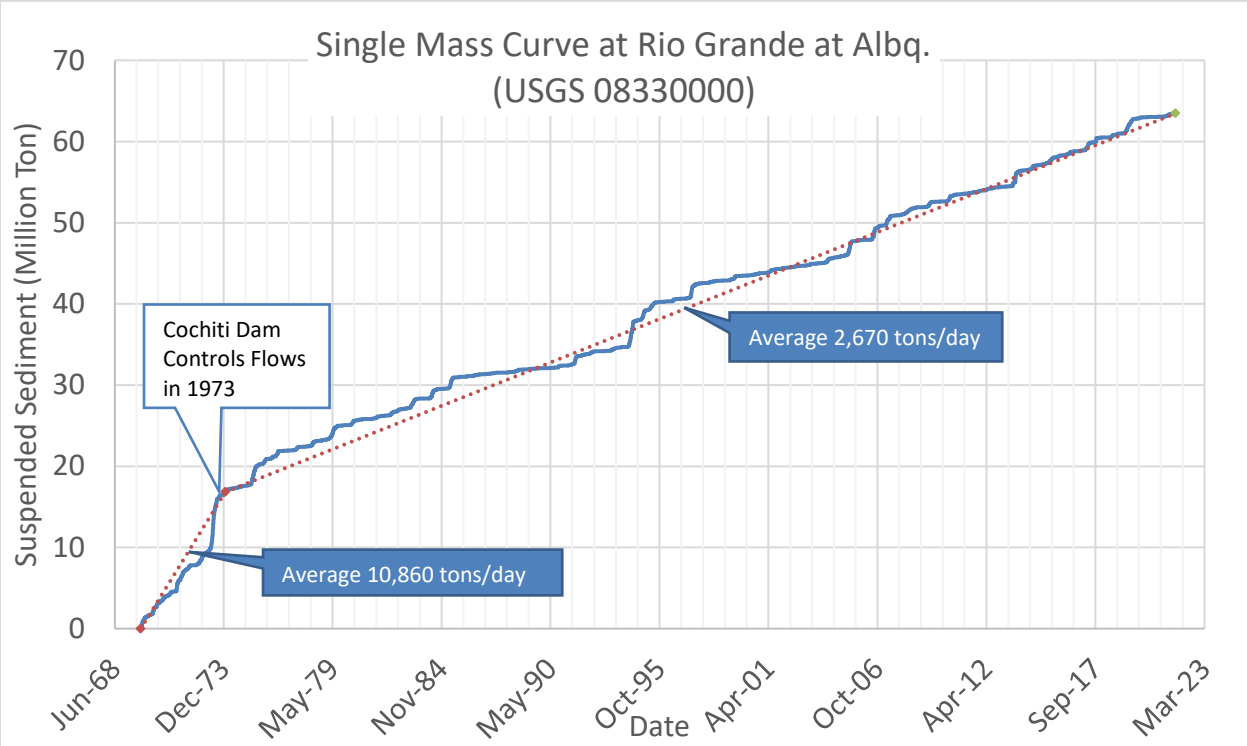

Figure 2-24 Suspended sediment discharge single mass curve for USGS gage 08330000 at Rio Grande at Albq, NM

2.3.2 Double Mass Curve

Double mass curves show how suspended sediment volume relates to the daily discharge volume. The slope of the double mass curve represents the mean sediment concentration. The double mass curve in **Figure 2-25** is for USGS gage Rio Grande at Albuquerque (USGS 08330000).

Figure 2-26 relates the cumulative average monthly suspended sediment at the Rio Grande at Albuquerque (USGS 08330000) gage (located just downstream of Montaño Bridge) to the cumulative precipitation at the Alameda Precipitation gage. The vertical steps show an increase in suspended sediment occurring without an increase in precipitation. The horizontal steps show an increase in precipitation without an increase in suspended sediment. This stair-step trend shows that at most times, there is not a significant correlation between precipitation and suspended sediment. However, there are monsoonal events that impact the suspended sediment in the Bernalillo and Montaño Reaches. The sections of steep slopes between the stair-step pattern indicate an increase in suspended sediment that is correlated with an increase in precipitation. These represent monsoonal events, such as those that occurred in August 2006 and September 2013.

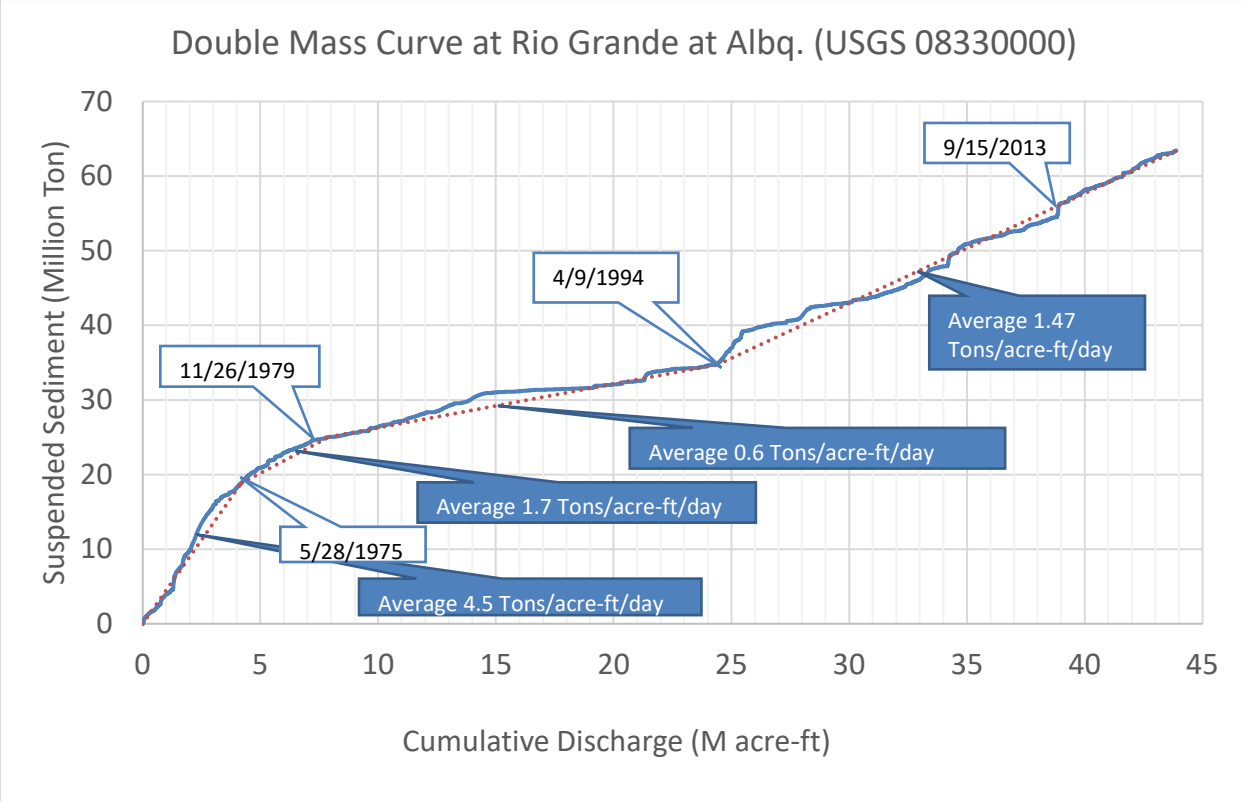

Figure 2-25 Double mass curve for USGS gage 08330000 at Rio Grande Near Albuquerque, NM

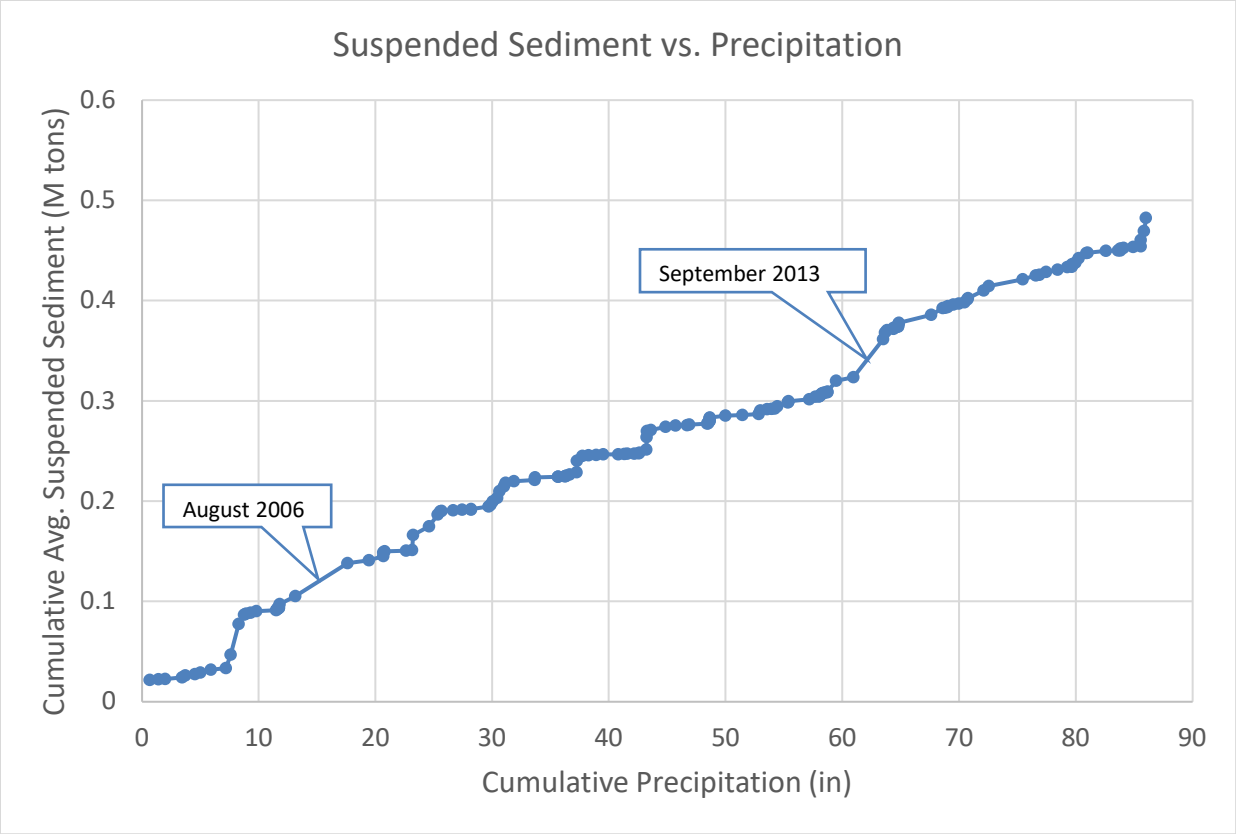

Figure 2-26 Cumulative suspended sediment (data from the Rio Grande at Albuquerque (USGS 08330000) gage) versus cumulative precipitation at the Alameda gage.

2.3.3 Monthly Sediment Variation

Plots of monthly average discharge and suspended sediment were created for the Jemez River (USGS 08329000), Rio Grande Below Cochiti (USGS 08317400), Rio Grande Near Bernalillo (USGS 08329500), and Rio Grande at Albuquerque (USGS 08330000) gages are shown in **Figure 2-27** to **Figure 2-34**, to help reveal any important seasonal trends. These figures show the seasonal trends of suspended sediment load and concentration, respectively, along with the discharges that correspond with the years. The spring snowmelt brings some of the larger flow rates associated with the larger quantities of sediment. However, the increased flows from the monsoonal storm events in the summer months were associated with the higher spikes in sediment concentration. There also peaks in suspended sediment from flood events that occurred prior to the construction of Cochiti Dam and from the 2013 flood. As shown in the figures below, a majority of the sediment flux is occurring during spring runoff associated with seasonal snowmelt in the region. Monsoonal events affect the sediment flux but are not the driving force for sediment movement in the Bernalillo and Montano Reaches of the MRG.

The primary sediment input into the MRG through the Bernalillo and Montano reaches is due to ephemeral tributaries (Fitzner 2018). The spring runoff brings sediment from these tributaries into the MRG. However, the sediment load at the Rio Grande Below Cochiti (USGS 08317400) shows the sediment being in phase with the flow and relatively lower sediment discharges and concentrations compared to the other gages. There are no uncontrolled ephemeral tributaries upstream of Cochiti, so the sediment and flow from Cochiti are both controlled by dam releases.

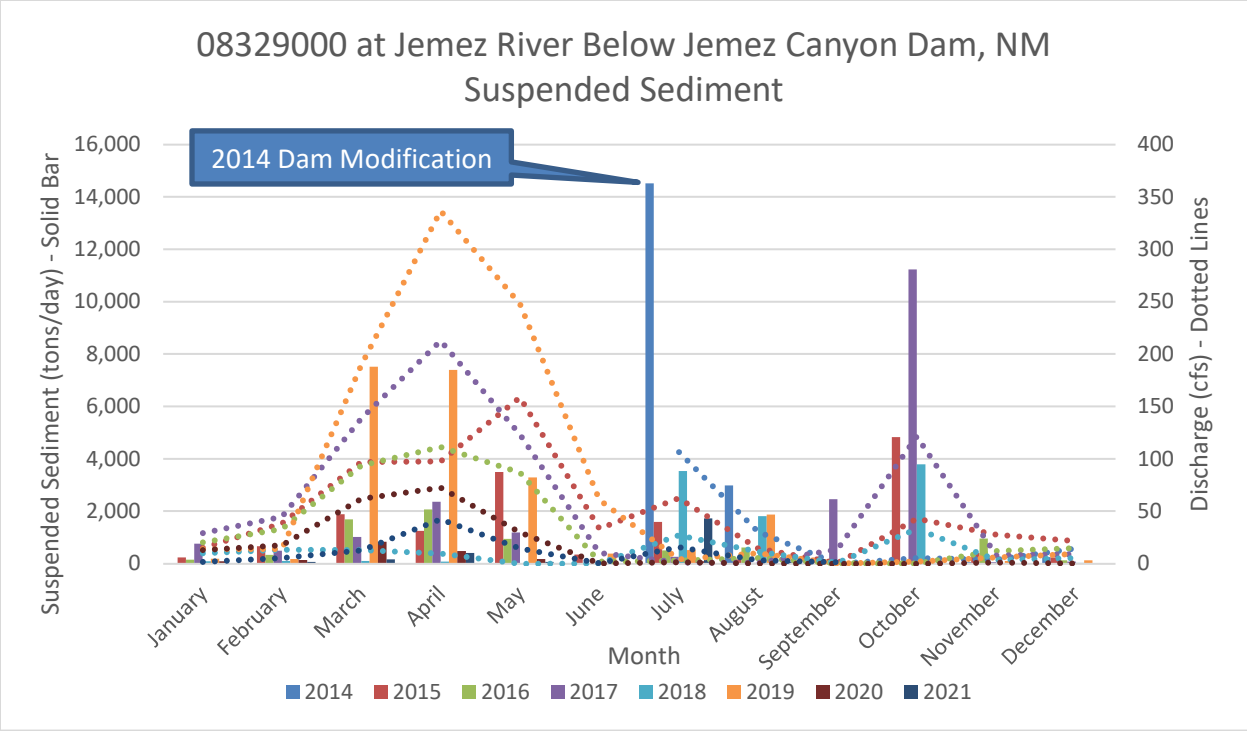

Figure 2-27 Monthly average suspended sediment and water discharge at USGS gage 08329000 at Jemez River Below Jemez Canyon Dam, NM

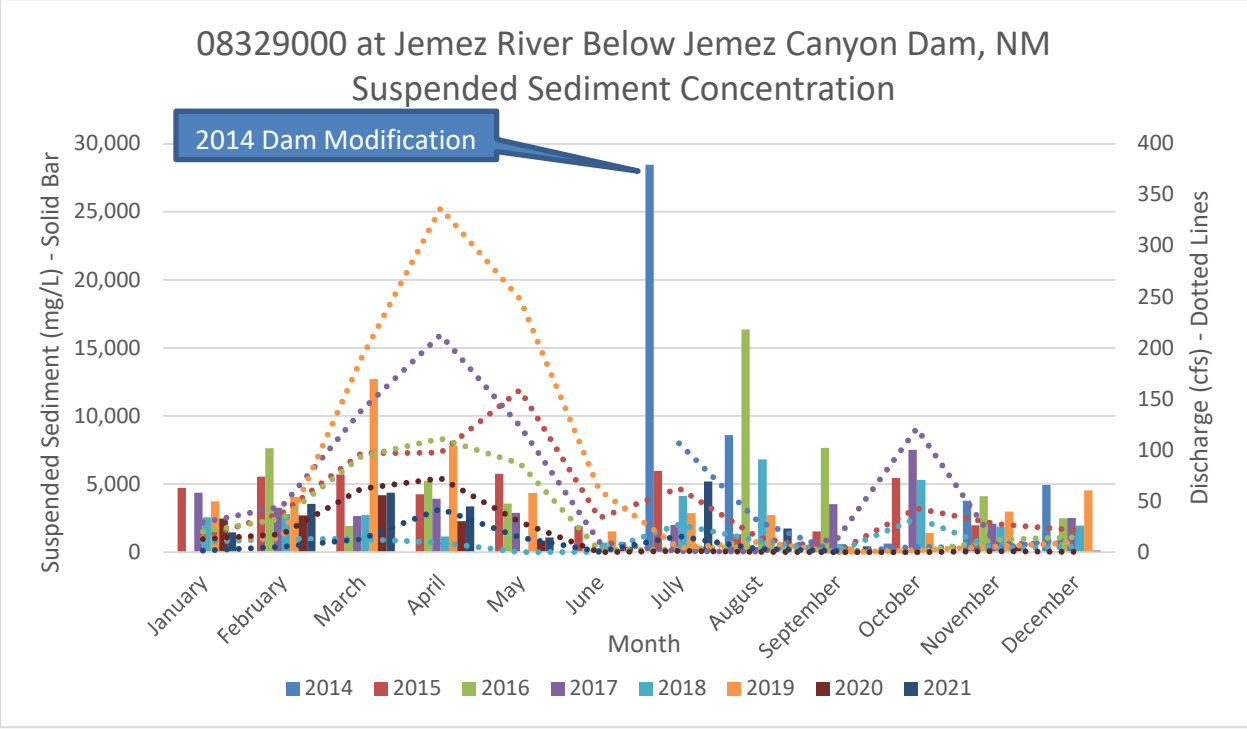

Figure 2-28 Monthly average suspended sediment concentration and water discharge at USGS gage 08329000 at Jemez River Below Jemez Canyon Dam, NM

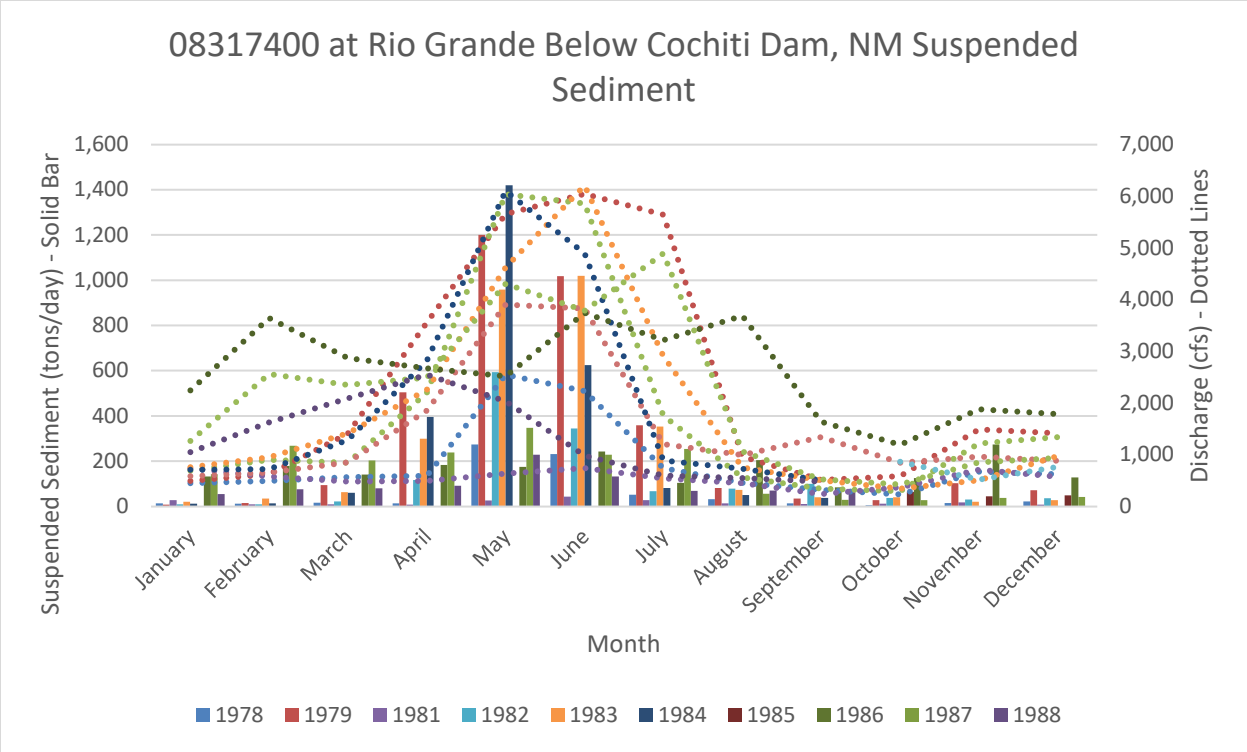

Figure 2-29 Monthly average suspended sediment and water discharge at USGS gage 08317400 at Rio Grande Below Cochiti Dam, NM

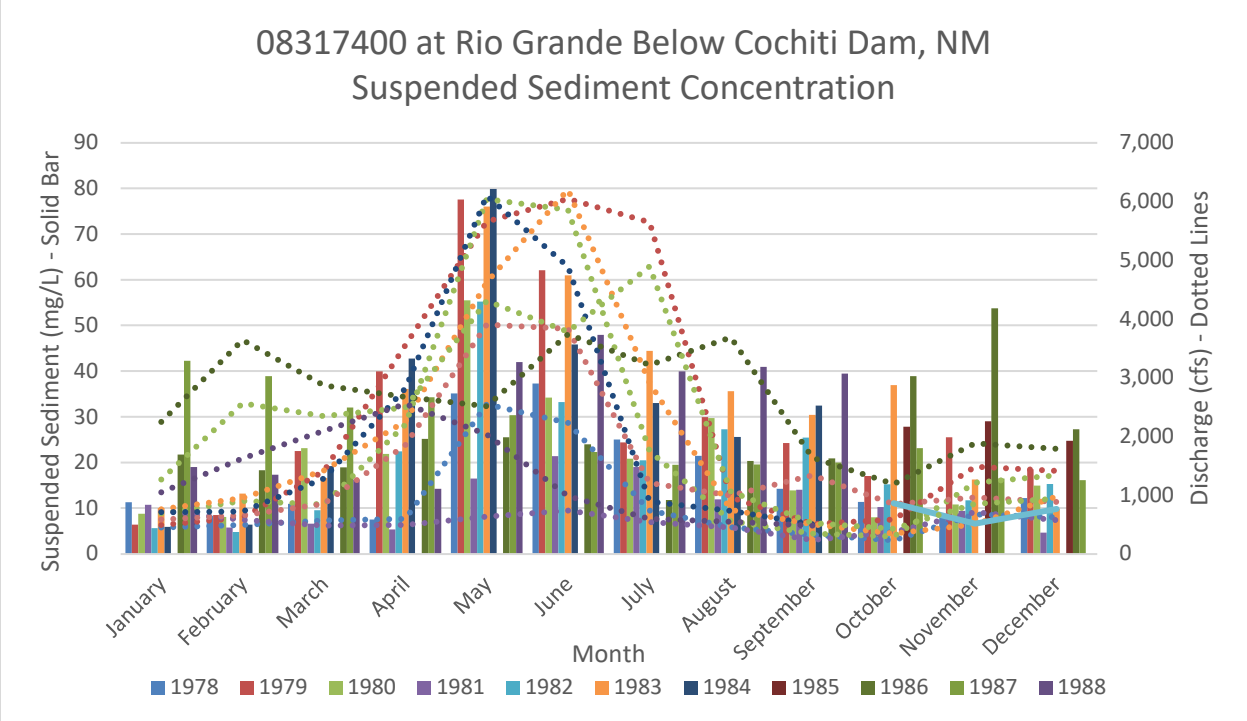

Figure 2-30 Monthly average suspended sediment concentration and water discharge at USGS gage 08317400 at Rio Grande Below Cochiti Dam, NM

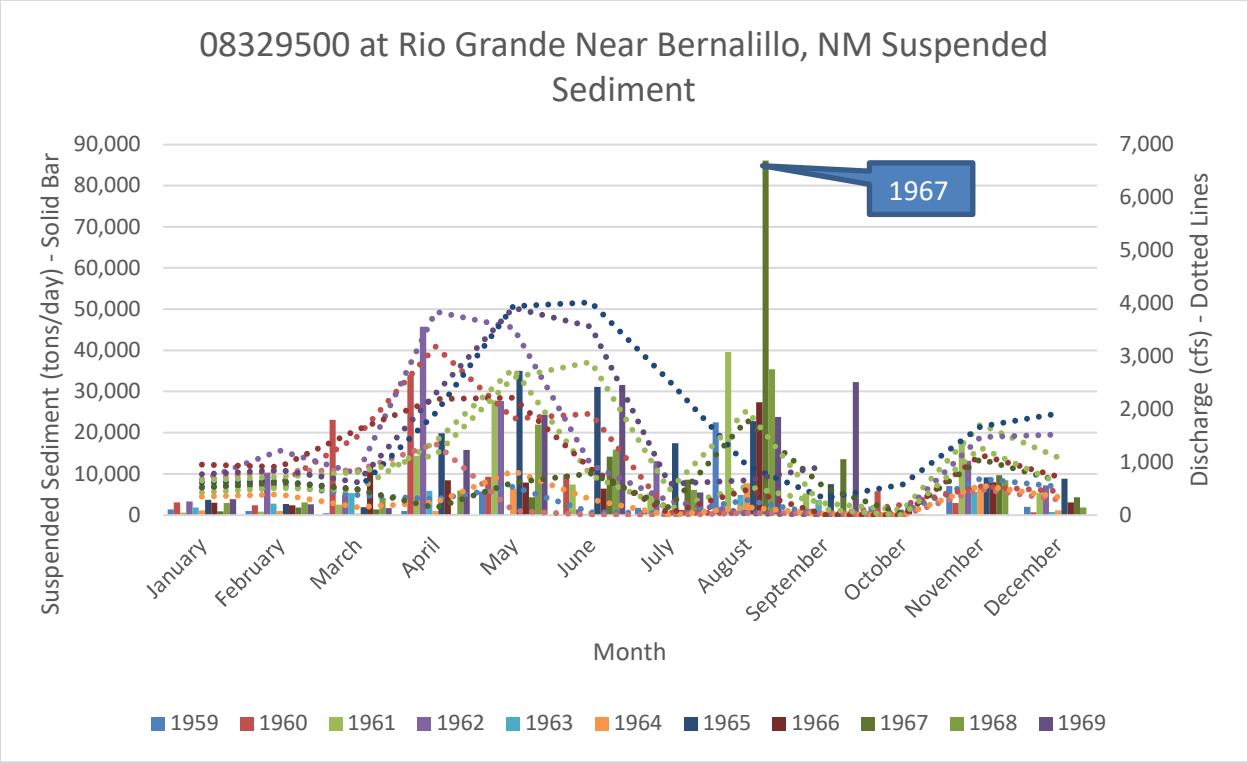

Figure 2-31 Monthly average suspended sediment and water discharge at USGS gage 08329500 at Rio Grande Near Bernalillo, NM

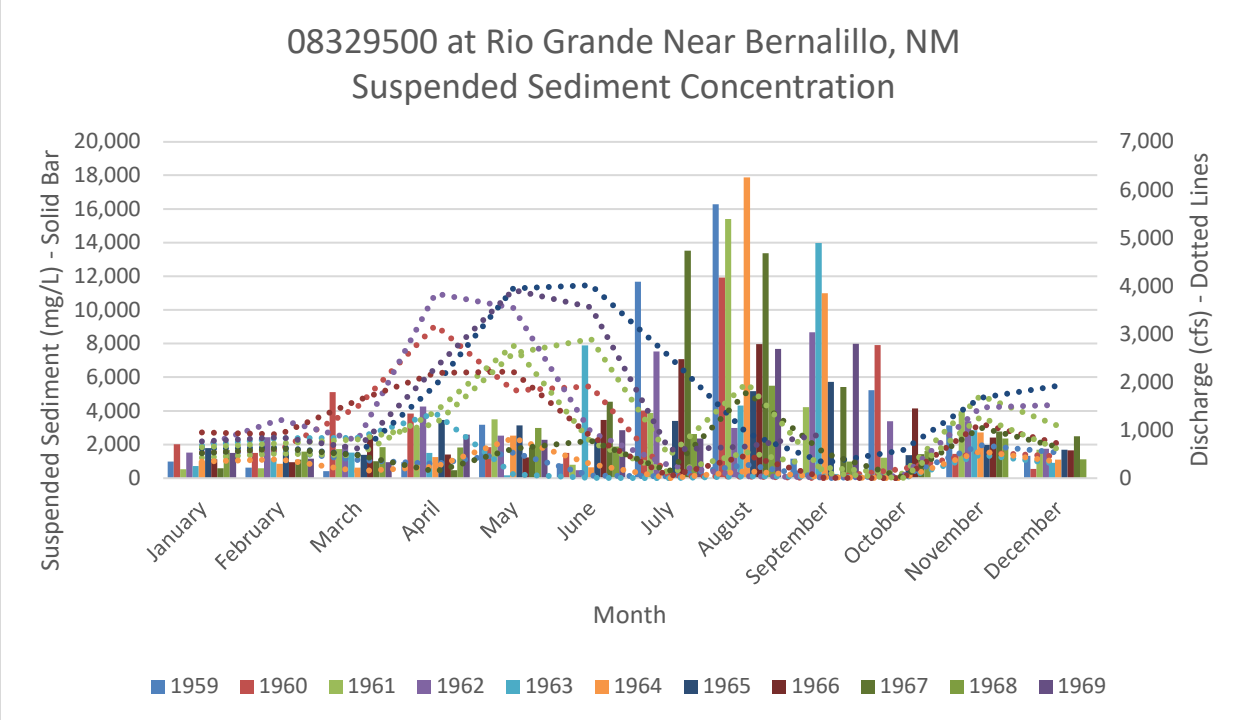

Figure 2-32 Monthly average suspended sediment concentration and water discharge at USGS gage 08329500 at Rio Grande Near Bernalillo, NM

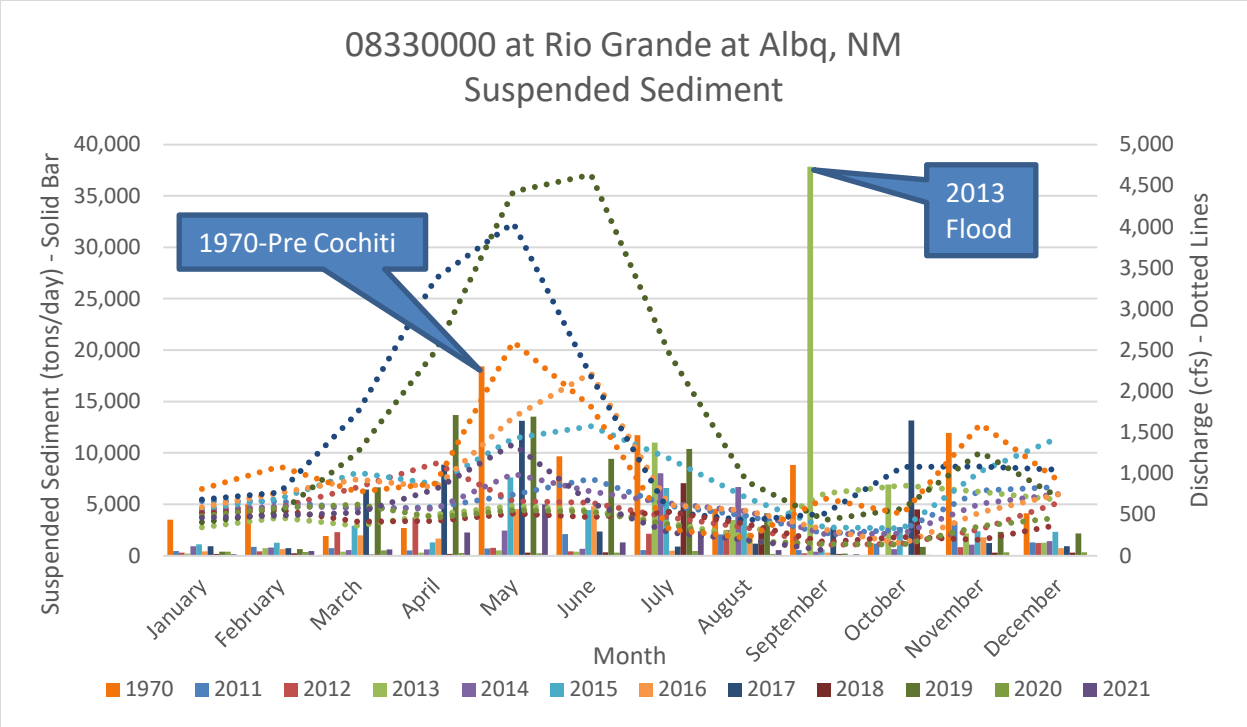

Figure 2-33 Monthly average suspended sediment and water discharge at USGS gage 08330000 at Rio Grande at Albq, NM

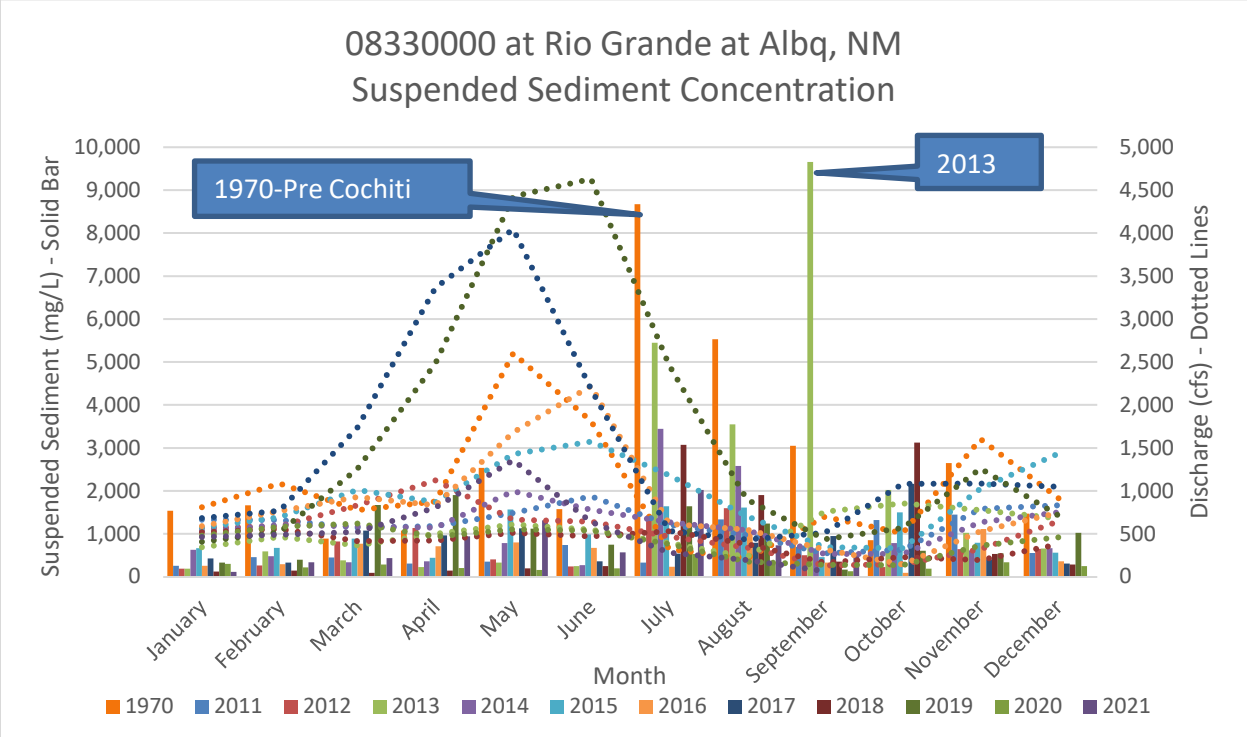

Figure 2-34 Monthly average suspended sediment concentration and water discharge at USGS gage 08330000 at Rio Grande at Albq, NM

2.3.4 Additional Jemez River Analysis

The Jemez River is a major tributary of the Bernalillo and Montaño reaches. The Jemez Dam was constructed in 1953. Sediment data was not collected prior to the construction of the dam. In 2014, the Jemez Dam underwent a modification that included a low flow channel. This modification and the subsequent effects on the suspended sediment were analyzed. **Figure 2-35** and **Figure 2-36** below show the single mass curves before and after the dam modification. It is important to note that there was a gap in sediment data collection between the years 1958-2014. It should be noted that while this analysis provides some insight into the sediment and flow characteristics for the Jemez River, the gaps in sediment data and the limited 7 years of record following modification of the Jemez Dam make it difficult to draw any definitive conclusions regarding impacts of the modification at this time.

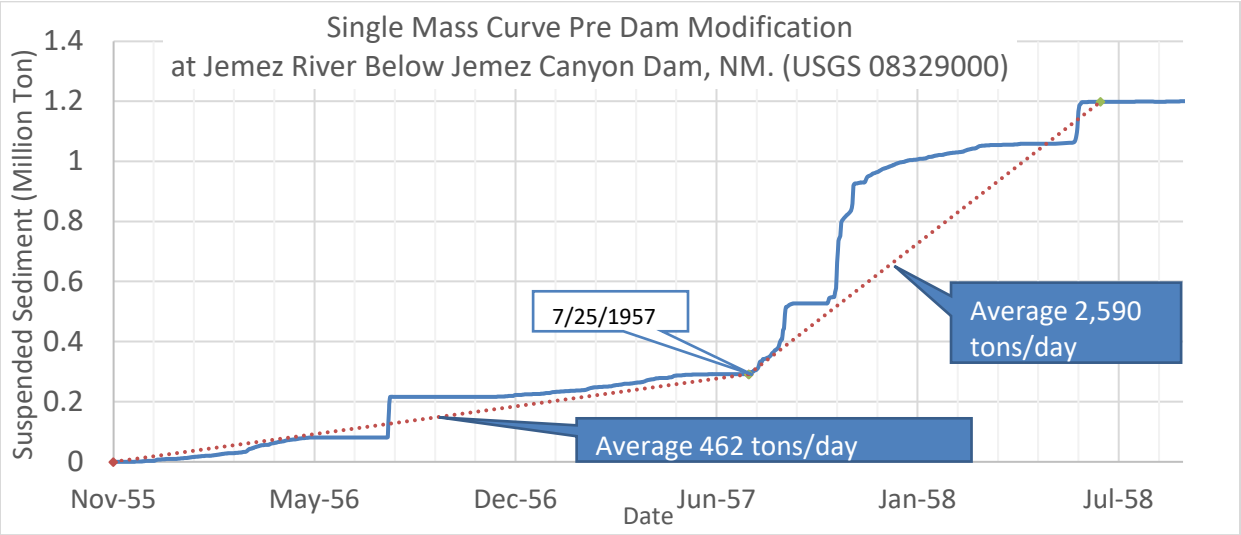

Figure 2-35 Suspended sediment discharge single mass curve for USGS gage 08329000 at Jemez River Below Jemez Canyon Dam, NM – Pre-Dam Modification

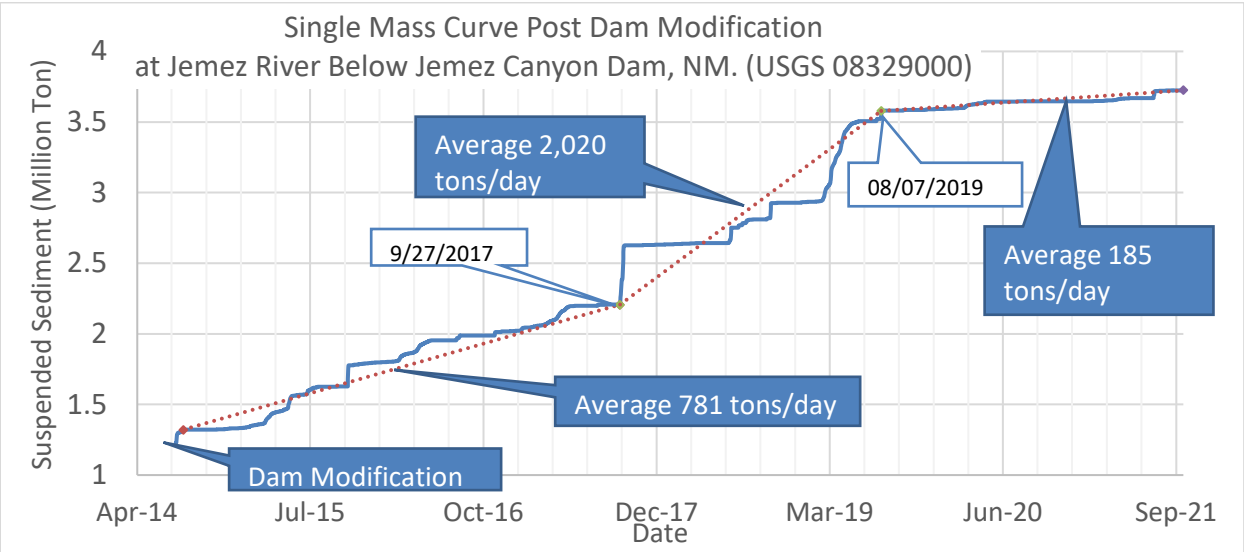

Figure 2-36 Suspended sediment discharge single mass curve for USGS gage 08329000 at Jemez River Below Jemez Canyon Dam, NM – Post-Dam Modification

The flow and sediment budget for the Middle Rio Grande through the Bernalillo and Montaño Reaches is dependent on the flow and suspended sediment coming from the Jemez River, from downstream of the Cochiti Dam, and from other sources such as ephemeral tributaries and channel erosion.

A flow budget, shown in **Figure 2-37** was determined using the gages at the outlet of the Jemez River (historical USGS Gage 08329000 and USGS Gage 08328950) along with either the Bernalillo (USGS Gage 08329500) or the Albuquerque (USGS Gage 08330000) gages located downstream of the outlet, depending on the year and data availability. The gage record was analyzed for the years of overlapping gage record between the Jemez River and the Rio Grande gages between 1944 and 2021. The Jemez contributed a total of 4% of the flow to the Bernalillo and Montaño reaches each year. The Jemez River flow contribution varied between 1.7% and 10.5%, depending on the year. The year 2021 saw the lowest contribution of flow, at 1.7%, while 1961 saw the highest contribution to flow of 10.5%.

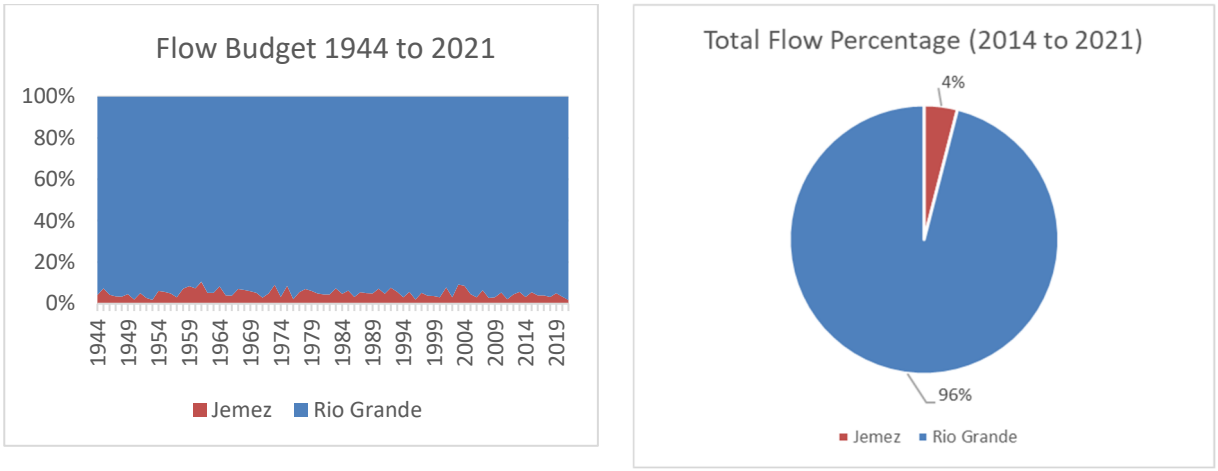

Figure 2-37 Flow Budget through the years between 1944 and 2021 (left) and total flow percentage between 2014 and 2021 (right) for the Jemez River at the Outlet and Rio Grande at Bernalillo and Albuquerque.

The slope of the single mass curves presented in this section and **Section 2.3.1**, provide average sediment discharges in tons/day for certain periods of time. The sediment budget was calculated for each year by using the average sediment discharges. The total sediment budget was approximated from either USGS Gage 08329500 at Rio Grande Near Bernalillo, NM or USGS Gage 08330000 at Rio Grande at Albuquerque, NM, since the two gages do not overlap available data and represent the furthest downstream gage, depending on the year and available data. An average sediment discharge rate from the Jemez and Cochiti gages was calculated from the slopes of the single mass curves. For the time periods past the available gage data at Cochiti, the same rate from the single mass curve of available data was used because the suspended sediment was consistent over time. **Figure 2-38** below shows sediment budgets for 1958 (pre-Jemez Dam modification), 2014 (the year the Jemez Dam modification was completed), and 2021 (post-Jemez Dam modification). The 1958 sediment budget does not include sediment from downstream of the Cochiti because the Cochiti Dam was not constructed then.

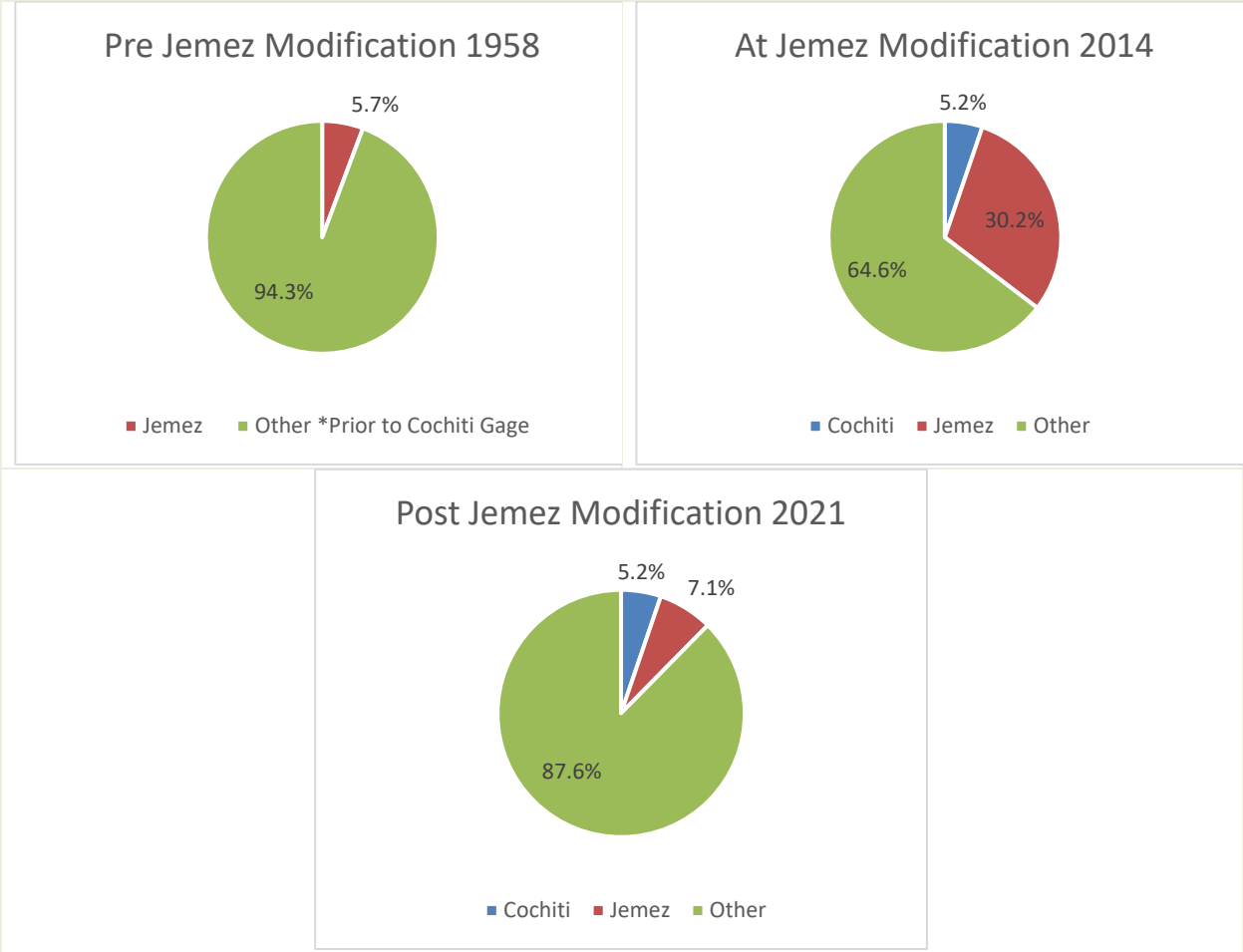

Figure 2-38 Sediment budgets pre-, at-, and post- Jemez Dam modification

Figure 2-39 below shows the average sediment budget for each year from 2014 to 2021 compared to the average sediment budget before the Cochiti Dam was constructed (1955 to 1973). The purpose is to show how the fraction of sediment contribution coming from the Jemez River changed after the construction of Cochiti Dam. The results showed that the percentage of sediment coming from the Jemez was significant in between 2014 and 2017, spiked in 2018 and 2019, and receded significantly in 2020 and 2021. The spike in sediment contribution between 2014 and 2019 may have been from release of sediment that had been held behind the dam that now can now move downstream. In general, the Jemez dam provided less sediment to the overall budget seen in Albuquerque before Cochiti Dam construction. This further illustrates that the construction of Cochiti Dam lowered the amount of sediment going through the reach between the Cochiti Dam location and the Jemez River tributary. **Figure 2-39** below also shows a spike in the Jemez River average sediment budget in 2018 and 2019 which could be due to some peak flow events that occurred during those times.

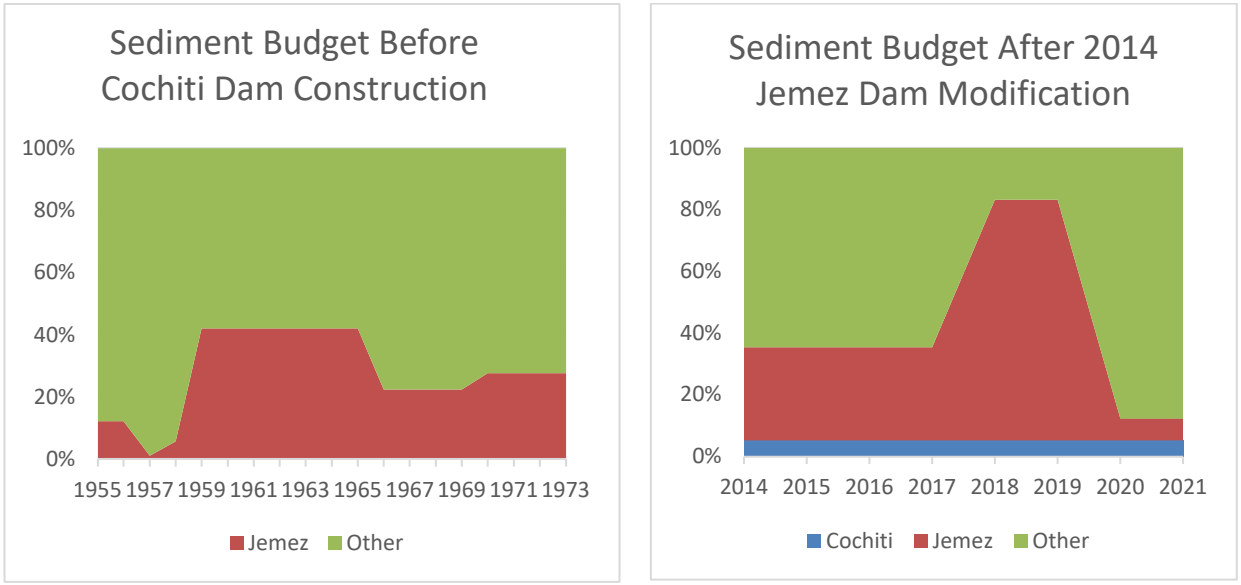

Figure 2-39 Average sediment budget comparison – before Cochiti Dam construction (left) and after Jemez Dam modification (right)

To better understand the sediment sources for the years since the Jemez Dam Modification, a total sediment budget by volume for the years 2014 through 2021 was created. Based on available data, the average daily sediment volume in tons was summed from July 30th, 2014 to September 30th, 2021. Similar to the average sediment budget analysis above, there was not sediment data for USGS Gage 08317400 at Rio Grande Below Cochiti Dam for the years 2014 to 2021. However, the average sediment budget of 135 tons/day (taken from the slope of the single mass curve) was used over the time period analyzed. **Figure 2-40** below shows the results. The Jemez River accounts for nearly 40% of the total volume during 2014 to 2021.

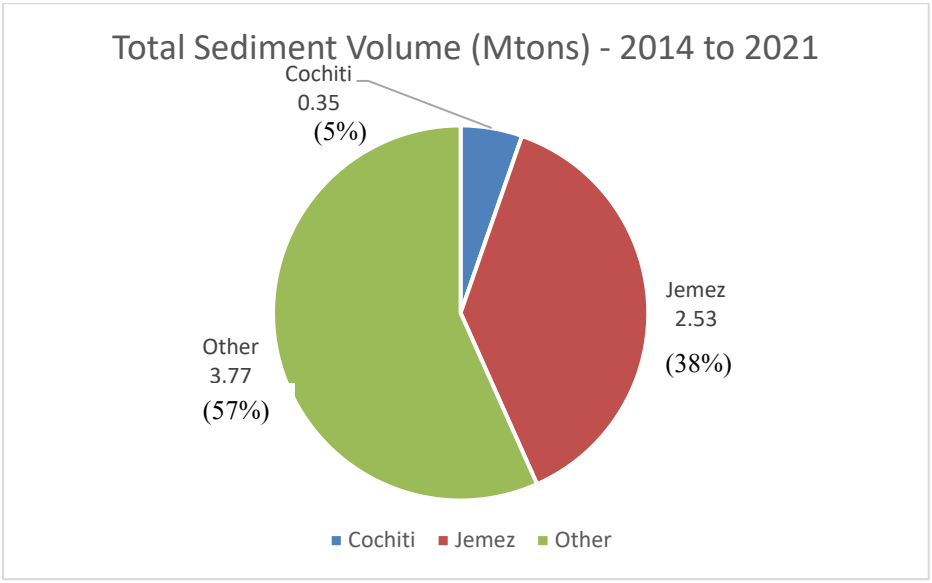

Figure 2-40 Total sediment volume budget in million tons at the USGS Gage 08330000 at Rio Grande at Albuquerque, NM from 2014 to 2021.

3 River Geomorphology

3.1 Wetted Top Width

Wetted top width can provide significant insight into hydraulic geometry. Typically, wetted top width in a compound trapezoidal channel would slowly increase as discharge values increase until there is a connection with the floodplain. At this point, the top wetted width would quickly increase as the water spills onto the floodplains. Then, a gradual increase in width would continue after this point. Analysis of the wetted top width can be used to help understand bankfull conditions and how they vary spatially and temporally in the Bernalillo Reach. A HEC-RAS model was created to analyze a variety of top width metrics. As discussed in **Section 4.1.1**, computational levees were used in HEC-RAS geometries for 1962 and 1972 and ineffective flow areas were used in the 2012 geometry to keep the water contained in the channel until bankfull is reached. An increment of 500 cfs up to 10,000 cfs was used in the top width analysis for the years with available data: 1962, 1972, 1992, 2002 and 2012.

Based on the analysis, Subreaches B1, B2, and B3 have experienced the most dramatic change in top width. Majority of the B1, B2, and B3 subreaches have shown a trend of narrowing since 1972. Subreach B4 has also shown a trend of narrowing over time, but at a smaller scale. Widening of the channel occurred throughout most of the Bernalillo Reach between 1962 and 1972. This widening could be a result of the large sediment discharge events that occurred post-1962 that caused aggradation of the channel. See **Section 2.3** for more detail on the sediment trends see in the Bernalillo Reach. The aggradation caused the channel invert to rise and the active top width to increase. Lateral bank erosion due to higher flow discharges could also be aiding in the channel widening. Post 1972, as a result of the construction of Cochiti Dam in 1973, the sediment supply was smaller in magnitude and the channel generally experienced degradation and narrowed active top widths. Between 2002 and 2012, effects from the AMAFCA North Diversion Channel can be seen. The AMAFCA North Diversion Channel outfall is located at the downstream end of Subreach B2. It acts as a grade control and is likely responsible for the slope stability throughout time as shown in Subreach B2. The sediment load from this tributary helps maintain a wide channel and nearby islands by helping control the aggradation/degradation trends seen in Subreach B3. See Section 3.3 for the aggradation/degradation analysis of the Bernalillo Reach. In addition, the width changes seen from 2002 and 2012 is thought to be also influenced by introduction of more flows during the summer months for RGSM which, in effect, has irrigated the bosque leading to woody vegetation growth that has narrowed the channel (Baird pers. Con. 2023). Additional figures from this analysis can be found in **Appendix C**, including plots with the corresponding top width for each agg/deg line rather than the moving average.

Figure 3-1 shows the moving cross sectional averaged top wetted width at 1,000 from the HEC-RAS model results. The moving cross sectional averaged width at each section is calculated by averaging the width for five cross sections at a time. These five cross sections include the cross section, two sections upstream, and the two sections downstream. The top width shown at each agg/deg line comes from the moving average from five consecutive cross sections: the identified agg/deg line, two upstream agg/deg lines, and two downstream agg/deg lines.

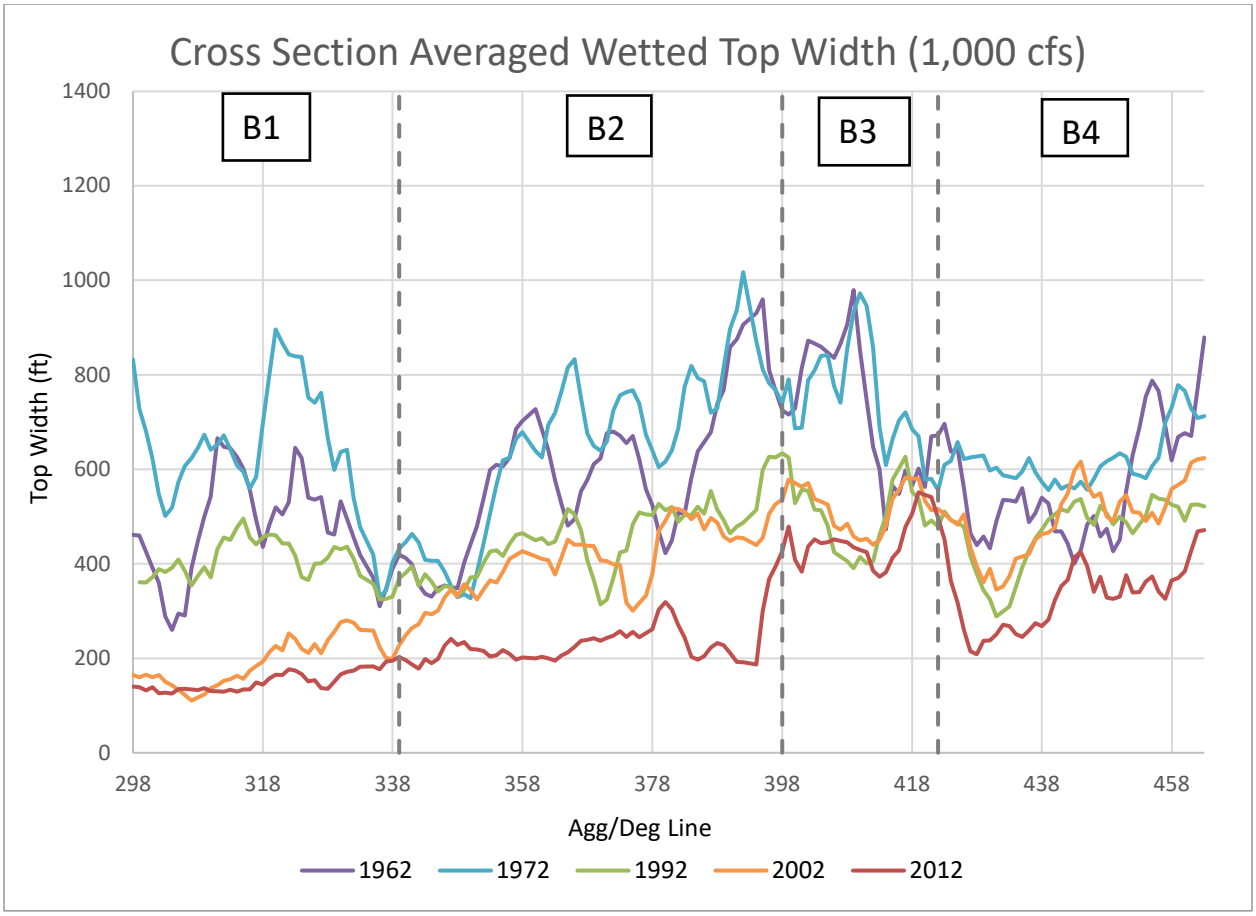

Figure 3-1 Moving cross-sectional average of the wetted top width at a discharge of 1,000 cfs.

Figure 3-2 shows the moving cross sectional averaged top wetted width at 3,000 cfs from the HEC-RAS model results. The channel width decreased dramatically in 1992 compared to 1962 and 1972. In the subsequent years at flow of 3,000 cfs, there is a steady decrease in top width in Subreaches B1 and B2. Subreaches B3 and B4 show a small decrease in top width. This is a similar trend when compared to the 1,000 cfs flow. This indicates that the floodplain might not be utilized and filled at 3,000 cfs.

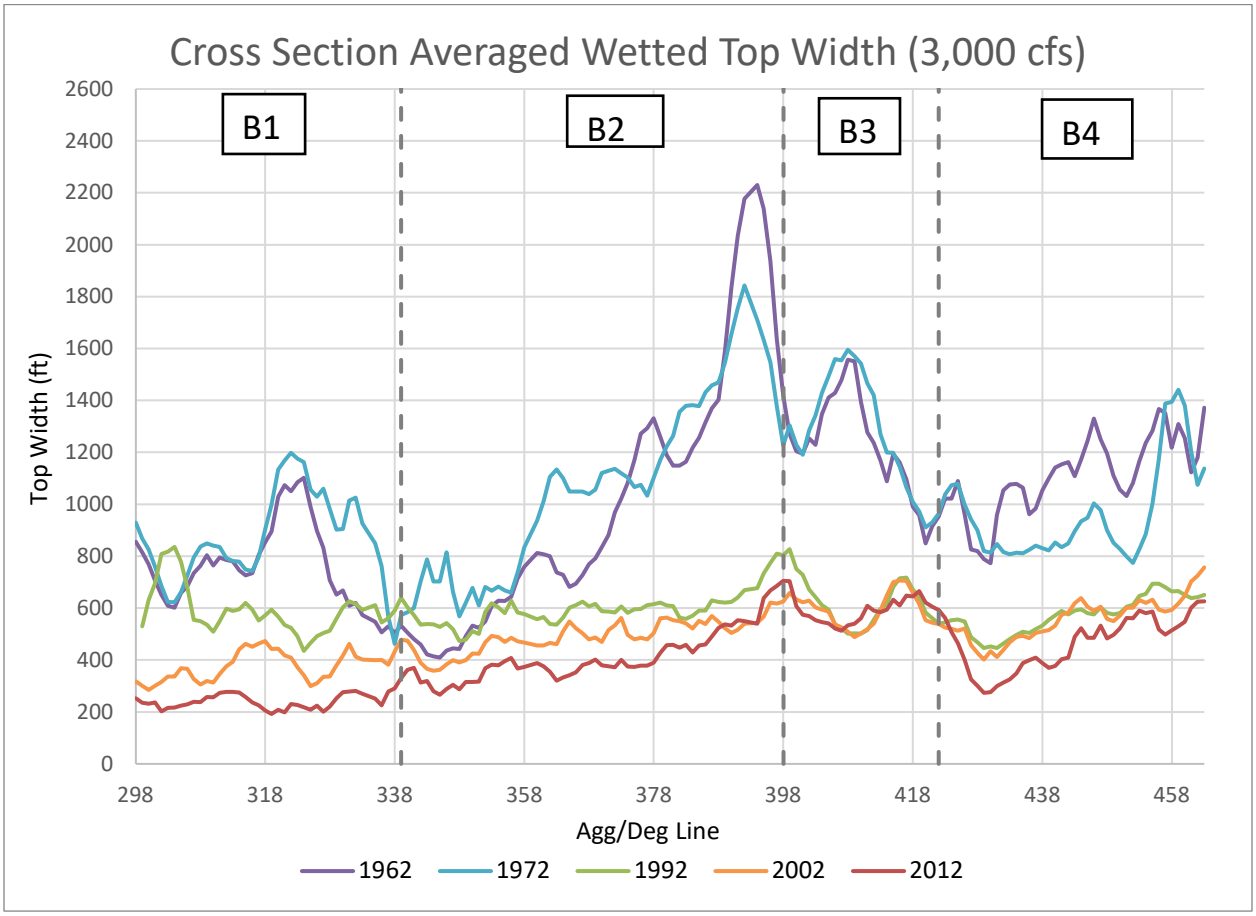

Figure 3-2 Moving cross-sectional average of the wetted top width at a discharge of 3,000 cfs.

Figure 3-3 shows the moving cross sectional averaged wetted top width at 5,000 cfs. The top width is fairly consistent from 1962 and 1972 in all of the subreaches. The top width generally decreases from 1972 to 2012, however, there are some locations within the reaches that have seen spikes in the top width. These spikes could indications sections of the channel are transiting from bankfull to the floodplain at 5,000 cfs.

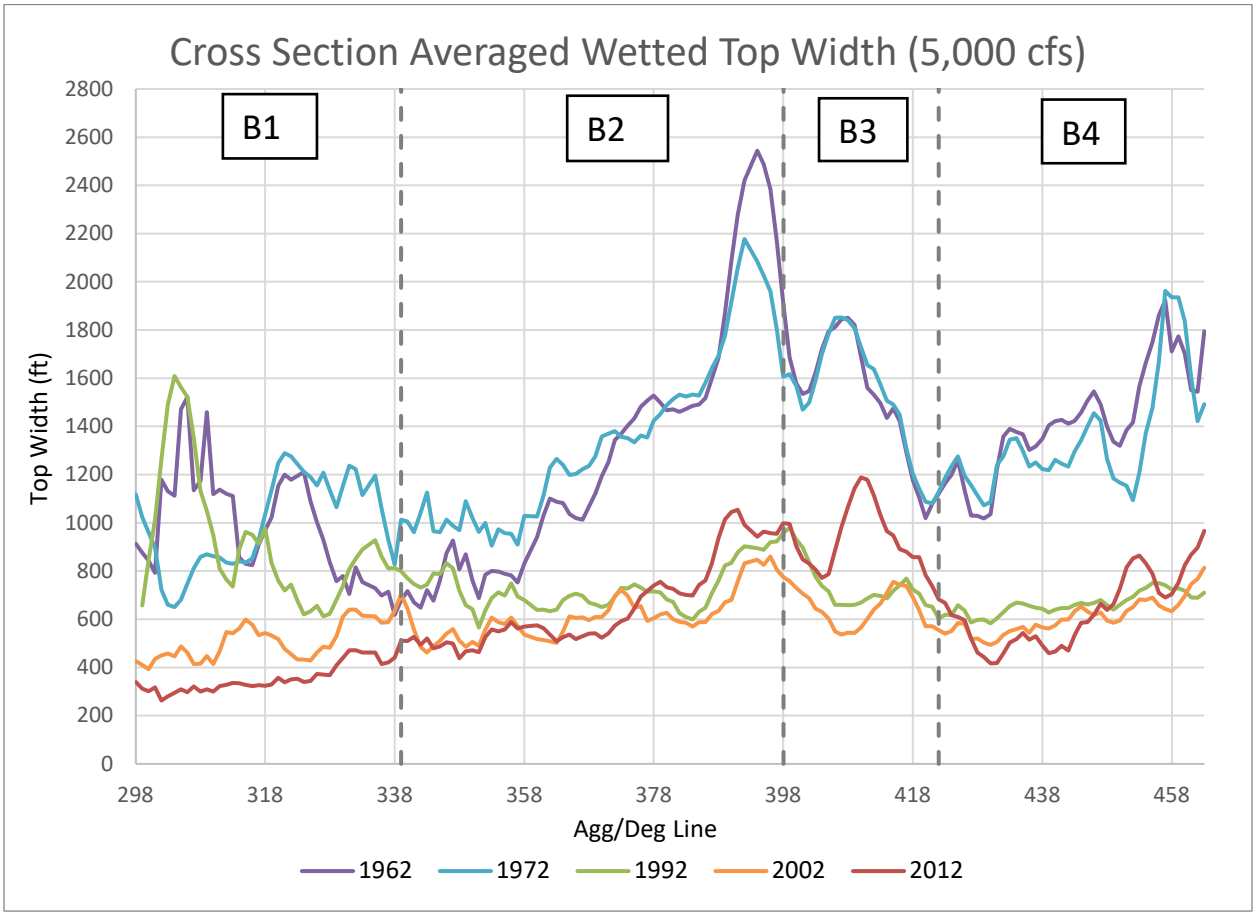

Figure 3-3 Moving cross-sectional average of the wetted top width at a discharge of 5,000 cfs.

Figure 3-4 to Figure 3-6 show the cumulative top width of the wetted cross sections. The cumulative width shows how the width through time varies within each subreach. In general, 1972 had the largest channel widths. As previously discussed, the increase in channel widths from 1962 to 1972 is due to aggradation and potential lateral bank erosion. Then in 1992 the channel is significantly narrower due to the impacts of Cochiti Dam. In 2012, the cumulative top width crosses the 2002 cumulative top width line in Subreach B3, indicating an increase in top width during that time frame. The AMAFCA North Diversion Channel outfall provides an increase in sediment load and islands are located in the vicinity as well. A combination of the additional islands, increase in sediment load, and the temporary backwatering impact of the ABCWUA adjustable height dam, could be the reasons why there are increases in top width from 2002 to 2012. The discussed channel characteristics are further corroborated in **Section 3.2 and 3.3**.

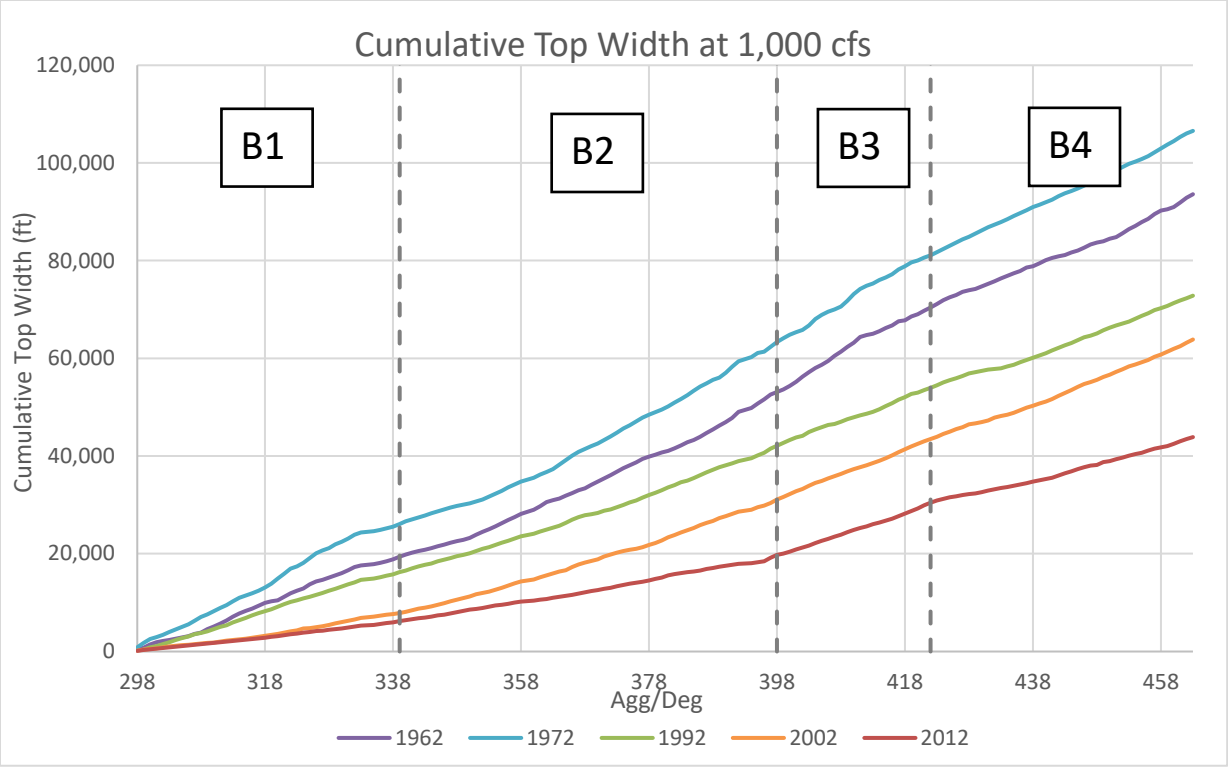

Figure 3-4 Cumulative top width at a discharge of 1,000 cfs.

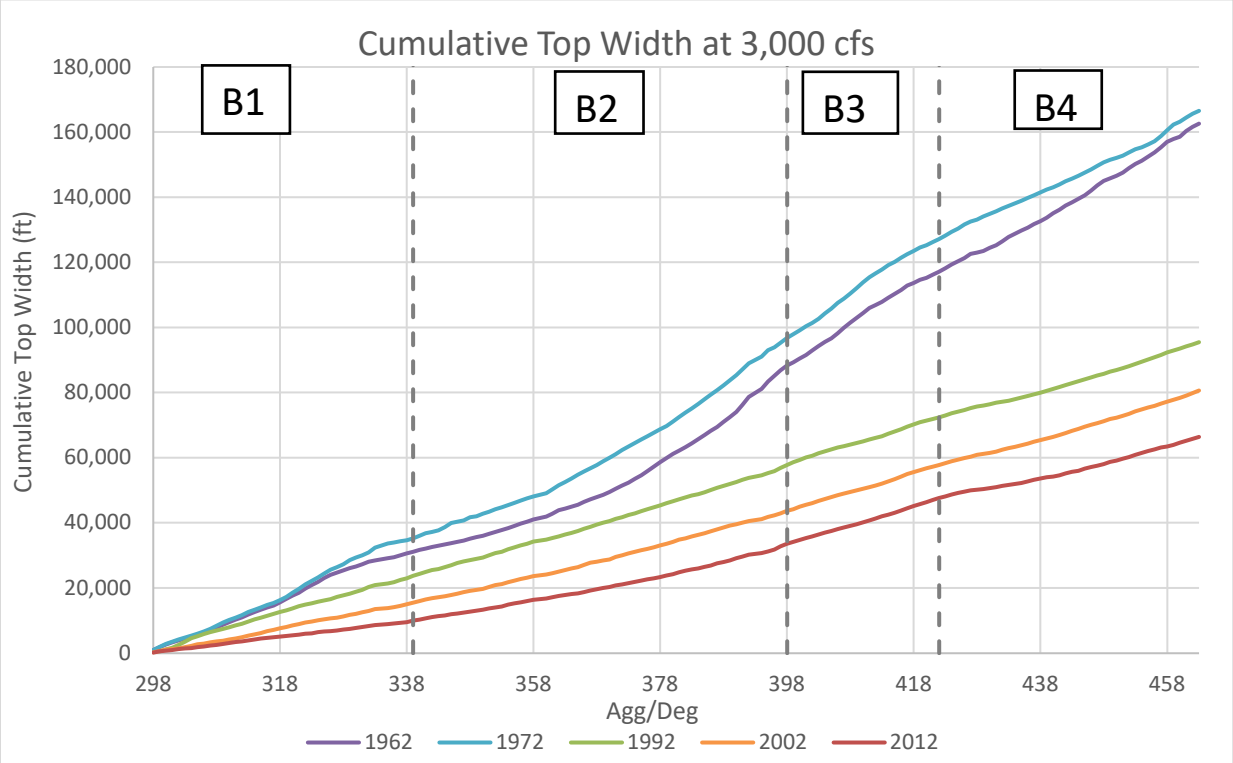

Figure 3-5 Cumulative top width at a discharge of 3,000 cfs.

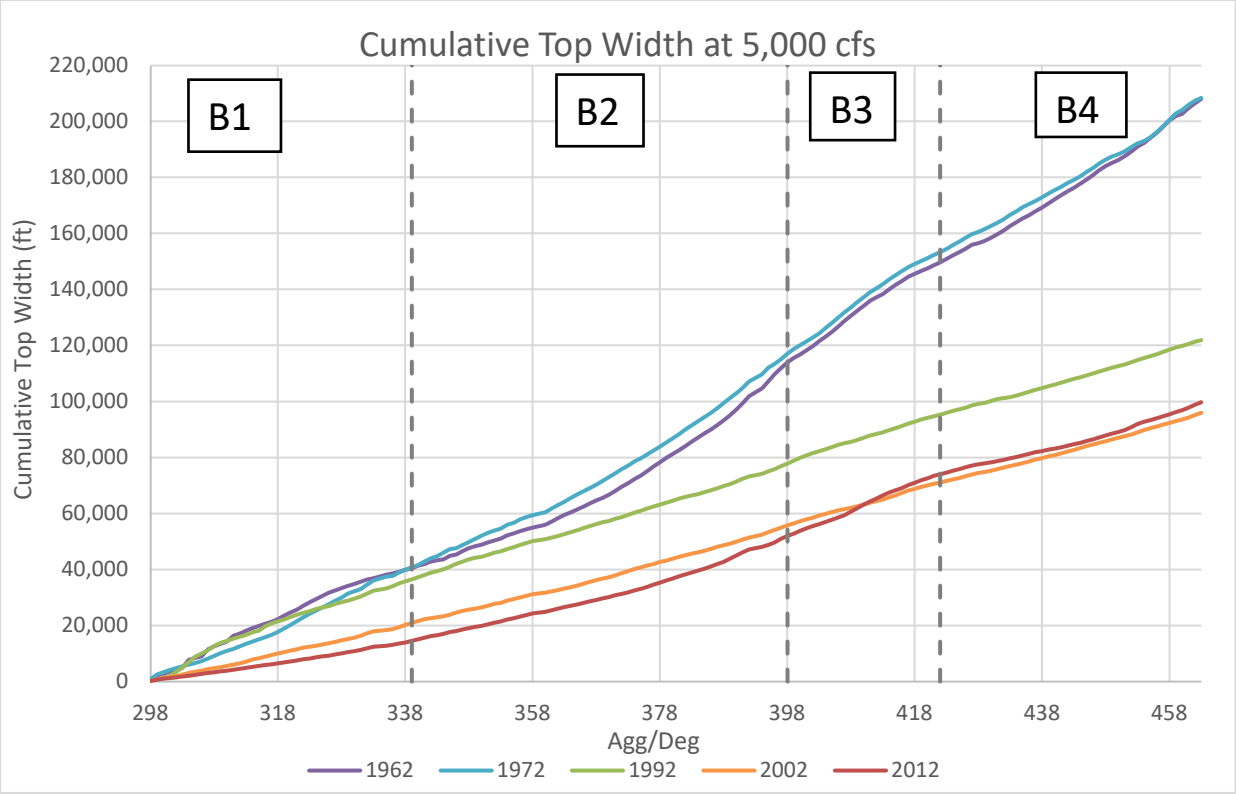

Figure 3-6 Cumulative top width at a discharge of 5,000 cfs.

The average top width for each subreach was also plotted for the years analyzed in **Figure 3-7** for discharges up to 10,000 cfs. From 1962 to 1972, the average top width for almost all of the subreaches increased. Then, from 1972 to 1992, there was a dramatic decrease in top width generally for all subreaches due to the impacts of the Cochiti Dam construction. The average top width for all reaches generally decreased between 1992 and 2012 showing narrowing of the channel. However, as previously discussed, the impacts of the AMAFCA North Diversion outfall and the temporary impacts of the ABCWUA Adjustable Height Dam resulting in an increase in top width in B2, B3, and B4 from 2002 to 2012. Subreaches B1, B2, B3 and B4 show a large range of top width changes throughout the years of widening then narrowing of the channel.

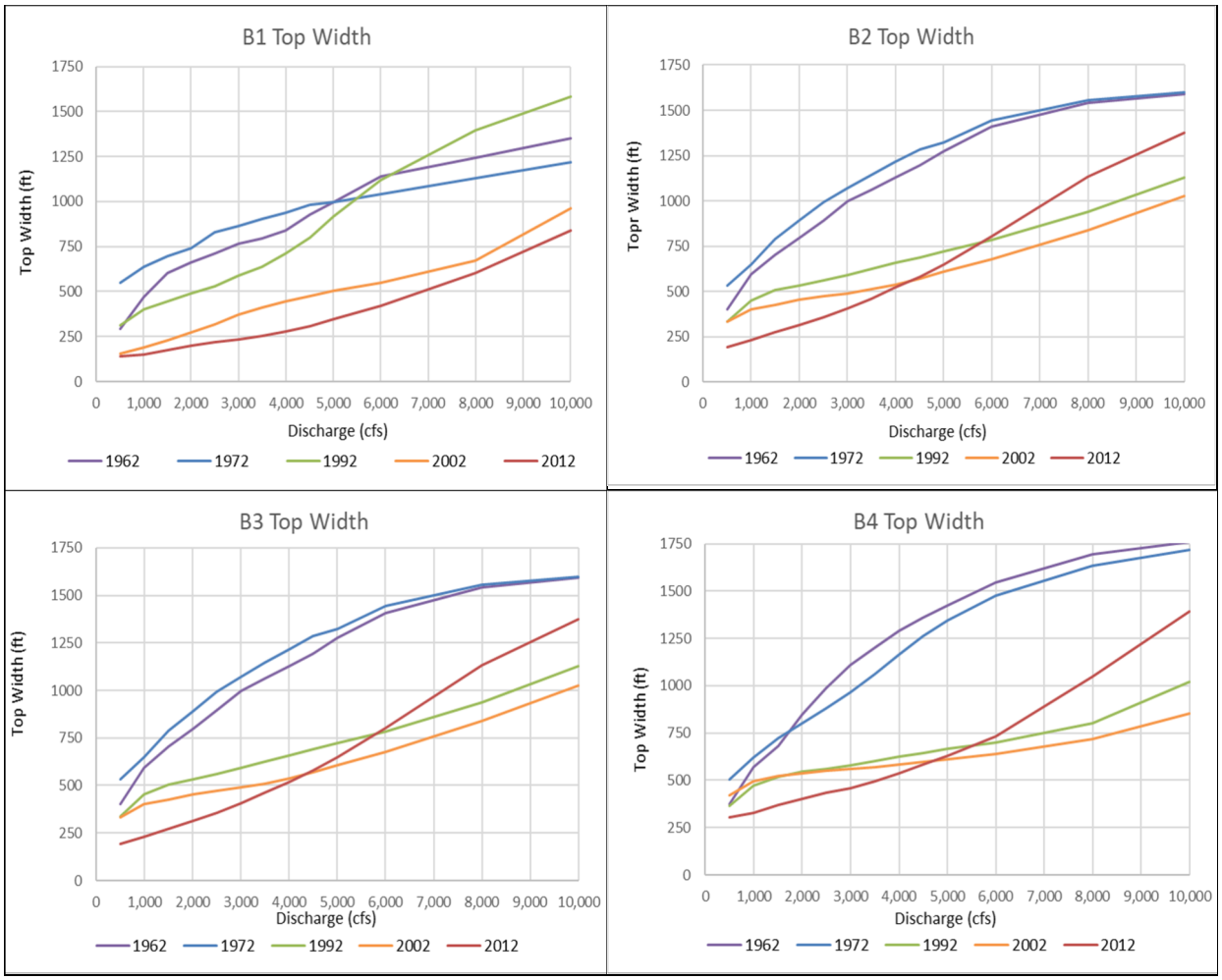

Figure 3-7 Average top width for B1 (top left), B2 (top right), B3 (bottom left), and B4 (bottom right) at discharges 500 to 5,000 cfs.

3.2 Width (Defined by Vegetation)

The width of the channel was found by clipping the agg/deg line to the width of the active channel, defined here as the non-vegetated channel based on aerial imagery. Aerial photographs were provided for years 1918 (digitized sketch), 1935 1962, 1972, 1992, 2001, 2002, 2004, 2005, 2006, 2008, 2012 and 2019. Additionally, active channel agg/deg polygons were provided by Reclamation's GIS and Remote Sensing Group for the years between 1918 and 1992. The average channel width of each subreach was calculated by averaging the width of all agg/deg lines within the subreach. **Figure 3-8** gives a breakdown of the average channel width by subreach.

Figure 3-8 shows a clear trend from a wider channel to a narrower channel for each subreach between 1918 and 2019. In 1935 for example, the average channel width in Subreach B1 was 650 feet. By 2019, the average channel width in Subreach B1 had narrowed to 240 feet. Channel width tends to become wider from upstream to downstream, with cross sections in Subreaches B3 and B4 that are on average wider than cross sections in B1 and B2. This is likely due to the greater degree of channel incision that occurred in the two upstream reaches compared with the two downstream reaches. Channel bank GIS data from 1918 gives a good indication of channel width prior to significant anthropogenic activity and development within the floodplain and tributaries.

In 1935, the channel width was significantly wider than it is today. This was particularly true in B3 and B4, where average channel width was 1,130 feet and 1,415 feet, respectively. Channel width generally showed significant narrowing after 1935. Between 1962 and 1992, the average channel width remained fairly consistent. For this 30-year period, the average channel width ranged between 500 feet and 620 feet for B1 and B2, while average channel width in B3 and B4 ranged between 580 feet and 780 feet. Another period of channel narrowing appears to have happened between 1992 and 2001. In the 11-year period between 2001 and 2012, the average vegetated channel width stabilized, ranging between 320 feet and 440 feet for B1 and B2 and between 450 feet and 580 feet for B3 and B4. Between 2012 and 2019, the river experienced another significant decrease in average channel width in B1, B2, and B4, but not B3. In the two upstream subreaches, average channel width dropped down to 240 feet, which is on average 100 feet and 80 feet narrower for B1 and B2, respectively, than the average channel width in 2012. Subreach B3 shows the least amount of channel narrowing in 2019. This may be impacted by the Albuquerque Bernalillo County Water Utility Authority (ABCWUA) Adjustable Height Dam constructed in 2005, which is likely preventing the channel directly upstream of this dam from further degrading and narrowing.

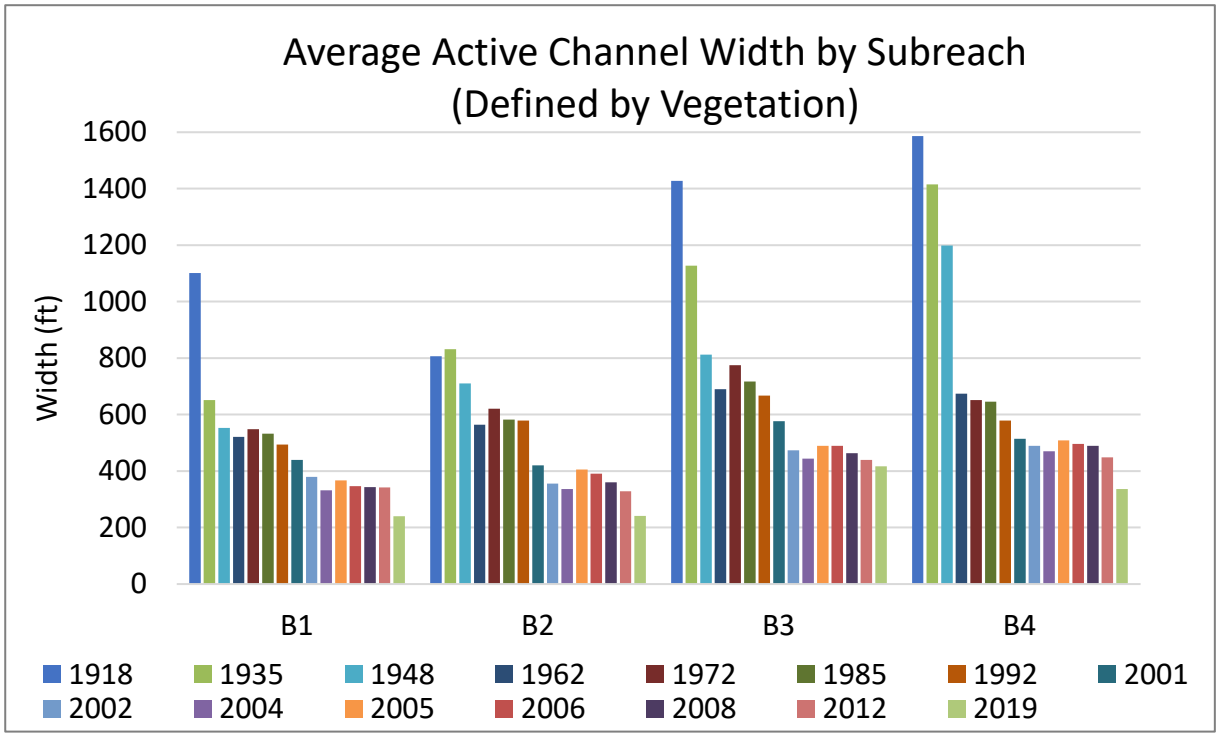

Figure 3-8 Averaged active channel width by subreach from historical imagery (defined by vegetation)

Throughout the century of georeferenced linen maps (1918) and available imagery (1935 – 2019) the average active channel has decreased by between 70% and 80%. The pre-channelized Rio Grande was wide, braided, and aggradational. Several impacts including changes land use to grazing led to a dramatic decline in the active channel width of the river between 1918 and 1949 (Scurlock, 1998). The first valley-wide levees began with the formation of the Irrigation District in 1925. Floods in 1929 set them back and in 1930 a more concerted effort began to control flooding with levees. Floods in the 40s set them back again, and the 50s is when the federal government stepped in to reconstruct levees and install jetty jacks, resulting in additional narrowing of the active channel (Scurlock, 1998). Upstream dams and reservoir storage also lead to a decrease in peak flows throughout this time period. Mowing operations cleared vegetation along the riverbanks from the 1960s to the 1980s (and into the early 1990s in various locations

along the MRG), which played a part in a slight widening of the river between 1972 and 1985, in addition to the increased flows as the period of drought came to an end. After another period of severe drought from the late 1990s to the late 2000s (though this drought is still on-going), the active channel width of the river has decreased once again and has since remained relatively stable.

Figure 3-9 shows an example section of channel in 1992 (blue bank lines) compared with the channel in 2019 (red bank lines) at the upstream limit of B2. Note that in 1992 the channel is wide and braided, with unvegetated sand bars and a slightly meandering low-flow channel. Conversely, the 2019 imagery shows vegetated channel banks and a single-thread meandering channel.

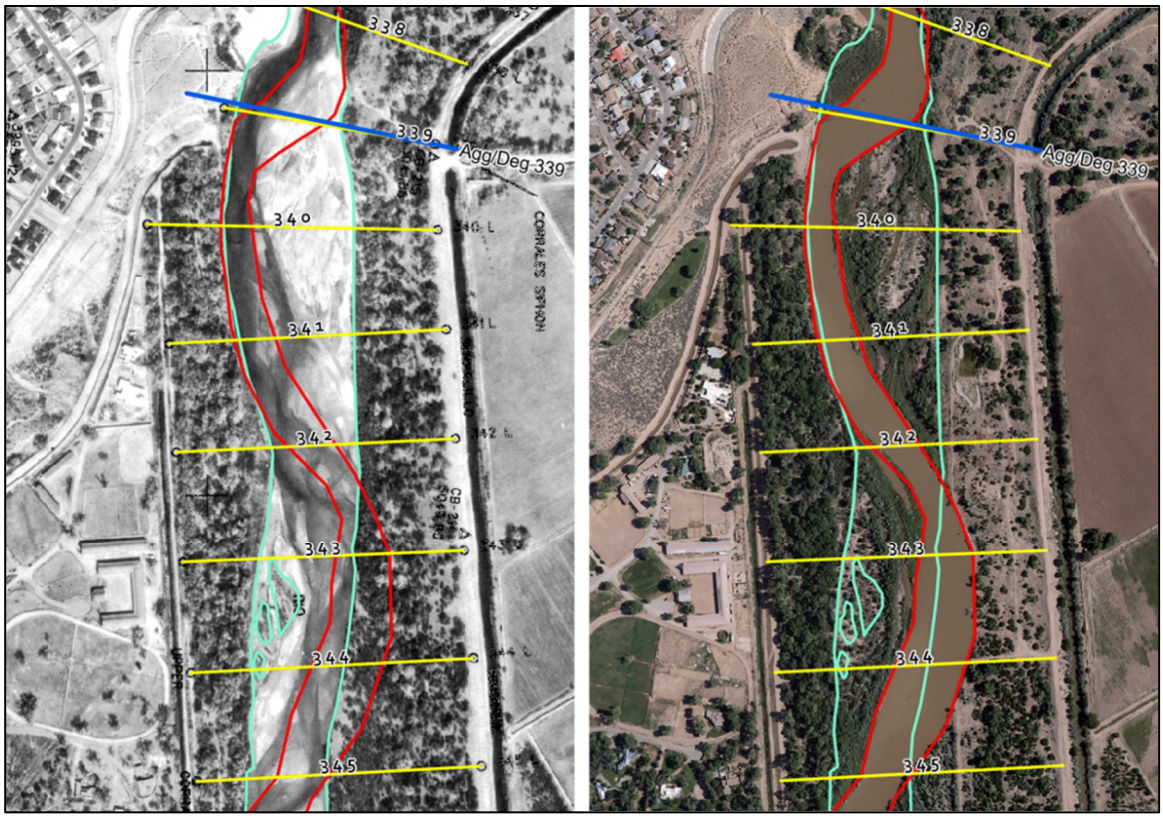

Figure 3-9 Channel in 1992 (left image, green bank lines) compared with channel in 2019 (right image, red bank lines)

3.3 Bed Elevation and Slope

The minimum channel bed elevation is used to evaluate the change in the longitudinal profile of the Bernalillo Reach. The bed elevation of the channel comes from an estimate generated by HEC-RAS, which is based on the discharge and the water surface elevation on the day of the aerial photography. While the minimum channel elevation points may not be exact, the overall trends can still be identified throughout the Bernalillo Reach. The minimum channel elevation was obtained at each cross-section from the HEC-RAS geometry files to generate a plot of the bed elevation throughout the reach, as seen in **Figure 3-10**.

In recent years, several grade controls are active throughout the reach and are identified on 2012 profile shown in **Figure 3-10**. The Corrales Siphon is exposed and is potentially holding grade, storing sediment, and creating backwater effects (pers. Comm. From Ari Posner, 2023). The AMAFCA North Diversion Channel outfall, located at the downstream end of B2, provided increased sediment loads and acts as grade

control by helping maintain channel width and islands and controlling the aggradation/degradation trends. It is important to note that the 2012 longitudinal profile crosses the 2002 longitudinal profile in the vicinity of the outfall, highlighting the effects of the increased sediment load from the outfall and the backwater effects from the islands. The ABCWUA Adjustable Height Dam, built in 2005, can also act as a temporary grade control. During the 2012 data collection, it appears that the dam was in the up position, though this is just a snapshot in time and the channel bed responds to changes in the dam height.

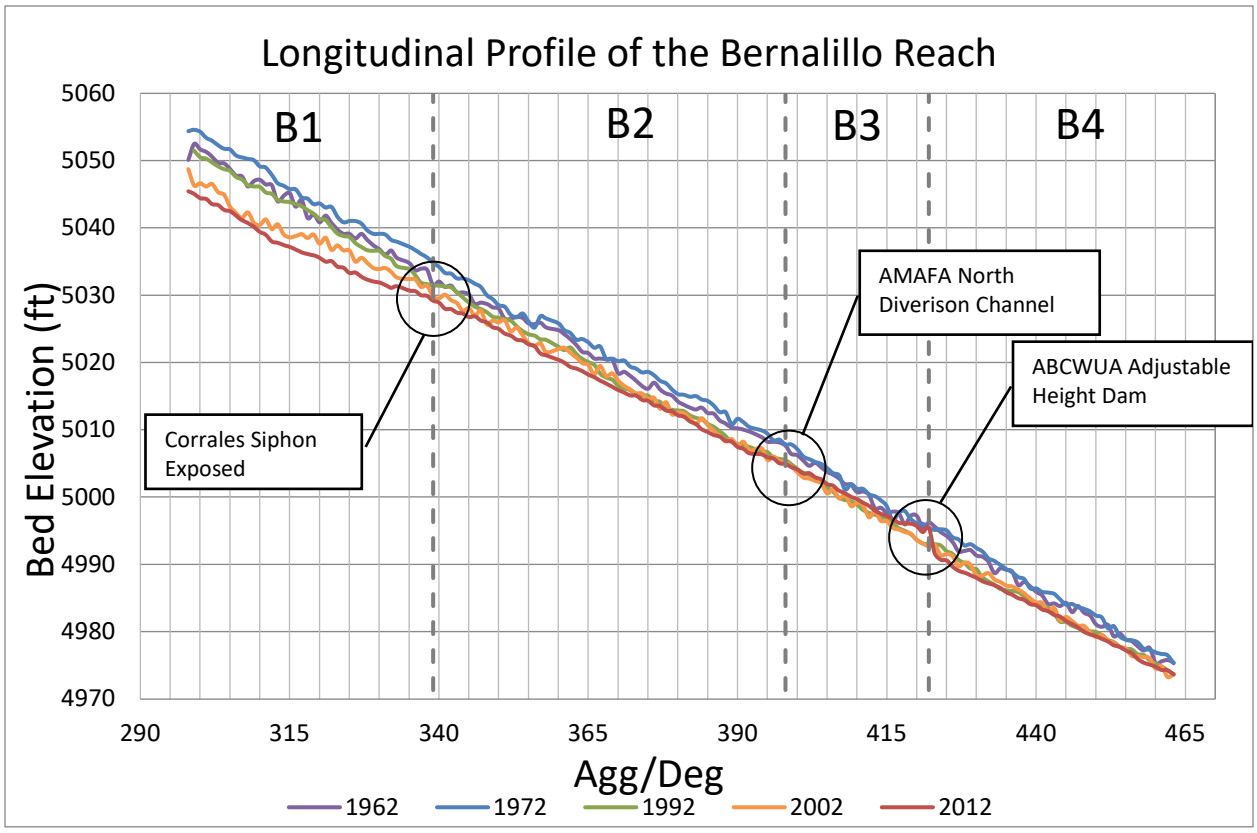

Figure 3-10 Longitudinal bed elevation profile.

In Subreaches B1, B2, and B4, a similar pattern of aggradation and degradation occurs throughout all years. Between the years 1962 to 1972, aggradation occurs through all subreaches. From 1972 to 2002, the river sees degradation in all subreaches. The rise in bed elevation from 2002 to 2012 in Subreach B3 is most likely a result of the increased sediment load from the AMAFA North Diversional Channel outfall and the temporary backwatering impacts of the ACBWUA Adjustable Height Dam. It appears that the upstream aggradation is contained within Subreach B3 and does not affect B1 and B2 subreaches. Upstream and downstream of B3, in Subreaches B1, B2, and B4, the degradation seen in the previous years has continued.

These trends can be observed and are analyzed in **Figure 3-11**, which shows the main channel aggradation and degradation of each subreach. The aggradation and degradation were found by first finding the average minimum channel elevation for each subreach and then subtracting the average bed elevation of the earlier year from the later year. A positive number indicates aggradation, and a negative number indicates degradation. This figure visualizes a direct comparison of trends in bed elevation between time intervals within individual subreaches. The period of 1962 to 1972 was the only period where there was aggradation throughout the entire Bernalillo Reach. This period of aggradation was followed by two periods, 1972 to 1992 and 1992 to 2002, of general degradation throughout the entire reach, which was heavily influenced

by the construction of Cochiti dam. There was some aggradation seen in B4 during the period of 1992 to 2002, but it is minor. The period of 2002 to 2012 were generally periods of degradation in all subreaches with exceptions in B3 which is due to the sediment load from AMAFA North Diversion outfall and temporary backwatering effects of the ABCWUA Adjustable Height Dam. The aggradation and degradation described in this section defines the channel slopes. For more detailed information on the channel slopes and how they have influenced the change in planform over time, see **Section 3.9**. The aggradation and degradation within the reach also impacts channel width (see **Section 3.2**) and bed material (see **Section 3.4**).

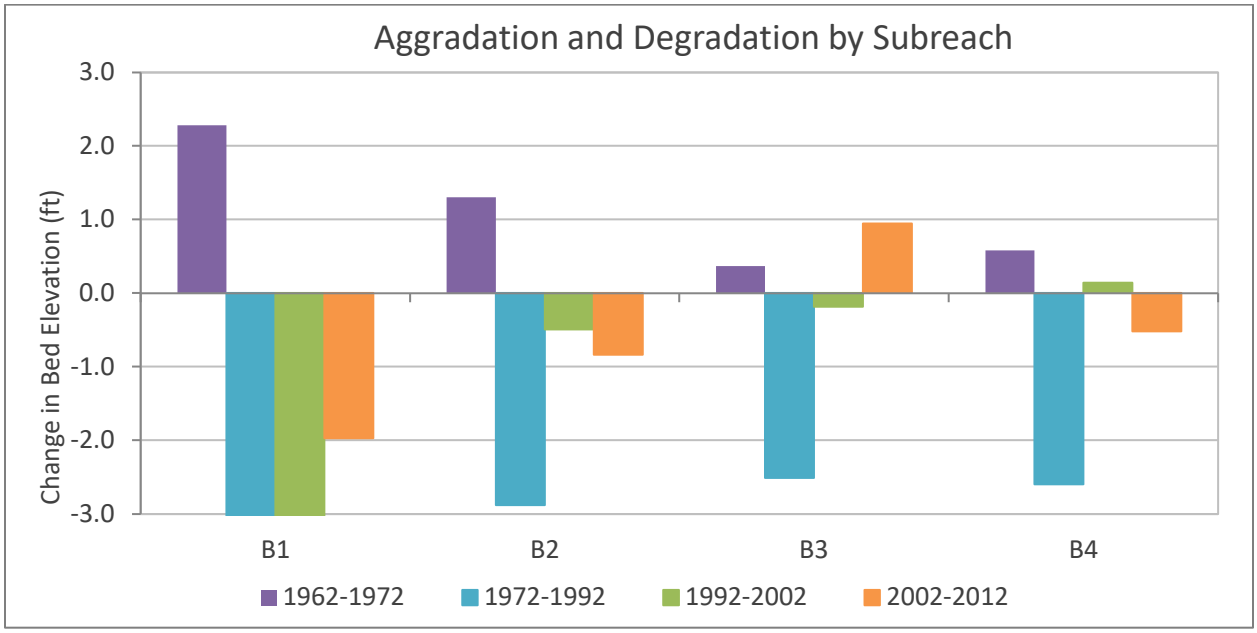

Figure 3-11 Aggradation and degradation by subreach

The bed slope was calculated by taking the slope of a linear fitted line for each subreach. The bed slope of the linear fitted line is shown in **Table 3-1** and **Figure 3-12** below. The left bar chart in **Figure 3-12** shows a water surface slope calculated off of the water surface profile at 500 cfs for each subreach, while the right bar chart in **Figure 3-12** shows the bed slope for each subreach. This slope has fluctuated but has stayed relatively stable, with a bed slope of around 0.0008 over the time interval of 1962 to 2012. Subreach B1 ultimately both dropped in bed slope from around 0.0009 to 0.00075 between 1992 and 2002. In 2005, the ABCWUA Adjustable Height Dam was constructed at the end of the B3 reach. Due to the aggradation and degradation that occurred upstream and downstream of the dam, respectively, the bed slopes between 2002 and 2012 decreased in B2, B3, and B4.

Changes in flow depth and slope often have an inverse relationship. **Table 3-1** presents bed slope by subreach. In general, as slope decreases the flow depth increases. This trend can be seen in the Bernalillo Reach, through all subreaches. As seen in **Figure 3-17** in **Section 3.6,** the hydraulic depth increases significantly from 1992 to 2012. The inverse trend in seen below in **Figure 3-12**, where the slope has decreased from 1992 to 2012. It is importat to note that these subreaches each have there own characteristics and trends where between 1962 and 2012. Those trends are further discussed in **Section 3.3** and **Section 3.9**.

Table 3-1. Channel bed slope by subreach

Subreach	1962	1972	1992	2002	2012
B1	0.00091	0.00094	0.00095	0.00075	0.00076
B2	0.00086	0.00089	0.00092	0.00087	0.00084
B3	0.00094	0.00100	0.00097	0.00095	0.00082
B4	0.00099	0.00099	0.00093	0.00093	0.00090

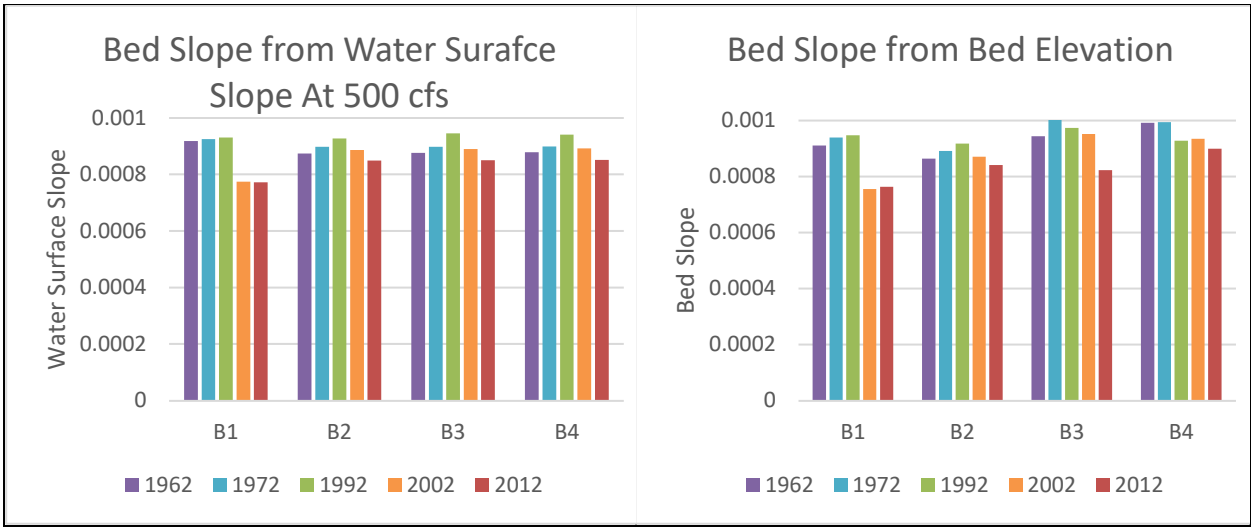

Figure 3-12 Water surface slope at 500 cfs (left) and channel bed slope (right).

3.4 Bed Material

Bed material samples were collected at various location in the river reach denoted by Agg/Deg locations. There are bed material samples available for analysis of the Bernalillo Reach from the years 1990 to 2020. **Figure 3-13** shows the median grain diameter of each sample versus Agg/Deg location downstream of the Highway 550 Bridge (i.e. the start of the Bernalillo Reach).

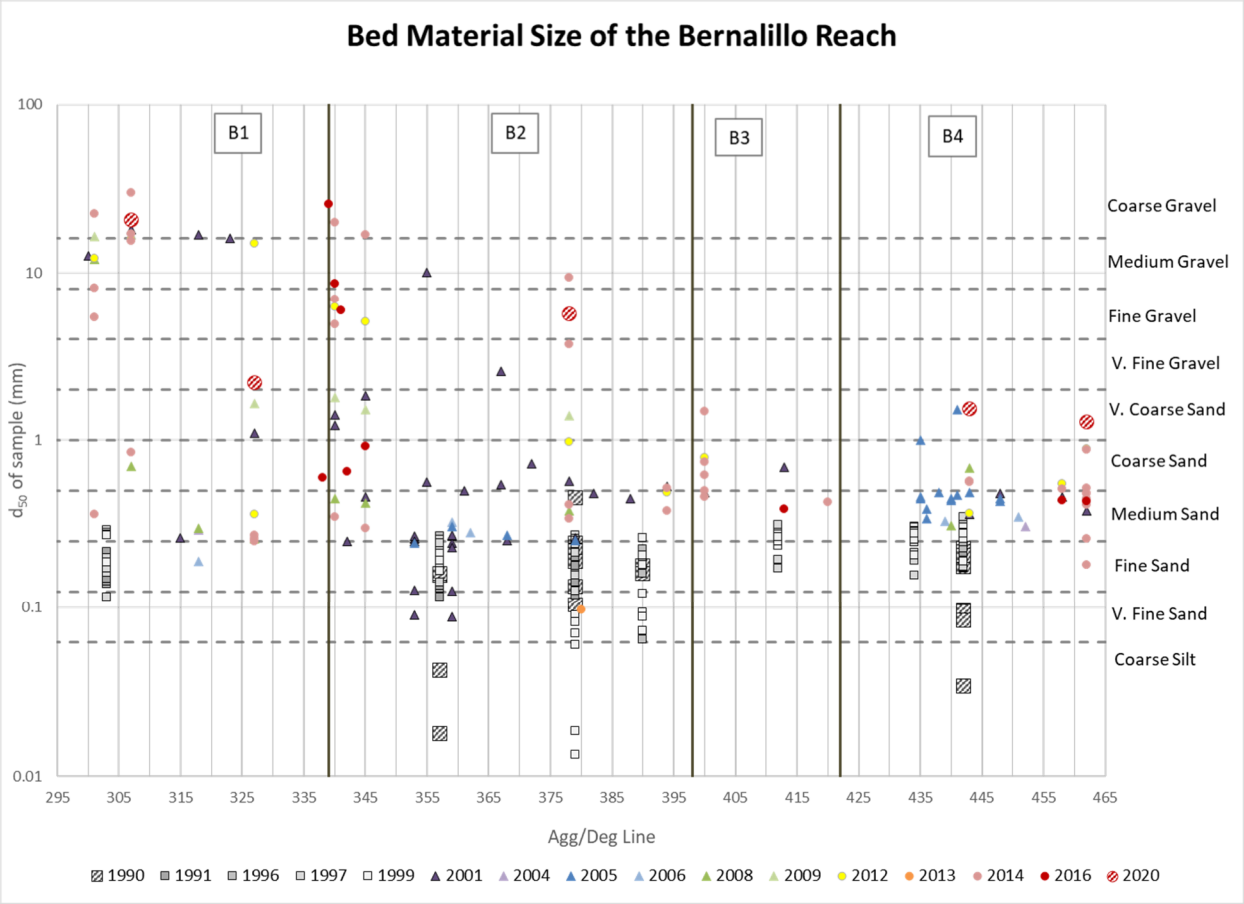

Figure 3-13 Median grain diameter size of samples taken throughout the Bernalillo Reach

Throughout the reach, the median diameter size of the samples typically varies between 0.0625 millimeter and 2 millimeter for the years in which data were collected. However, larger grain sizes, up to coarse gravel, were found in the upstream stream subreaches, B1 and B2, particularly in more recent years. **Figure 3-14** shows how the average bed material has changed over time in each subreach. In general, the has been a trend of the bed material coarsening over time. However, for a majority of the Bernalillo Reach, the grain size diameters correspond with classifications of fine sand to fine gravel, emphasizing the majority of Bernalillo Reach is a sand-bed river with some coarse silt and some gravels.

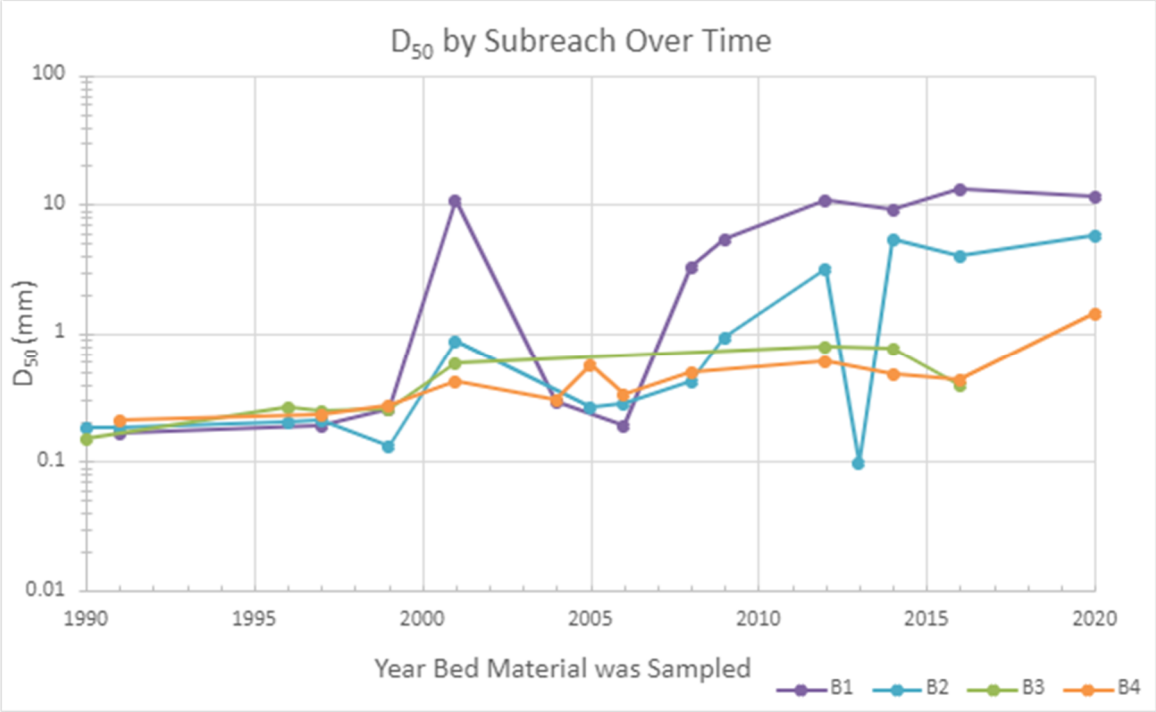

Figure 3-14 D50 change over time by subreach

3.5 Sinuosity

Channel sinuosity was calculated by dividing the river length by the valley length within each subreach. This was accomplished using historical aerial imagery and digitized channel centerlines provided by Reclamation's GIS and Remote Sensing Group. The results of this analysis are presented in **Figure 3-15.**

The Bernalillo Reach can generally be described straight or as having low sinuosity throughout the last century. A straight channel is classified as having a sinuosity between 1.00 and 1.05, while a low sinuosity channel can be classified as having a sinuosity between 1.06 and 1.3 (Brierley and Fryirs 2005). The average sinuosity in the Bernalillo Reach varies between 1.01 and 1.12. No trend of increasing or decreasing sinuosity is clear based on this data; however, Subreach B3 has tended to have the greatest degree of sinuosity over the years. In 2019, all four subreaches can be classified as straight channels.

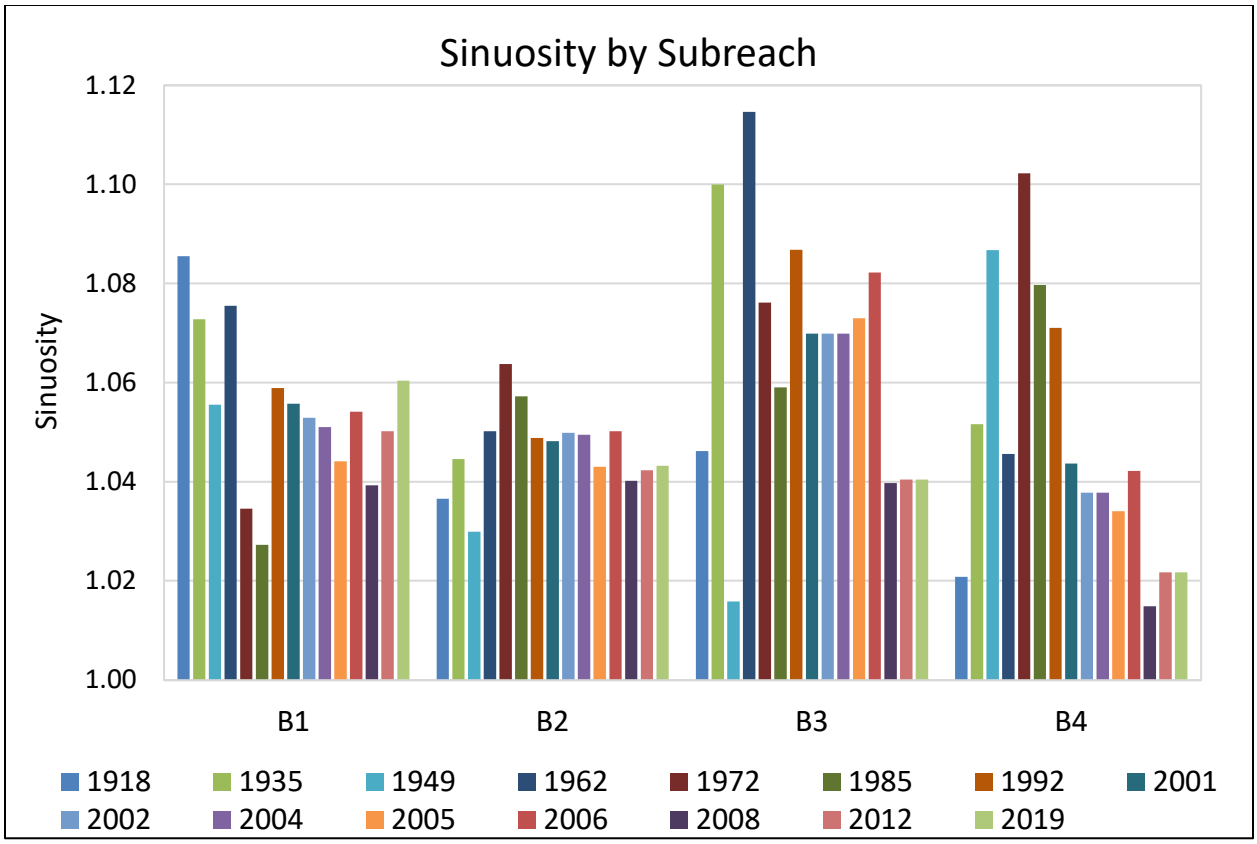

Figure 3-15 Average sinuosity by subreach

3.6 Hydraulic Geometry

Flow depth, velocity, width, wetted perimeter of the main channel, and bed slope are obtained using HEC-RAS 6.2.0 with a discharge of 3,000 cfs and 5,000 cfs. 3,000 cfs was selected because it is the approximate bankfull condition of previously studied reaches on the Middle Rio Grande (Sperry 2022 and Scheid et al. 2022). 5,000 cfs was selected because it is the discharge that most likely represents bankfull conditions in the Bernalillo and Montaño reaches. Bankfull conditions are the maximum discharges with limited likelihood of overbanking (LaForge et al., 2019 and Yang et al., 2019). It is important to note that at some locations in 2012, 3,000 cfs and 5,000 cfs flows activate the floodplain and could be considered greater than bankfull discharge. This can be seen in Habitat Maps found in **Appendix E**. A discharge of 3,000 cfs has a daily exceedance of around 9.9%, and a 5,000 cfs discharge has a daily exceedance of 3.3% for the time period after Cochiti Dam construction. For this same time period, 1,000 cfs, has a daily exceedance probability around 33.8%. Since the 1,000 cfs flow is a more common flow in the subreach, it was also included in the hydraulic geometry analysis. For the plots of the hydraulic geometry variables, the values were averaged by subreach for each year analyzed.

The HEC-RAS results shown in **Figure 3-16** show a general trend that matches the trend seen in **Sections 3.1 and 3.2**. For all flows, there is generally an increase in wetted top width from 1962 to 1972, except in subreach B4 at 3,000 cfs and 5,000 cfs. From 1972 to 1992, there is a large decrease in wetted top width. From 1992 to 2012, there is generally a decrease in top width, except at 5,000 cfs. The fluctuation between 1962 to 1972 is a results of the aggradation occurring from sediment discharge in the river and the potential lateral erosion occurring due to higher flow discharges. From 1972 to 2012 the degradation trends that the

Bernalillo Reach experienced was due to decrease in the sediment loads and flow magnitudes caused by the construction of Cochiti Dam in 1973.

Because top width and hydraulic depth are typically inversely related for the same discharge, it is expected that the change in hydraulic depth results over time will have the opposite trend that the change in wetted top width results showed from subreach to subreach. **Figure 3-17** shows the HEC-RAS calculated hydraulic depths (area over top width) at discharges of 1,000 cfs, 3,000 cfs, and 5,000 cfs. In general, the HEC-RAS calculated results are similar to what is expected at 1,000 cfs. However, at 3,000 cfs and 5,000 cfs, the hydraulic depth in B1 should be higher in 1962 than in 1972 because the river is wider in 1972 than 1962.

Figure 3-16 HEC-RAS Wetted top width of channel at 1,000 cfs (top left), 3,000 cfs (top right), and 5,000 cfs (bottom middle)

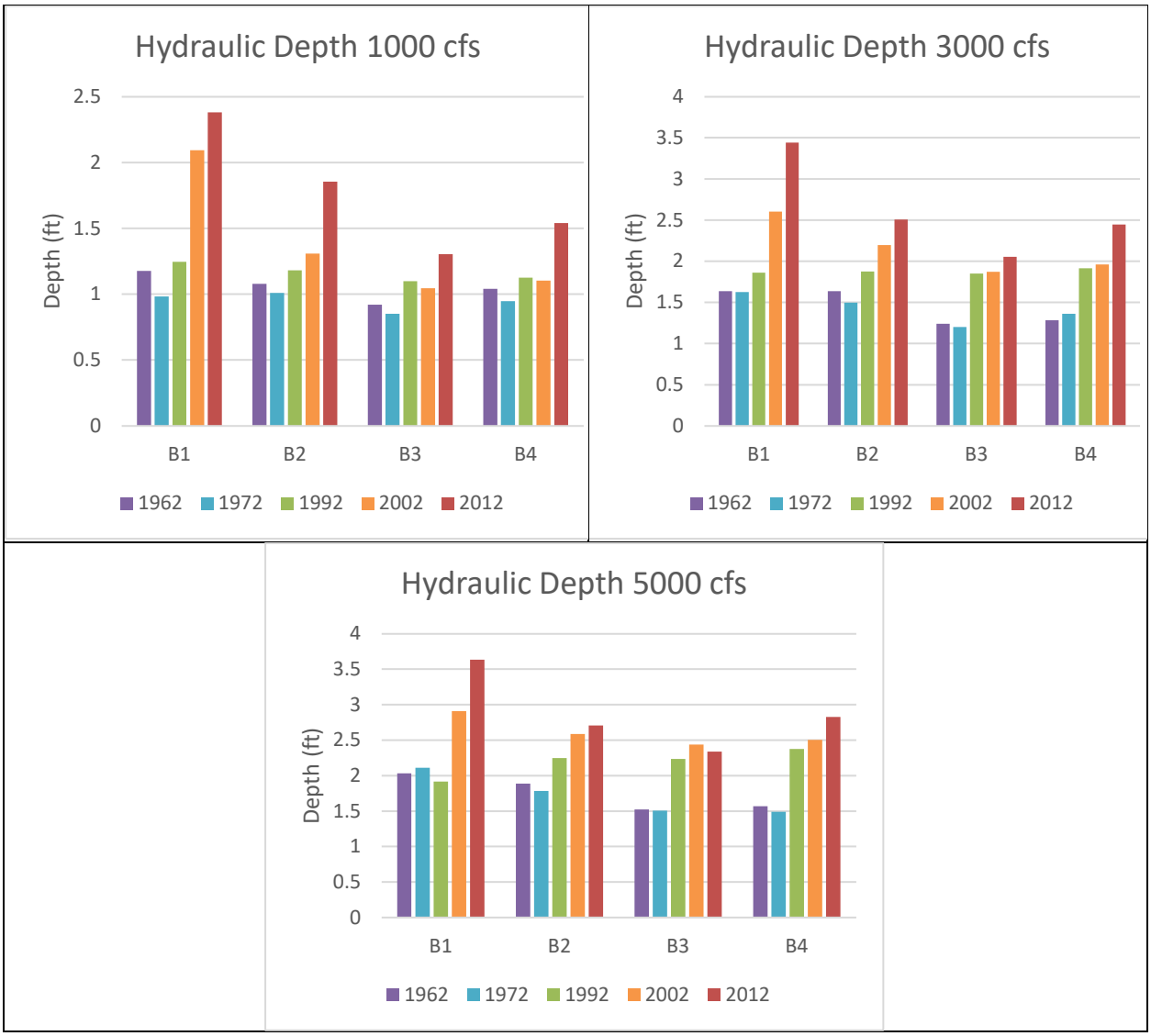

Figure 3-17 HEC-RAS Hydraulic depth at 1,000 cfs (top left), 3,000 cfs (top right), and 5,000 cfs(bottom)

The results for the wetted perimeter of the main channel were obtained by using HEC-RAS and is represented by **Figure 3-18.** Generally, the main channel wetted perimeter follows a similar trend to the top width. All of the subreaches generally show a steady decline in main channel wetted perimeter throughout the time interval analyzed. There are exceptions in some of the subreaches where the is an increase in wetted perimeter from 1962 to 1972, following by a decrease for the remaining periods. This matches the trends seen for the wetted top widths in **Section 3.1** and is due to the aggradation and degradation trends shown in **Section 3.3**. It is important to note that the wetted perimeter is confined to the main channel and shows how the main channel has changed over time.

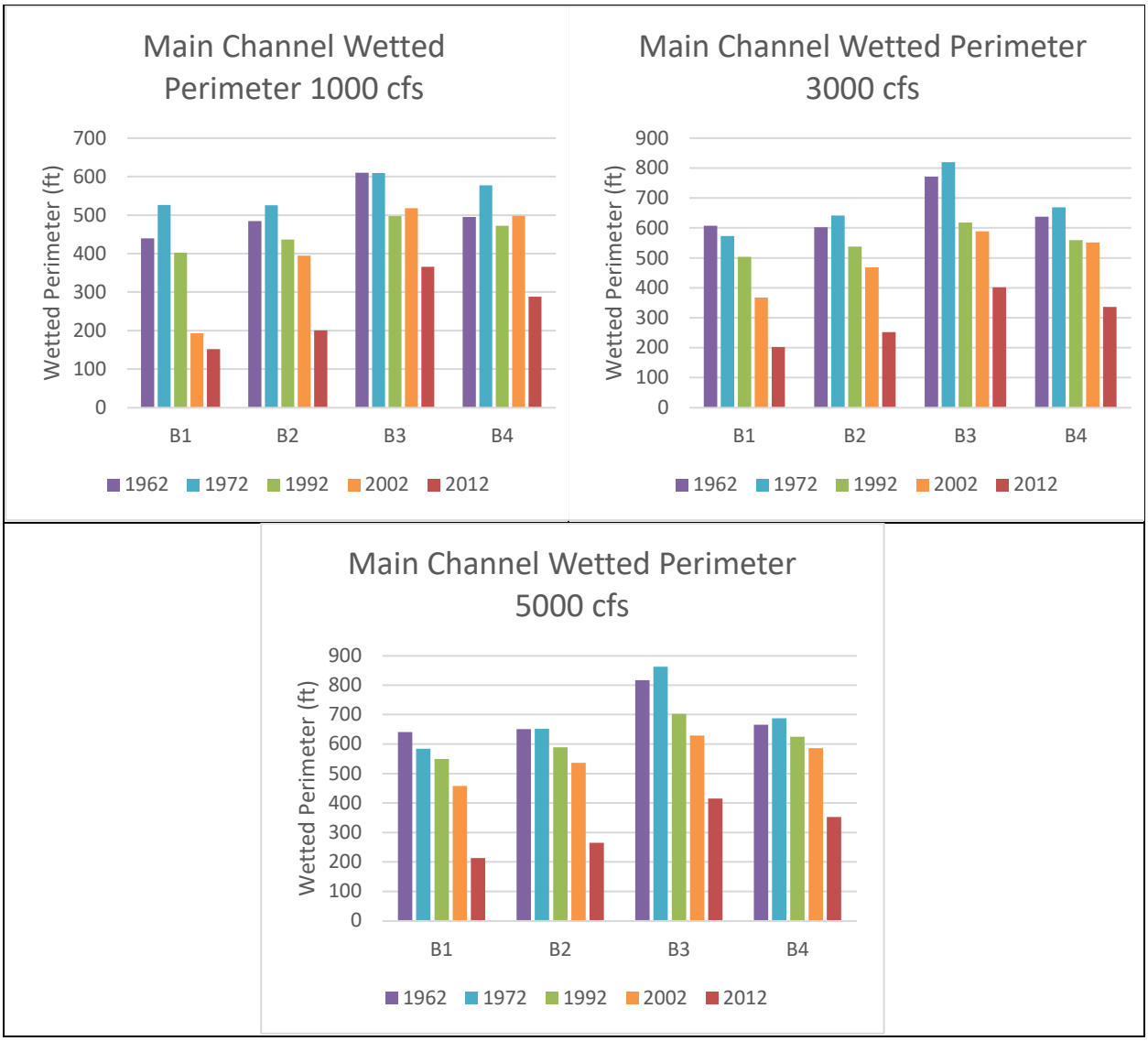

Figure 3-18 HEC-RAS Main Channel Wetted Perimeter at 1,000 cfs (top left), 3,000 cfs (top right), and 5,000 cfs (bottom middle).

3.7 Number of Channels

At low flows, the number of vegetated mid-channel bars and islands at each agg/deg line is measured from digitized planforms from aerial photographs provided by the Reclamation. In some locations, multiple channels were present at one agg/deg line due to a vegetated bar or island bifurcating the flow. Note that the stage of a river can affect the number of visible islands and bars. A limitation in this analysis is that for some aerial images it is not clear what the discharge was, and as a result, some vegetated islands may be obscured by higher flows. This adds some degree of uncertainty regarding whether the difference between years in terms of number of channels were due to a variation in stage or a change in channel morphology. However, this analysis is still helpful in comparing general trends over a longer time period.

The number of channels at each agg/deg line, averaged across each subreach, are presented in **Figure 3-19.** For all four subreaches, the channel had very few vegetated islands for the years of 1972 and 1985. In contrast, Subreaches B2, B3, and B4 averaged more than 1.5 channels between the years of 2001 and 2012.

The year 1972 generally shows the least number of channels per subreach, ranging between 1.0 and 1.04 channels, on average. The year 2001 generally shows the greatest number of channels per subreach, ranging between 1.65 and 2.04 channels, on average. In 2019, the average number of channels per subreach ranged between 1.3 and 1.7.

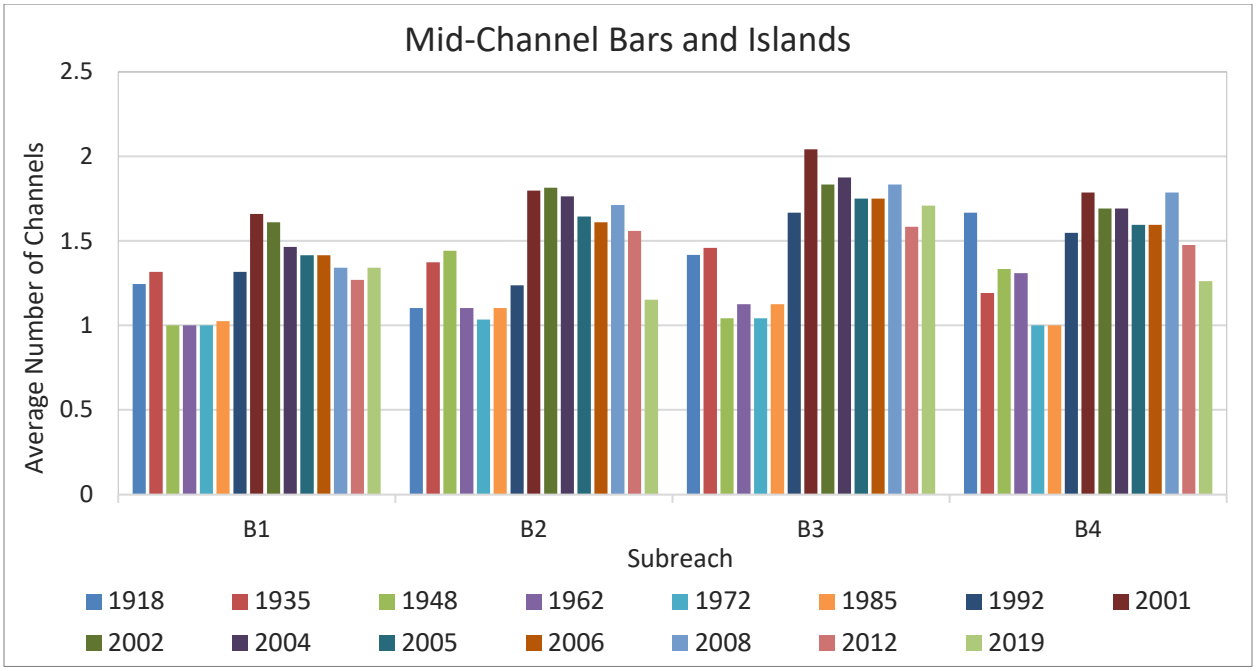

Figure 3-19 Average number of mid-channel bars and islands by subreach

Figure 3-20 gives the percentage of agg/deg lines with multiple flow paths per year, which gives a rough idea of the percentage of the Bernalillo Reach that contains multiple channels in any given year. Across all agg/deg lines, there were between 1 and 5 channels in any given year. 1935 shows a spike in agg/deg lines with multiple channels, with 30% of the Bernalillo Reach having 2-3 flow paths and 70% having 1 flow path. Between 1972 and 1985, there are few vegetated islands in all four subreaches due to channel maintenance. During this period, the islands were annually cleared of vegetation and roots were removed, which made it possible for the next high flow events to mobilize the islands (Baird pers. Con. 2023). This practice of annually clearing islands of vegetation stopped in 1985 (Baird pers. Con. 2023).

The number of agg/deg lines crossing multiple channels steadily increases until 2001. This time period during the late 1990s coincides with a drought characterized by lower peak flows that were incapable of wiping out the vegetation or re-working the bars and islands. Between 2001 and 2004, nearly 60% of the agg/deg lines have between 2 and 5 flow paths. This number of paths declines to 50% between 2005 and 2008, coinciding with a return to normal flows that facilitated denser vegetation growth but also likely mobilized some of the islands. In 2019, the percentage of channels dropped to 30% due to channel narrowing (Baird pers. Con. 2023). One way in which channels can become narrower is when islands become bank attached bars, which reduces the number of channels (Baird pers. Con. 2023).

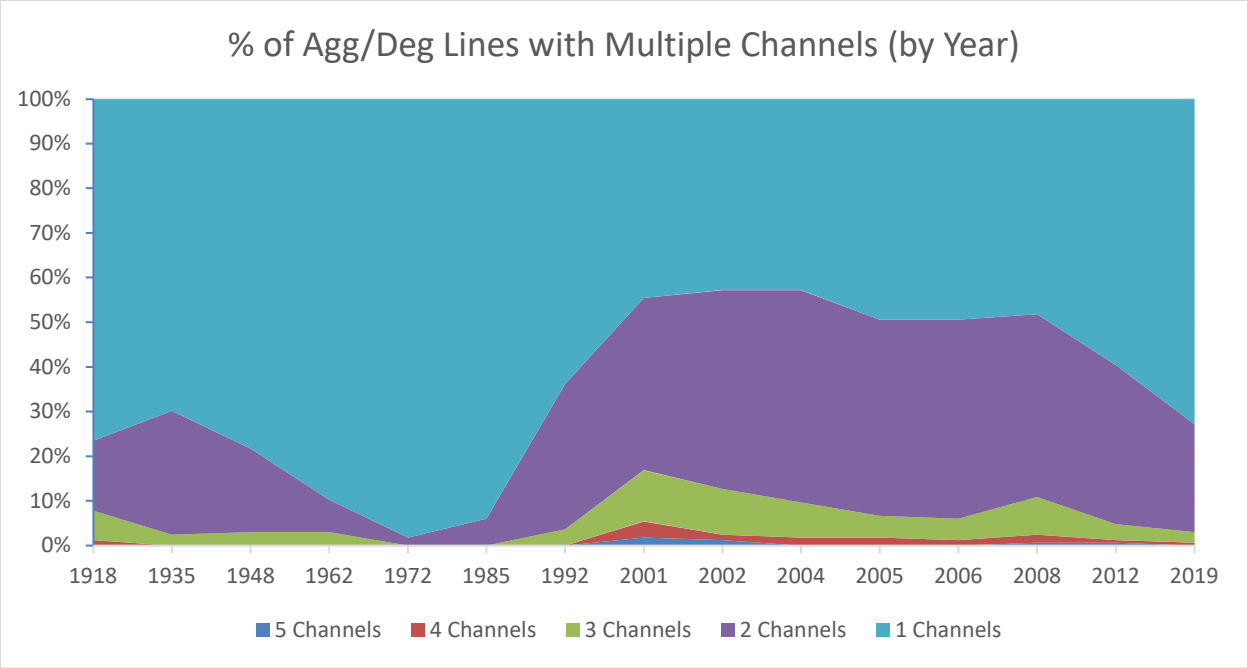

Figure 3-20 Percentage of agg/deg lines with multiple channels, by year, segregated by number of channels between 1 and 5.

Figure 3-21 shows a comparison of aerial imagery for the years 1972, 2002, and 2019. Note the wide channel and lack of vegetated islands in 1972, the formation of mid-channel vegetated islands in 2002, and the gradual incorporation of the islands to the floodplain in 2019.

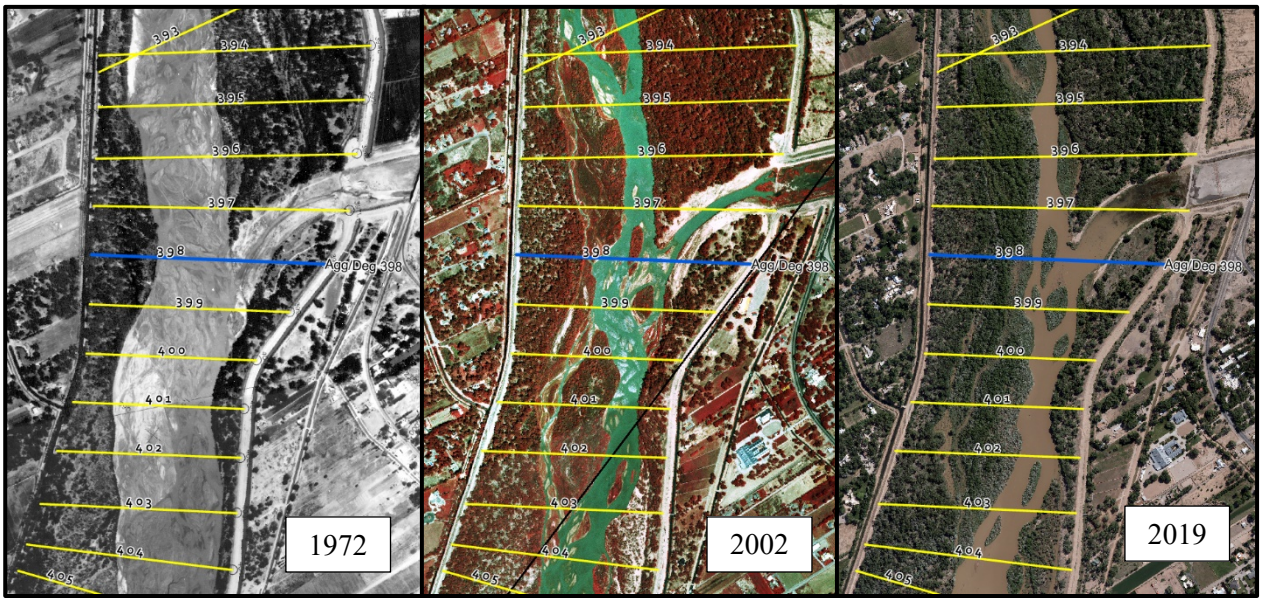

Figure 3-21 Aerial photograph showing evolution of vegetated bars and islands at Agg/Deg 398 in 1972 (left), 2002 (center) and 2019 (right).

3.8 Channel Response Models

The Julien and Wargadalam (JW) equations were used to predict the equilibrium channel width for each Montano Subreach. These equations predict the width and depth likely to result from a given discharge (typically bankfull), grain size, and slope based on empirical analysis of over 700 rivers and channels (Julien & Wargadalam, 1995):

$$h = 0.2Q^{\frac{2}{6m+5}}D_s^{\frac{6m}{6m+5}}S^{\frac{-1}{6m+5}}$$

$$W = 1.33Q^{\frac{4m+2}{6m+5}}D_s^{\frac{-4m}{6m+5}}S^{\frac{-1-2m}{6m+5}}$$

Where: $m = 1/\left[2.3\log\left(\frac{2h}{D_s}\right)\right]$, h is the flow depth, W is the channel width, Q is the flow discharge, D_s is the median grain size, and S is the slope.

Microsoft Excel was used to solve for h and W iteratively. A discharge of 5,000 cfs was used to represent the bankfull discharge. The slope and grain size values were obtained from **Section 3.3** and **Section 3.4**, respectively. The predicted equilibrium channel width results were compared to the observed active channel widths (from the GIS analysis of the digitized planforms) and are shown in **Table 3-2** and represented graphically in **Figure 3-22** and **Figure 3-23**. Median grain size, D50, values with a (*) symbol indicate data that does not match the specified year – see **Appendix B** for the median grain sizes used and an additional 3,000 cfs JW analysis for comparison with previous reach reports. The percent difference was calculated as follows:

$$\text{Percent Difference} = 100 * \left(\frac{\text{predicted width} - \text{observed width}}{\text{observed width}}\right)$$

Table 3-2 Julien-Wargadalam channel width prediction for 5,000 cfs

Year	Subreach	Ds (mm)	Slope	Predicted Width (ft)	Observed Width (ft)	Precent Difference
1992	B1	0.168*	0.0010	305	493	-38%
	B2	0.182*	0.0009	308	578	-47%
	B3	0.149*	0.0010	304	668	-54%
	B4	0.211*	0.0009	307	579	-47%
2002	B1	10.830*	0.0008	338	379	-11%
	B2	0.869*	0.0009	315	356	-11%
	B3	0.590*	0.0010	309	473	-35%
	B4	0.420*	0.0009	309	489	-37%
2012	B1	10.822	0.0008	338	342	-1%
	B2	3.206	0.0008	323	329	-2%
	B3	0.789	0.0008	319	439	-27%
	B4	0.602	0.0009	312	448	-30%

*See Table B-1 in Appendix B for specific years used for Ds values.

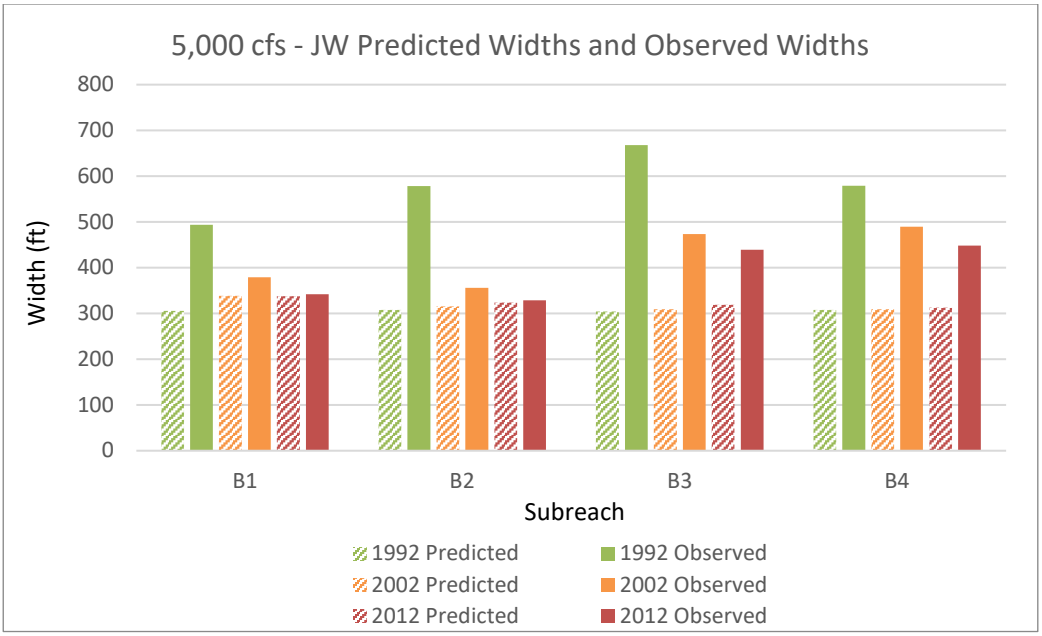

Figure 3-22 Julien and Wargadalam predicted widths and observed widths of the channel for 5,000 cfs

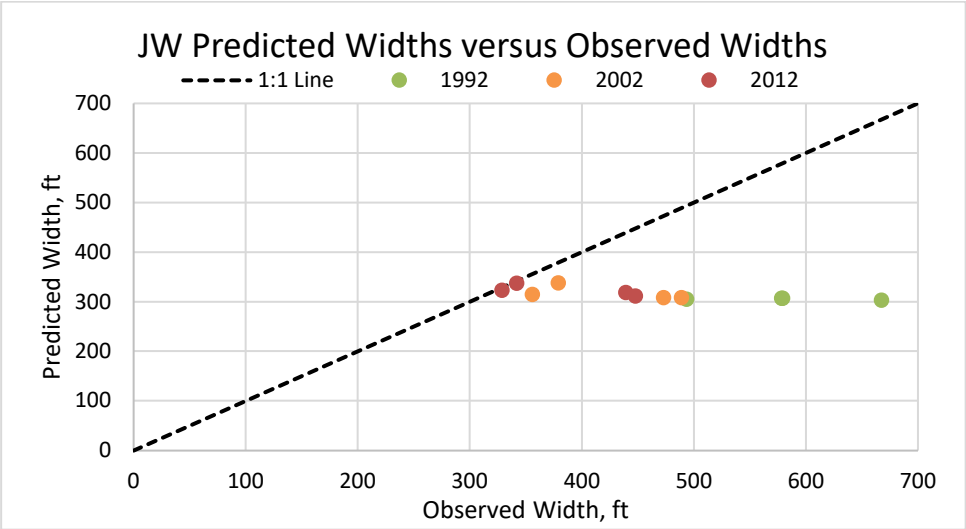

Figure 3-23 Julien and Wargadalam predicted widths versus observed widths with 1:1 line for 5,000 cfs

The predicted JW widths are narrower than the observed widths for all subreaches in the Bernalillo Reach – this indicates that the equilibrium width is narrower than the observed 2012 width. This predicted equilibrium channel width is about 300 ft. The percent error decreases from 1992 to 2012, see **Figure 3-22**, from a maximum error of 54% to 30% respectively. However, Subreaches B1 and B2 show very small percent differences for 2012, indicating that the subreaches could be reaching equilibrium. The sources of error are: a single discharge (bankfull) is used when a spectrum of discharges flow through the MRG, some D50 values are not associated with the years calculated (though large changes in grain size are required to see substantial changes to predicted width), and these equations are based on single-thread channels (the MRG is naturally a braided system). It is important to note that the JW equations represent a river whose morpho-dynamics are in equilibrium. The morpho-dynamic equilibrium assumes there would be no aggradation or degradation occurring.

3.9 Geomorphic Conceptual Model

Massong et al. (2010) developed a channel planform evolution model for the MRG based on historical observations. The sequence of planform evolution is outlined in **Figure 3-24**. **Stage 1** describes a wide, shallow channel with a high sediment load and large floods, which results in an active channel with constantly changing bars and dunes and little vegetation encroachment. The evolution from these more transient dunes and bars to more stable, higher relief bars and islands transitions the river into **Stage 2**. This transition generally occurred throughout the MRG between 1999 and 2004, which was characterized by sparse flooding and dry summer months. As the islands and bars become vegetated, they stabilize and begin to act more like floodplains, indicating that the river is transitioning to **Stage 3**. This transition occurred following a return to higher flows in 2005 and 2006. During this time, flow was high enough to inundate and erode some of the bars that had formed during the preceding 5-year dry period, but most of the bars survived and became well-vegetated during these wetter years.

The sediment transport capacity then becomes the determining factor of the future course of the river to either an aggrading river or a migrating river. A deficiency in sediment transport capacity, meaning the sediment supply is exceeding the transport capacity, leads to *aggradation* in the main channel and the flow eventually shifts onto the lower surrounding floodplain (**Stages A4-A6**). This typically forms in areas where the reach slopes are less than 0.0007 ft/ft. When the sediment transport capacity exceeds the sediment supply, bank material erodes both laterally and vertically, leading to a *meandering* river (**Stages M4 to M8**). This typically happens where average channel slopes are larger than 0.0009 ft/ft. Transitions or complex combinations between the M stages and the A stages can occur, typically in areas where the average channel slope adjusts or in areas where neither A nor M stages dominate (typically where slopes are between 0.0007 ft/ft and 0.0009 ft/ft). However, a reset to Stage 1 always requires a large, prolonged flood to overcome the vegetation encroachment and widen the floodplain (Massong et al., 2010).

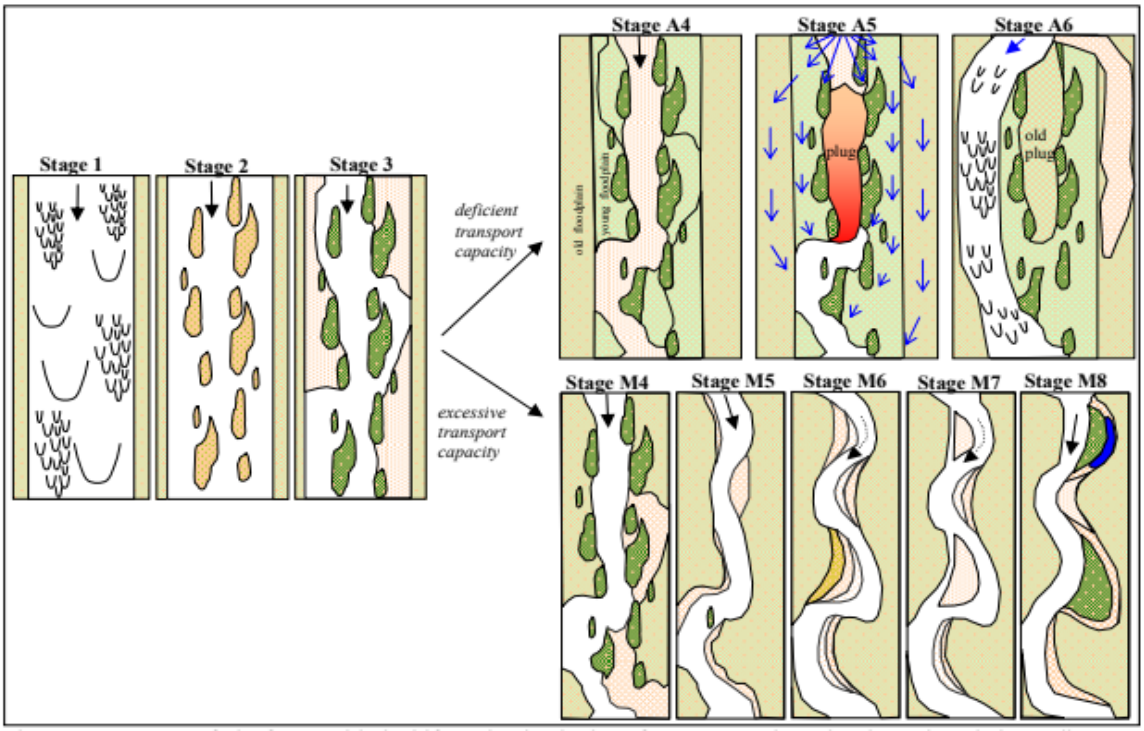

Figure 3-24 Planform evolution model from Massong et al. (2010). The river undergoes stages 1-3 first and then continues to Stages A4-A6 or stages M4-M8 depending on the sediment transport capacity.

The reach-averaged slope for the Bernalillo Reach has adjusted through-out the years as a result of incision, particularly in the upstream-most subreach (B1). Between 1962 and 1992 the slope for B1 remained relatively stable, ranging between 0.00091 and 0.00095. However, by 2002, the channel slope had flattened significantly to a slope of 0.00075. The slope for Subreach B3 remained consistent between 1962 and 2002, but experienced a significant drop between 2002 and 2012, from 0.00095 to 0.00082. This can be attributed to the temporary impacts of ABCWUA Adjustable Height Dam that was constructed in 2005. During the time of 2012 survey, it is believed that the adjustable height dam was in the up position, which led to aggradation and a subsequent flattening of the slope behind the sill that primarily occurred in the B3 subreach. The increased sediment load from the AMAFA North Diversion outfall also attributed to this aggradation. Other reaches generally saw a less significant changes in slope between 1962 and 2012, though they all show a downward trend. Refer to **Table 3-1** and **Figure 3-10 (Section 3.6**) for more detailed values of bed slope over the years for each subreach.

In 2012, the bed slope for B1, B2, B3, and B4 are 0.00076, 0.00084, 0.00082, and 0.0009, respectively. According to Massong et al. (2010), these reaches fall within a grey-area range of bed slopes, where neither the meandering process nor the aggradation process is clearly dominant. However, it is apparent from the available data that the Bernalillo Reach of the MRG has evolved through the meandering planform changes between 1992 and 2012, not the aggrading planform changes. Factors such as channel bed coarsening and degradation progressing to a point where the bank height exceeds the root depth of the riparian vegetation are more important than slope in assessing plan view stage for reaches where the sediment supply is less than transport capacity. Signs of this evolutionary track towards a meandering river include channel incision and narrowing rather than aggradation, coarsening of the bed, meander planform visible within the aerial imagery, and an absence of sediment plugs.

Figure 3-25 shows the stages for a meandering river course in plan view (Massong et al. 2010) as well as cross-section view. During **Stage M4**, a dominant channel is typically established, while secondary channels begin to aggrade and will only become inundated during higher flows. Vegetation begins to encroach into these secondary channels, and they begin to transition from a channel to floodplain. During **Stage M5**, the channel continues to incise until the channel reaches a stable slope or runs into a coarser bed layer. This form is generally single threaded and straight or slightly sinuous. The channel may begin to meander, as shown by **Stage M6,** if the channel thalweg is below the root zone. This allows for erosion of the bank material beneath the soil layer that is more consolidated by roots. Meanders progress and typically form side channel cuts (chutes) through the point bar on the inside of the bend (**Stage M7**). These gradually become larger until it eventually able to convey all of the flow, leading to the eventual abandonment of the old channel. The old channel fills with sediment and becomes part of the floodplain (**Stage M8**). Note that the plan view classification system has been expanded to include representative cross sections for each stage.

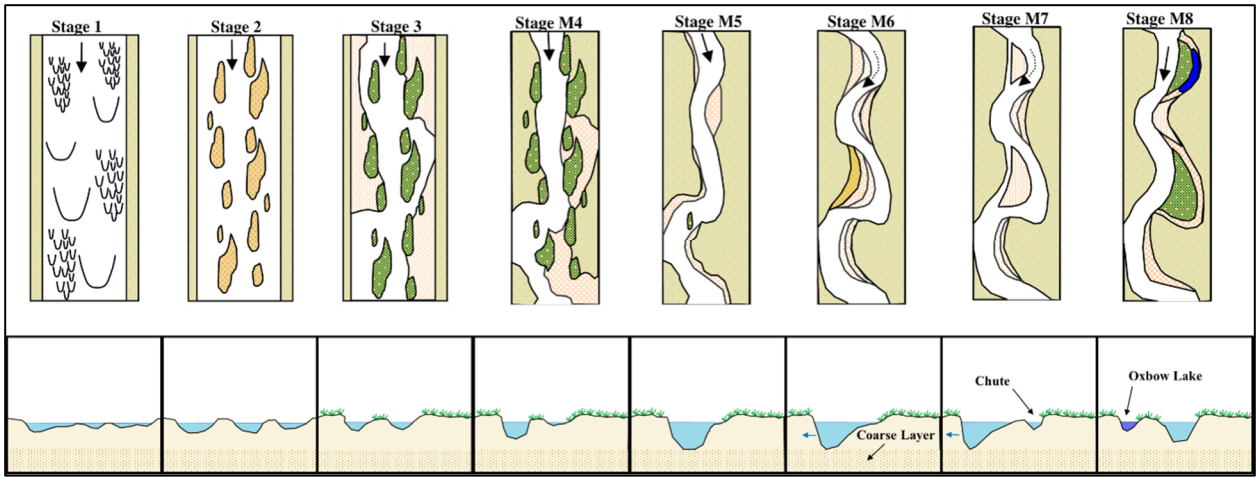

Figure 3-25 Planform evolution model from Massong et al. (2010) applied to channel cross sectional view left to right looking downstream (modified by Brianna Corsi, 2022)

Figure 3-26 shows the evolution of the channel in the upstream-most subreach using a representative cross section at Agg/Deg 318 for the years 1962, 1972, 1992, 2002, and 2012.

In Subreach B1, the channel aggraded between 1962 and 1972. The 1962 cross-section shows a more clearly defined low flow channel that is approximately 150 feet wide and 2 foot deep. In contrast, the 1972 cross-

section shows no clearly defined low flow channel. Between 1972 and 2012, the channel gradually degraded, narrowed, and became more clearly distinguishable from the floodplain. The channel dropped by 2 feet in the 20-year period between 1972 and 1992, by 4 feet in the 10-year period between 1992 and 2002, and another 3 feet in the 10-year period between 2002 and 2012, for a total of around 9 feet of degradation in 40 years at this cross-section. Subreach B1 shows the greatest drop in channel bed of the four subreaches within the Bernalillo Reach.

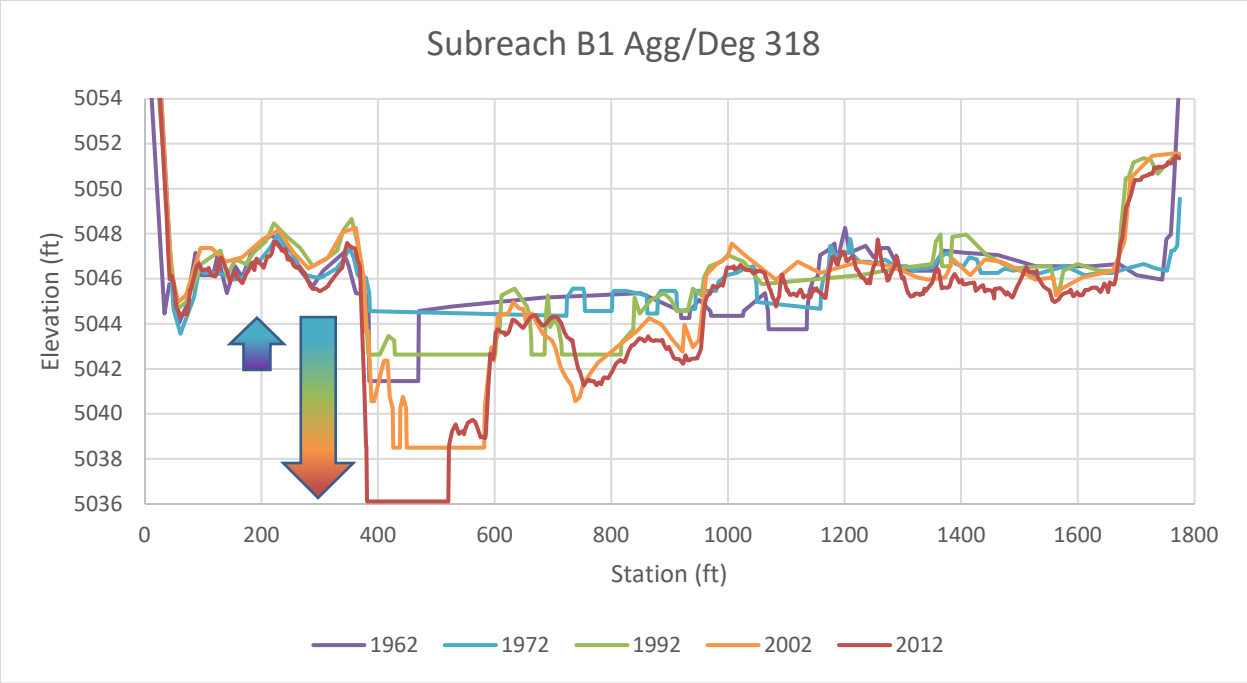

Figure 3-26 Subreach B1: Channel evolution of representative cross section Agg/Deg 318. Significant channel degradation and narrowing occurred between 1972 and 2012.

Figure 3-27 gives a synthesis of the likely channel form based on the Massong classification (left), the channel cross section (center) and aerial imagery (right) for Agg/Deg 318 in Subreach B1 for each evaluated year. River discharge is unknown at the time that the aerial imagery was flown.

Between 1962 and 1972, Subreach B1 appears to be in Stage 1, with a wide, undefined channel and transient bars and islands. Between 1972 and 1992, the channel has shifted into Stage 2, with some vegetation encroachment along the left side of the channel as well as the formation of more clearly defined bars and islands. Between 1992 and 2002, the left channel has deepened considerably and become the dominant channel, while vegetation has continued to encroach and become established along the banks and islands, indicating that the channel has evolved into Stage M4 single thread channel. The channel cross-section from 2012 shows additional channel degradation (increased bank height), narrowing, and lateral migration indicating that the channel has evolved into Stage M5.

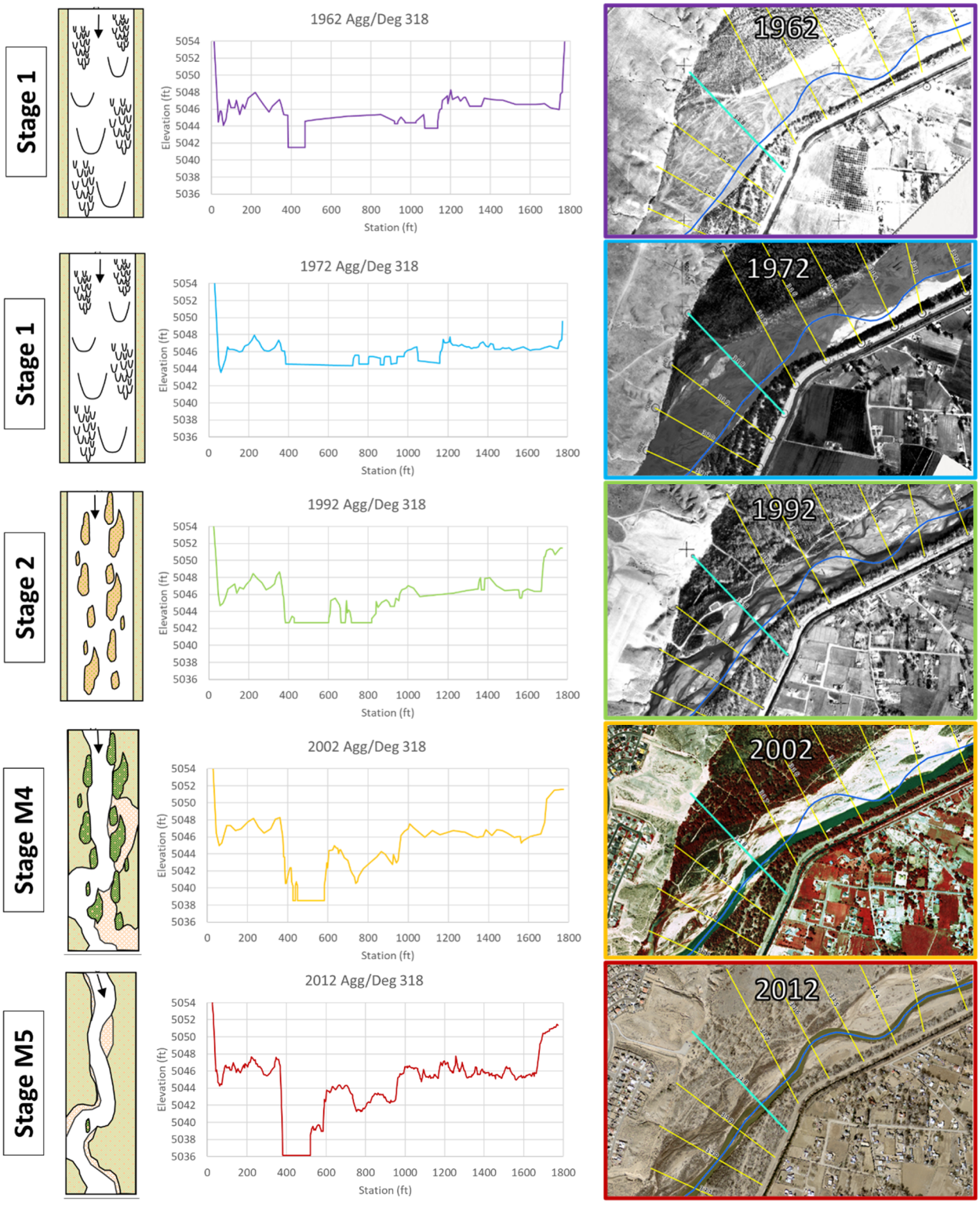

Figure 3-27 Subreach B1: Massong et al. (2010) classification (left), historical cross section profiles (center) and corresponding aerial images with channel centerline shown in blue (right) at Agg/Deg 318

Figure 3-28 shows the evolution of the channel in Subreach B2 using a representative cross section at Agg/Deg 368 for the evaluated years.

Subreach B2 is currently bound by potential grade controls, the Corrales Siphon on the upstream end, and the AMAFA North Diversion Channel outfall on the downstream end. In Subreach B2, the channel neither aggraded nor degraded between 1962 and 1972 at Agg/Deg 368. Between 1972 and 2012, the channel gradually degraded, narrowed, and became more clearly distinguishable from the floodplain. Approximately 3 feet of degradation occurred between 1972 and 1992. The channel and floodplain remain relatively static between 1992 and 2002, with approximately 2 feet aggradation filling a side-channel within the left floodplain (between stations 400 ft and 600 ft). Between 2002 and 2012, the right channel degrades by 1 foot and becomes more dominant, while the left channel (between stations 650 ft and 850 ft) begins to shrink. A total of 5 feet of degradation occurred in the 40 years between 1972 and 2012.

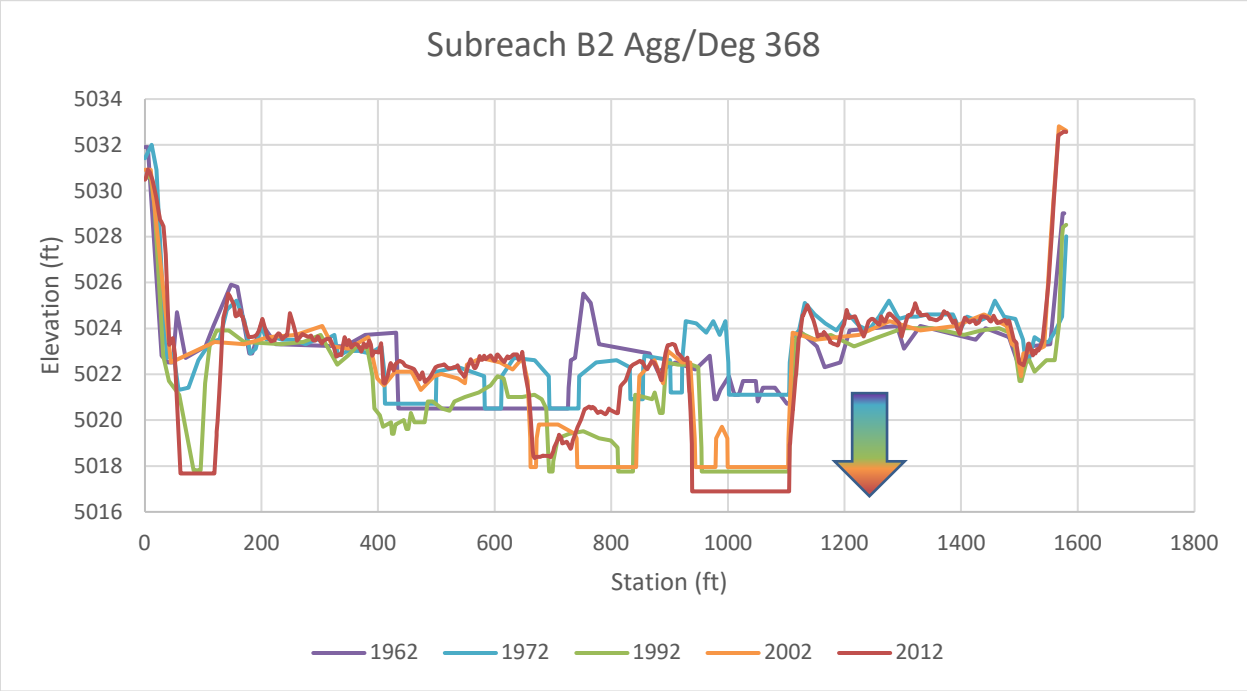

Figure 3-28 Subreach B2: Channel evolution of representative cross section Agg/Deg 368. Significant channel degradation and narrowing occurred between 1972 and 2012. Note: it appears that the side channel thalweg at station 100 ft was missed in the 2002 survey.

Figure 3-29 gives a synthesis of the likely channel form based on the Massong classification (left), the channel cross section (center) and aerial imagery (right) for Agg/Deg 368 in Subreach B2 for each evaluated year.

Between 1962 and 1972, Subreach B2 appears to be in Stage 1, with a wide, undefined channel and transient bars and islands. Between 1972 and 1992, the channel has shifted into Stage 2, with the formation of more clearly defined braids, bars, and islands. The channel in 2002 appears to be at Stage 3. Some of the side channels have aggraded, and vegetation is well-established along the banks and islands. At Agg/Deg 368, the flow is split into two evenly sized channels, with neither yet becoming the dominant flow path. In 2012, the right channel at station 1050 ft has become more dominant, indicating that the channel is transitioning into Stage M4, though there are still side channels that become inundated during relatively low flood events along the left floodplain.

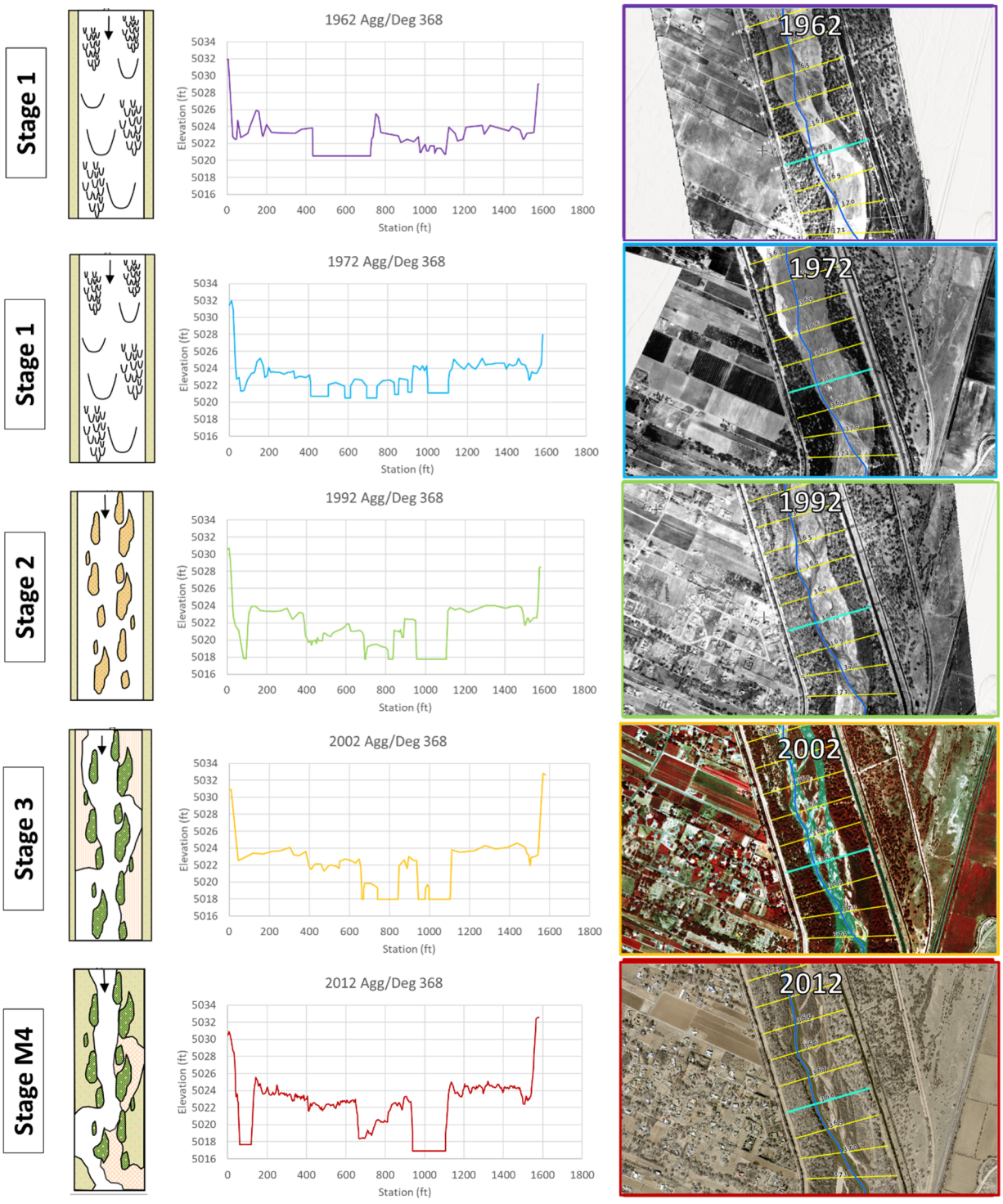

Figure 3-29 Subreach B2: Massong et al. (2010) classification (left), historical cross section profiles (center) and corresponding aerial images with channel centerline shown in blue (right) at Agg/Deg 368

Figure 3-30 shows the evolution of the channel in Subreach B3 using a representative cross section at Agg/Deg 418 for the evaluated years.

In Subreach B3, the channel aggraded by 2 feet between 1962 and 1972 at Agg/Deg 368. The 1962 cross-section shows a more clearly defined low flow channel that is approximately 60 feet wide and 2 foot deep. In contrast, the 1972 cross-section shows no clearly defined low flow channel. Between 1972 and 1992, the channel degraded by 3 feet and became more clearly distinguishable from the floodplain. The channel and floodplain remain relatively static between 1992 and 2002, with approximately 1 foot of aggradation at the mid-channel island between stations 700 ft and 800 ft. Between 2002 and 2012, 1 foot of aggradation has occurred in the channel. This is due to construction of the ABCWUA Adjustable Height Dam in 2005, which is located approximately 2,000 feet downstream of Agg/Deg 418 at Agg/Deg 422. While approximately 2-3 feet of net degradation has occurred in this reach over the last 40 years, the channel width has not been impacted as significantly as the channel in Subreaches B1 and B2.

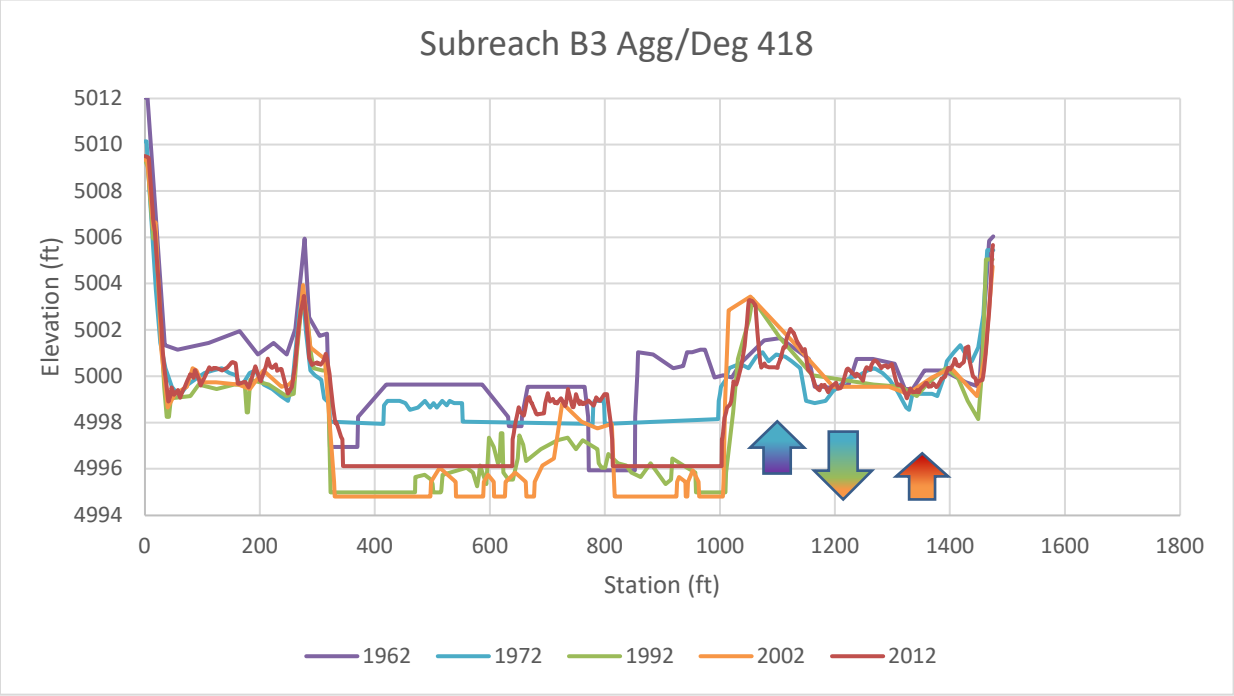

Figure 3-30 Subreach B3: Channel evolution of representative cross section Agg/Deg 418. Note less degradation and narrowing than seen in Subreaches B1 and B2.

Figure 3-31 gives a synthesis of the likely channel form based on the Massong classification (left), the channel cross section (center) and aerial imagery (right) for Agg/Deg 418 in Subreach B3 for each evaluated year.

Between 1962 and 1972, Subreach B3 appears to be in Stage 1, with a wide, undefined channel and transient bars and islands. Between 1972 and 1992, the channel has shifted into Stage 2, with the formation of more clearly defined braids, bars, and islands. The channel in 2002 and 2012 appears to be at Stage 3. Vegetation is well-established along the banks as well as the large mid-channel island. At Agg/Deg 418, the flow is split into two evenly sized channels, with neither yet becoming the dominant flow path. This subreach of the Bernalillo Reach appears not to be evolving as quickly into a meandering channel as Subreach B1 and B2. This process is likely slowed or halted by the construction of the ABCWUA Adjustable Height Dam directly downstream, which will prevent the channel from degrading further below the sill height for the section of channel that is directly upstream of the dam.

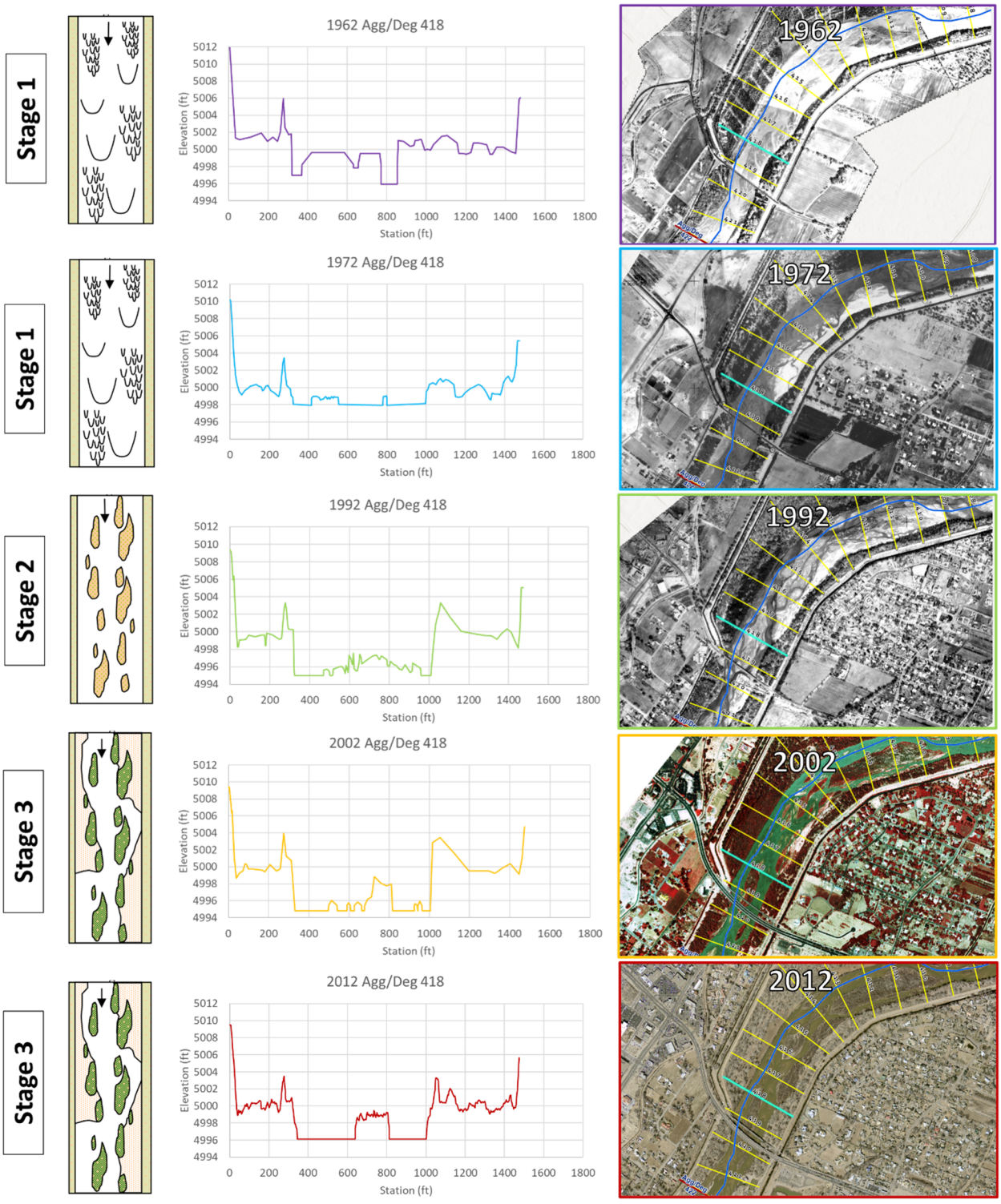

Figure 3-31 Subreach B3: Massong et al. (2010) classification (left), historical cross section profiles (center) and corresponding aerial images with channel centerline shown in blue (right) at Agg/Deg 418

Figure 3-32 shows the evolution of the channel in Subreach B2 using a representative cross section at Agg/Deg 442 for the evaluated years.

In Subreach B4, the channel aggraded between 1962 and 1972. The 1962 cross-section shows a more clearly defined low flow channel that is approximately 100 feet wide and 2 feet deep. In contrast, the 1972 cross-section shows a much wider channel with no clearly defined low flow channel. Between 1972 and 1992, the channel degraded by 2 feet and formed a deeper main channel (right) and side channel (left). Roughly 0.5 feet of degradation occurred between 1992 and 2002. Between 2002 and 2012 the channel did not degrade at Agg/Deg 442, but the left side channel, previously 100 feet wide in 2002, aggrades and becomes incorporated into the floodplain in 2012. Overall, a total of 3 feet of degradation occurred in the 40 years between 1972 and 2012.

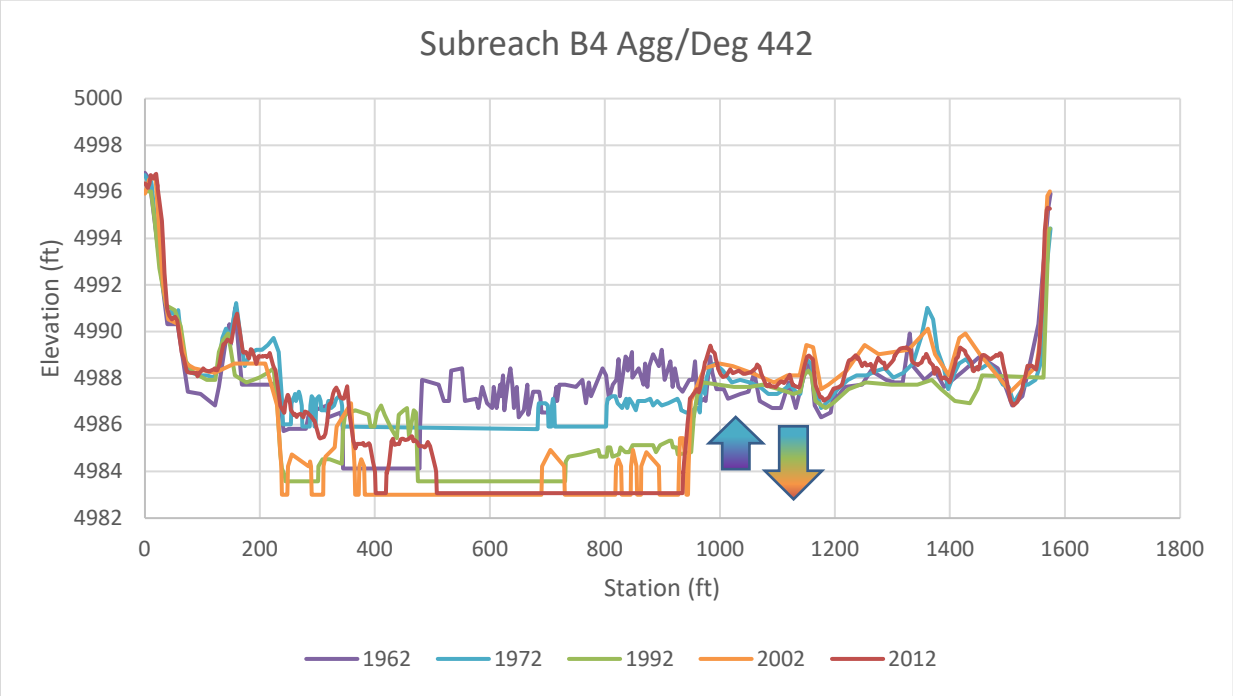

Figure 3-32 Subreach B4: Channel evolution of representative cross section Agg/Deg 442.

Figure 3-33 gives a synthesis of the likely channel form based on the Massong classification (left), the channel cross section (center) and aerial imagery (right) for Agg/Deg 442 in Subreach B4 for each evaluated year.

Although Agg/Deg 442 appears to be located at a narrow section of the channel in 1962, overall, Subreach B4 appears to be in Stage 1 at this time. By 1972, Agg/Deg 442 has widened considerably, likely due to a large flood event. The channel in 1972 is wide and undefined, again indicating a Stage 1 plan form. Between 1972 and 1992, the channel has shifted into Stage 2, with the formation of more clearly defined braids, bars, and islands. The channel in 2002 appears to be at Stage 3 based on the cross-section and aerial imagery, which shows vegetation establishment on the islands. Unlike Subreach B3, Subreach B4 appears to be transitioning into Stage M4 in 2012 as side channels begin to aggrade and the right main channel becomes more dominant. However, the channel remains wide at this location and does not show the same level of degradation and narrowing that is seen in Subreaches B1 and B2.

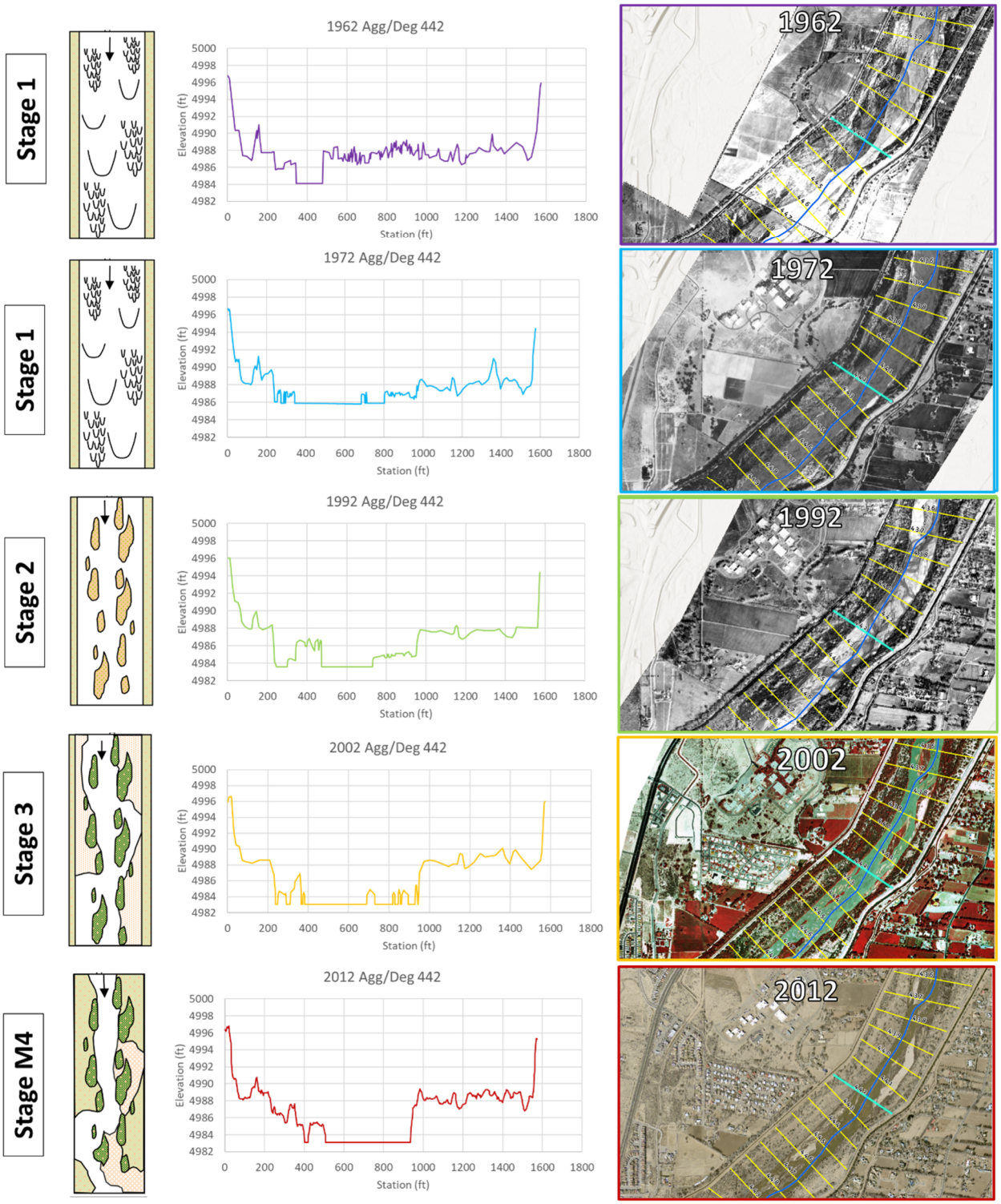

Figure 3-33 Subreach B4: Massong et al. (2010) classification (left), historical cross section profiles (center) and corresponding aerial images with channel centerline shown in blue (right) at Agg/Deg 442

4 HEC-RAS Modeling for Silvery Minnow Habitat

The Rio Grande Silvery Minnow (RGSM or silvery minnow) is an endangered fish species that is native to the Middle Rio Grande. Currently, it occupies only about seven percent of its historical range (U.S. Fish and Wildlife Service, 2010). It was listed on the Endangered Species List by the US Fish and Wildlife Service in 1994.

One of the most important aspects of silvery minnow habitat is the connection of the main channel to the floodplain. Spawning is stimulated by peak flows in late April to early June. These flows should create shallow water conditions on the floodplains, which is ideal nursery habitat for the silvery minnow (Mortensen et al., 2019). Silvery minnows require specific velocity and depth ranges depending on the life stage that the fish is in. **Table 4-1** outlines these velocity and depth guidelines. Fish population counts are available prior to 1993 to the present. Therefore, analysis of silvery minnow habitat will not begin prior to 1992. In preparation for the process linkage report, figures relating the geomorphology of the river and RGSM habitat availability are included in **Appendix F**.

Table 4-1 Rio Grande Silvery Minnow habitat velocity and depth range requirements (from Mortensen et al., 2019)

	Velocity (cm/s)	Velocity (ft/s)	Depth (cm)	Depth (ft)
Adult Habitat	<40	<1.31	>5 and <60	>0.16 and <1.97
Juvenile Habitat	<30	<0.98	>1 and <50	>0.03 and <1.64
Larvae Habitat	<5	<0.16	<15	<0.49

4.1 Modeling Data and Background

The data available to develop these models varies year by year. Cross section geometry was available for the years 1962, 1972, 1992, 2002, and 2012. In 2012, additional LiDAR data of the floodplain was available, which allowed the development of a terrain for RAS-Mapper. Therefore, RAS-Mapper was used in 2012 only, while comparisons across years are done using 1-D techniques. See **Appendix G** for information on boundary conditions and manning's n values.

4.1.1 Levee and Ineffective Flow Analysis

HEC-RAS distributes water within the channel by filling each available cross section from the lowest elevation upwards. Because HEC-RAS fills cross-sectional area from the bottom up, it is possible to show flow in low-lying areas when in reality the area is disconnected from the main channel. Ineffective areas were used to address this by setting them at an elevation that roughly prevented effective flow in these low-lying areas when the area in upstream cross-sections were not inundated. These areas of ineffective flow were excluded from the habitat analysis. However, due to the two-dimensional nature of split flow, this procedure is a highly iterative process in 1D modeling, and some disconnected areas remained during certain analyzed flows. Much of the MRG is either perched or has been altered with levees, so this can lead to inaccurate predictions of the flow distribution within the cross sections (overpredicting water in the floodplains), therefore, overpredicting hydraulically suitable habitat. However, these disconnected areas that remain in the analysis can be beneficial in that they have potential for indicating future restoration projects. See **Section 4.6** for additional discussion on disconnected areas.

Initial analysis of the years 1962 – 2012 showed that the years 1962, 1972, and 2012 were most likely overpredicting the amount of floodplain inundation in the two upstream subreaches. The initial no levee HEC-RAS top width results were compared with the width defined by vegetation from **Section 3.2** and cross checked with aerial imagery to determine that some areas of disconnected flow would not naturally

occur due to bridge crossings, tributary outlets, levees, etc. Computational levees were used in HEC-RAS geometries for 1962 and 1972 to keep the water contained in the channel until bankfull is reached. Most of the levee adjustments occurred along the right floodplain in the B1 and B2 subreaches where the floodplain is wide. At this location, the newly constructed Highway 550 and a new ditch connection to the river effectively cut off a large, wide side channel along the right bank. Without levee placement, this resulted in unrealistic predictions of wide, shallow flow and model results that were likely not representative of actual conditions at the site. The computational levees were either placed at the high points along the bank closest to the channel or at an elevation of a high point in the cross section upstream where there isn't a flow path connecting the two in the aerials.

By 2012, the channel had narrowed and deepened, which disconnected many of the side channels at lower flood events. However, as discussed above, since a 1-D HEC-RAS model fills from the bottom up, sections of the side channels were beginning to fill at lower flood events despite not being connected to the main channel upstream or downstream. To resolve this, ineffective flow areas were added along the floodplains. The elevation of ineffective areas were generally set at elevations that allowed for flow conveyance when flow was connected, but prevented flow conveyance at lower flow events when these areas were not connected upstream to downstream.

4.2 Width Slices Methodology

Without a terrain for 1962-2002, additional methods had to be considered to determine a metric of fish habitat in area per distance and in length of river. HEC-RAS has the capability to perform a flow distribution analysis to calculate the laterally varying velocities, discharges, and depths throughout a cross section as described in chapter 4 of the HEC-RAS Hydraulic Reference Manual (US Army Corps of Engineers, 2016). HEC-RAS allows each cross-section to be divided into 45 slices. Although other reaches of the RGSM relies heavily on floodplains for habitat (due to higher velocities and depths in the main channel), the Bernalillo Reach main channel contains more variability than the floodplains contain, so 10 width slices were assigned in each floodplain and 25 width slices were assigned in the main channel. An example of the flow distribution in a cross-section is shown in **Figure 4-1**. The velocity and depth of each slice were analyzed to determine the total width at each agg/deg line that meets the RGSM larval, juvenile, and adult criteria. Because the agg/deg lines are spaced approximately 500 feet apart, the hydraulically suitable widths were multiplied by 500 feet to obtain an area of hydraulically suitable habitat per length of river.

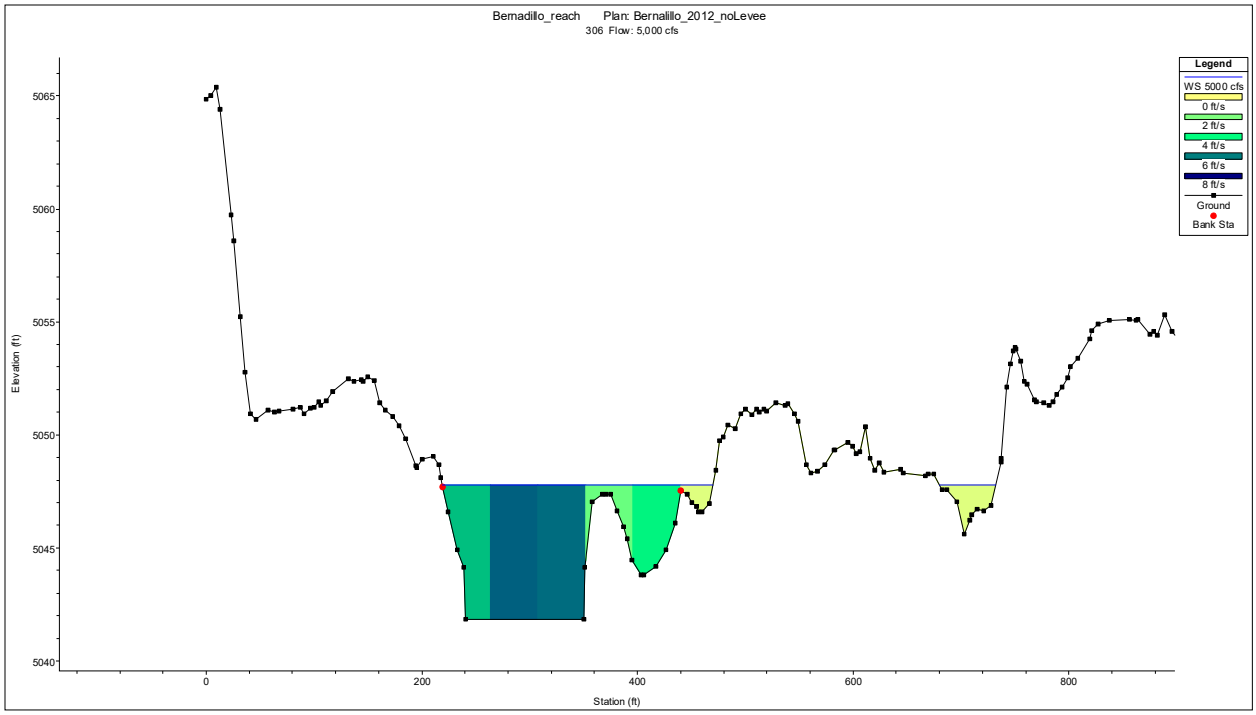

Figure 4-1 Cross-section with flow distribution from HEC-RAS with 20 vertical slices in the floodplains and 25 vertical slices in the main channel. The yellow and green slices are small enough that the discrete color changes look more like a gradient.

4.3 Width Slices Habitat Results

The width slices method was first used to analyze the habitat availability throughout the Bernalillo Reach at a reach scale for the years of 1962, 1972, 1992, 2002, and 2012. For the discharges at which the water is contained in the main channel, there is less habitat availability. In general, when the discharge increases and the water can spill out onto the floodplains, there is suddenly an increase in area where the depth and velocity criteria are met, as shown in **Figure 4-2 to Figure 4-4** below. For the years 1992 – 2012, increased flow in the channel resulted in an increase in habitat availability. For the earlier years, there is a steady increase in habitat availability with flow until 8,000 cfs, then the availability decreases as the depths and velocity exceed the Rio Grande Silvery Minnow habitat velocity and depth range requirements.

Throughout the Bernalillo Reach, the results follow a similar trend for larvae, juvenile, and adult stage habitat. There was more habitat availability during the years of 1962 and 1972. There is a dramatic decrease in habitat between 1972 and 1992, which corresponds to the degradation and the decrease in active top width that the reach experiences during that time frame due to the construction of Cochiti Dam. See **Section 3** for more information on the change in channel characteristics between time periods. There is limited available larvae habitat in comparison to the juvenile and adult available habitats, although it slightly increases as the flow increases through the channel and more of the floodplain is activated. As seen in **Figure 3-17** in **Section 3.6**, as flow increases, the hydraulic depths do not change by a large amount, so the there is more consistent habitat available.

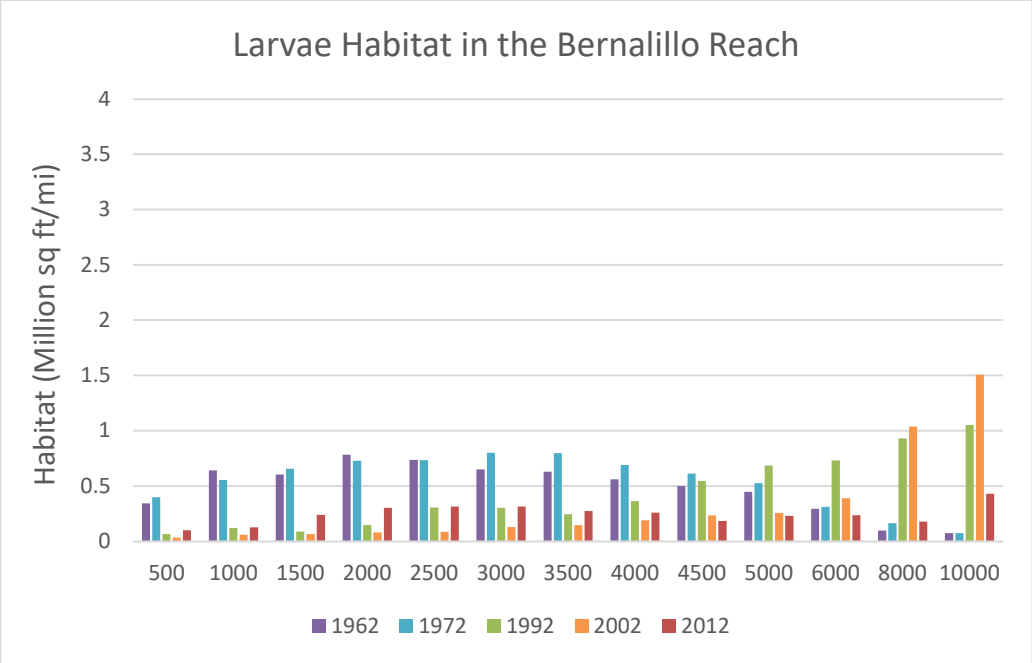

Figure 4-2 Larval RGSM habitat availability throughout the Bernalillo Reach

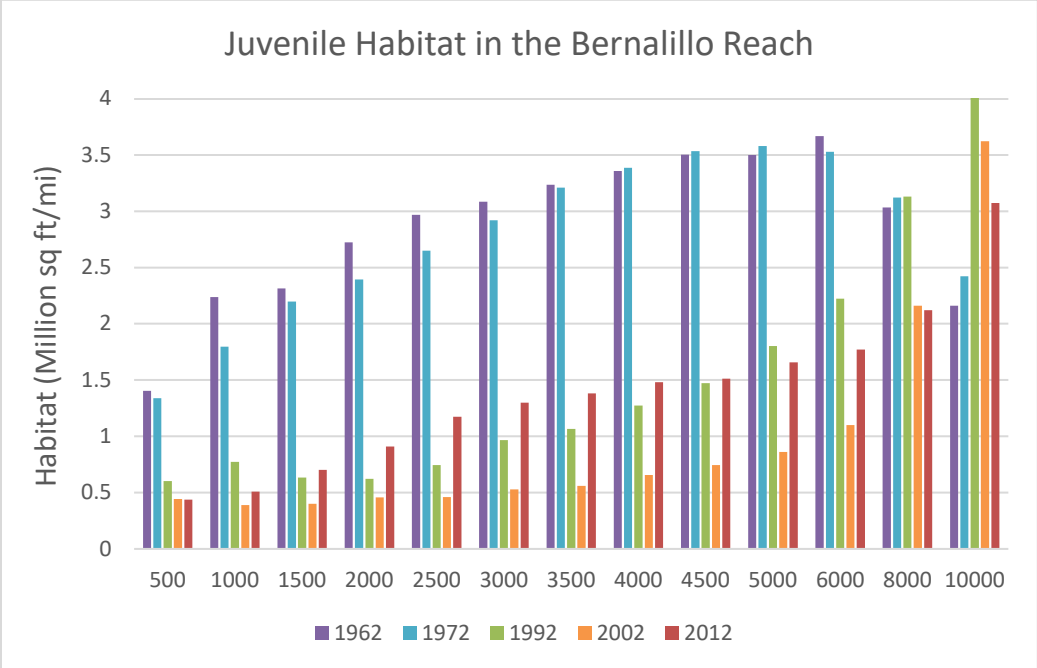

Figure 4-3 Juvenile RGSM habitat availability throughout the Bernalillo Reach

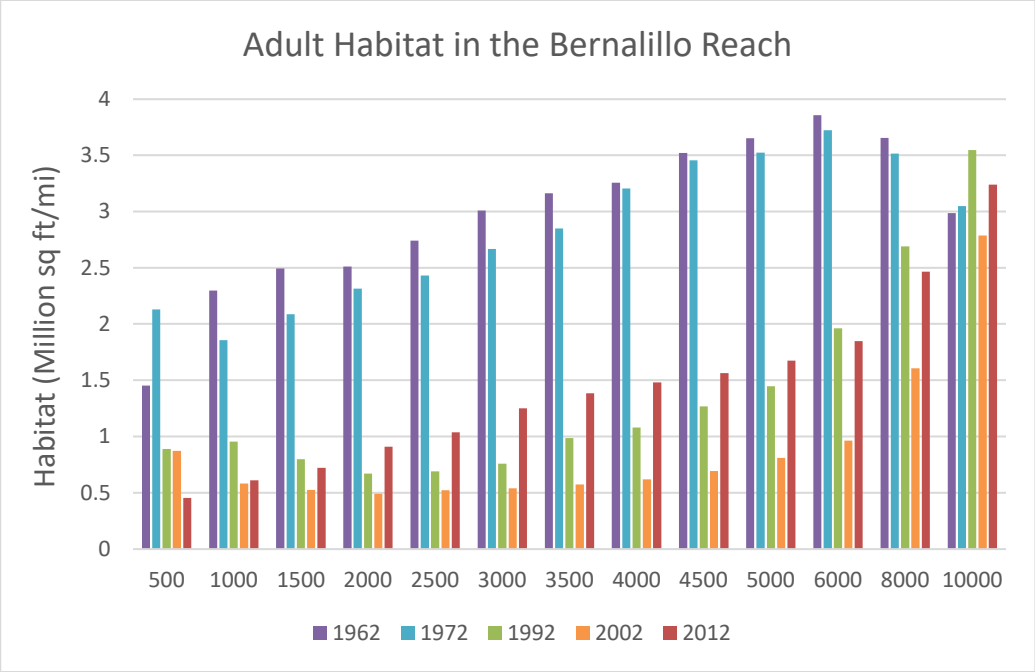

Figure 4-4 Adult RGSM habitat availability throughout the Bernalillo Reach

The width slices method was also used to analyze the habitat availability throughout the Bernalillo Reach at a subreach level. Stacked habitat bar charts were created to portray the spatial variation of hydraulically suitable habitat of the RGSM throughout the Bernalillo Reach. The bar charts display the width of habitat at different discharges for 2012. To convert the hydraulically suitable habitat to an area, these values would be multiplied by 500 ft, which is approximate the distance between each agg/deg line. **Figure 4-5** shows the 2012 habitat availability from 500 cfs to 10,000 cfs for Subreaches B1 through B4.

Based on this method, applied to the 2012 data, Subreach B3 consistently had the most hydraulic suitable habitat for larvae, juvenile, and adult life stages at the discharges lower than 1500 cfs. Above 1500cfs, Subreaches B2 and B3 had the most juvenile and adult hydraulic suitable habitat and had similar magnitudes while B1 and B2 offered more larva habitat during those flows. At 10,000 cfs, B4 had a similar magnitude as B2 and B3 for the juvenile and adult life stages. For the larvae, B1 spiked to the highest magnitude at 10,000 cfs.

The channel form of B2 and B3 may be more efficient at reaching the RGSM's habitat criteria of velocity and flow depth for the juvenile and adult life stages, while B1 and B2 may be for efficient for the larvae. As seen in **Section 3.9**, B1 and B2 generally have wider floodplains, so this indicates that the floodplains are most suitable for the larvae while the channels might be more suitable for the juveniles and adults. Additional bar charts for all subreaches and life stages are located in **Appendix D**.

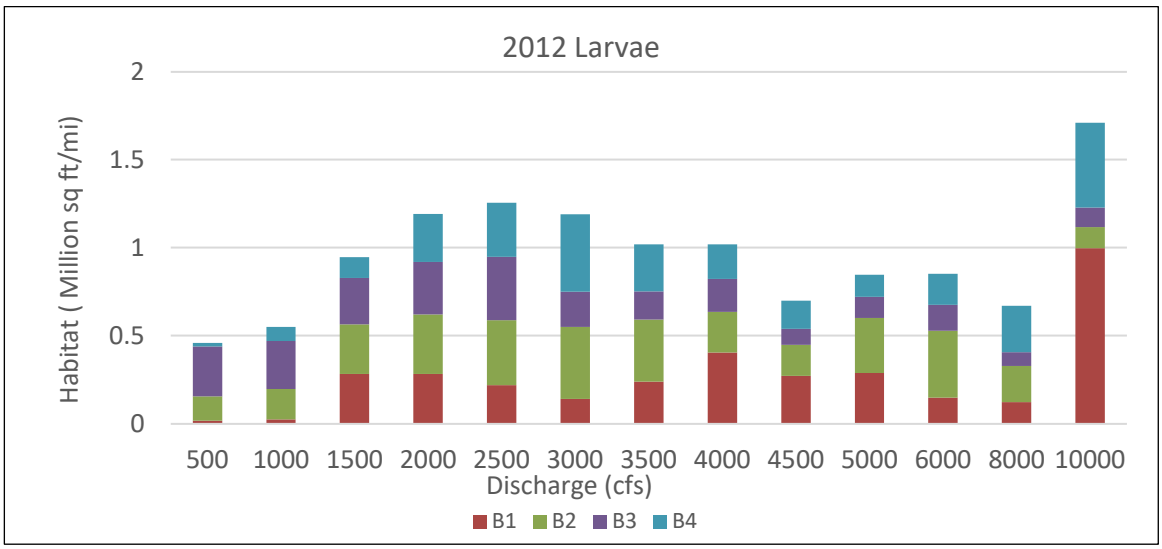

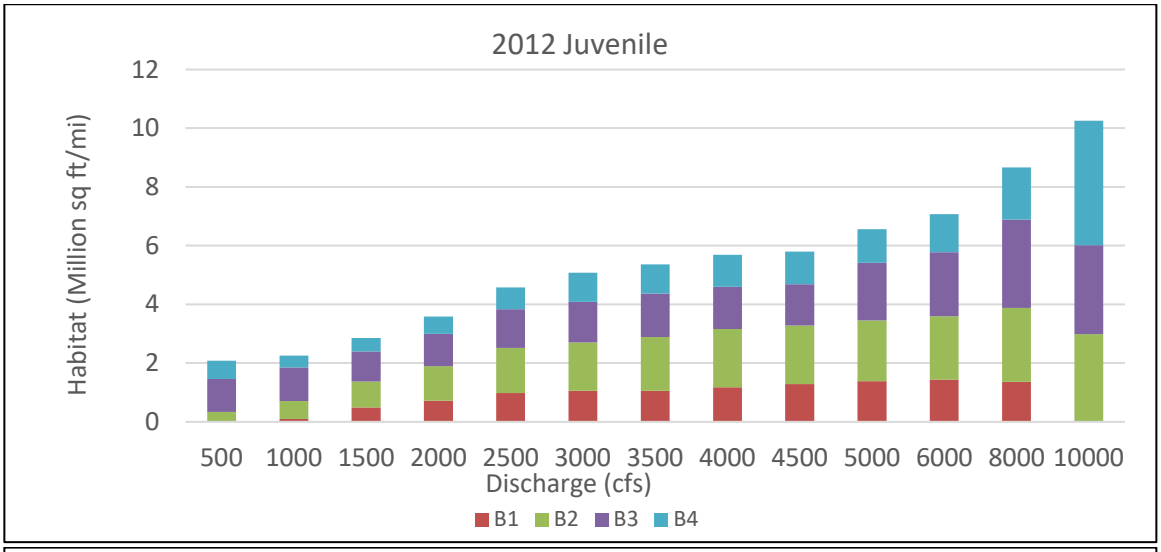

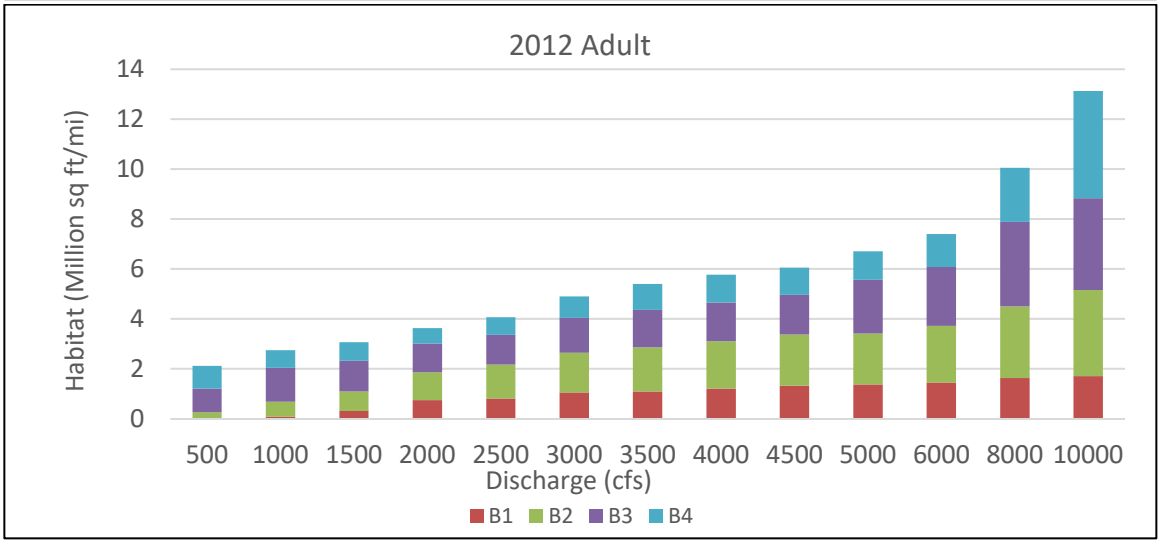

Figure 4-5 Stacked habitat charts at different scales to display spatial variations of habitat throughout the Bernalillo Reach in 2012

4.4 RAS-Mapper Methodology

By using RAS-Mapper, the goal was to transform the 1-D habitat estimates into pseudo two-dimensional (2-D) results. RAS-Mapper overlays the water onto a prescribed terrain and interpolates the water surface elevation to create an estimate of the location of water inundation, which can then be used to predict locations of hydraulically suitable habitat for the Rio Grande Silvery Minnow (RGSM).

The HEC-RAS geometry data that was necessary for the RAS-Mapper analysis (geo-referenced cross-sections and a LiDAR surface to generate a terrain) was available only for the year 2012. Therefore, only 2012 results were processed in RAS-Mapper. The original 2012 LiDAR data was used to develop a raster on ArcGIS Pro software (intellectual property of ESRI), which could be imported as a terrain from RAS-Mapper. The RAS-Mapper application distributes the water throughout the terrain, interpolating between the cross-sections, which results in a more thorough understanding of where water is present in a channel.

RAS-Mapper will also predict the flow depth and velocity at a given discharge. It should be noted that while the cross-sectional data has a low-flow channel stamped into each cross section, the LiDAR surface used for mapping does not include channel data below the water surface. As a result, the water depth in the channel generated from RAS-Mapper underestimates the flow depth by around 2 feet throughout the entire reach and will not show accurate habitat mapping within the main channel. Given that suitable habitat is generally found in the floodplain, this was not as great of a concern. Additionally, the habitat graphs discussed in **Sections 4.2** and **4.3** account for the low flow channel and are therefore not subject to this same error.

ArcGIS Pro was used to combine the RAS-Mapper generated raster datasets for velocity and depth so that RGSM depth and velocity criteria could be applied to identify the areas of potential suitable habitat. The results were used to create maps that show the areas of hydraulically suitable habitat for each life stage of the RGSM throughout the Bernalillo Reach.

4.5 RAS-Mapper Habitat Results in 2012

While the width slice method quantitatively determined areas with increased potential for habitat, RAS-Mapper was used to spatially depict the areas of potential RGSM habitat throughout the Bernalillo Reach of the MRG and display the results on a map of the river. The hydraulically suitable habitat for each life stage was mapped at discharges of 1,500 cfs, 3,000 cfs, and 5,000 cfs, which have post-dam daily exceedance probabilities of around 20.2%, 9.9%, and 3.3%, respectively (**Figure 2-17**). The habitat maps for each reach at these discharges are available in Appendix E.

The hydraulically suitable habitat is primarily seen in the side channels where velocities are slower and channel depths are smaller. According to the RAS-Mapper results and the habitat graphs (**Figure 4-5**), there is more hydraulically suitable habitat for all life stages in Subreaches B2 and B3 than there are in Subreaches B1 and B4. B1 shows the least amount of suitable habitat for juveniles and adults at the more frequent 1,500 cfs magnitude flood events, although it does show more potential for larvae habitat along the side channels. The 2,000 cfs to 3,000 cfs range of flood events show the most potential for larvae habitat among the four subreaches, while suitable larvae habitat is generally reduced as flow depth increases within the side channels at higher magnitude flood events. Conversely, suitable habitat for juveniles and adults generally increases with increased flood magnitude.

Figure 4-6, **Figure 4-7**, and **Figure 4-8** show an example of potentially suitable habitat at the downstream section of Subreach B2 at flow rates of 1,500 cfs, 3,000 cfs, and 5,000 cfs, respectively. At this location, the greatest degree of larvae suitable habitat occurs at 1,500 cfs, and generally begins to disappear as flow

rate increases. A greater amount of juvenile and adult habitat can be found along the side channels at 3,000 cfs as these channels become more activated. At 5,000 cfs, suitable habitat begins to shift from the side channels to the islands, which become submerged at the higher flow rate. This results in an overall increase in juvenile and adult habitat at 5,000 cfs.

All habitat mapping for the Bernalillo Reach of the MRG can be found in **Appendix E**.

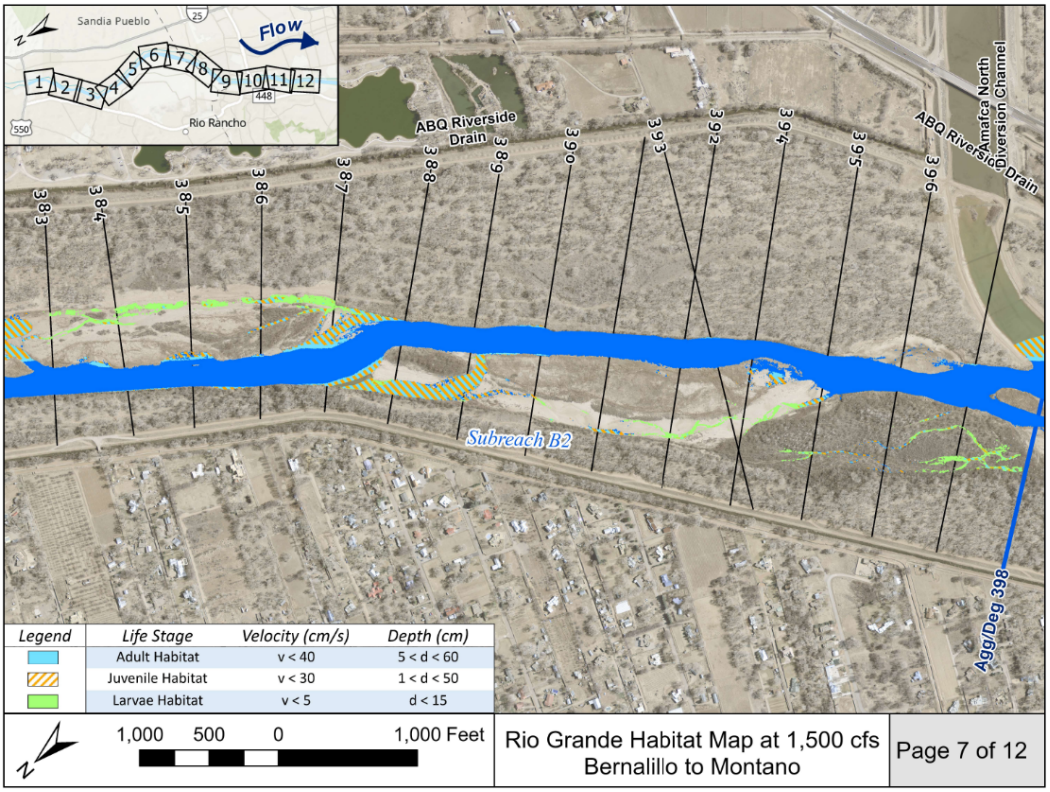

Figure 4-6 Suitable habitat in 2012 for each life stage at 1,500 cfs at the downstream section of B2. Dark blue inundation area are not suitable for habitat at any life stage.

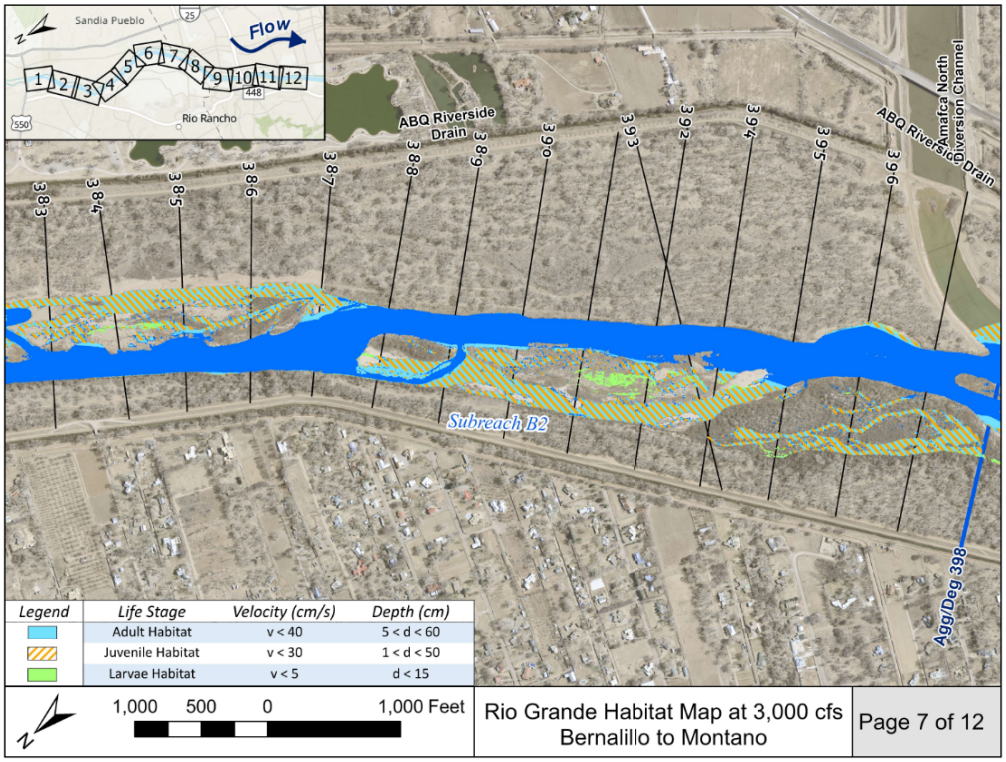

Figure 4-7 Suitable habitat in 2012 for each life stage at 3,000 cfs at the downstream section of B2. Dark blue inundation area are not suitable for habitat at any life stage.

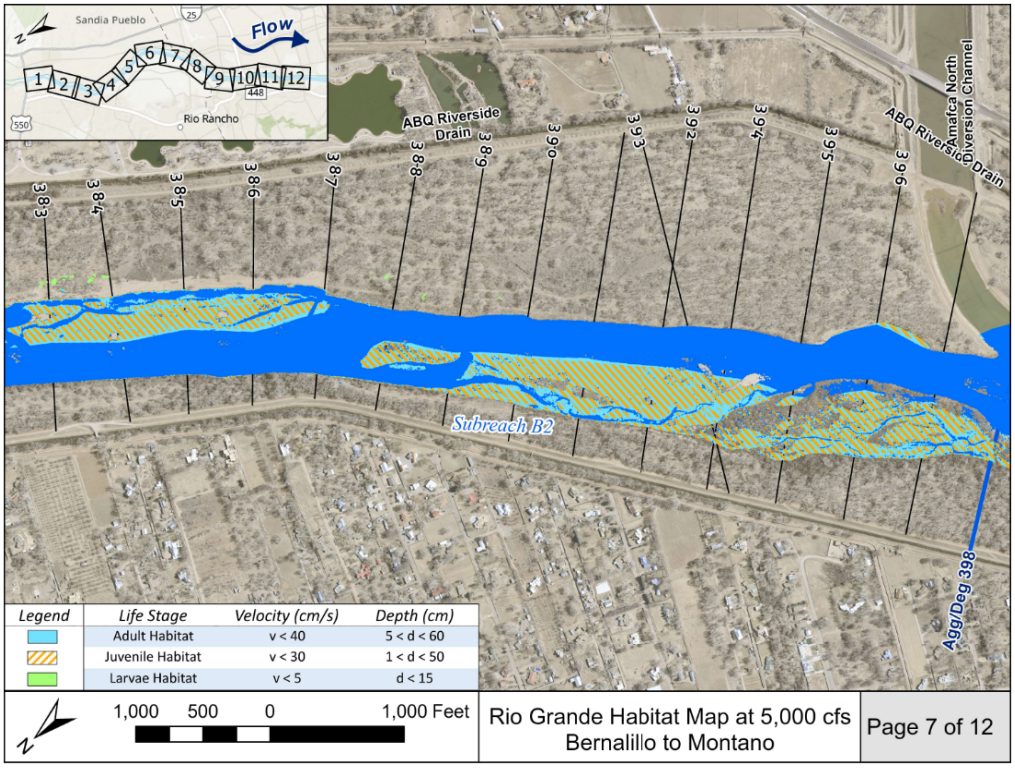

Figure 4-8 Suitable habitat in 2012 for each life stage at 5,000 cfs at the downstream section of B2. Dark blue inundation area are not suitable for habitat at any life stage.

4.6 Disconnected Areas

RAS-Mapper provides the opportunity to identify areas that likely meet the velocity and depth requirements of the RGSM at specified discharges. RAS-Mapper may also be beneficial for identifying areas throughout the reach than may contain water but are not connected to the main channel (see **Section 4.6**). These may be possible areas of focus for restoration efforts to increase habitat potential.

By connecting several of these disconnected areas, the RGSM may gain a great amount of possible habitat. **Figure 4-9** shows one instance of a disconnected area in Subreach B2. The disconnected area is emphasized by the red rectangles. These low-laying areas appear to contain side channels that historically became inundated at lower magnitude flood events, but over time have become disconnected from the main channel due to aggradation. The disconnected areas could identify problem areas for the RGSM by indicating that there are areas where fish may become stranded in months when the river contains less water and disconnected areas form. Conversely, these areas could become possible restoration sites leading to an increase in hydraulically suitable RGSM habitat.

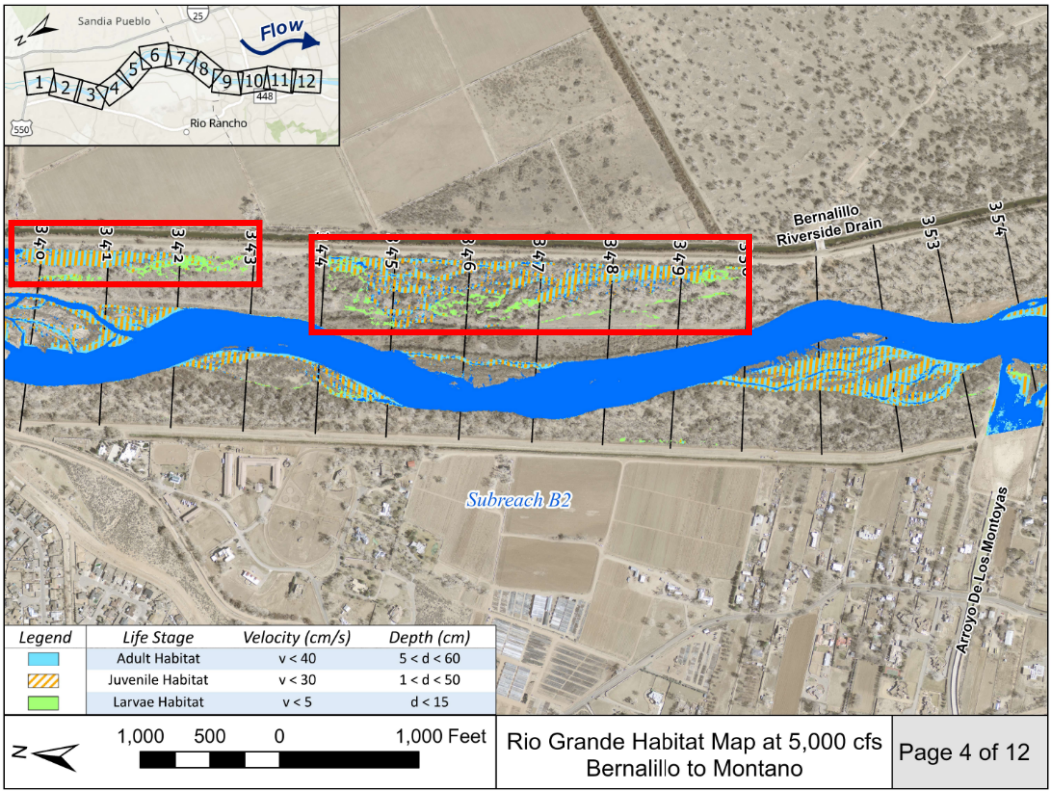

Figure 4-9 Disconnected low-laying areas that are no longer connected to the main channel at 5,000 cfs in Subreach B2.

Figure 4-10 shows another example of a disconnected area in Subreach B3. If this area were to be reconnected to the floodplain through restoration efforts, it may be particularly beneficial in increasing suitable larvae habitat at this location.

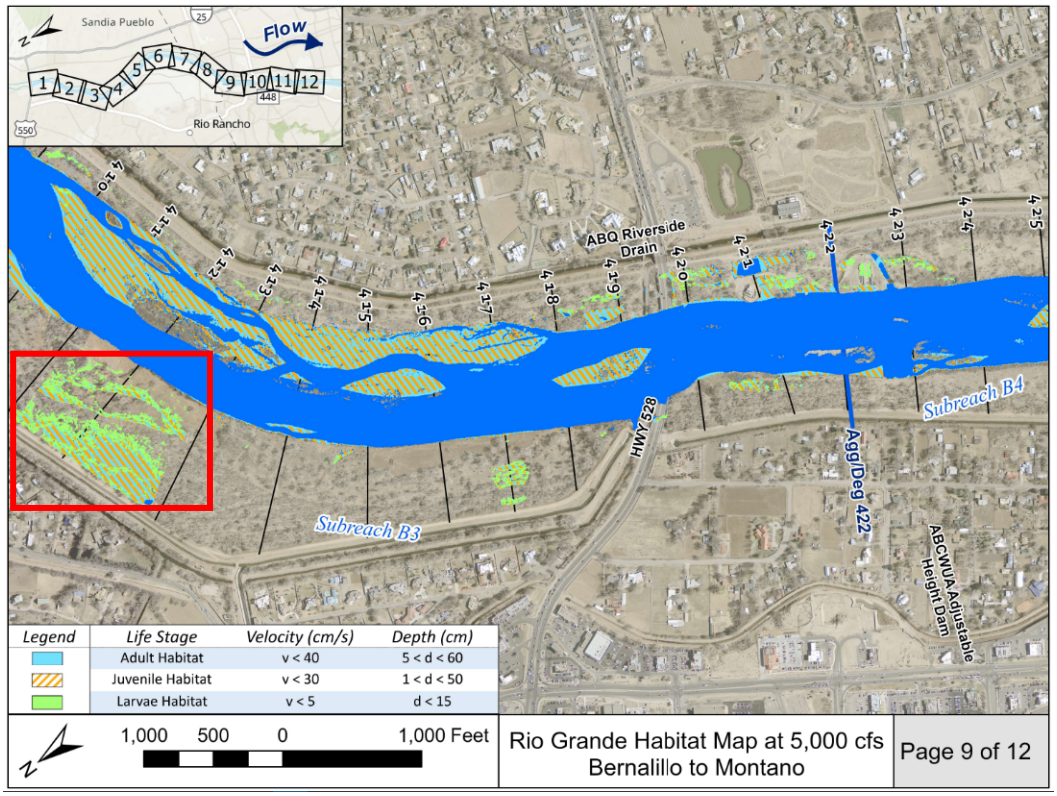

Figure 4-10 Disconnected low-laying areas that are no longer connected to the main channel at 5,000 cfs in Subreach B3.

5 Bernalillo Reach Synthesis

In the Bernalillo Reach, the channel morphology is influenced by upstream reservoir construction, flow diversions, channel maintenance, and periods of drought and high annual flow volumes. Changes in flow peaks, annual flow volume, and sediment supply have influenced channel width, depth, and velocity. The flow and sediment drivers have caused changes in bed elevation, which has altered the discharge at which flows overbank the channel and access the floodplain. In this section, results presented throughout the report are synthesized to link the effects of the geomorphic drivers (sediment and water supply) with the observed changes in channel morphology.

5.1 Hydrology

The first step in understanding the underlying processes driving changes to the Bernalillo Reach is to examine trends in the hydrology. Raster hydrographs shown in **Section 2.2.2** show that the Rio Grande typically experiences higher flows from snowmelt runoff in April through June, low flows throughout the late summer months, and medium flows through the winter. Historically the Rio Grande experienced greater flow variability and larger magnitude flood events than it does in present day. This is due in large part to the construction of the Cochiti Dam (**Figure 2-8**). Between 1926 and 1970, the Bernalillo Reach of the MRG experienced 11 flood events with an average daily peak greater than 10,000 cfs in 44 years (**Figure 2-7**). In other words, a flood event greater than 10,000 cfs occurred, on average, once every four years. Between 1970 and present day, this reach of the Rio Grande has not experienced a flood event greater than 9,000 cfs in 52 years of gage record (**Figure 2-8**).

While the largest flood events are clearly impacted by the upstream dam, smaller floods and lower flows do not appear to be significantly impacted by the dam. This can be seen clearly in the flow duration relationships described in **Section 2.2.5** and shown by **Table 2-2** and **Figure 2-17**. Prior to completion of the dam, the 1% daily exceedance probability for this reach was around 9,300 cfs where-as after completion, the 1% exceedance probability was closer to 6,200 cfs. A daily exceedance probability of 10% is roughly the point where pre- and post-dam flood magnitudes begin to diverge. The flow duration curve shown in **Figure 2-17** indicates that flows roughly greater than 3,000 cfs (10% daily exceedance probability) are reduced due to impacts from the dam, while flows less than 3,000 cfs are not noticeably impacted.

The Rio Grande has cycled through wetter and drier periods, which can be seen clearly in the cumulative discharge curves described in **Section 2.2.4**. Between 1926 and 1970, the daily discharged averaged at around 1,100 – 1,300 cfs, with the exception of an uncharacteristically wet period between 1941 and 1942, which had a daily average discharge of 3,900 cfs. This timing corresponds with the two largest flood events in the gage record. Between 1970 and 1979, the average discharge is reduced to around 970 cfs. Following this drier period there is a 16-year span of time of larger flows between 1979 and 1995, where the average daily discharge is around 1,700 cfs. Much of the period between 1995 and present day can be characterized as a drought. During this time, the average daily flow rate was around 970 cfs.

5.2 Sediment Load

As previously determined from the cumulative discharge plot in **Section 2.2.1**, the large increases in flow in the Bernalillo and Montaño Reaches occurred in the spring from snowmelt, with some increases in the summer from seasonal thunderstorms. Spring snowmelt typically supplies the greatest water and sediment discharge volumes, and some occasional monsoonal thunderstorms often transport the greatest concentration of suspended sediment for a short period of time. The sediment flux into the river seems to be primarily driven by snowmelt drains into the ephemeral tributaries and nearby arroyos that wash

sediment into the MRG. Monsoonal events occurred in both 2006 and 2014 that created large amounts of suspended sediment in the MRG.

The Jemez River outlets upstream of the Bernalillo and Montaño Reaches. In 1953, the Jemez Dam was constructed. There is not sediment data prior to the Jemez Dam construction, however, there was sediment data collected after construction. The dam was most likely restricting the sediment input into the Bernalillo and Montaño Reaches. In 2014, the Jemez dam was modified to add a low flow channel that allows for passage of both flow and sediment. This allowed the sediment from behind the dam to flush into the MRG. Given the gaps in sediment data record and the limited years of data following dam modification, it is not yet clear whether the modification has resulted in significant changes to sediment loads to the MRG. However, it is apparent that the Jemez River contributes a large portion of sediment to the MRG. Between 2014 and 2021, the Jemez River contributed roughly 38% of sediment to the Albuquerque gage while only contributing 4% of flow.

The single mass curve for the Albuquerque USGS shows a steep slope, representing an average sediment discharge of 9,380 tons/day, prior to the completion of the Cochiti Dam. After construction, the average sediment discharge decreased to about 2,590 tons/day and has stayed at a steady slope ever since. This means that although most of the sediment entering the Bernalillo and Montaño Reaches is coming from the ephemeral streams, the Cochiti Dam is likely responsible for helping to keep a constant sediment discharge throughout the reach.

5.3 Channel Morphology

Changes to the hydrology and sediment regimes impact channel morphology. Lower peak flows, lower annual flow volumes, and lower sediment loads have resulted in channel narrowing and degradation, increased mean flow depth, and decreased wetted perimeter. Subreach B1 of the Bernalillo reach has begun to experience some lateral channel migration. Lateral migration typically begins to occur when the bank height exceeds the depth of the riparian woody vegetation root zone. In all four reaches, the active channel width has decreased over time (see **Section 3.2** and **Figure 3-8**). This reduction in channel width roughly corresponds with periods of droughts, which have lower annual flows that don't have enough stream power to activate side channels and prevent encroachment of vegetation. Between 1962 and 1992, the average channel width remained fairly consistent, which roughly corresponds to a period of higher annual flow volumes (occurring roughly between 1979 and 1995). By 2001, a notable drop in channel width had occurred, corresponding to a drier period in the early 2000s and changes in channel maintenance practices. This allowed for additional vegetation encroachment and island formation (shown by **Figure 3-19** and **Figure 3-20)**. The channel widened slightly in 2005, corresponding to a relatively large flood event that occurred in 2005. This flood event likely removed some islands and vegetation but was not enough to completely remove all of the islands and vegetation that had established in the proceeding years.

The spring seasons of 2017 and 2019 both saw flood events peaking at around 6,000 cfs. These flood events may have helped to further establish and recruit vegetation along the channel bars because by 2019, vegetation had again encroached considerably and the flood events were not large enough to disrupt that process, particularly in the two upstream reaches. **Figure 3-20** indicates that between 2008 and 2019, many of the islands began to disappear. This decrease is likely a result of channel maintenance practices and vegetated islands connecting with the channel banks and becoming part of the floodplain as the channel narrows, deepens, and becomes more single-threaded.

In addition to impacting the hydrology, construction of the Cochiti Dam had a significant impact on sediment transport and bed elevation changes through the reach. Between 1962 and 1972, the Bernalillo

Reach was in the process of aggrading, with the greatest degree of aggradation occurring in Subreaches B1 and B2. This aggradation led to an increase in bed elevation and steepening in channel slope during this decade. Following the completion of the dam the channel began to incise, with the most significant channel bed degradation occurring in Subreach B1 and B2 (see **Section 3.3** and **Section 3.9**). The greatest degradation in the channel occurs at the upstream boundary of Subreach B1. In Subreach B1, the channel bed has degraded by 8 feet, on average, between 1962 and 2012 (**Figure 3-11**) and the channel slope has flattened considerably from 0.00094 ft/ft to 0.00076 ft/ft. In Subreach B2, the channel degraded by 4 feet while the channel bed slope has remained relatively stable over the decades. This could be due to the AMAFCA North Diversion Channel outlet, located at the downstream end of Subreach B2, acting as a sediment source and holding grade (pers. comm. from Ari Posner, 2023).

In 2005, the ABCWUA Adjustable Height Dam was constructed at the end of the B3 reach. Although it is just a snapshot in time and the channel bed responds to changes in dam height, the dam seems to be in the up position at the time of 2012 survey. This dam height raised the bed elevation and caused aggradation to occur immediately upstream and degradation to occur immediately downstream. Note that Subreach B3 shows the least amount of channel narrowing between 2005 and 2019 (**Figure 3-8**). This is likely to the adjustable height dam and the increased sediment loads from the AMAFCA North Diversion Channel outlet, which may be preventing further narrowing of the channel as it aggrades. In the 2012 data collection, the Corrales Siphon, located at the downstream end of Subreach B1, is exposed and is potentially acting as a grade control (pers. comm. from Ari Posner, 2023).

A coarsening of bed material from sand to gravel can also be indicative of a degrading reach as finer material is winnowed away or the channel degrades to an underlying gravel layer. This coarsening of the channel bed can slow or halt bed degradation and may eventually cause the channel to begin to meander laterally. In **Section 3.4**, **Figure 3-13 and Figure 3-14** indicate that the bed material samples collected in Subreaches B1 and B2 have ranged widely between coarse silt to coarse gravel over the years. The bed material seems to have become coarser over time. For example, in 2020, the bed material samples in B1 and B2 ranged from fine gravel to coarse gravel. Conversely, nearly all of the bed material samples collected in Subreach B3 over the years between 1990 and 2020 have been between fine sand and coarse sand.

Table 5-1 summarizes the hydrology, sediment, and geomorphic trends between 1962 and 2012. Most of the subreaches in the Bernalillo Reach follow similar trends for many of the geomorphic trends. Between the years 1962 to 1972, all the subreaches except B4 saw an increase in bed elevation, width and slope. This aligns with the high volume of suspended sediment in that time frame. All of the subreaches saw an increase in mid-channel bars and islands from the years 1972 to 2002 followed by a decrease from 2002 to 2012. Although notable trends are the change in bed elevation and slope after the construction of the ABCWUA Adjustable Height Dam in 2005.

Table 5-1 Geomorphic Trends Over Time by Subreach

	Period	Hydrology	Suspended Sediment	Change in Bed Elevation	Change in Width	Change in Slope	Change in Sinuosity	Mid-Channel Bars and Islands
Subreach B1	1962-1972	Average	High	Increase	Increase	Increase	Decrease	No Change
	1972-1992	Wet	Low	Decrease	Decrease	Increase	Increase	Increase
	1992-2002	Average	Low	Decrease	Decrease	Decrease	Decrease	Increase
	2002-2012	Drought	Low	Decrease	Decrease	Increase	Decrease	Decrease
Subreach B2	1962-1972	Average	High	Increase	Increase	Increase	Increase	Decrease
	1972-1992	Wet	Low	Decrease	Decrease	Increase	Decrease	Increase
	1992-2002	Average	Low	Decrease	Decrease	Decrease	Increase	Increase
	2002-2012	Drought	Low	Decrease	Both (Increase after 4,000 cfs)	Decrease	Decrease	Decrease
Subreach B3	1962-1972	Average	High	Increase	Increase	Increase	Decrease	Decrease
	1972-1992	Wet	Low	Decrease	Decrease	Decrease	Increase	Increase
	1992-2002	Average	Low	Decrease	Decrease	Decrease	Decrease	Increase
	2002-2012	Drought	Low	Increase	Both (Increase after 4,000 cfs)	Decrease	Decrease	Decrease
Subreach B4	1962-1972	Average	High	Increase	Decrease	No Change	Increase	Decrease
	1972-1992	Wet	Low	Decrease	Decrease	Decrease	Decrease	Increase
	1992-2002	Average	Low	Increase	Decrease	No Change	Decrease	Increase
	2002-2012	Drought	Low	Decrease	Both (Increase after 5,000 cfs)	Decrease	Decrease	Decrease

5.4 Massong Classification Summary

The Massong et al. (2010) classification system was used to evaluate channel planform over time with the use of historical aerial imagery and a representative channel cross-section from each subreach. Between 1962 and 2012, the Bernalillo Reach appears to be progressing through the meandering (M) planform stages. This indicates that the Bernalillo Reach tends to have excess transport capacity, meaning that the channel tends to erode rather than deposit sediment through the reach. Factors such as channel bed coarsening and degradation progressing to a point where the bank height exceeds the root depth of the riparian vegetation are more important than slope in assessing plan view stage for reaches where the sediment supply is less than transport capacity. Signs that the Bernalillo reach on the evolutionary track towards a meandering river include channel incision and narrowing rather than aggradation, coarsening of the bed, meander planform visible within the aerial imagery, and an absence of sediment plugs. The Massong et al. (2010) Meandering (M) planform stages along with a cross-section representation is given by **Figure 5-1** (also see **Section 3.9**). Note that the plan view classification system has been expanded to include representative cross sections for each stage.

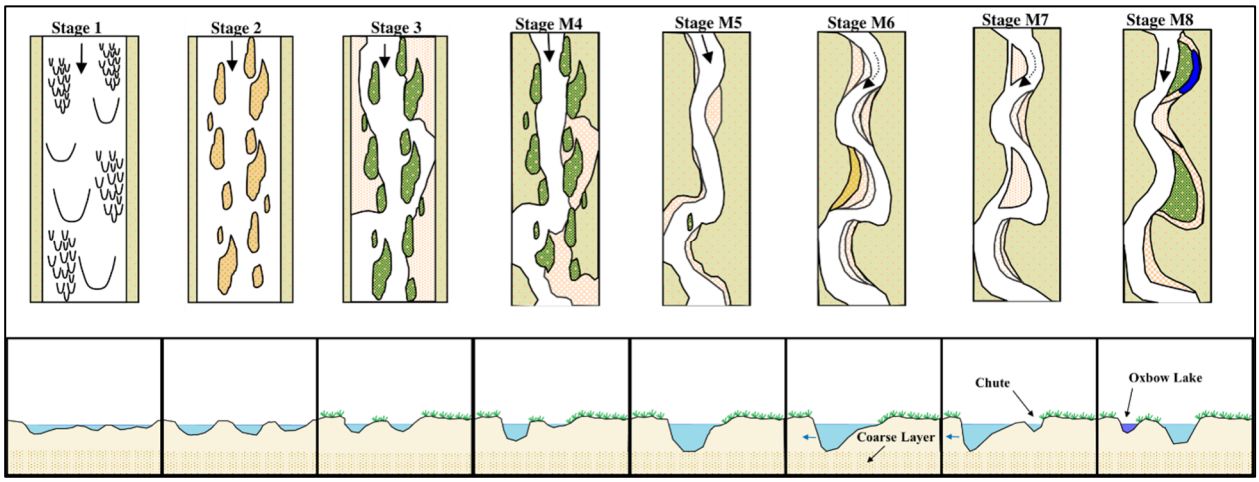

Figure 5-1 Planform evolution model from Massong et al. (2010) applied to channel cross sectional view left to right looking downstream (modified by Brianna Corsi, 2022).

In 1960, all subreaches were classified as Stage 1. Stage 1 describes a wide, shallow channel with a high sediment load and large floods, which results in an active channel with constantly changing bars and dunes and little vegetation encroachment. While this appears to be the case in the 1960s, the recent width decreases and channel evolution were minor compared to what occurred between the early and mid-1900s based on the digitized sketch from 1918 and available aerial imagery in 1935 and 1948.

By 2012, Subreach B1 appears to have progressed more quickly than the other subreaches to Stage M5, which is characterized by a deep, slightly meandering single-threaded channel. The faster rate at which Subreach B1 progressed through to stage M5 is likely tied to the large degree of channel incision through this reach, which increased flow conveyance within the channel and reduced floodplain connection at lower flows. Subreach B2 has progressed to Stage M4, though there are still side channels that become inundated at relatively low flood events. Subreach B3 generally appears to have only progressed through Stage 3, with an abundance of islands and no clear dominant flow path. This subreach of the Bernalillo Reach appears not to be evolving as quickly into the meandering channel planforms as Subreaches B1 and B2, which again is likely due in part to the construction of the ABCWUA Adjustable Height Dam at the downstream end of the subreach. Subreach B4 appears to have progressed into Stage M4 by 2012, with side channels and sand

bars that have not yet become fully vegetated and that still become inundated at low flood events. While B4 is classified as the same stage as Subreach B2, it has maintained a wider channel width and shallower flow depth.

5.5 Habitat

HEC-RAS modeling was completed to evaluate habitat for the Rio Grande Silvery Minnow (RGSM). One of the most important aspects of the RGSM is the connection of the main channel to the floodplain. In general, flows that go over bank and access the floodplain results in significant habitat availability. The Bernalillo Reach has a significant portion of its available habitat within side channels and, during higher flow events, within mid-channel bars and islands. In 2012, the normalized habitat availability quantities showed that Subreach B3 consistently had the most hydraulicly suitable habitat for larvae, juvenile, and adult life stages at discharges lower than 1,500 cfs. Above 1,500 cfs, Subreaches B2 and B3 had the most juvenile and adult hydraulicly suitable habitat and had similar magnitudes, while B1 and B2 offered more larvae habitat during those flows. The channel form of B2 and B3 may be more efficient at reaching the RGSM's habitat criteria of velocity and flow depth for the juvenile and adult life stages, while B1 and B2 may be for efficient for the larvae.

Minnow habitat and the associated link to geomorphology and hydraulics is shown in the maps provided in **Appendix F** and will be discussed further in a separate process linkage report.

6 Conclusions

The Bernalillo Reach extends from the Hwy 550 bridge crossing in Bernalillo and ends at the Montaño bridge crossing in Albuquerque, New Mexico. The purpose of the report is to analyze the hydrologic, hydraulic, and geomorphic trends between 1918 and 2021. HEC-RAS and GIS were used to find geomorphic and river characteristics such as sinuosity, width, bed elevation and other hydraulic parameters. Hydraulically suitable RGSM habitat was determined quantitatively and spatially throughout the reach.

The major findings of this study are listed below:

- The hydrograph of the Bernalillo Reach was impacted by the construction of Cochiti Dam. Prior to the dam completion, there was a greater frequency and magnitude of large flood events. Flow events above a daily exceedance probability of 10% have been most impacted by the Cochiti Dam construction. The MRG has cycled through dry and wet periods, and it currently in a dry period.
- Spring snowmelt typically supplies the greatest water and sediment discharge volumes. Some occasional monsoonal thunderstorms transport the greatest concentrations of suspended sediment, but only for short periods of time. The sediment flux into the river seems to be primarily driven by snowmelt drains into the ephemeral tributaries and nearby arroyos that wash sediment into the MRG. The Jemez River contributes a large portion of sediment to the MRG. Between 2014 and 2021, the Jemez River contributed roughly 38% of sediment to the Albuquerque gage while only contributing 4% of flow.
- Between 1962 and 1972, the Bernalillo Reach was in the process of aggrading, with the greatest degree of aggradation occurring in Subreaches B1 and B2. This aggradation led to an increase in bed elevation and steepening in channel slope during this decade. Following the completion of the Cochiti dam the channel began to incise, with the most significant channel bed degradation occurring in Subreach B1 and B2. In recent years, several grade controls are active throughout the reach. The Corrales Siphon is exposed and is potentially storing sediment and creating backwater effects. The AMAFCA North Diversion Channel outfall, located at the downstream end of B2, provided increased sediment loads and acts as grade control by helping maintain channel width and control the aggradation/degradation trends. The ABCWUA Adjustable Height Dam can also act as a temporary grade control where the channel bed responds to changes in the dam height.
- The bed material samples collected in Subreaches B1 and B2 have ranged widely between coarse silt to coarse gravel over the years. The bed material samples in these two reaches have generally indicated that the channel has become coarser over time. Conversely, nearly all of the bed material samples collected in Subreach B3 over the years between 1990 and 2020 have been between fine sand and coarse sand.
- The average sinuosity in the Bernalillo Reach varies between 1.01 and 1.12. No trend of increasing or decreasing sinuosity is clear based on this data. However, several low radius beds do occur and increases in sinuosity tend to be concentrated in specific locations. For example, Subreach B3 has tended to have the greatest degree of sinuosity over the years. In 2019, all four subreaches can be classified as straight channels.
- Between 1962 and 2012, the Bernalillo Reach appears to be progressing through the meandering (M) planform stages. This indicates that the Bernalillo Reach tends to have excess transport capacity, meaning that the channel tends to erode rather than deposit sediment through the reach.
- The Subreaches B2 and B3 may be more efficient at reaching the Rio Grande Silvery Minnow's habitat criteria of velocity and flow depth for the juvenile and adult life stages, while B1 and B2 may be more efficient for the larvae.

7 Bibliography

Anderson, T and Julien, P.Y. (2022). Draft Report. "Middle Rio Grande Montaño Reach Report: Morpho-dynamic Processes and Silvery Minnow Habitat from the Montaño Road Bridge Crossing to the Isleta Diversion Dam," Submitted to the U.S. Bureau of Reclamation, Albuquerque, New Mexico.

Beckwith, T and Julien, P.Y. (2020) "Middle Rio Grande Escondida Reach Report: Morpho-dynamic Processes and Silvery Minnow Habitat from Escondida Bridge to US-380 Bridge (1918-2018.)" Colorado State University, Fort Collins, CO.

Brierley, G. J. and Fryirs, K. A. (2005). Geomorphology and river management: Applications of the river styles framework. Blackwell Publishing.

Bovee, K.D., Waddle, T.J., and Spears, J.M. (2008). "Streamflow and endangered species habitat in the lower Isleta reach of the middle Rio Grande." U.S. Geological Survey Open-File Report 2008-1323.

Fogarty, C and Julien, P.Y. (2020). Linking Morphodynamic Processes and Silvery Minnow Habitat Conditions in the Middle Rio Grande – Isleta Reach, New Mexico. Colorado State University, Fort Collins, CO.

Doidge, S and Julien, P.Y. (2019). Draft Report. Middle Rio Grande San Acacia Reach: Morphodynamic Processes and Silvery Minnow Habitat from San Acacia Diversion Dam to Escondida Bridge, Colorado State University, Fort Collins, CO.

Fitzner, A. (2018). Draft Report "Reclamation Managing Water in the West." Bureau of Reclamation Draft Lower Reach Plan, Albuquerque Area Office, Albuquerque, NM, 36 p.

Greimann B., and Holste N. (2018). "Analysis and Design Recommendations of Rio Grande Width", Technical Service Center, Sedimentation and River Hydraulic Group, U.S. Bureau of Reclamation, Denver, CO

Holste, N. (2020) "One-Dimensional Numerical Modeling of Perched Channels." U.S. Bureau of Reclamation, Denver, CO.

Julien, P.Y. (2002). River Mechanics, Cambridge University Press, New York

Julien, P. Y., and Wargadalam, J. (1995). "Alluvial channel geometry: theory and applications." Journal of Hydraulic Engineering, American Society of Civil Engineers, 121(4), 312–325.

Klein, M., Herrington, C., AuBuchon, J., and Lampert, T. (2018a). Isleta to San Acacia Geomorphic Analysis, U.S. Bureau of Reclamation, Reclamation River Analysis Group, Albuquerque, New Mexico.

Klein, M., Herrington, C., AuBuchon, J., and Lampert, T. (2018b). Isleta to San Acacia Hydraulic Modeling Report, U.S. Bureau of Reclamation, Reclamation River Analysis Group, Albuquerque, New Mexico.

LaForge, K., Yang, C.Y., Julien, P.Y., and Doidge, S. (2019). Draft Report. Rio Puerco Reach: Hydraulic Modeling and Silvery Minnow Habitat Analysis, Colorado State University, Fort Collins, CO.

Larsen, A. (2007). Hydraulic modeling Analysis of the Middle Rio Grande-Escondida Reach, New Mexico. M.S thesis, Civil Engineering Department, Colorado State University, Fort Collins, CO.

Makar, P. (2006). "Channel Widths Changes Along the Middle Rio Grande, NM." Proceedings of the Eith Federal Interagency Sedimentation Conference, Bureau Of Reclamation, Denver, CO. 943 p.

Makar, P., Massong, T., and Bauer, T. (2006). "Channel Widths Change Along the Middle Rio Grande, NM." Joint 8th Federal Interagency Sedimentation Conference, Reno, NV, April 2 -April6, 2006.

Massong, T., Paula, M., and Bauer, T. (2010). "Planform Evolution Model for the Middle Rio Grande, NM." 2nd Joint Federal Interagency Conference, Las Vegas, NV, June 27 - July 1, 2010.

MEI. (2002). Geomorphic and Sedimentologic Investigations of the Middle Rio Grande between Cochiti Dam and Elephant Butte Reservoir, Mussetter Engineering, Inc., Fort Collins, CO, 220 p.

Mortensen, J.G., Dudley, R.K., Platania, S.P., and Turner, T.F. (2019). Draft report. Rio Grande Silvery Minnow Habitat Synthesis, University of New Mexico with American Southwest Ichthyological Researchers, Albuquerque, NM.

Mortensen, J.G., Dudley, R.K., Platania, S.P., White, G.C., and Turner, T.F., Julien, P.Y., Doidge, S, Beckwith, T., Fogarty, C. (2020). Draft Report. Linking Morpho-Dynamics and Bio-Habitat Conditions on the Middle Rio Grande: Linkage Report 1- Isleta Reach Analyses. Submitted to the U.S. Bureau of Reclamation, Albuquerque, New Mexico.

Owen, T. E., Anderson, K., and Julien, P. (2011). Elephant Butte Reach: South boundary of Bosque del Apache NWR to Elephant Butte Reservoir hydraulic modeling analysis, 1962- 2010. Colorado State University, Fort Collins, CO.

Owen, T. E., (2012). Geomorphic Analysis Of the Middle Rio Grande - Elephant Butte Reach, New Mexico. Colorado State University, Fort Collins, CO.

Pinson, A.O., Scissons, S.K., Brown, S.W., Walther, D.E. (2014). Post Flood Report: Record Rainfall and Flooding Events during September 2013 in New Mexico, Southeastern Colorado and Far West Texas, U.S. Army Corps of Engineers, Albuquerque, New Mexico.

Pinson, A.O., Scissons, S.K., Brown, S.W., Walther, D.E. (2014). Post Flood Report: Record Rainfall and Flooding Events during September 2013 in New Mexico, Southeastern Colorado and Far West Texas, U.S. Army Corps of Engineers, Albuquerque, New Mexico

Posner, A. J. (2017). Draft report. Channel conditions and dynamics of the Middle Rio Grande River, U.S. Bureau of Reclamation, Albuquerque, New Mexico.

Scurlock, D. (1998). "From the Rio to the Sierra: an environmental history of the Middle Rio Grande Basin." General Technical Report RMRS-GTR-5. Fort Collins, CO: US Department of Agriculture, Forest Service, Rocky Mountain Research Station, 440 p.

Shah-Fairbank, S. C., Julien, P. Y., and Baird, D. C. (2011). "Total sediment load from SEMEP using depth-integrated concentration measurements." Journal of Hydraulic Engineering, 137(12), 1606–1614.

Schied, A., Sperry, D. J., and Julien, P.Y. (2022). Middle Rio Grande Bosque Reach Report: Morpho-dynamic Processes and Silvery Minnow Habitat from US-380 Bridge to Southern Boundary of Bosque Del Apache National Wildlife Refuge (BDANWR). Final report prepared for the United States Bureau of Reclamation. Colorado State University, Fort Collins, CO.

Shrimpton, C. P, (2012). Analysis of Sediment Plug Hypotheses Middle Rio Grande, NM. Colorado State University, Fort Collins, CO.

Sperry, D.J., Scheid, A., and Julien, P.Y. (2022). Middle Rio Grande Elephant Butte Reach Report: Morpho-dynamic Processes and Silvery Minnow Habitat from the Southern Boundary of the Bosque Del Apache National Wildlife Refuge to Elephant Butte Reservoir. Final report prepared for the United States Bureau of Reclamation. Colorado State University, Fort Collins, CO.

Towne, L. (2007). "Infrastructure and Management of the Middle Rio Grande." The Middle Rio Grande Today, Bureau of Reclamation, 17 p.

U.S. Bureau of Reclamation. (2012). "Middle Rio Grande River Maintenance Program - Comprehensive Plan and Guide." Albuquerque Area Office, Albuquerque, New Mexico, 202p.

U.S. Bureau of Reclamation. (2021). "Water Operations: Historical Data." Online Resource. https://www.usbr.gov/rsvrWater/HistoricalApp.html

U.S. Fish and Wildlife Service. (2007). “Rio Grande Silvery Minnow (Hybognathus amarus).” Draft Revised Recovery Plan, Albuquerque, New Mexico, 174 p.

Varyu, D. (2013). *Aggradation / Degradation Volume Calculations: 2002-2012*. U.S. Department of the Interior, Bureau of Reclamation, Technical Services Center, Sedimentation and River Hydraulics Group. Denver, CO.

Varyu, D. (2016). *SRH-1D Numerical Model for the Middle Rio Grande: Isleta Diversion Dam to San Acacia Diversion Dam*. U.S. Department of the Interior, Bureau of Reclamation, Technical Services Center, Sedimentation and River Hydraulics Group. Denver, CO.

Yang, C.Y. (2019). *The Sediment Yield of South Korean Rivers*, Colorado State University, Fort Collins, CO.

Yang, C.Y. and Julien, P.Y. (2019). “The ratio of measured to total sediment discharge.” *International Journal of Sediment Research*, 34(3), pp.262-269.

Yang, C.Y., LaForge, K., Julien, P.Y., and Doidge, S. (2019). Draft Report. *Isleta Reach: Hydraulic Modeling and Silvery Minnow Habitat Analysis*, Colorado State University, Fort Collins, CO.

Appendix A

Bernalillo and Montaño Subreach Delineation Report Submitted May 2022
(includes Attachments)

Bernalillo and Montaño Subreach Delineation Report

Prepared by Tristen Anderson, Brianna Corsi, Chelsey Rasmussen
Prepared for Ari Posner
May 20, 2022

Reach Definition

The area of interest includes two consecutive reaches in the Middle Rio Grande River spanning approximately 35 miles. The first reach, referred to as the Bernalillo reach, spans approximately 16 miles and begins at Highway 550 in Bernalillo, NM (Agg/Deg Line 298) and ends just upstream of the Montaño Bridge in Albuquerque, NM (Agg/Deg Line 463). The second reach, referred to as the Montaño Reach, spans approximately 19 miles and begins just upstream of the Montaño Bridge in Albuquerque, NM (Agg/Deg Line 463) and ends just downstream of the Isleta diversion dam (Agg/Deg 657). Both of these reaches are located within an urban river corridor. For purposes of hydraulic analysis, these two reaches were split into multiple subreaches based on notable urban and geomorphic features, as described below.

Bernalillo Subreach Delineation

The Bernalillo reach was delineated into four subreaches based on notable urban features such as bridge crossings or drainage tributary outlets. Table 1 below summarizes each subreach. Attachment 1 shows the aerial imagery of the reach delineation.

Table 1: Bernalillo Sub-Reach Delineation

Subreach Name	Agg/Deg Lines	Approximate Distance	Description
B-1	298 – 339	4.0 miles	Highway 550 Bridge to Rio Rancho Bosque Preserve (siphon crossing)
B-2	339 - 398	5.6 miles	Rio Rancho Bosque Preserve (siphon crossing) to Amafca North Diversion Channel (tributary)
B-3	398 - 422	2.4 miles	Amafca North Diversion Channel (tributary) to ABCWUA Adjustable Height Dam
B-4	422 - 463	4.0 miles	ABCWUA Adjustable Height Dam to Montaño Bridge

An analysis of the flood widths at a discharge of 3,000 cfs (Figure 1 and 2 in Attachment 1) as well as channel widths identified by the bank stationing (Figures 3 and 4 in Attachment 1) were considered. Other analyses preformed include the longitudinal profile of the reach (Figure 5 in Attachment 1) and the particle distribution through the reach (Figure 6 in Attachment 1). All analyses preformed identified boundaries consistent with the subreach delineation.

Montaño Subreach Delineation

The Montaño reach was delineated into four subreaches on notable urban features such as bridge crossings or drainage outlets. Table 2 below summarizes each subreach. Attachment 2 shows the aerial imagery of the reach delineation.

Table 2: Montaño Subreach Delineation

Subreach Name	Agg/Deg Lines	Approximate Distance	Description
M-1	463 – 494	3.0 miles	Montaño Bridge to Coronado Fwy (I-40)
M-2	494 – 528	3.5 miles	Coronado Fwy (I-40) to Bridge Blvd
M-3	528 – 575	4.5 miles	Bridge Blvd to Tijeras Arroyo (tributary)
M-4	575 – 623	4.5 miles	Tijeras Arroyo to I-25 Bridge
M-5	623 – 657	3.5 miles	I-25 Bridge to Isleta Diversion Dam

An analysis of the flood widths at a discharge of 3,000 cfs (Figure 1 and 2 in Attachment 2) as well as channel widths identified by the bank stationing (Figures 3 and 4 in Attachment 2) were considered. Other analyses preformed include the longitudinal profile of the reach (Figure 5 in Attachment 2). The particle distribution through the reach (Figure 6 in Attachment 2), could not be completed because the particle size data could not be located. If the data can be located the analysis can be performed and amended into the report. All analyses preformed identified boundaries consistent with the subreach delineation.

Attachment 1 – Bernalillo Subreach Delineation

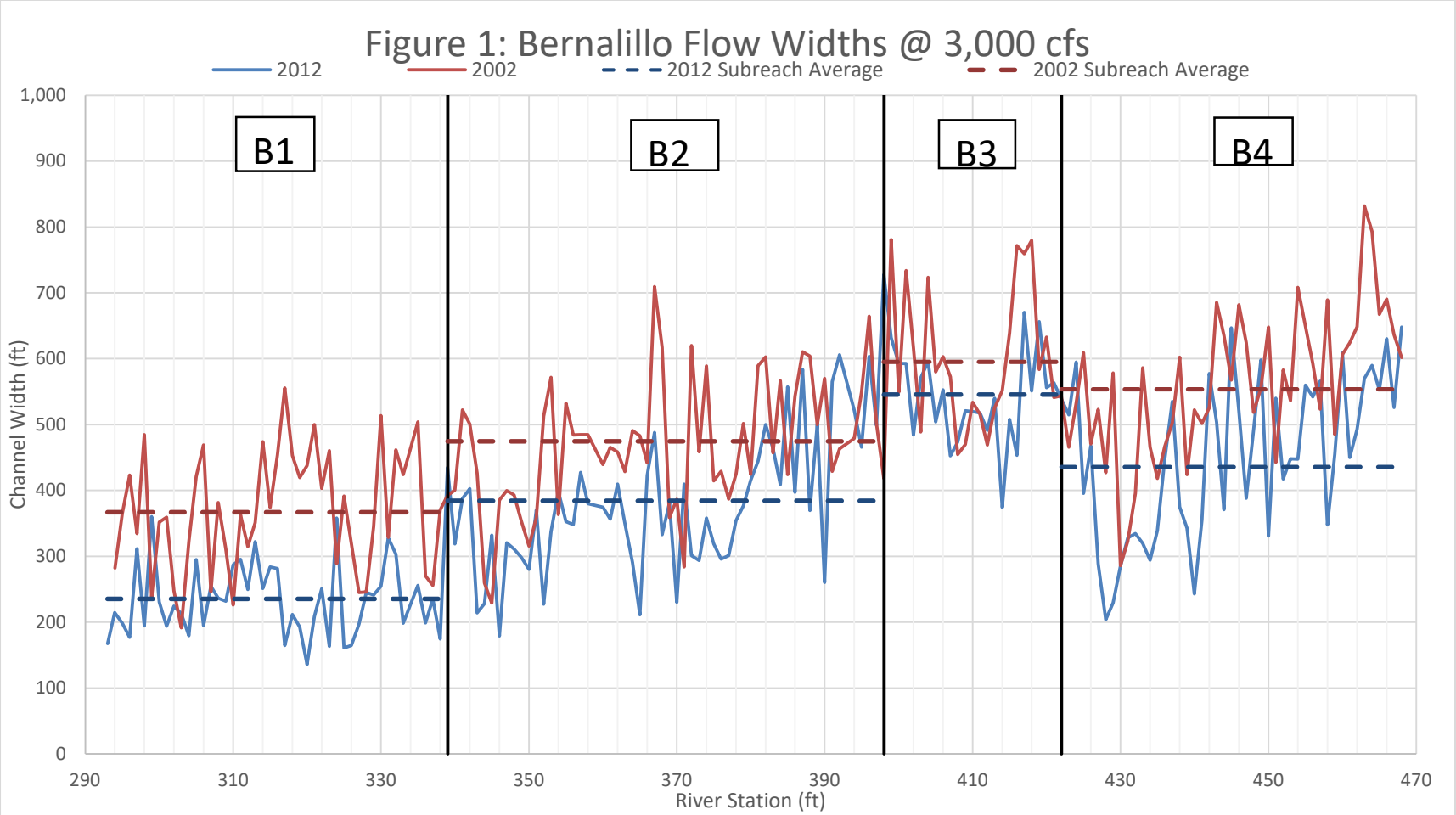

2002		
Subreach	**Average Flow Width, ft**	**Standard Deviation**
B1	367.0	90.9
B2	474.9	105.2
B3	595.4	104.1
B4	553.7	111.9

2012		
Subreach	**Average Flow Width, ft**	**Standard Deviation**
B1	235.5	54.3
B2	384.3	109.2
B3	545.6	74.9
B4	435.8	114.9

Figure 2: Cumulative Bernalillo Flow Widths @ 3,000 cfs
2012
2002
B1
B2
B3
B4
Width (ft)
90,000
80,000
70,000
60,000
50,000
40,000
30,000
20,000
10,000
0
290
310
330
350
370
390
410
430
450
470
River Station (ft)

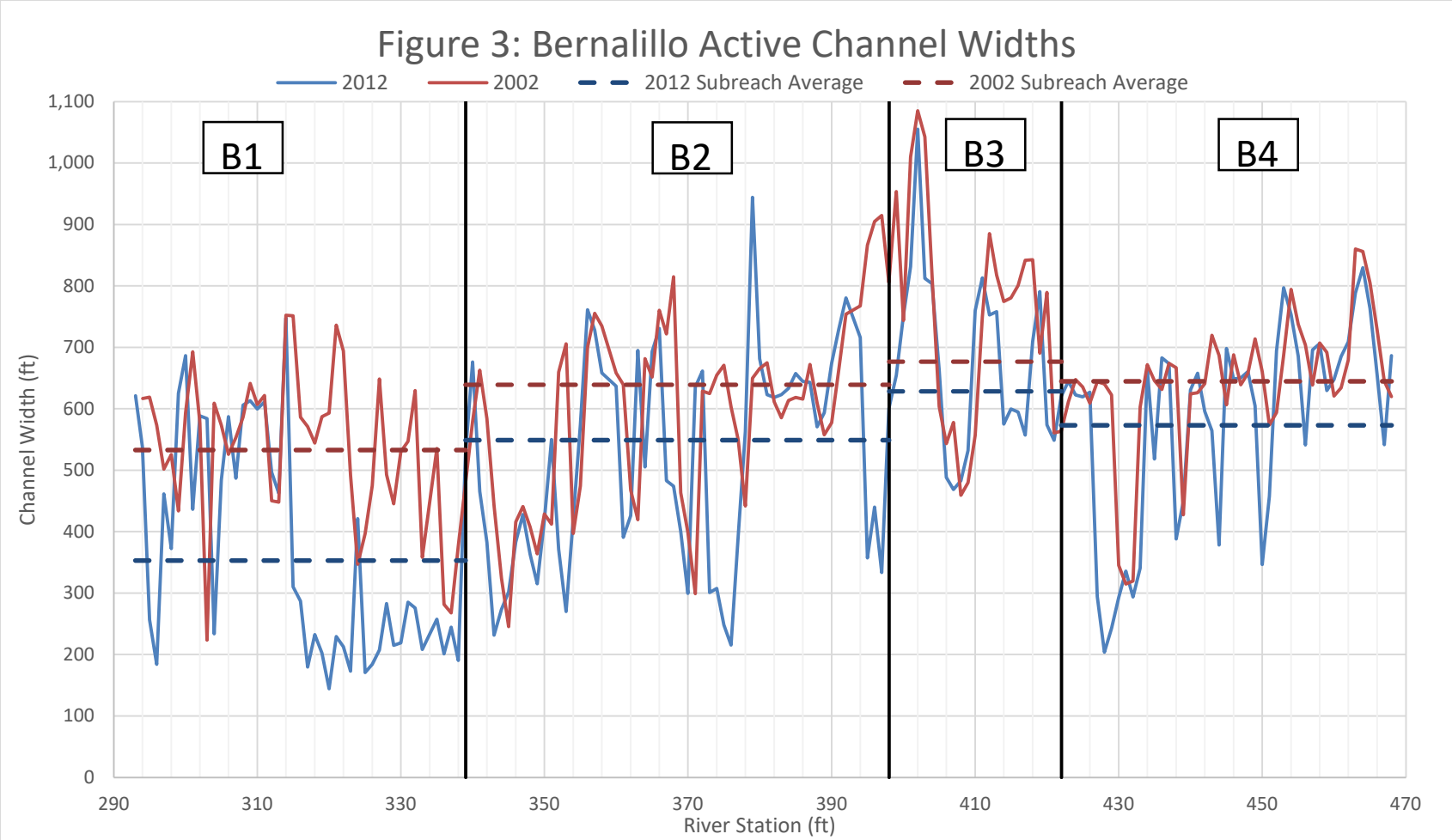

2012		
Subreach	**Average Active Channel Width, ft**	**Standard Deviation**
B1	353.1	172.0
B2	549.0	185.7
B3	628.5	124.8
B4	573.3	167.3

2002		
Subreach	**Average Active Channel Width, ft**	**Standard Deviation**
B1	533.0	120.3
B2	639.1	180.5
B3	676.8	120.9
B4	644.9	114.5

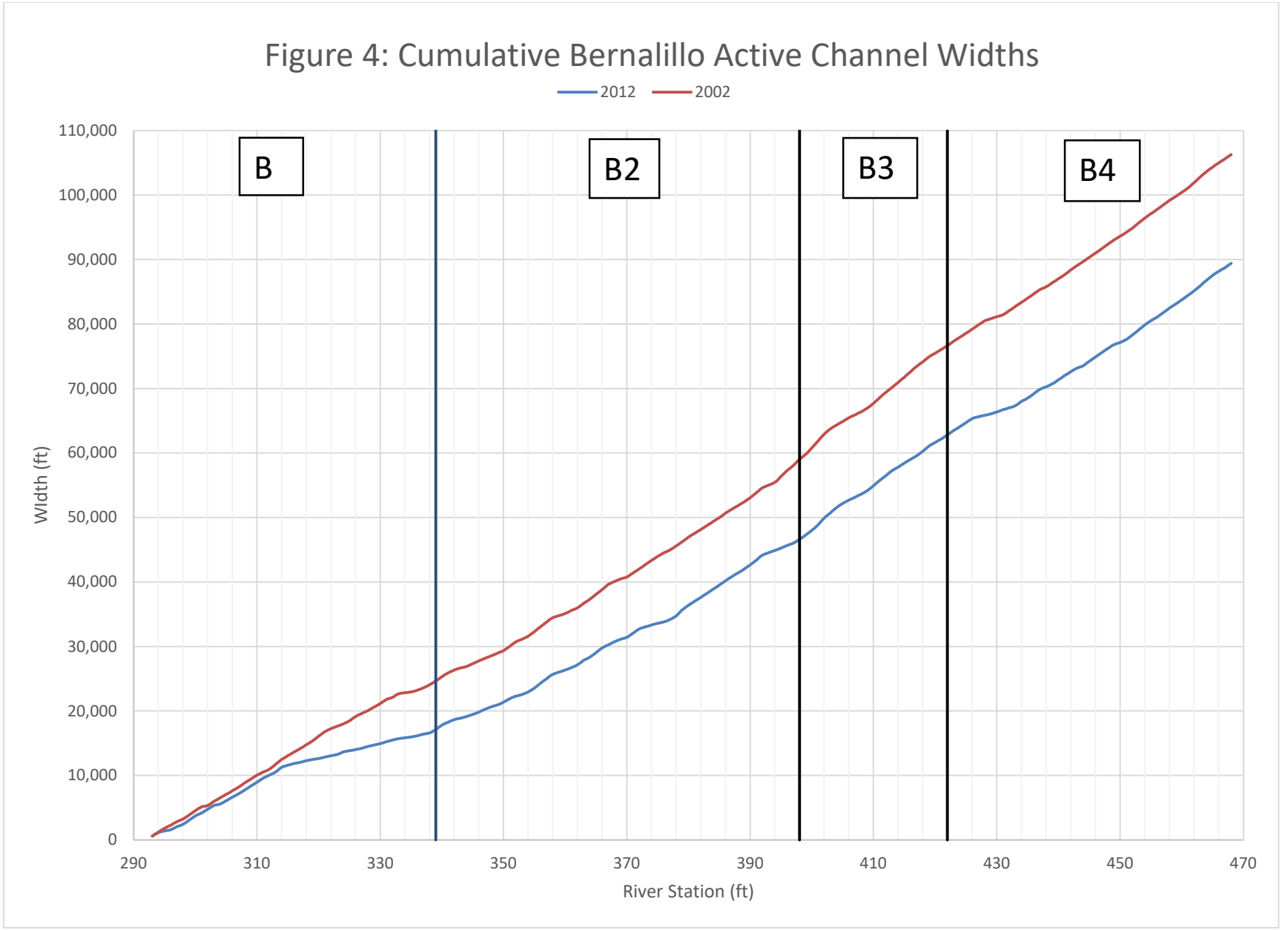
Figure 4: Cumulative Bernalillo Active Channel Widths
2012
2002
B
B2
B3
B4
Width (ft)
110,000
100,000
90,000
80,000
70,000
60,000
50,000
40,000
30,000
20,000
10,000
0
290
310
330
350
370
390
410
430
450
470
River Station (ft)

Figure 5: Longitudinal Profile of Bernalillo Reach

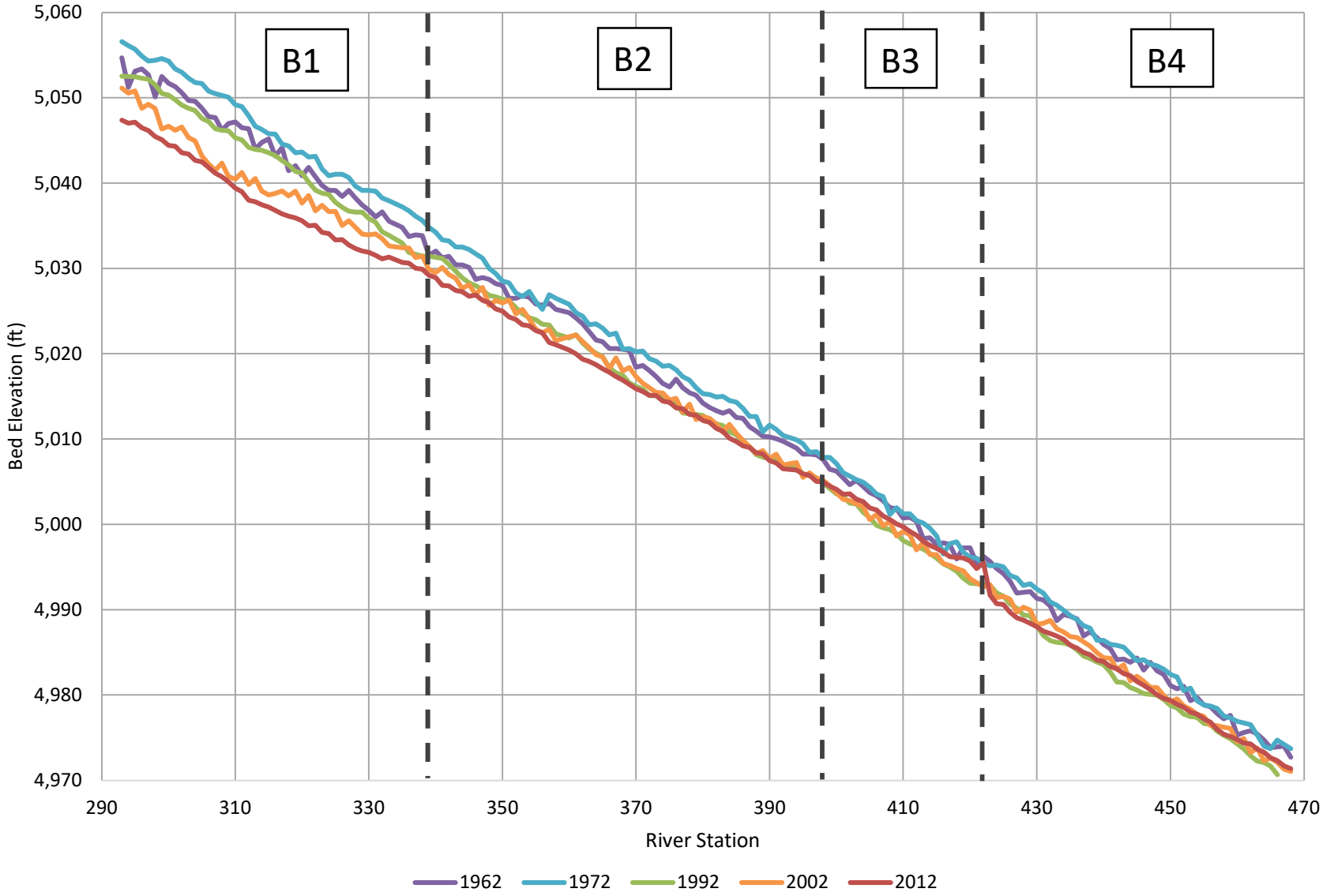

Figure 6: 2012 Bed Material Size of the Bernalillo Reach

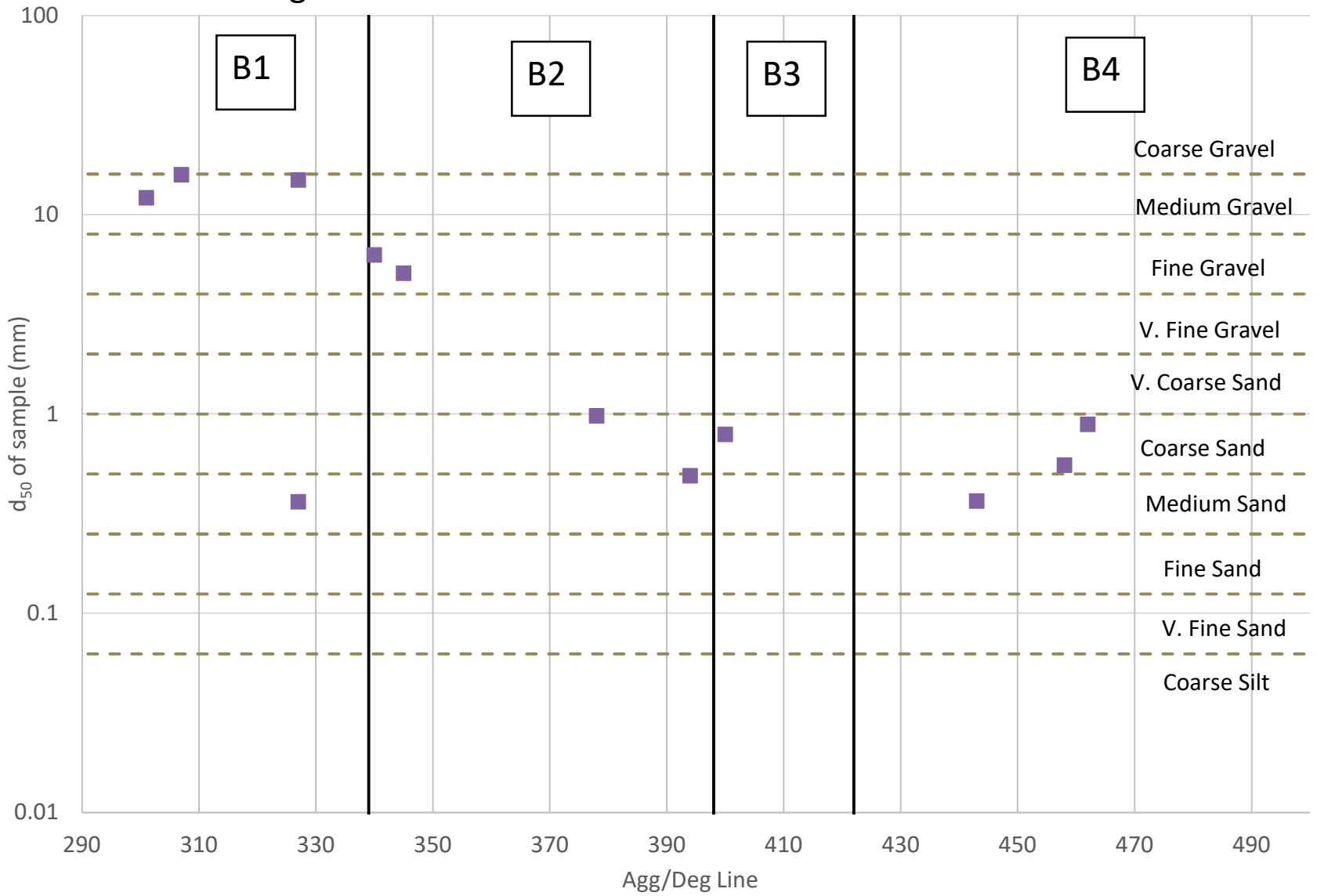

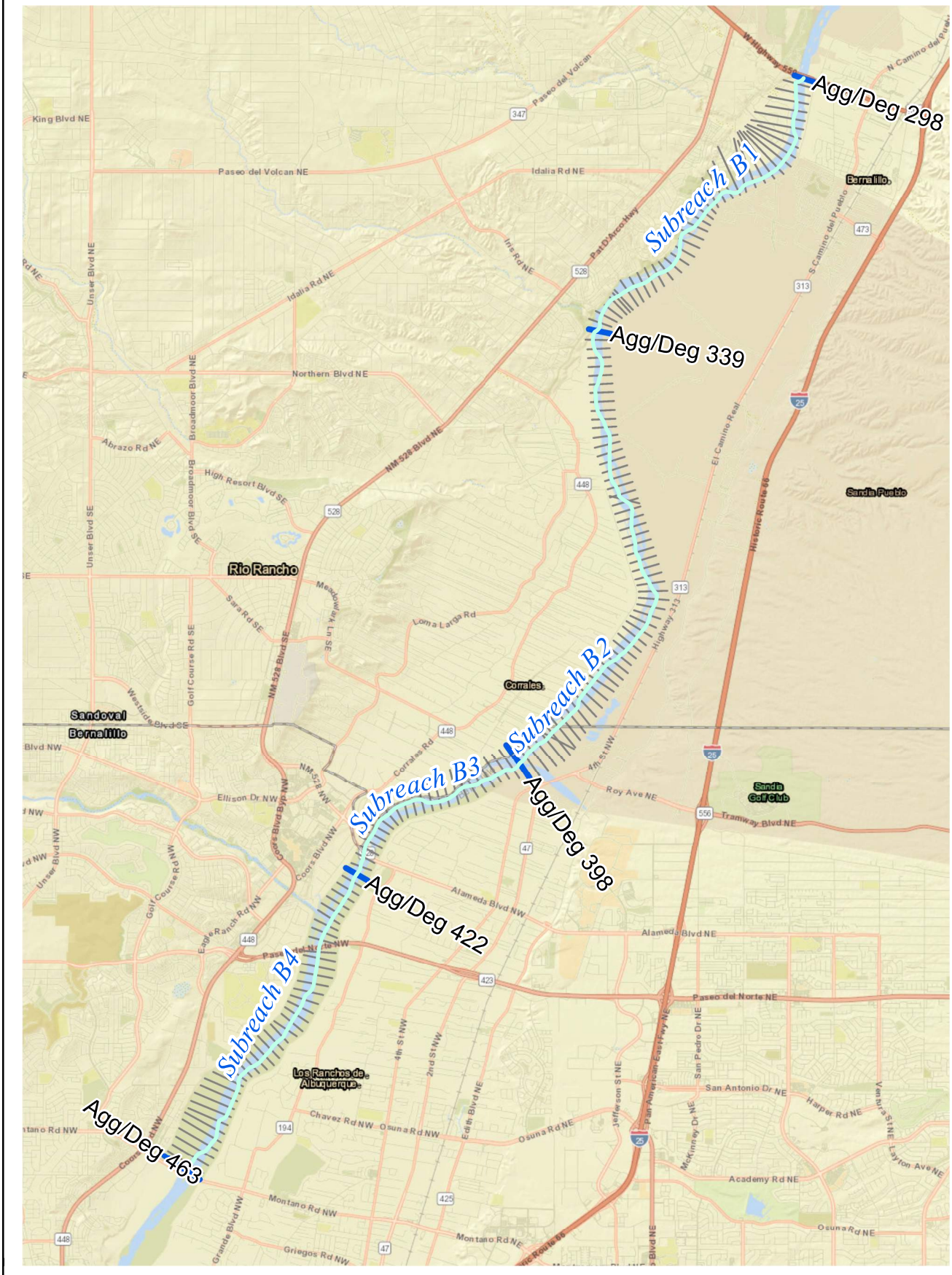

N

10,000 5,000 0 10,000 Feet

Bernalillo Subreach
Overview Map

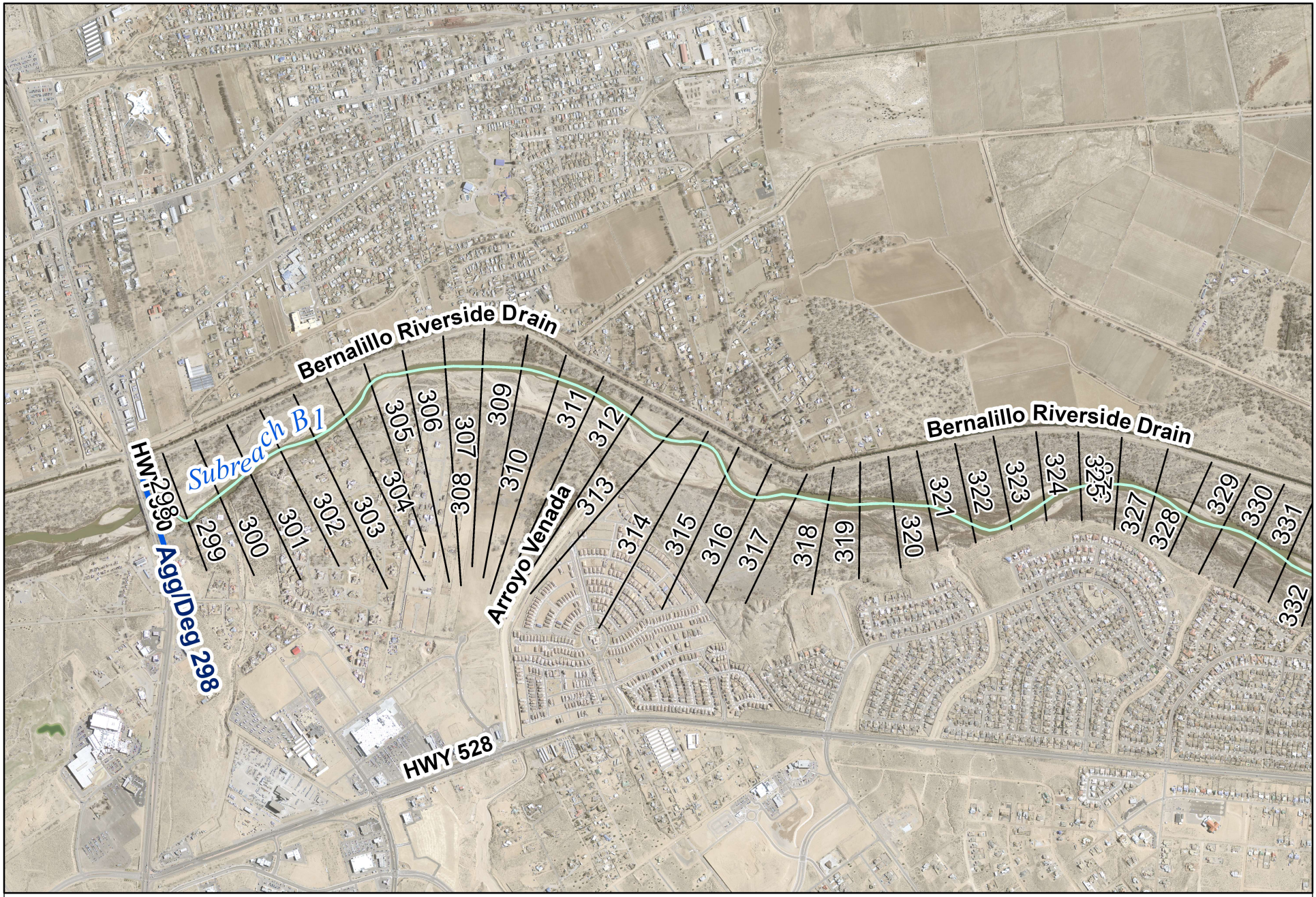

2,500 1,250 0 2,500 Feet

N

Rio Grande Subreach Map
Bernalillo to Montano

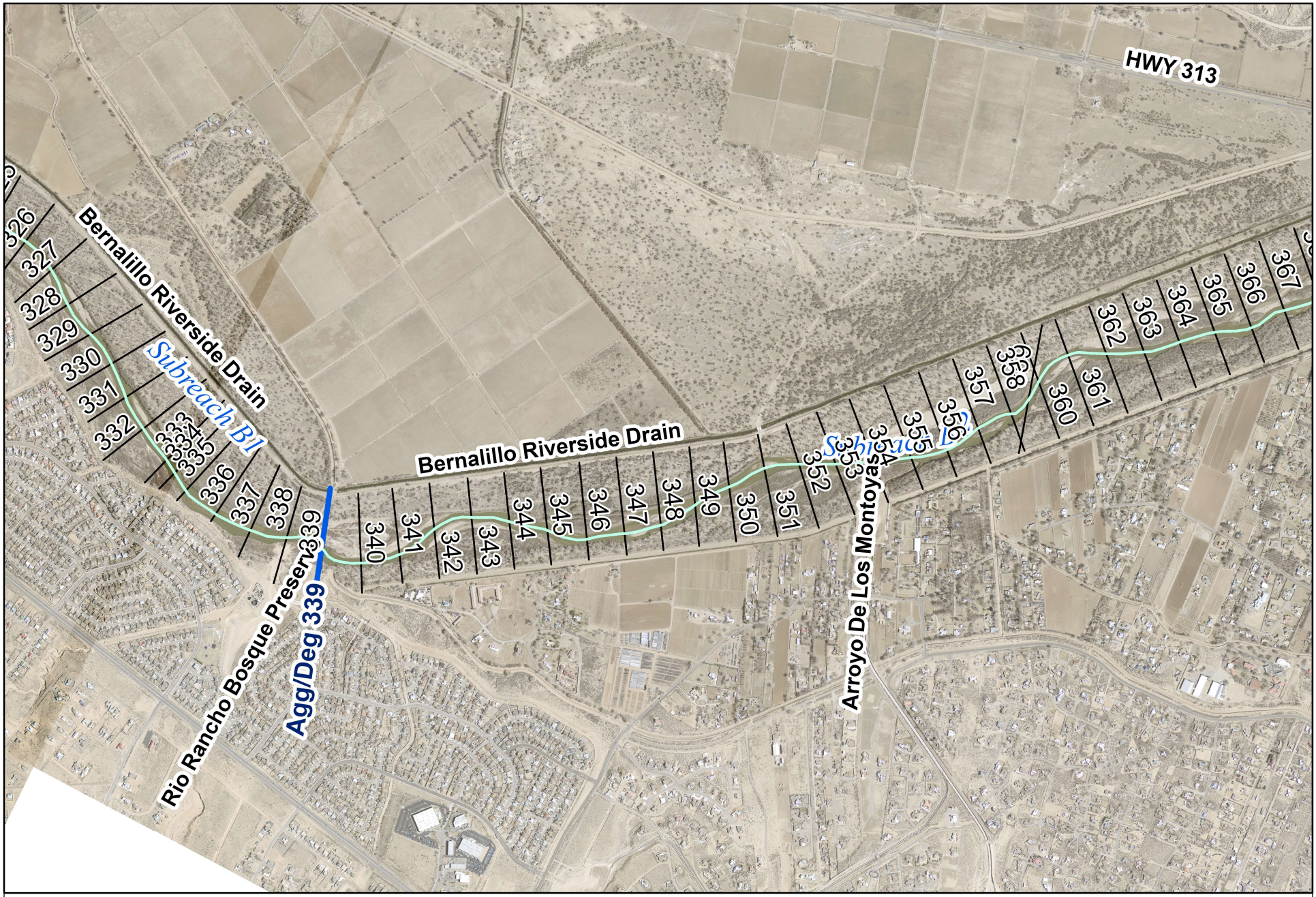

N

2,500 1,250 0 2,500 Feet

Rio Grande Subreach Map
Bernalillo to Montano

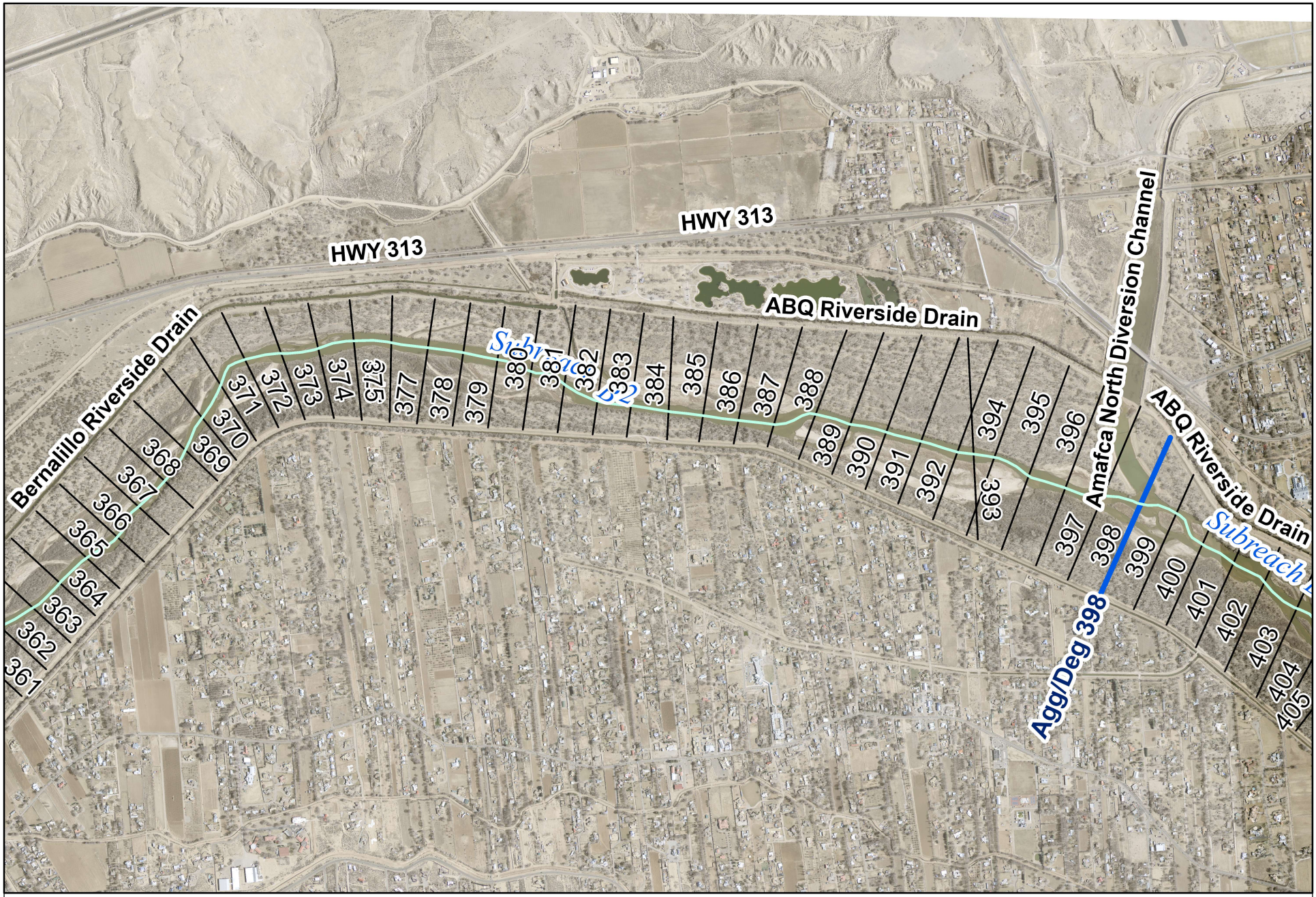

Rio Grande Subreach Map
Bernalillo to Montano

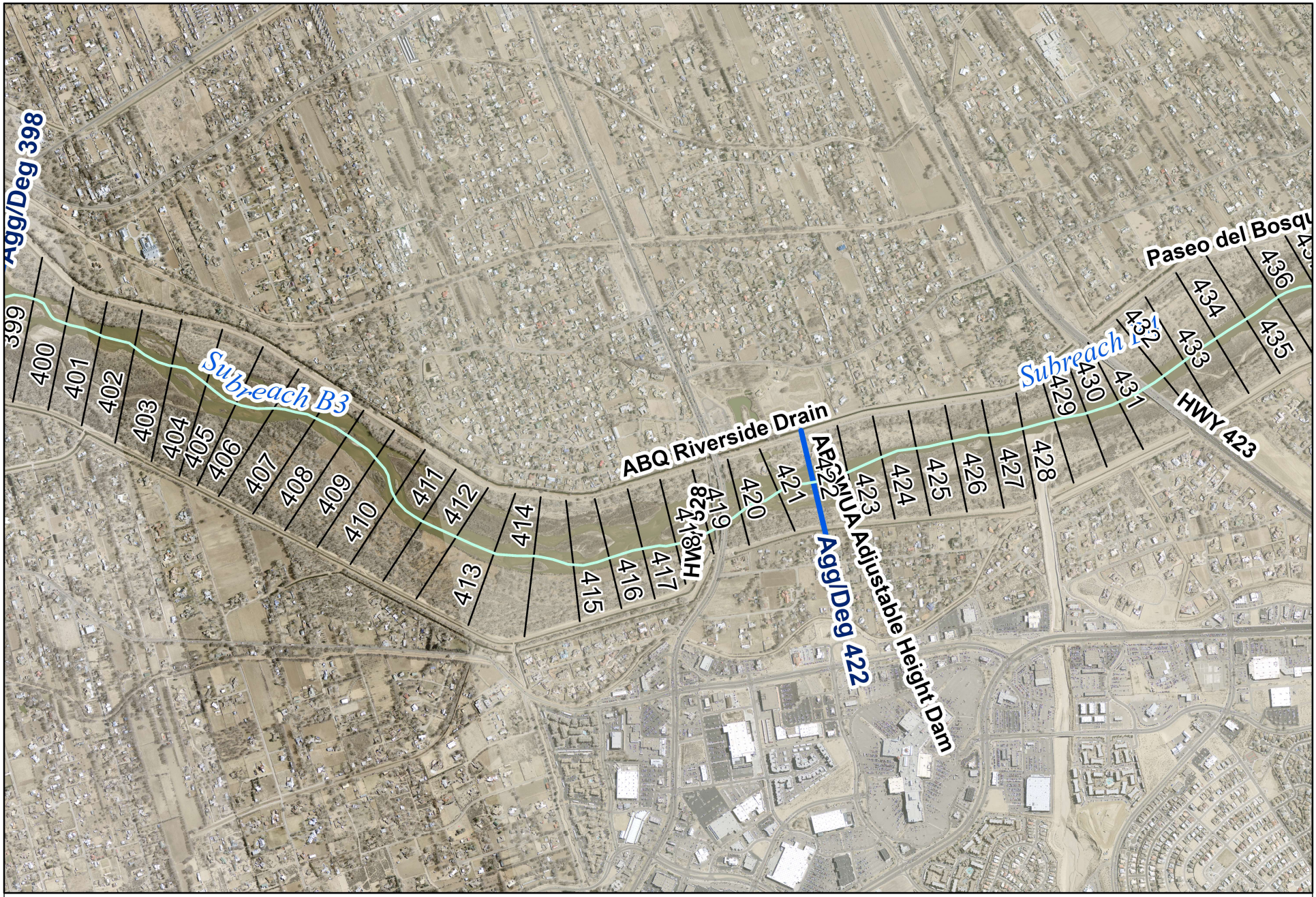

Rio Grande Subreach Map
Bernalillo to Montano

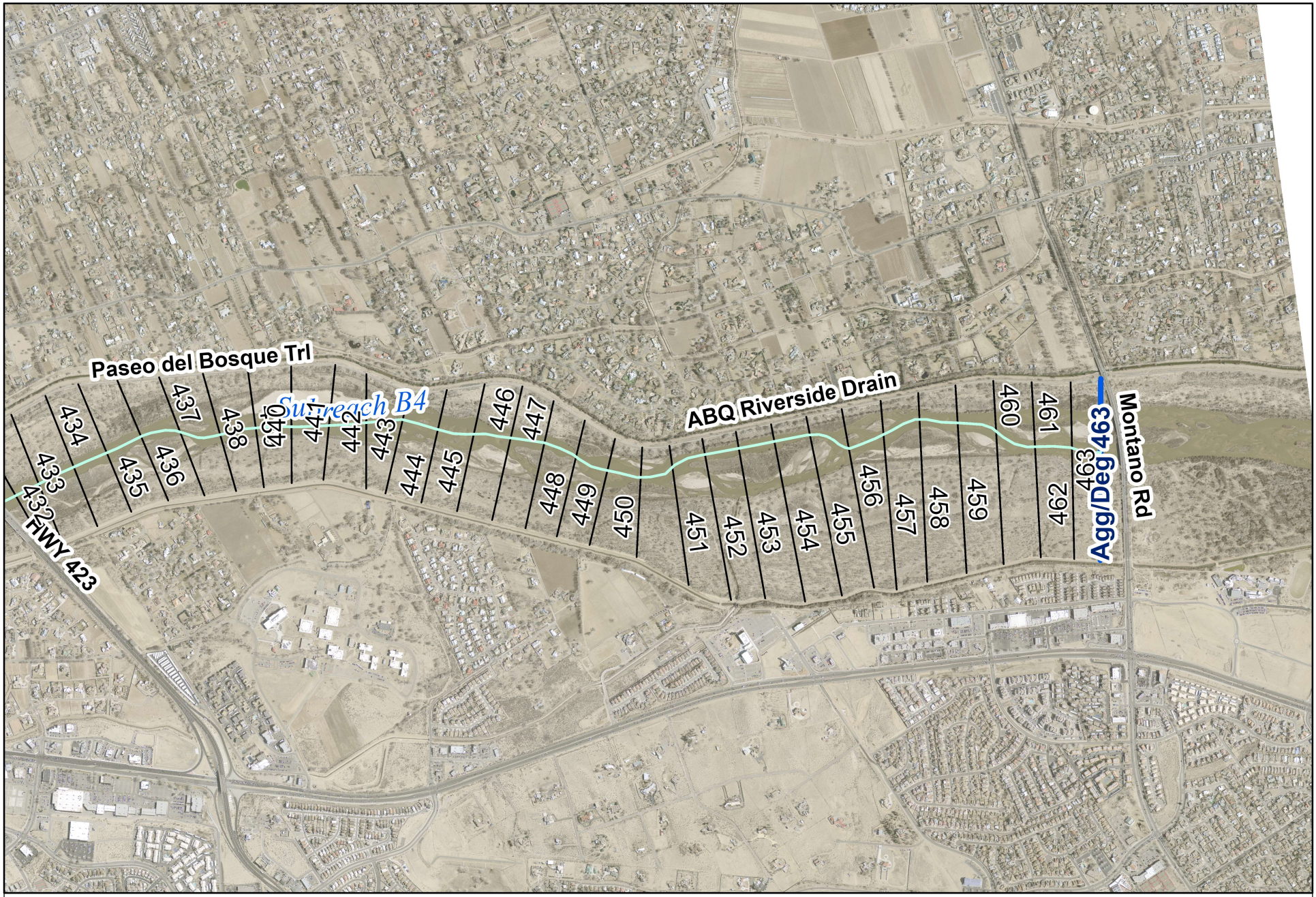

2,500 1,250 0 2,500 Feet

N

Rio Grande Subreach Map
Bernalillo to Montano

Appendix B

Years used in JW Calculations for D50, 3,000 cfs JW Analysis

Table B-1: Years used in JW Calculations for D50

Year Analyzed	Subreach	Year Used
1992	B1	1991
	B2	1991
	B3	1990
	B4	1991
2002	B1	2001
	B2	2001
	B3	2001
	B4	2001
2012	B1	2012
	B2	2012
	B3	2012
	B4	2012

The 3,000 cfs JW analysis are provided below for comparison with previous reports.

Table B-2: 3,000 cfs Julien-Wargadalam channel width prediction

Year	Subreach	Ds (mm)	Slope	Predicted Width (ft)	Observed Width (ft)	Precent Difference
1992	B1	0.168*	0.0010	255	493	-48%
	B2	0.182*	0.0009	257	578	-56%
	B3	0.149*	0.0010	254	668	-62%
	B4	0.211*	0.0009	257	579	-56%
2002	B1	10.830*	0.0008	284	379	-25%
	B2	0.869*	0.0009	264	356	-26%
	B3	0.590*	0.0010	258	473	-45%
	B4	0.420*	0.0009	258	489	-47%
2012	B1	10.822	0.0008	283	342	-17%
	B2	3.206	0.0008	271	329	-18%
	B3	0.789	0.0008	267	439	-39%
	B4	0.602	0.0009	261	448	-42%

*See Table B-1 in above for specific years used for Ds values.

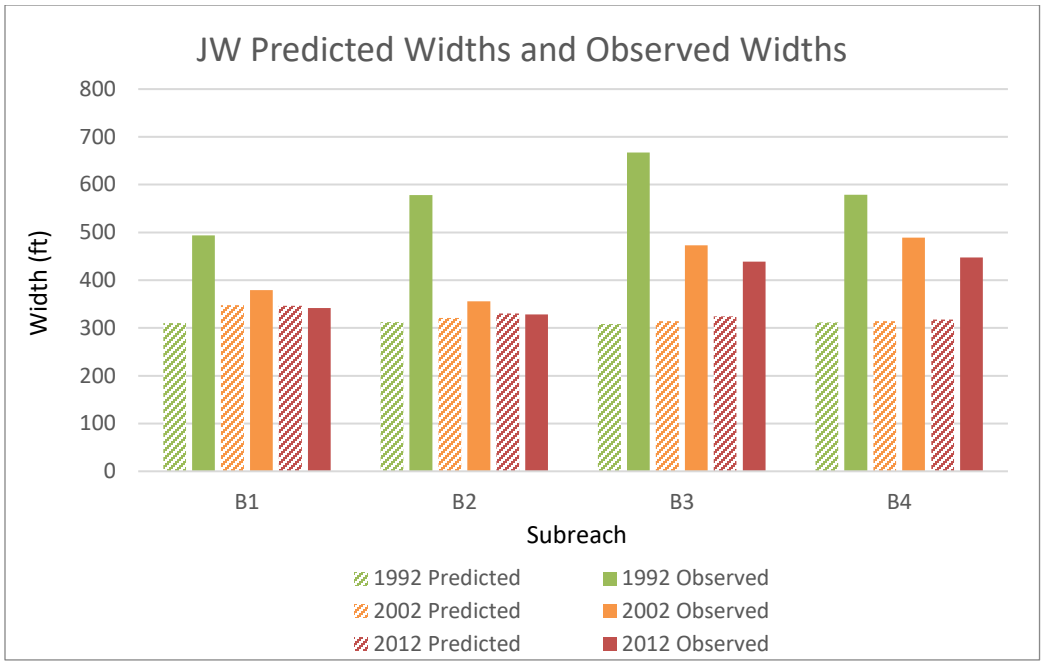

Figure B-1 Julien and Wargadalam predicted widths and observed widths of the channel

Appendix C

Additional Figures from Geomorphology Analyses

(Sediment Rating Curve/Alpha Method Example)

Wetted Top Width Plots

In Section 3.1, the cross-section moving averaged top width was plotted for all agg/deg lines in the Bernalillo Reach. Figures C-1, C-2, and C-3 show each cross-section top width plotted against the agg/deg lines rather than the moving average at discharges of 1,000 cfs, 3,000 cfs, and 5,000 cfs.

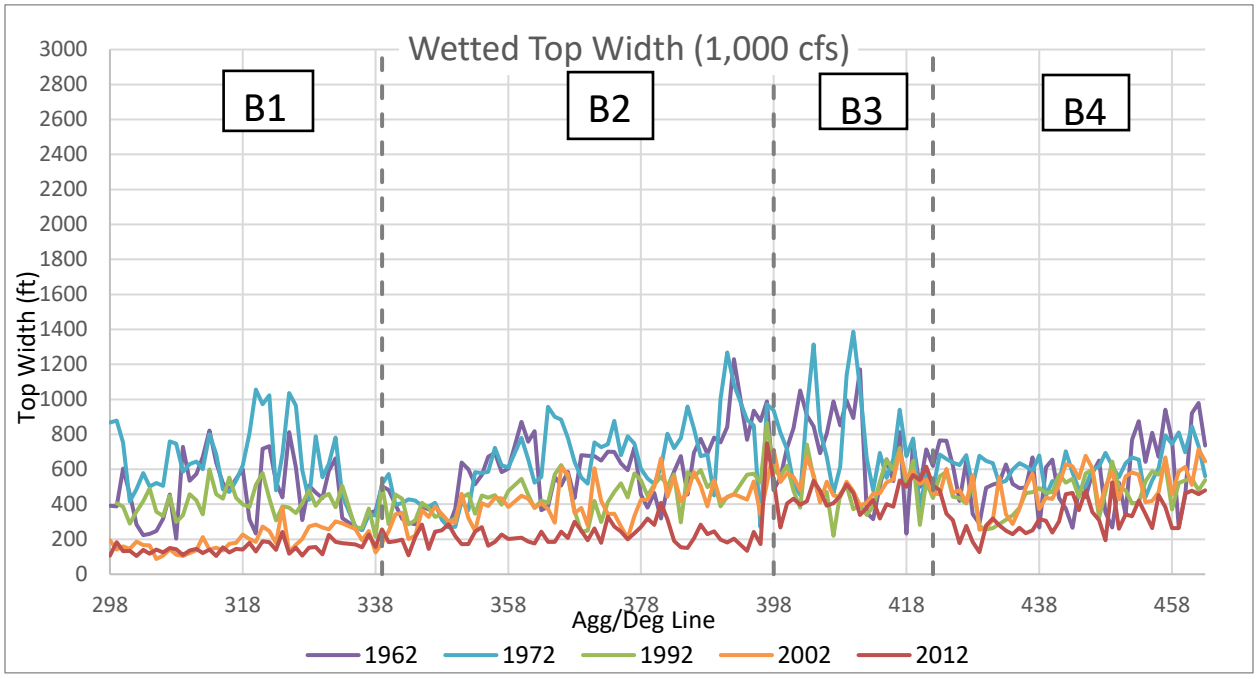

Figure C-1 Wetted top width at each agg/deg line in the Bernalillo Reach at a discharge of 1,000 cfs

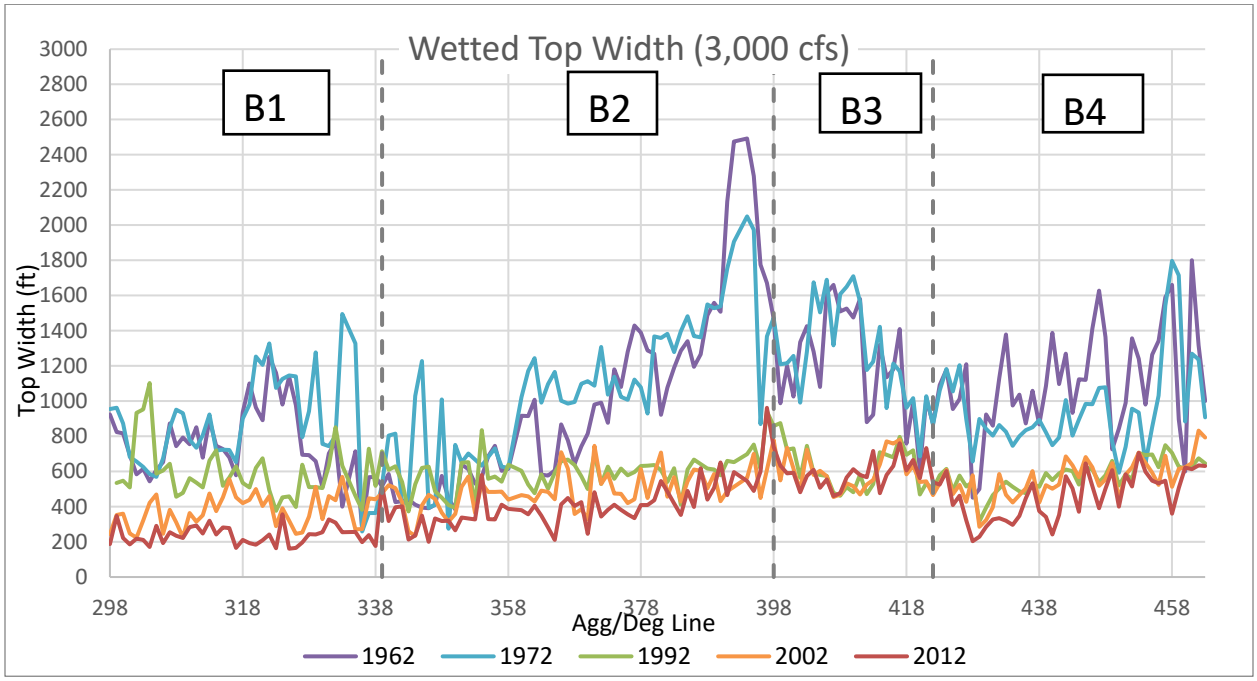

Figure C-2 Wetted top width at each agg/deg line in the Bernalillo Reach at a discharge of 3,000 cfs

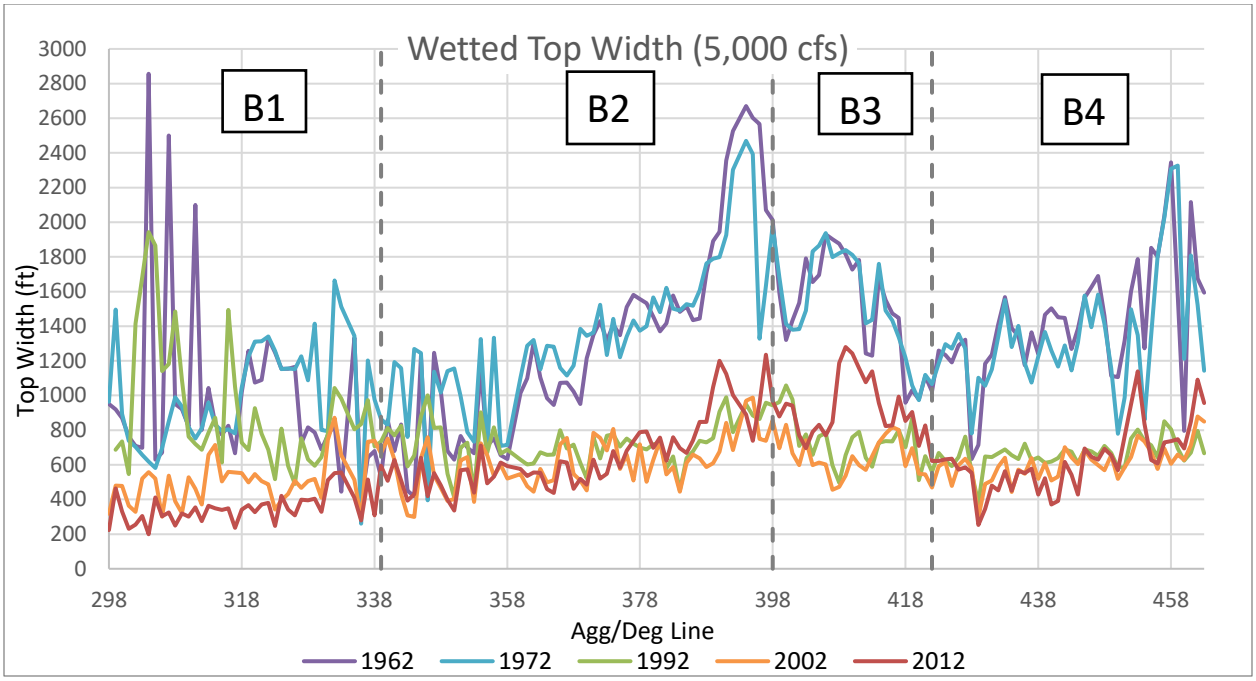

Figure C-3 Wetted top width at each agg/deg line in the Bernalillo Reach at a discharge of 5,000 cfs

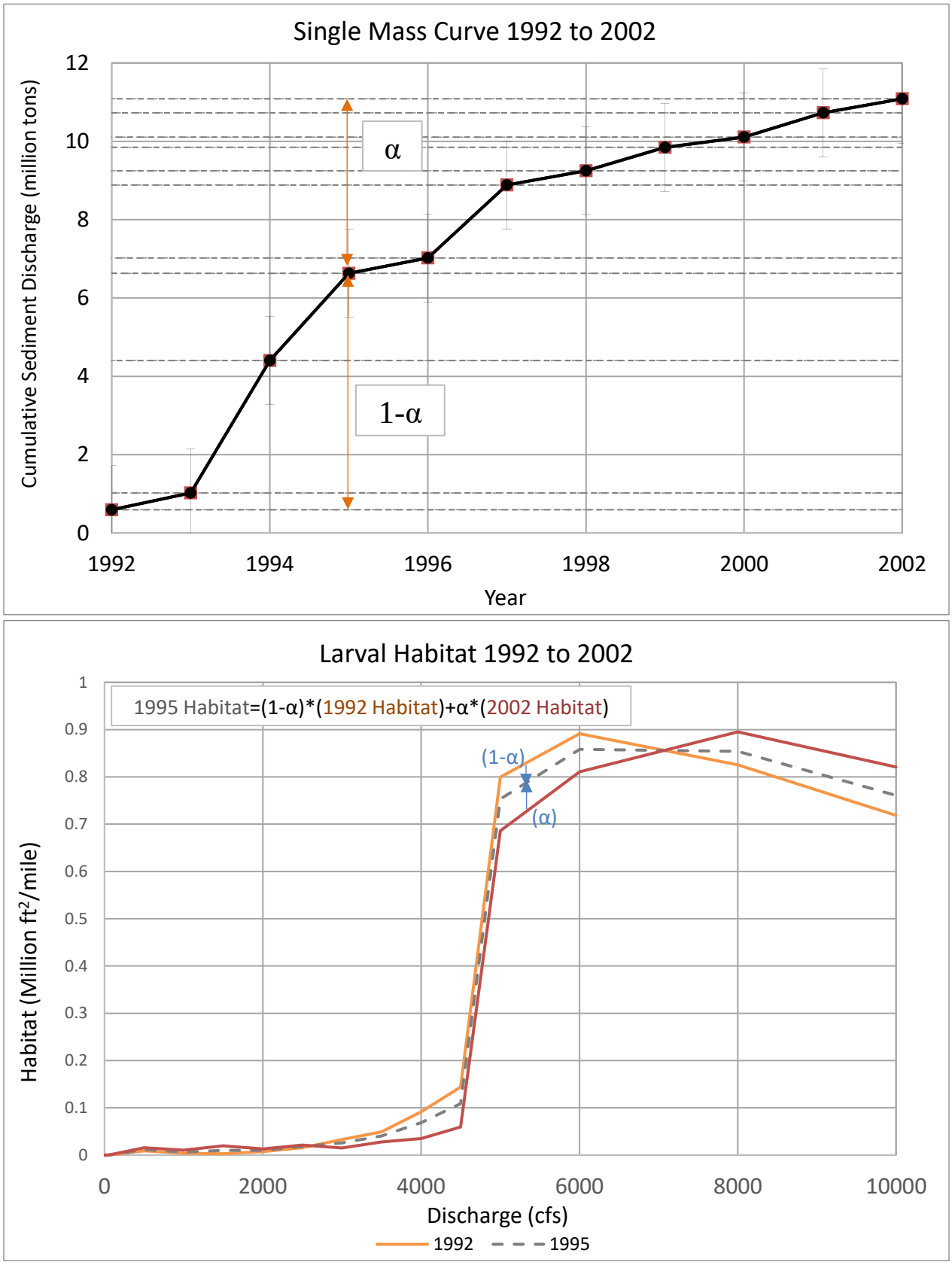

Figure C-4 Example of annual habitat interpolating using the sediment rating curve and alpha technique

Appendix D

Additional Figures from Habitat Analyses

(Habitat Charts by Subreach, Spatially Varying Habitat Charts, Habitat Curves)

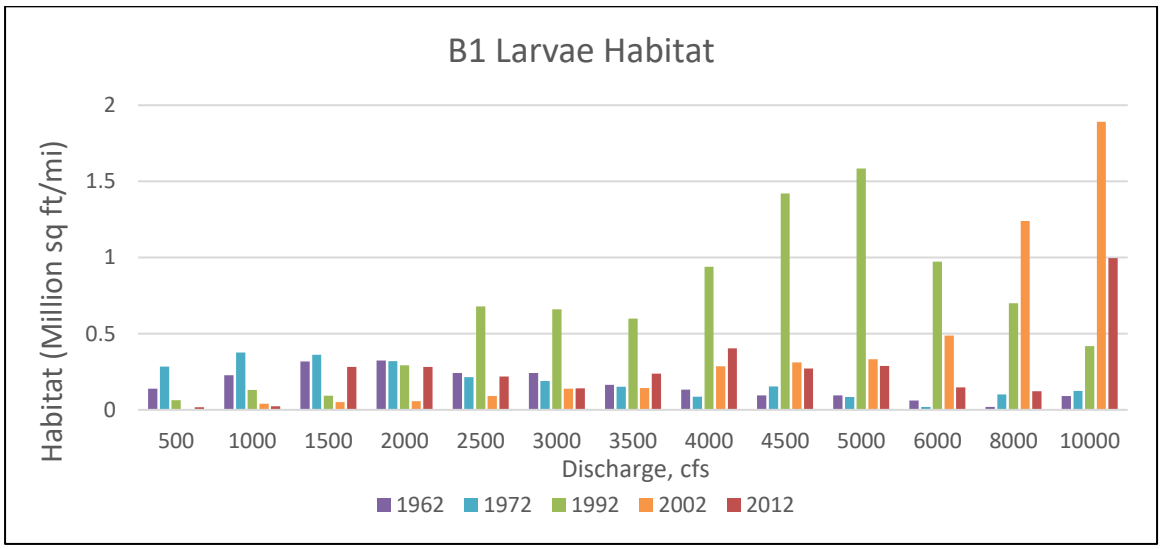

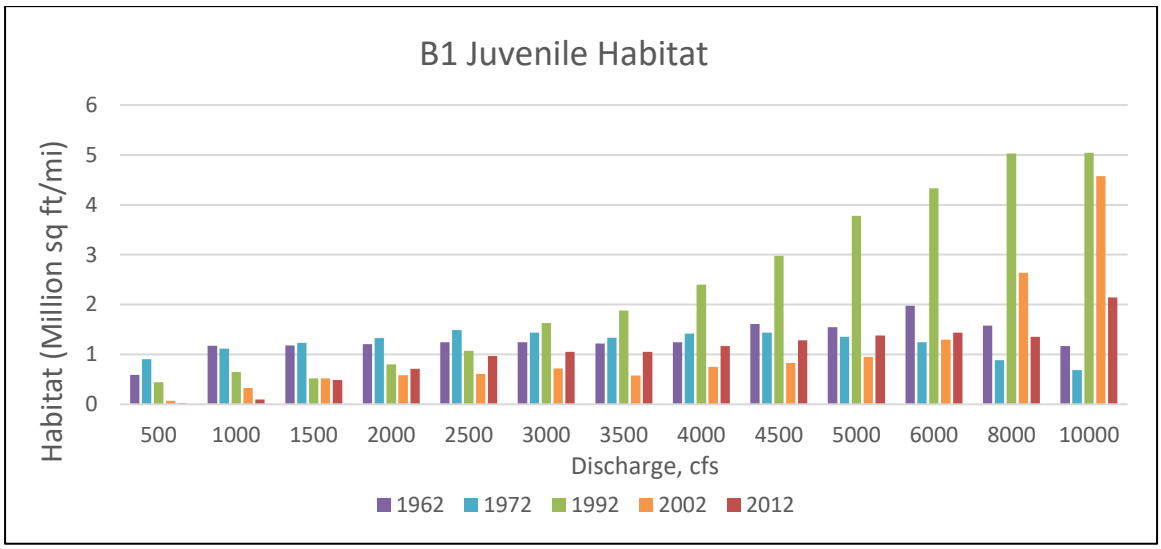

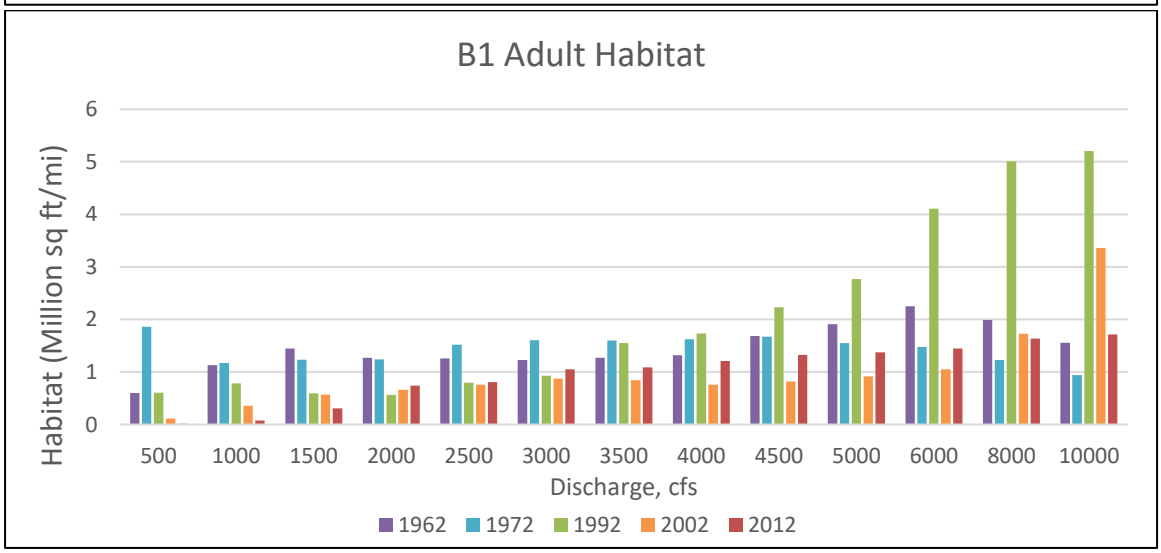

Figure D-1 RGSM habitat availability in Bernalillo Subreach, B1

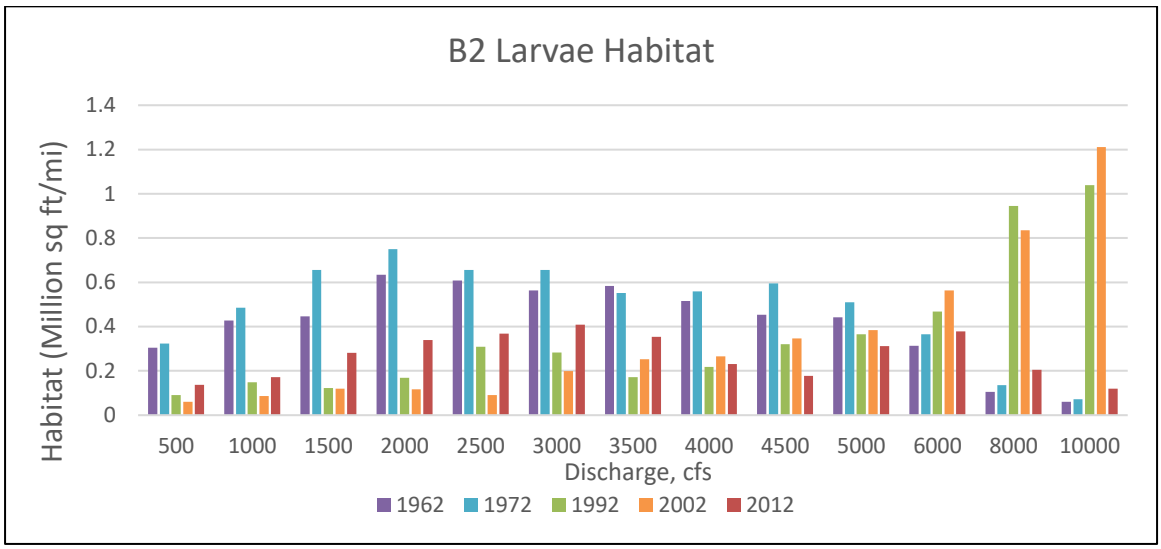

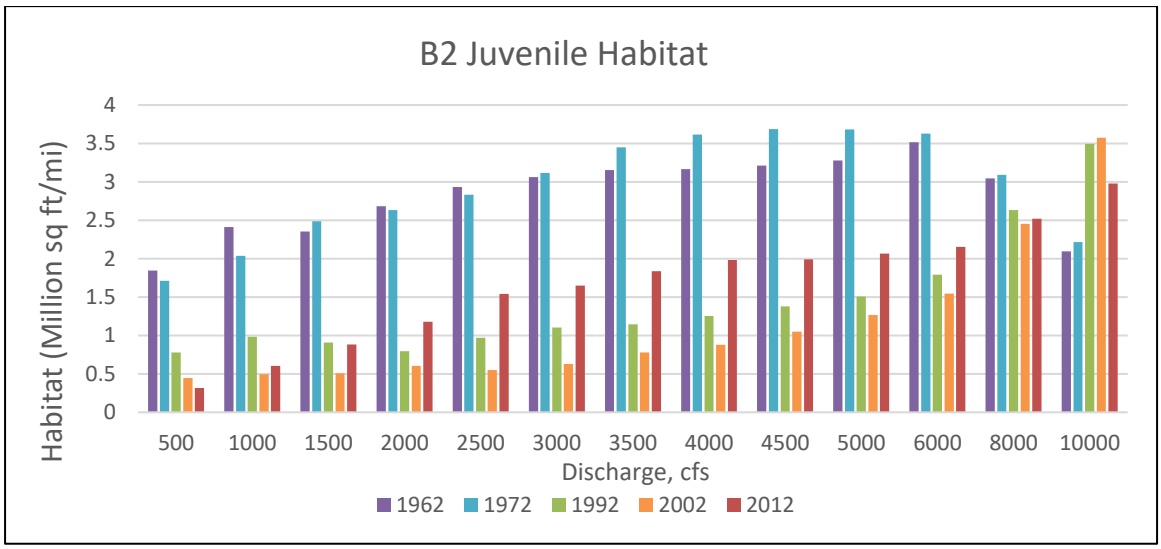

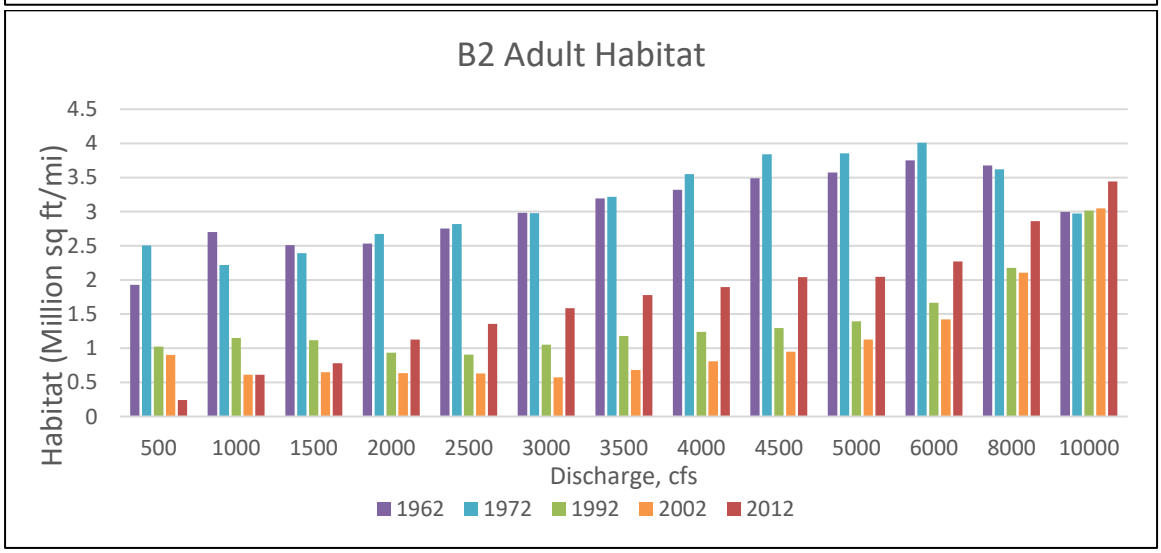

Figure D-2 RGSM habitat availability in Bernalillo Subreach, B2

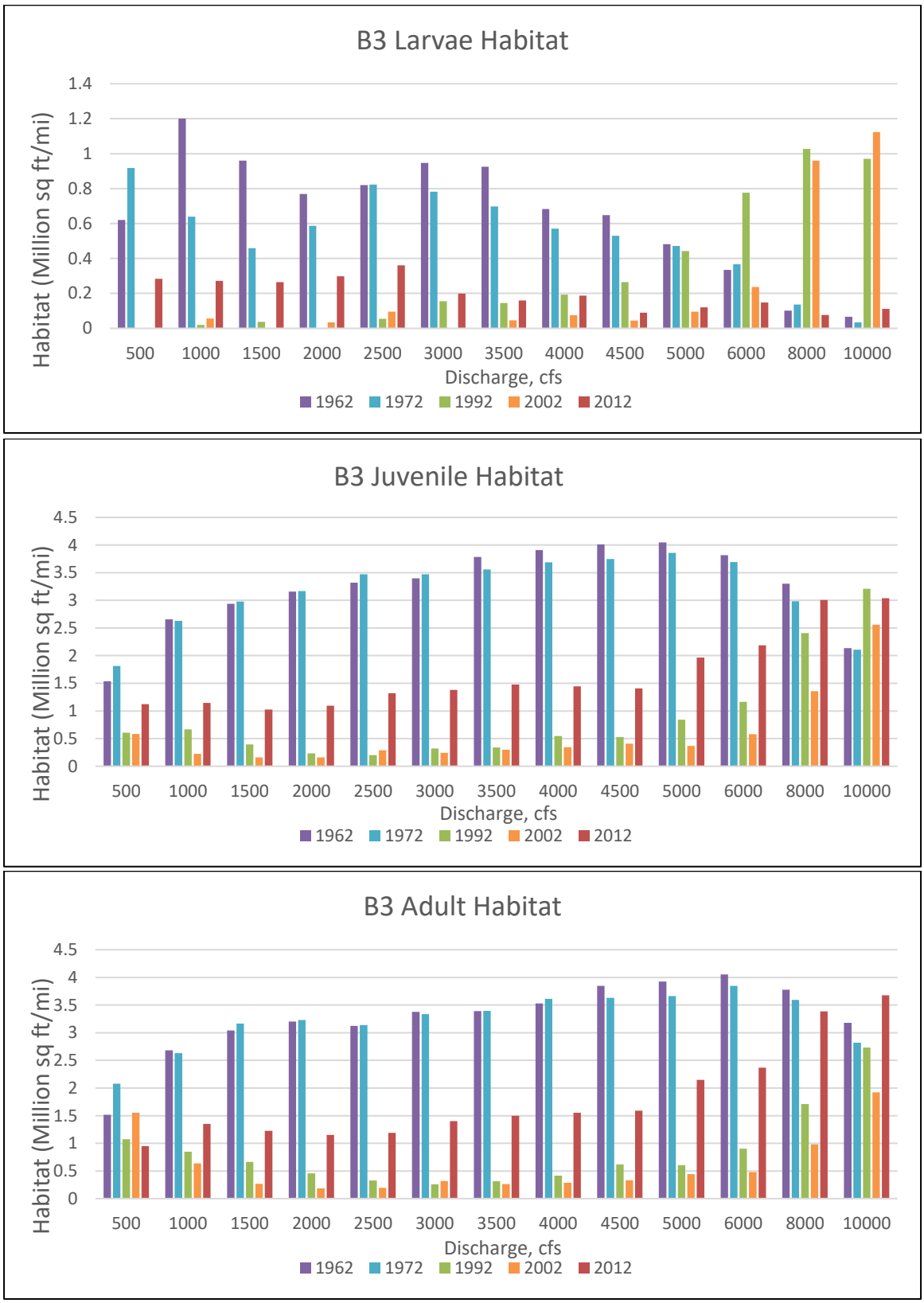

Figure D-3 RGSM habitat availability in Bernalillo Subreach, B3

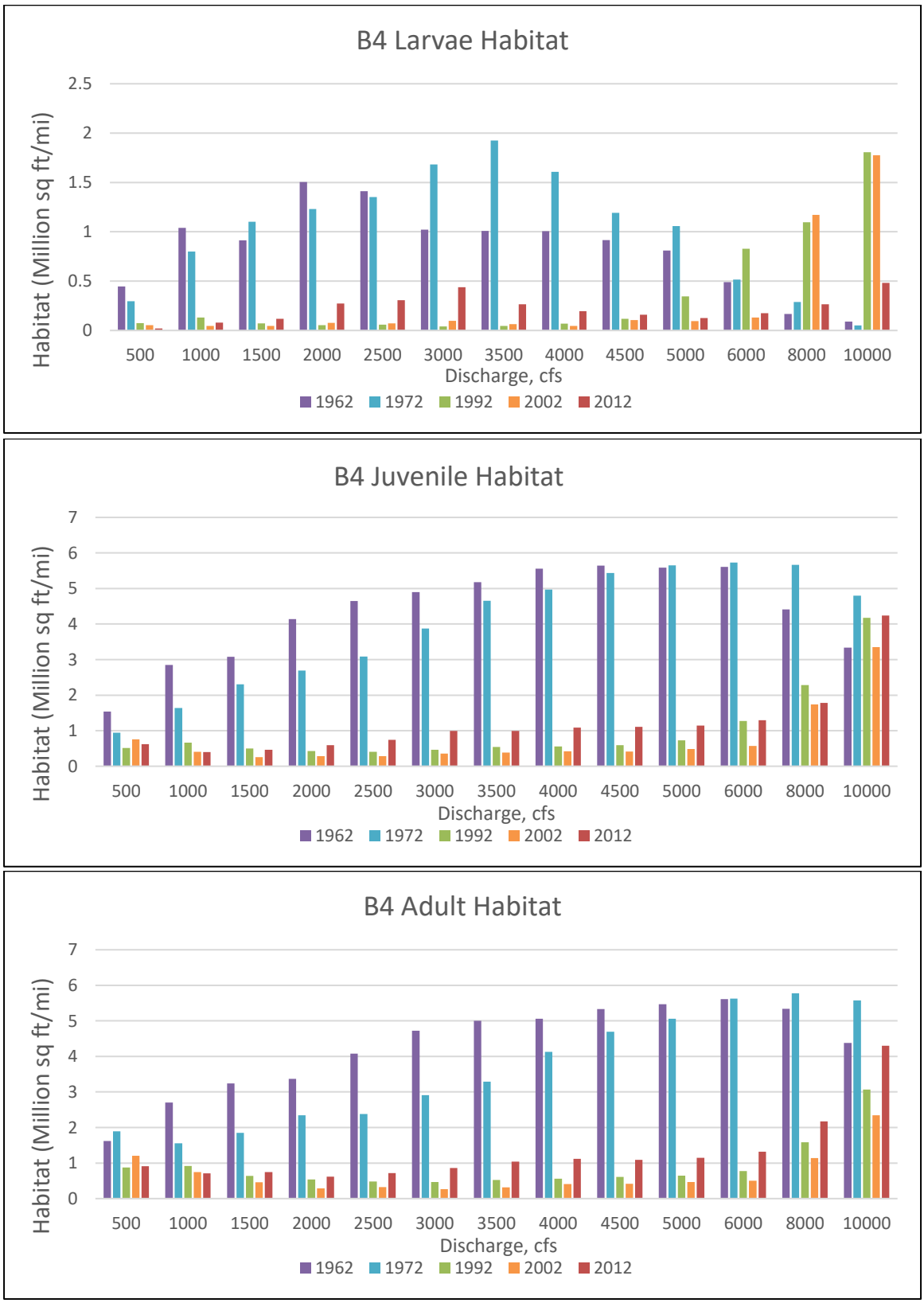

Figure D-4 RGSM habitat availability in Bernalillo Subreach, B4

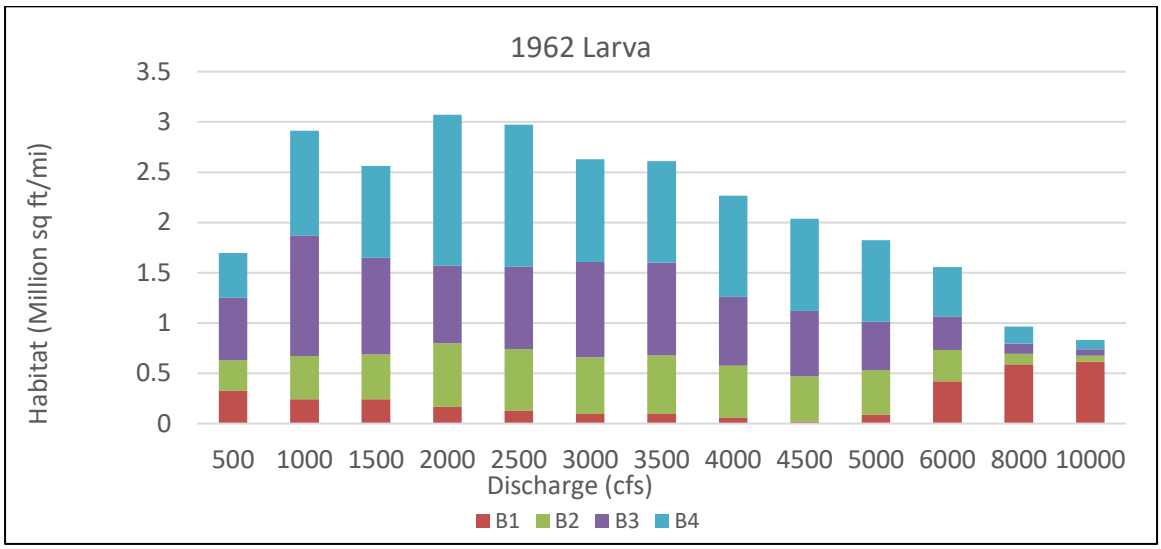

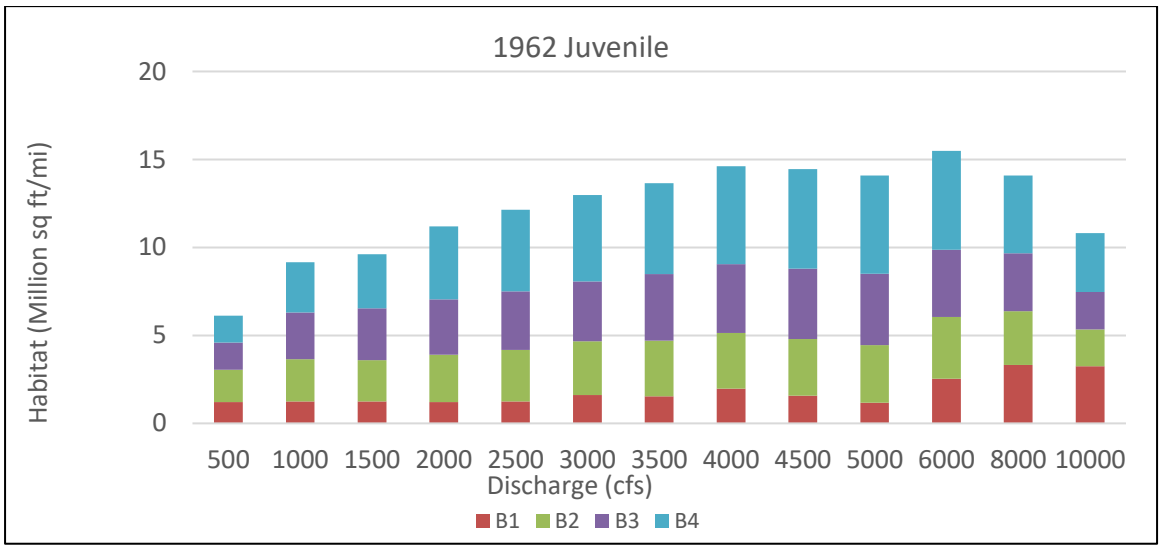

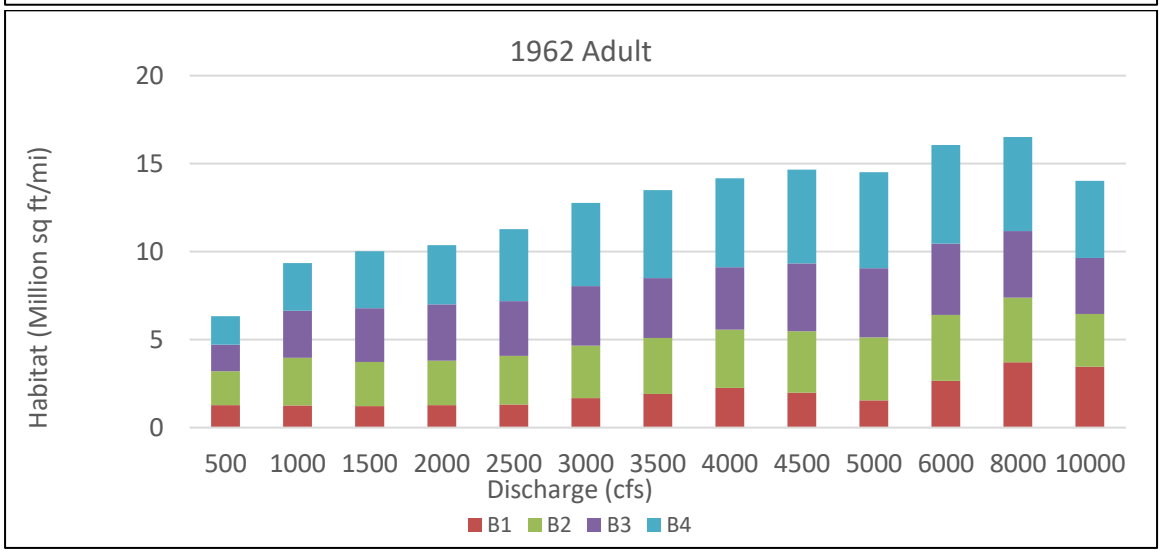

Figure D-5 Stacked habitat charts at different scales to display spatial variations of habitat throughout the Bernalillo reach in 1962

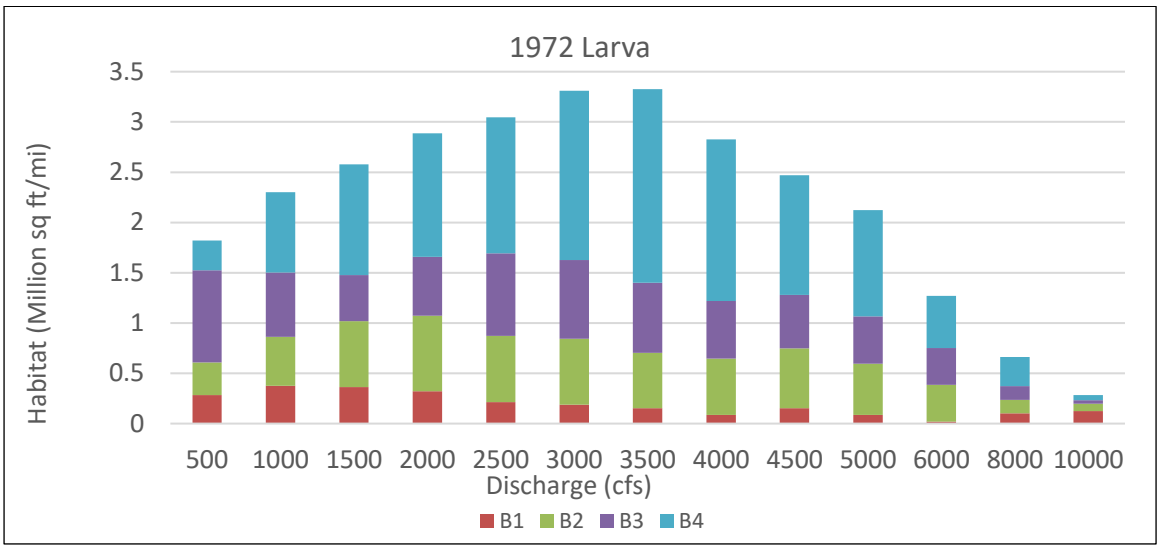

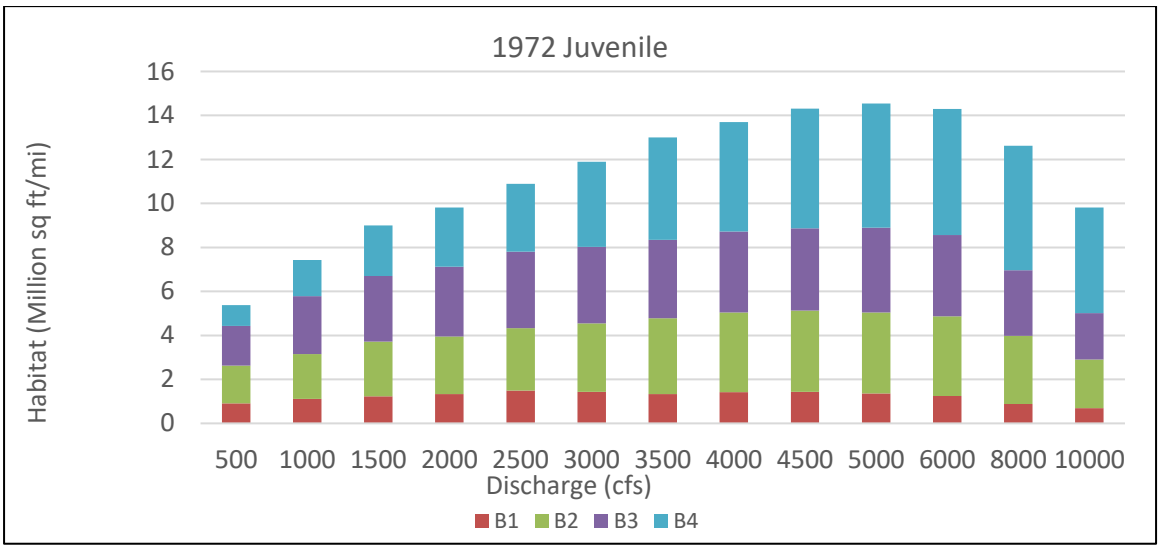

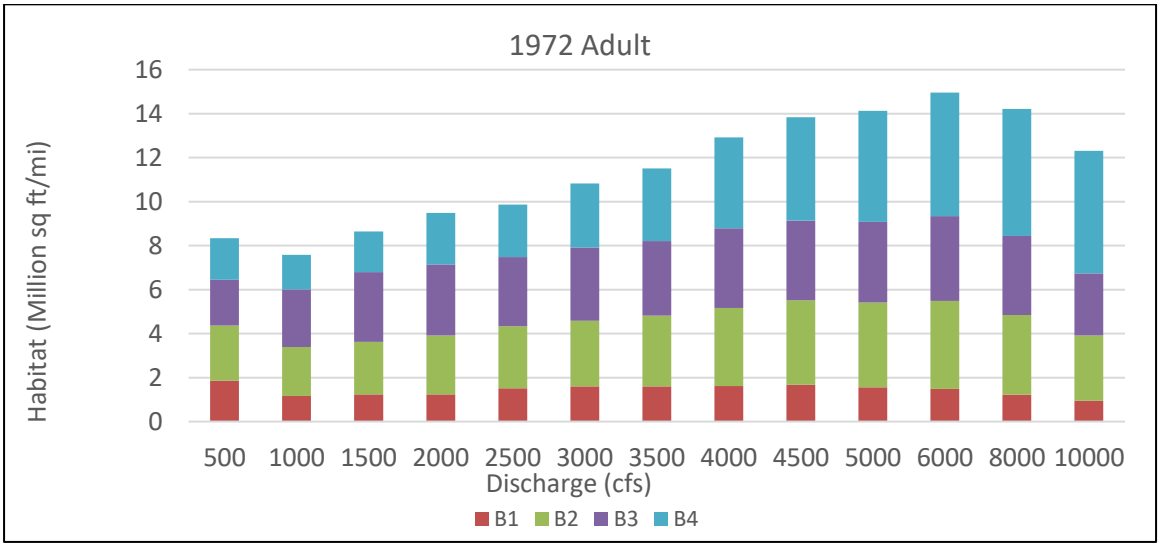

Figure D-6 Stacked habitat charts at different scales to display spatial variations of habitat throughout the Bernalillo reach in 1972

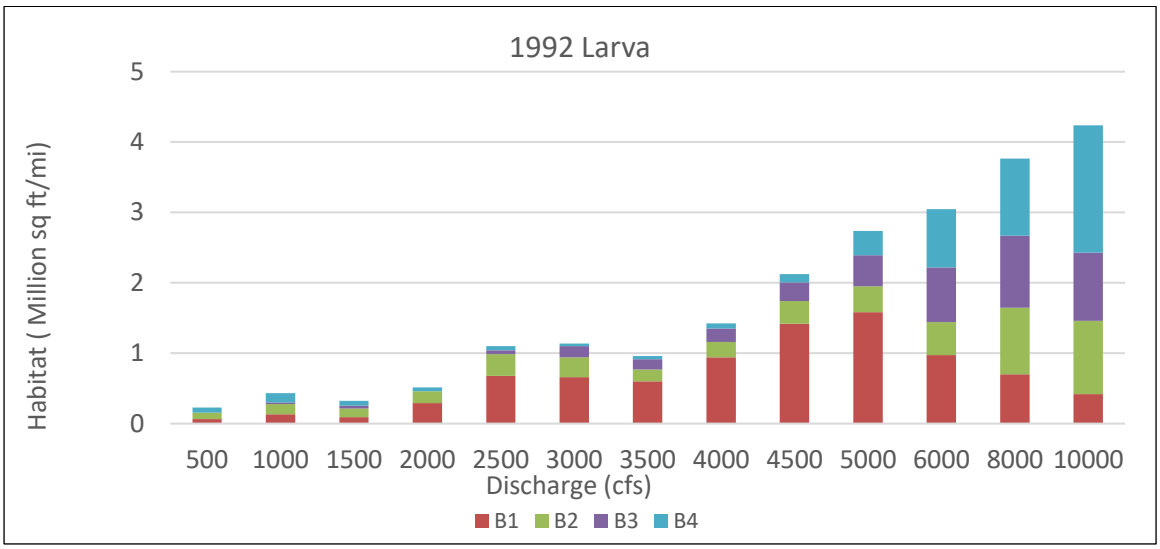

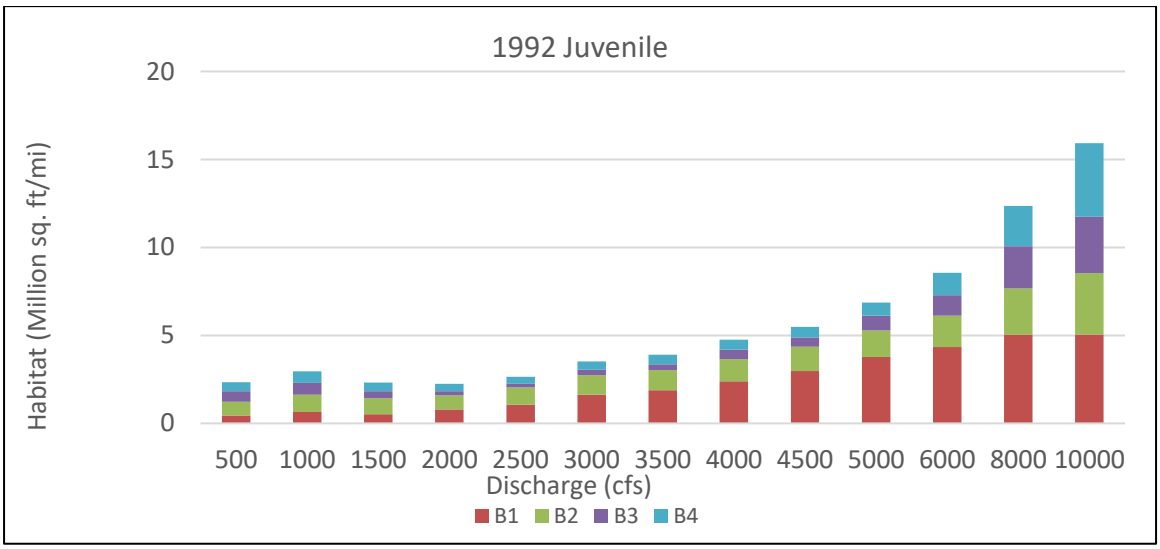

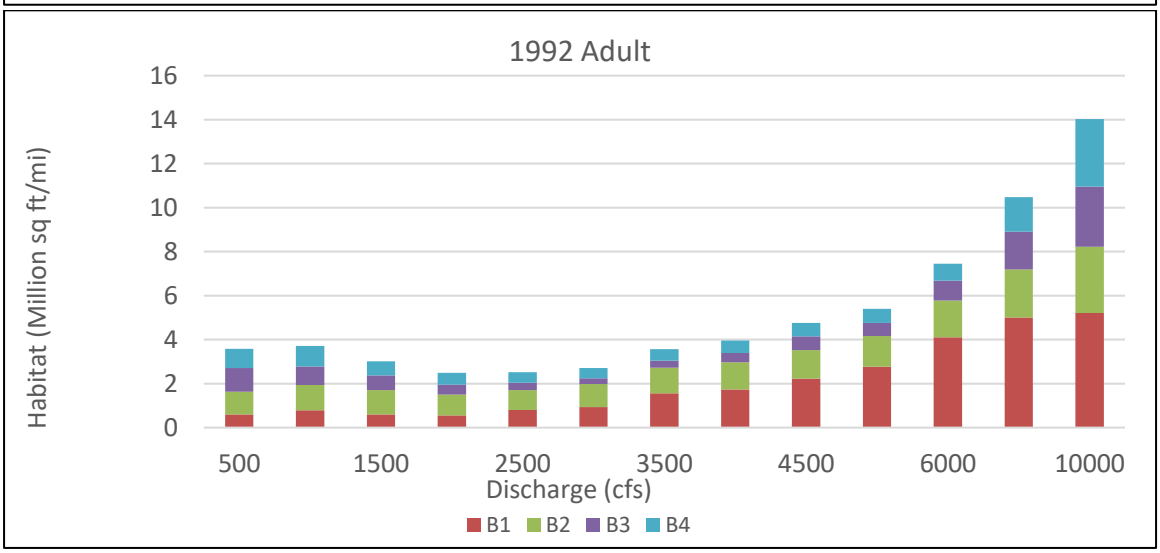

Figure D-7 Stacked habitat charts at different scales to display spatial variations of habitat throughout the Bernalillo reach in 1992

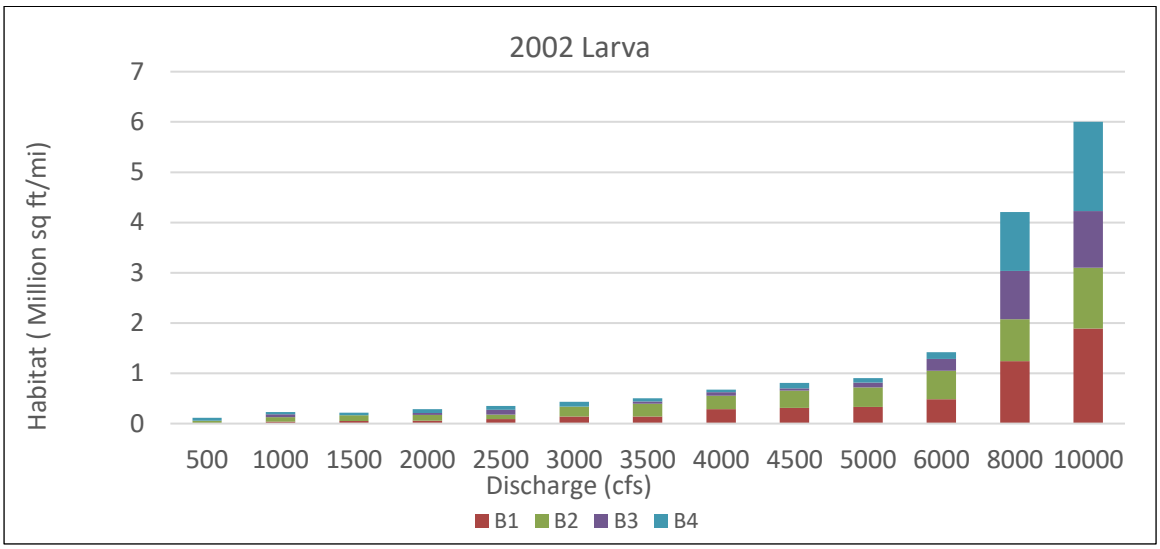

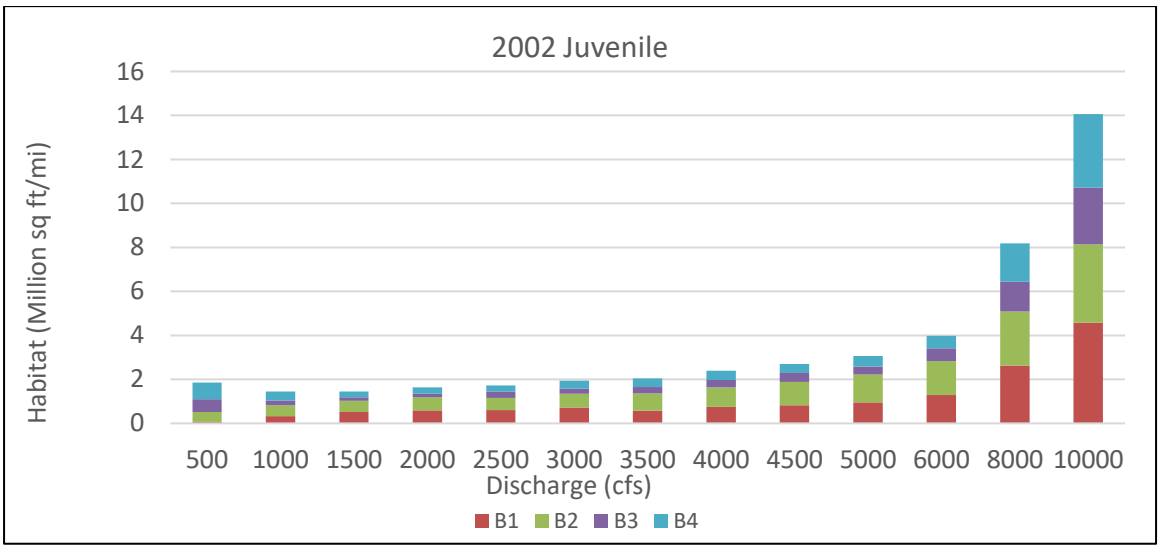

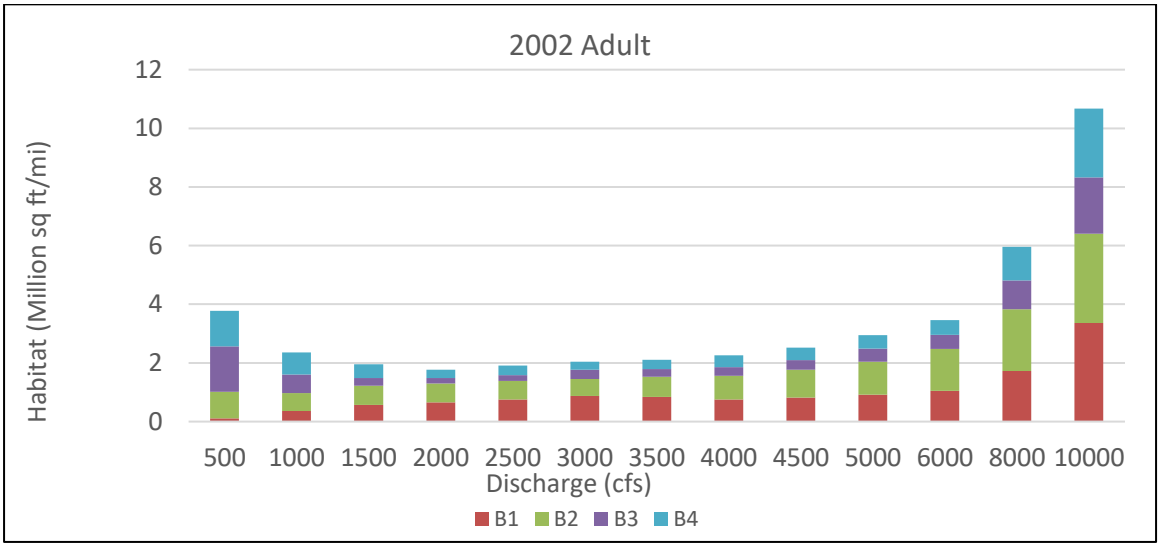

Figure D-8 Stacked habitat charts at different scales to display spatial variations of habitat throughout the Bernalillo reach in 2002

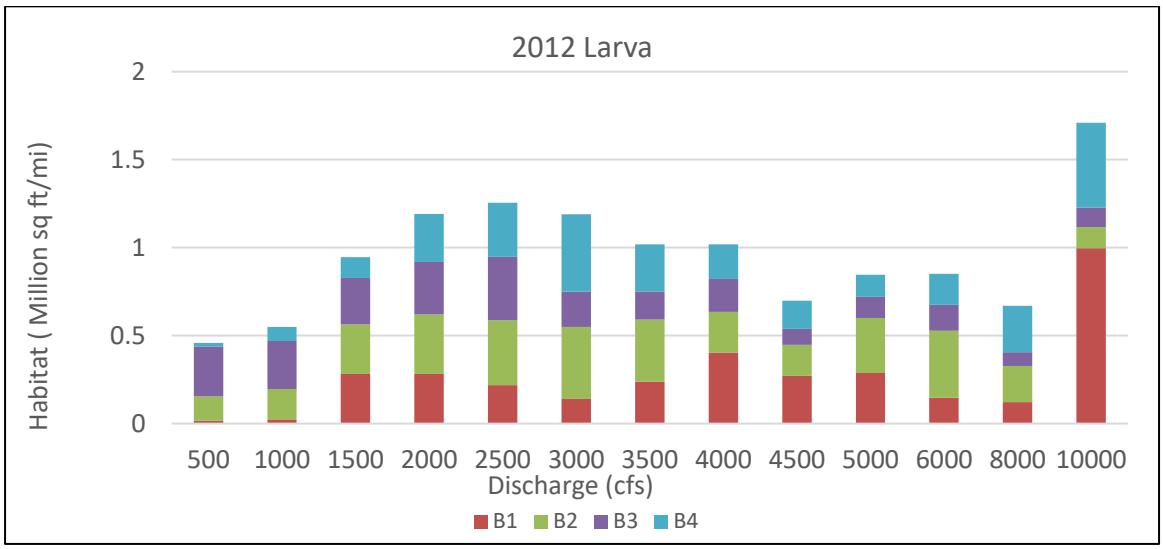

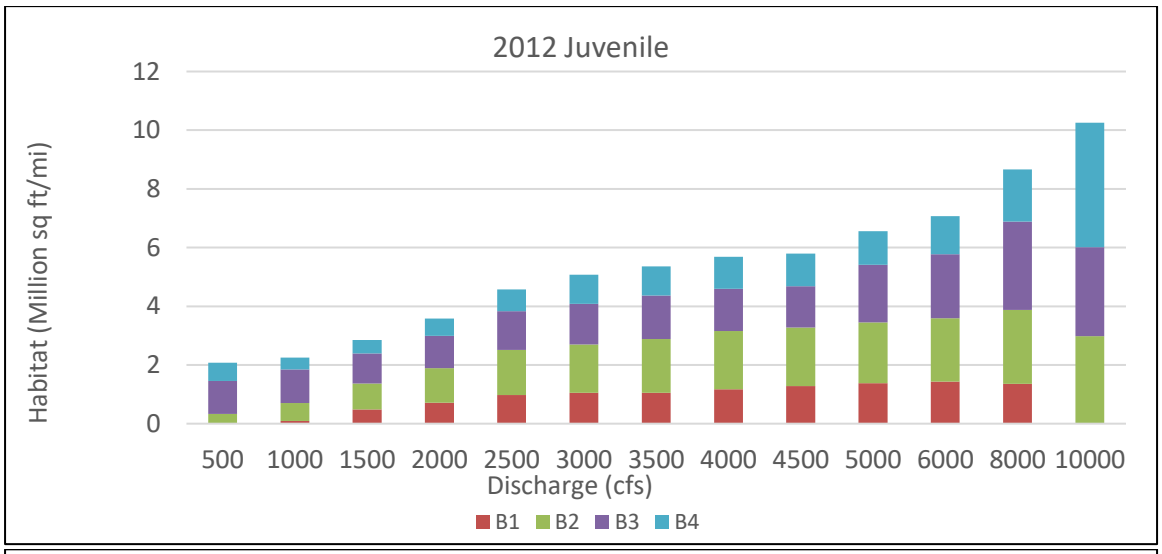

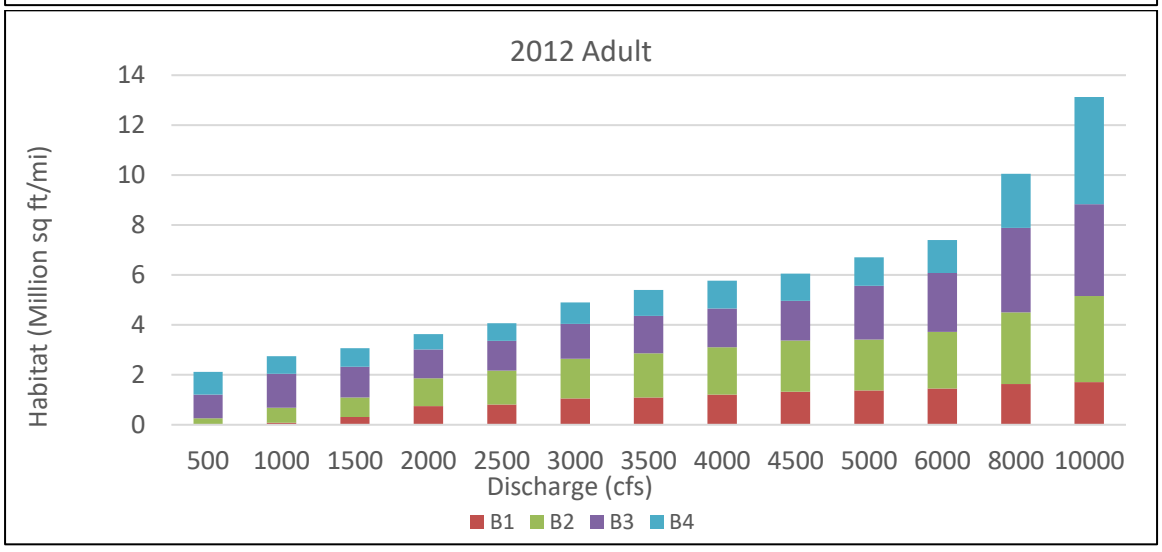

Figure D-9 Stacked habitat charts at different scales to display spatial variations of habitat throughout the Bernalillo reach in 2012

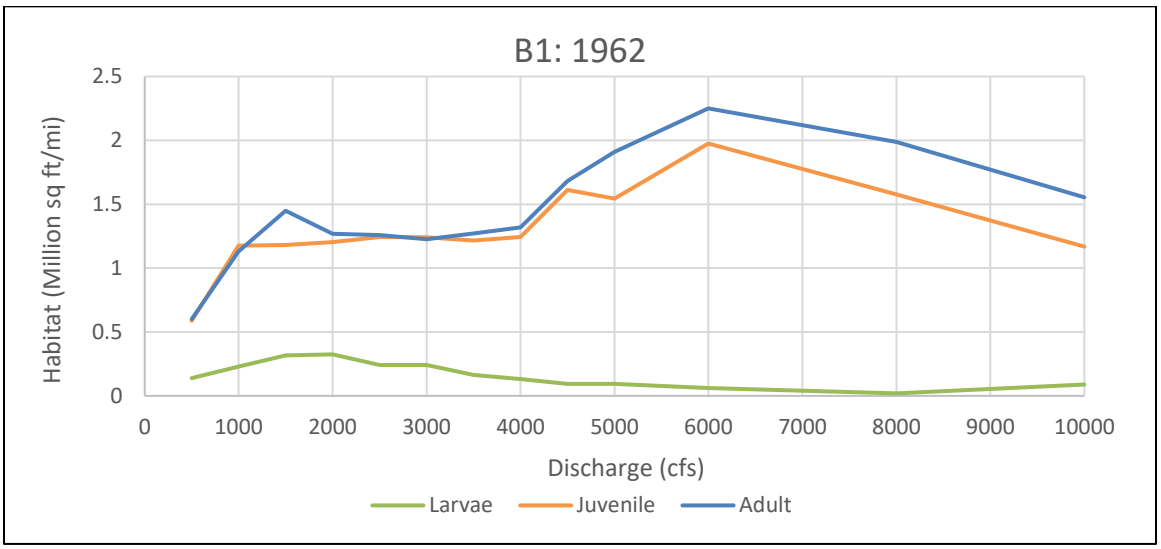
B1: 1962
Habitat (Million sq ft/mi)
2.5
2
1.5
1
0.5
0
0
1000
2000
3000
4000
5000
6000
7000
8000
9000
10000
Discharge (cfs)
Larvae
Juvenile
Adult

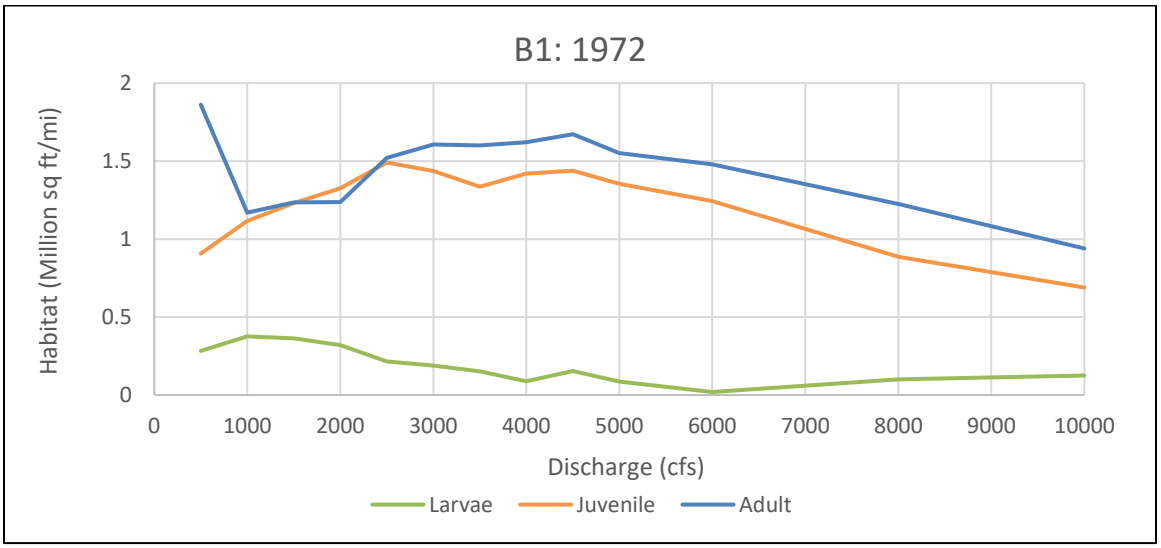
B1: 1972
Habitat (Million sq ft/mi)
2
1.5
1
0.5
0
0
1000
2000
3000
4000
5000
6000
7000
8000
9000
10000
Discharge (cfs)
Larvae
Juvenile
Adult

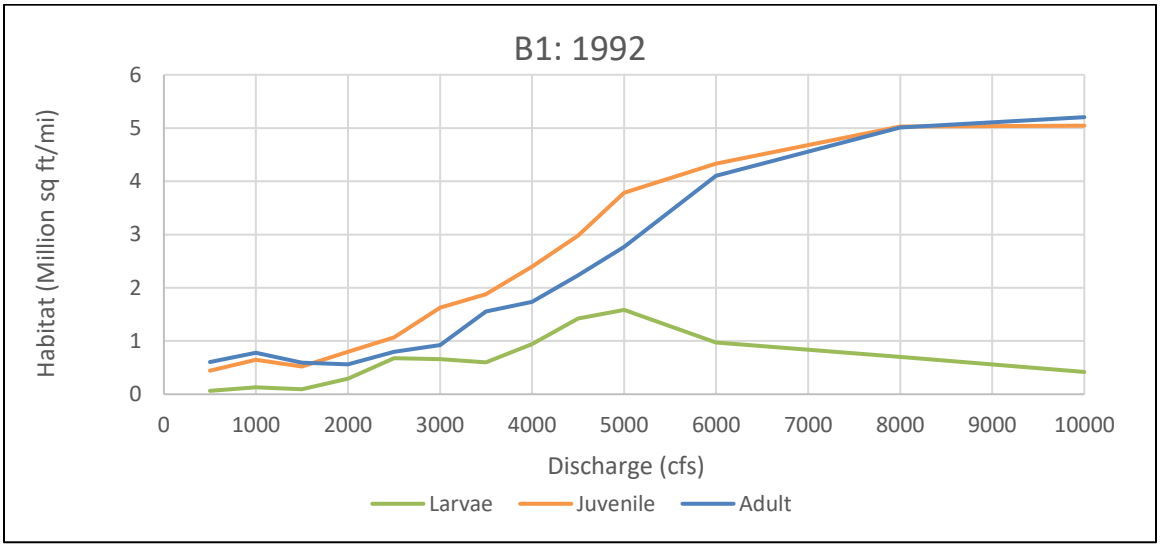
B1: 1992
Habitat (Million sq ft/mi)
6
5
4
3
2
1
0
0
1000
2000
3000
4000
5000
6000
7000
8000
9000
10000
Discharge (cfs)
Larvae
Juvenile
Adult

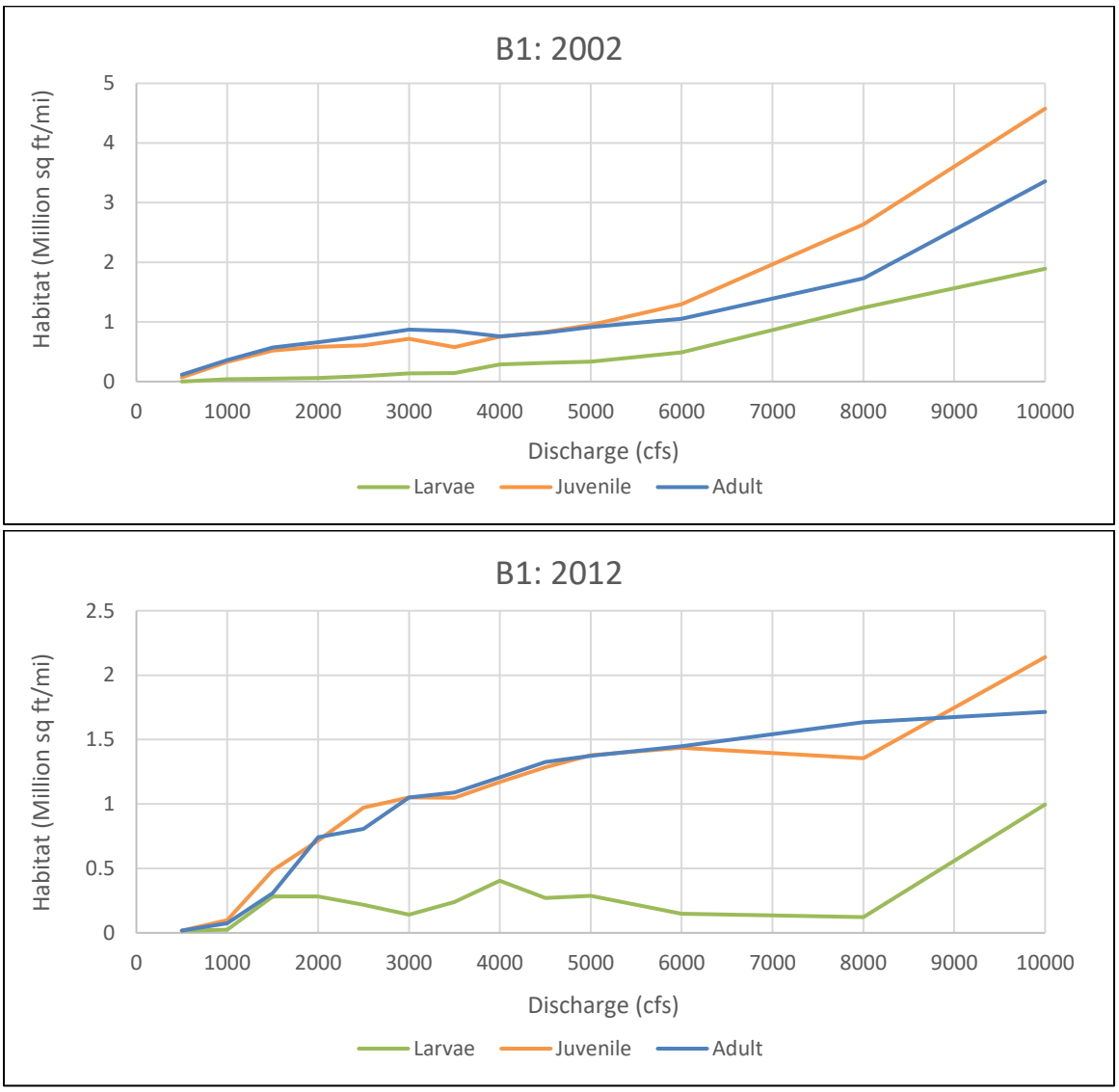

Figure D-10 Life stage habitat curves for Bernalillo Subreach B1 for the years 1962 to 2012.

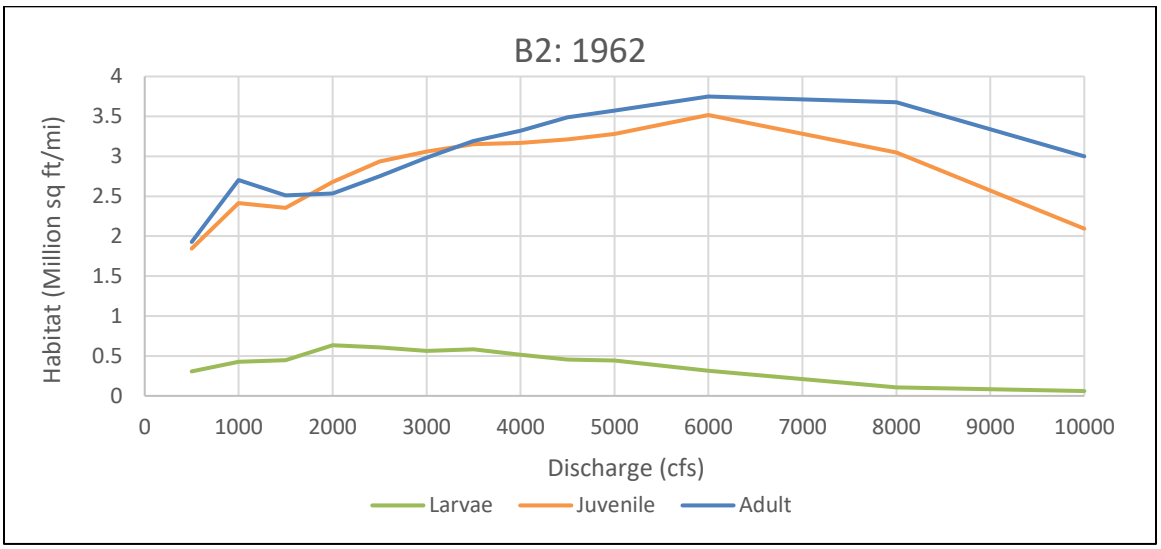
B2: 1962
Habitat (Million sq ft/mi)
4
3.5
3
2.5
2
1.5
1
0.5
0
0
1000
2000
3000
4000
5000
6000
7000
8000
9000
10000
Discharge (cfs)
Larvae
Juvenile
Adult

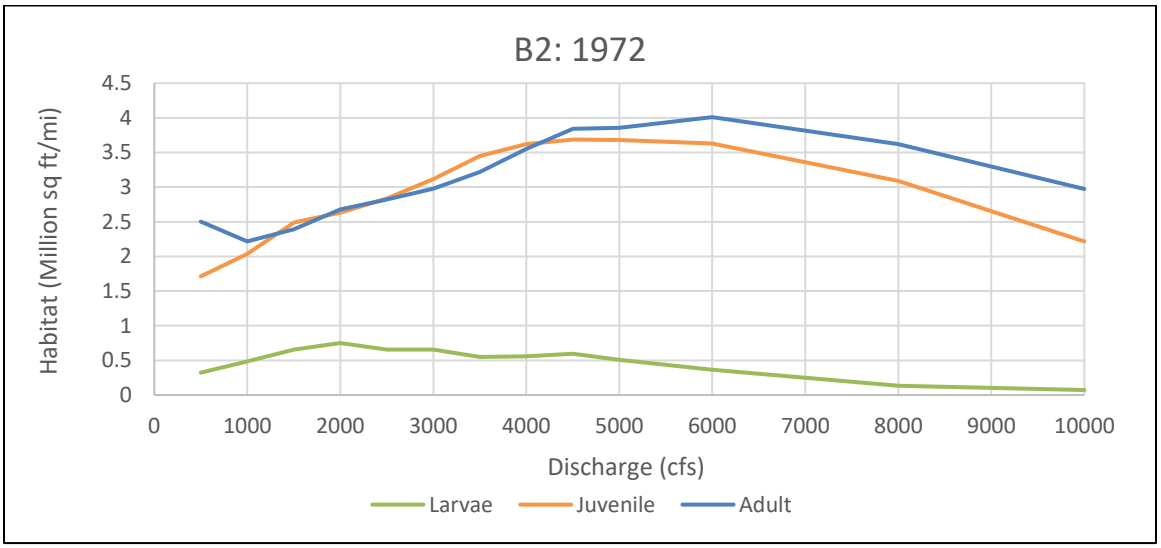
B2: 1972
Habitat (Million sq ft/mi)
4.5
4
3.5
3
2.5
2
1.5
1
0.5
0
0
1000
2000
3000
4000
5000
6000
7000
8000
9000
10000
Discharge (cfs)
Larvae
Juvenile
Adult

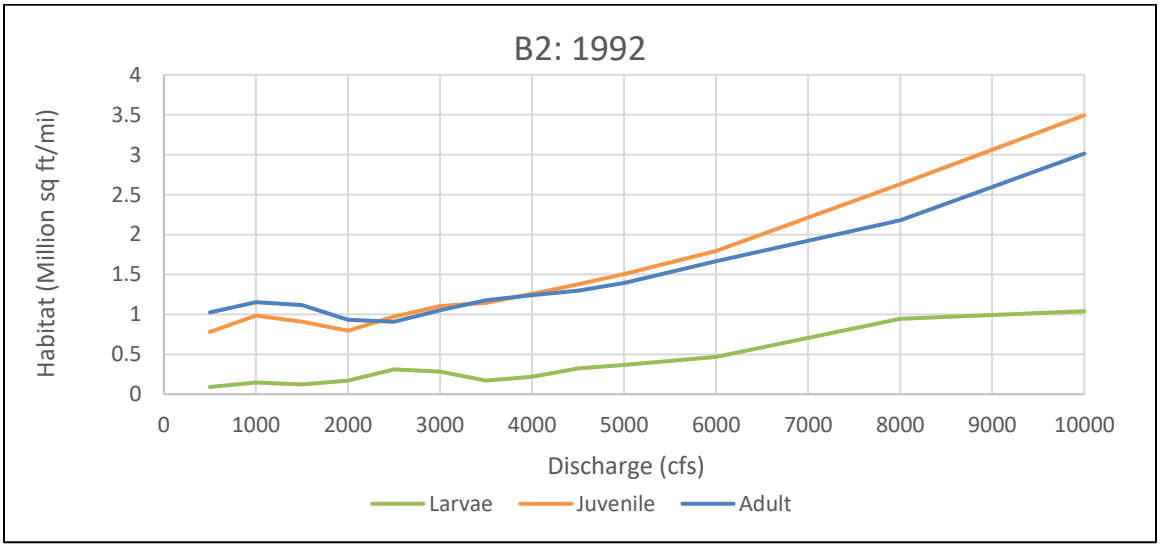
B2: 1992
Habitat (Million sq ft/mi)
4
3.5
3
2.5
2
1.5
1
0.5
0
0
1000
2000
3000
4000
5000
6000
7000
8000
9000
10000
Discharge (cfs)
Larvae
Juvenile
Adult

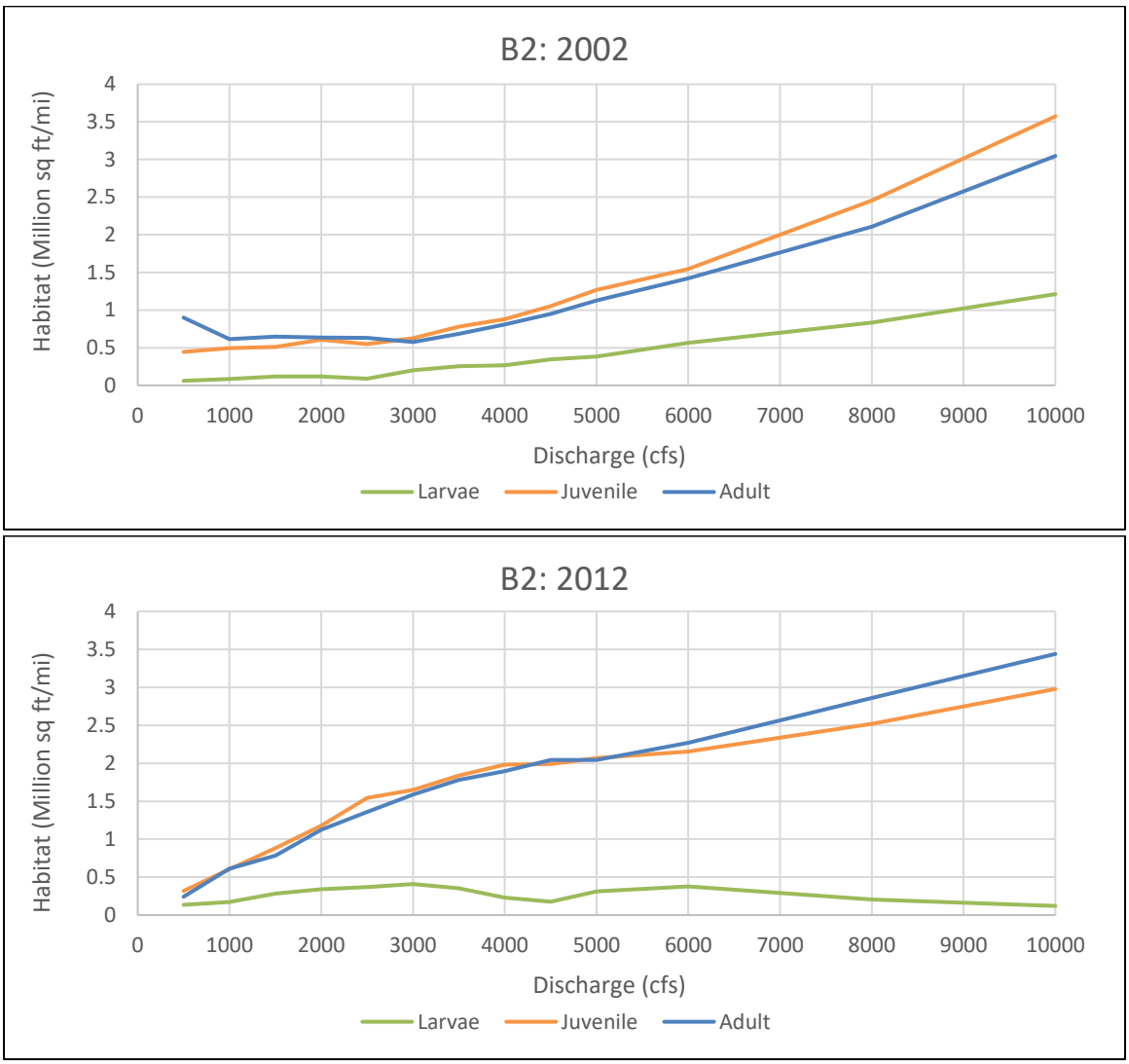

Figure D-11 Life stage habitat curves for Bernalillo Subreach B2 for the years 1962 to 2012.

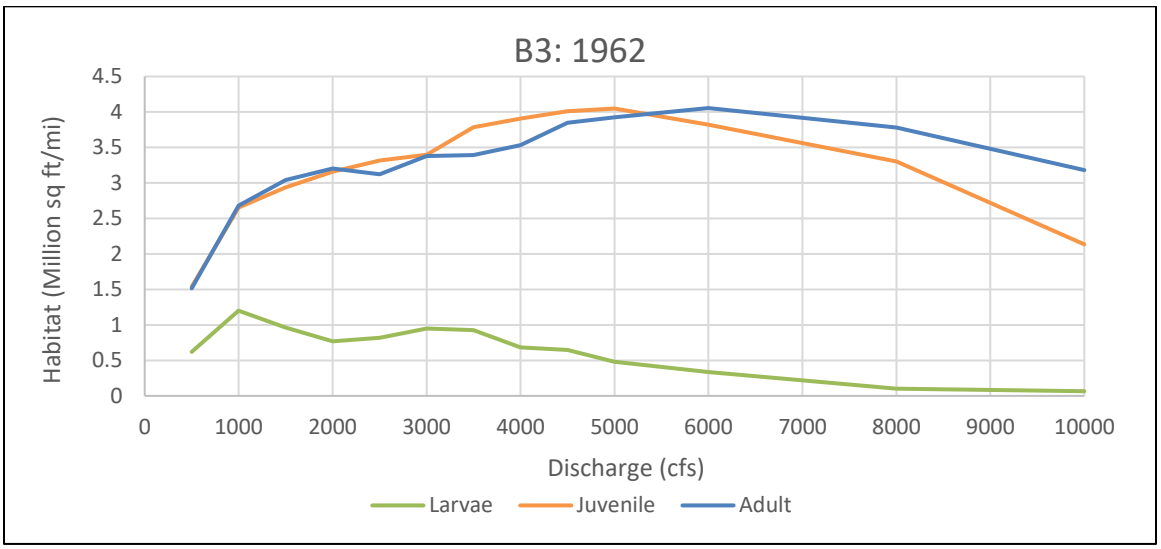
B3: 1962
Habitat (Million sq ft/mi)
4.5
4
3.5
3
2.5
2
1.5
1
0.5
0
0
1000
2000
3000
4000
5000
6000
7000
8000
9000
10000
Discharge (cfs)
Larvae
Juvenile
Adult

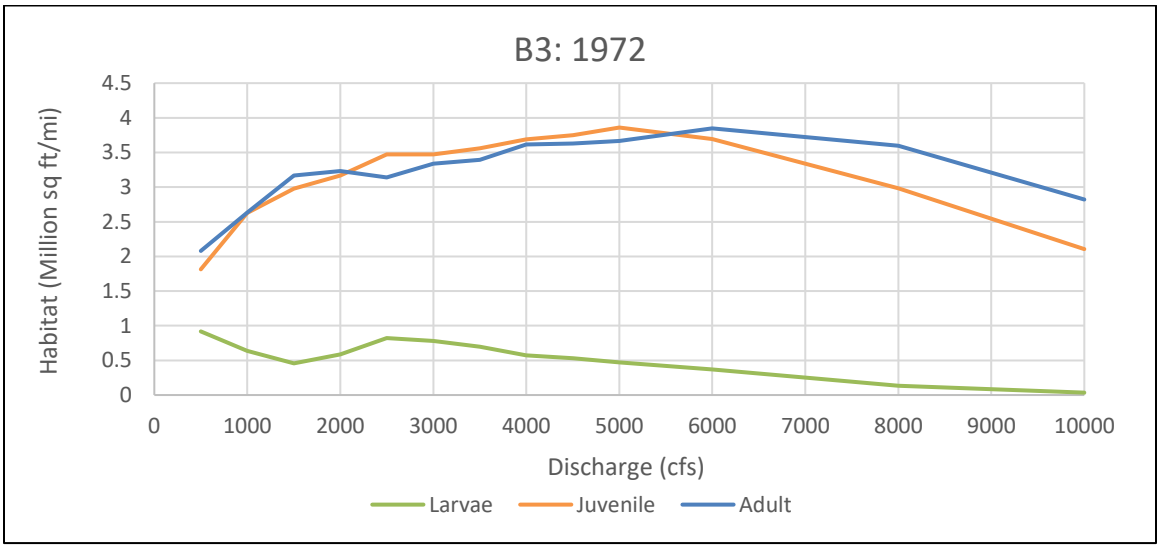
B3: 1972
Habitat (Million sq ft/mi)
4.5
4
3.5
3
2.5
2
1.5
1
0.5
0
0
1000
2000
3000
4000
5000
6000
7000
8000
9000
10000
Discharge (cfs)
Larvae
Juvenile
Adult

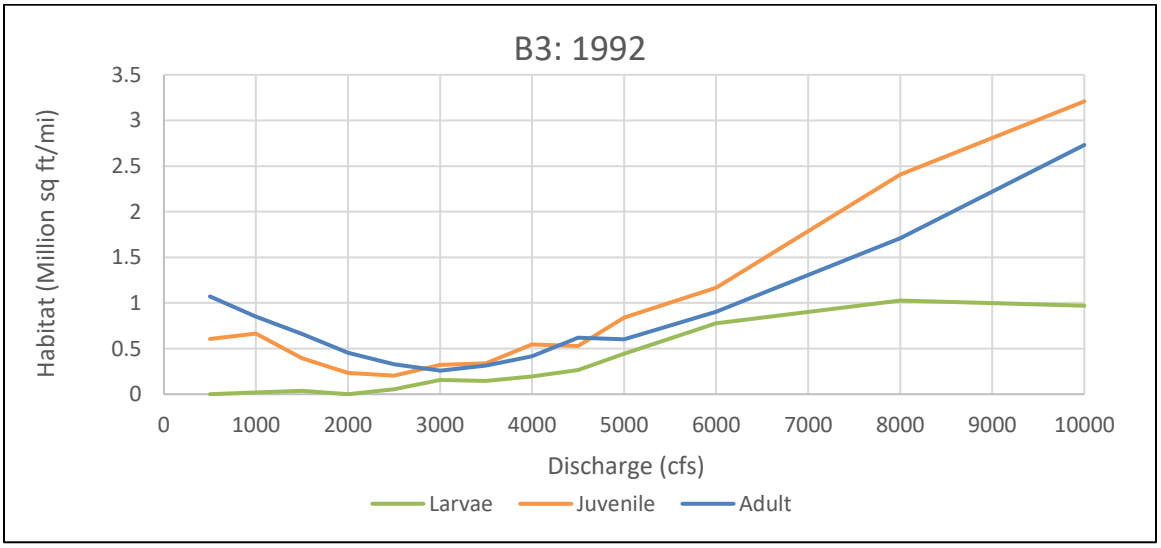
B3: 1992
Habitat (Million sq ft/mi)
3.5
3
2.5
2
1.5
1
0.5
0
0
1000
2000
3000
4000
5000
6000
7000
8000
9000
10000
Discharge (cfs)
Larvae
Juvenile
Adult

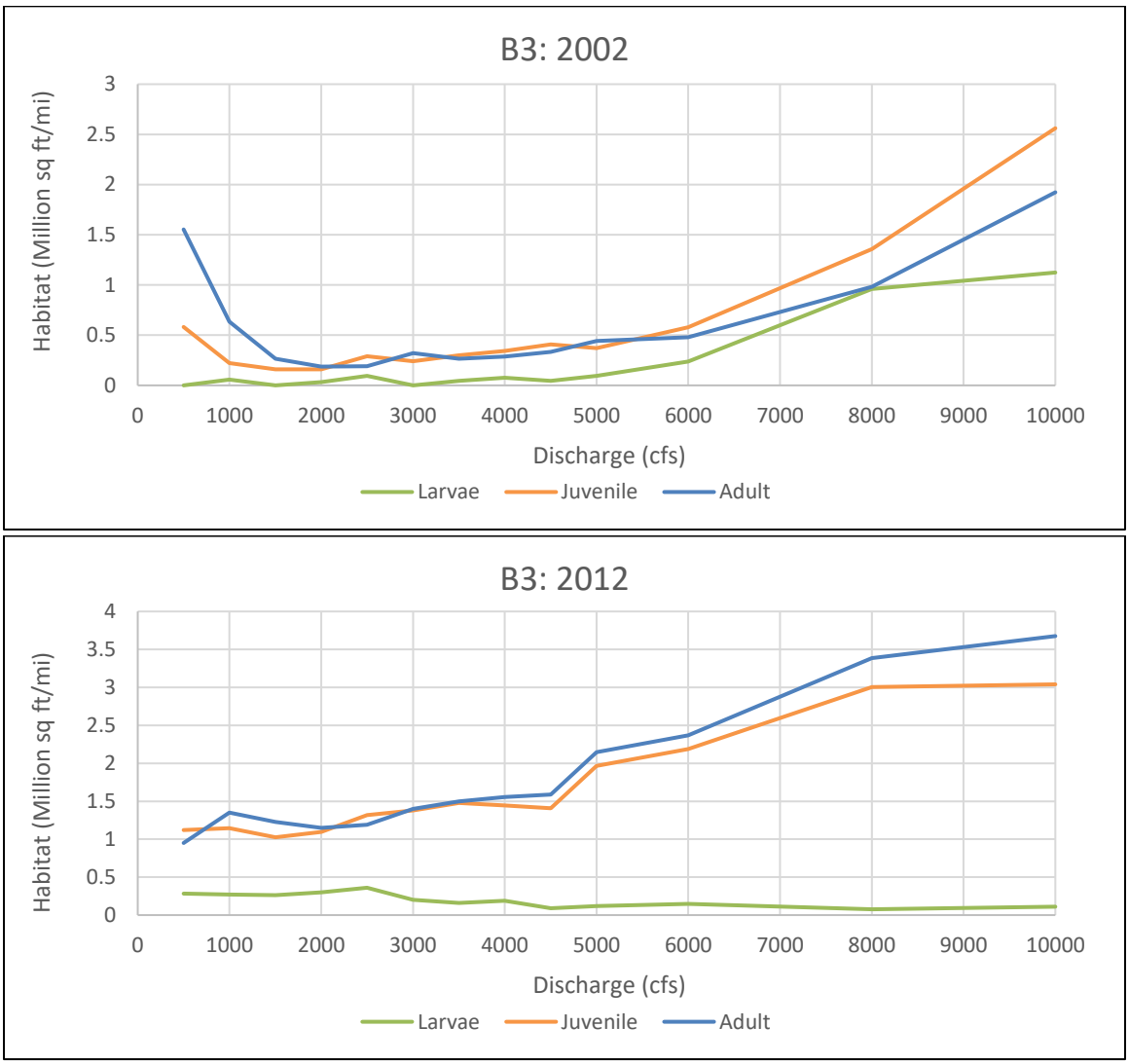

Figure D-12 Life stage habitat curves for Bernalillo Subreach B3 for the years 1962 to 2012.

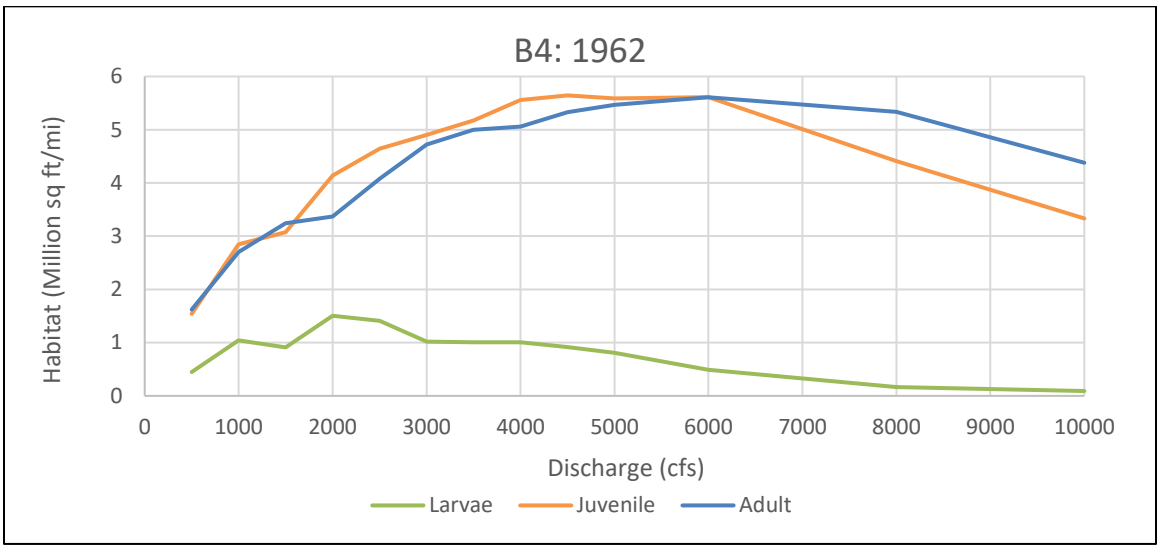
B4: 1962
Habitat (Million sq ft/mi)
0
1
2
3
4
5
6
0
1000
2000
3000
4000
5000
6000
7000
8000
9000
10000
Discharge (cfs)
Larvae
Juvenile
Adult

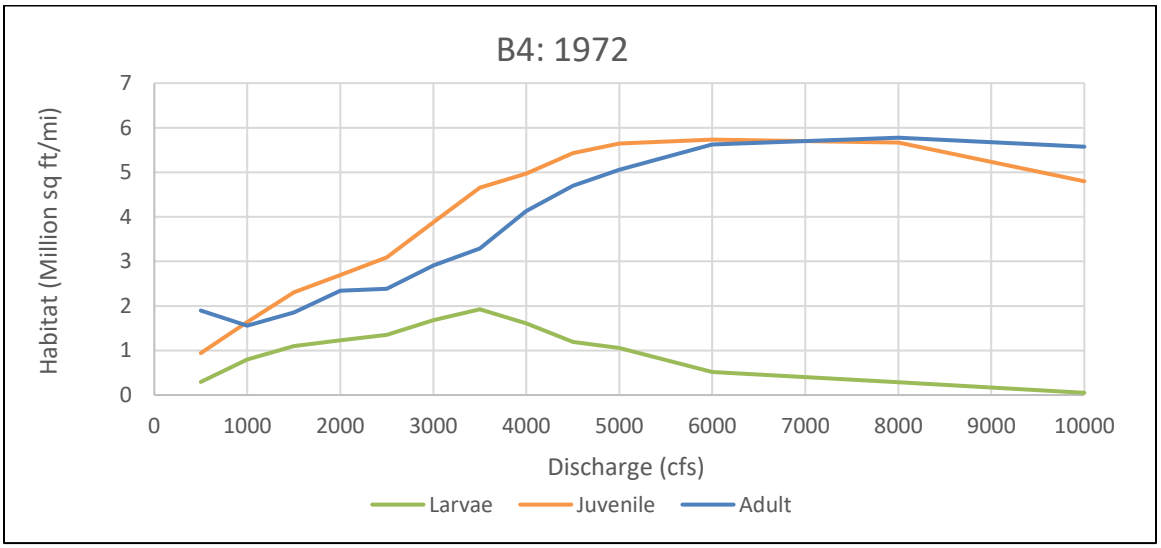
B4: 1972
Habitat (Million sq ft/mi)
0
1
2
3
4
5
6
7
0
1000
2000
3000
4000
5000
6000
7000
8000
9000
10000
Discharge (cfs)
Larvae
Juvenile
Adult

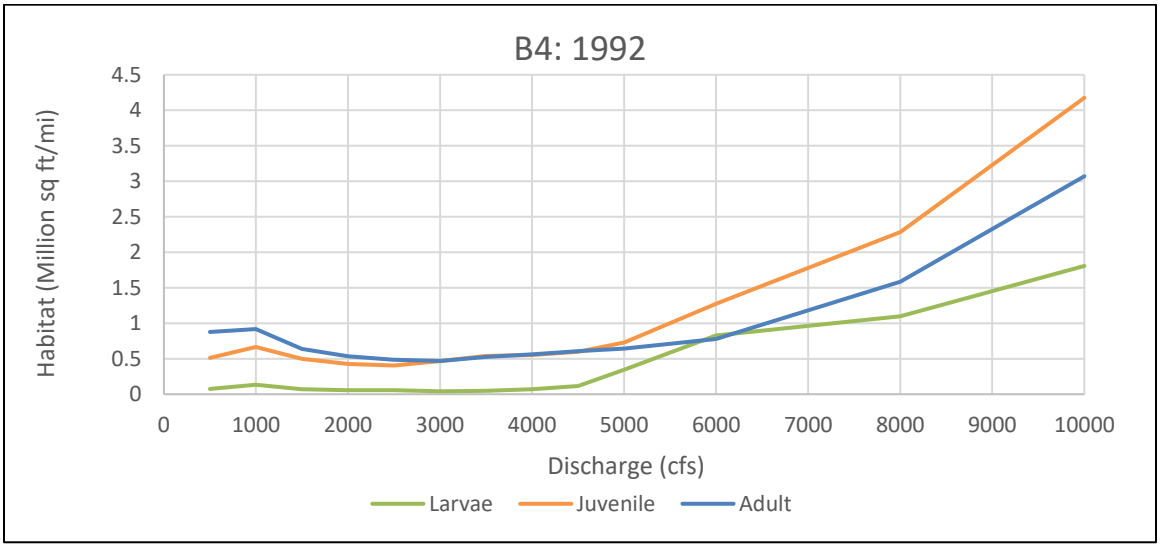
B4: 1992
Habitat (Million sq ft/mi)
0
0.5
1
1.5
2
2.5
3
3.5
4
4.5
0
1000
2000
3000
4000
5000
6000
7000
8000
9000
10000
Discharge (cfs)
Larvae
Juvenile
Adult

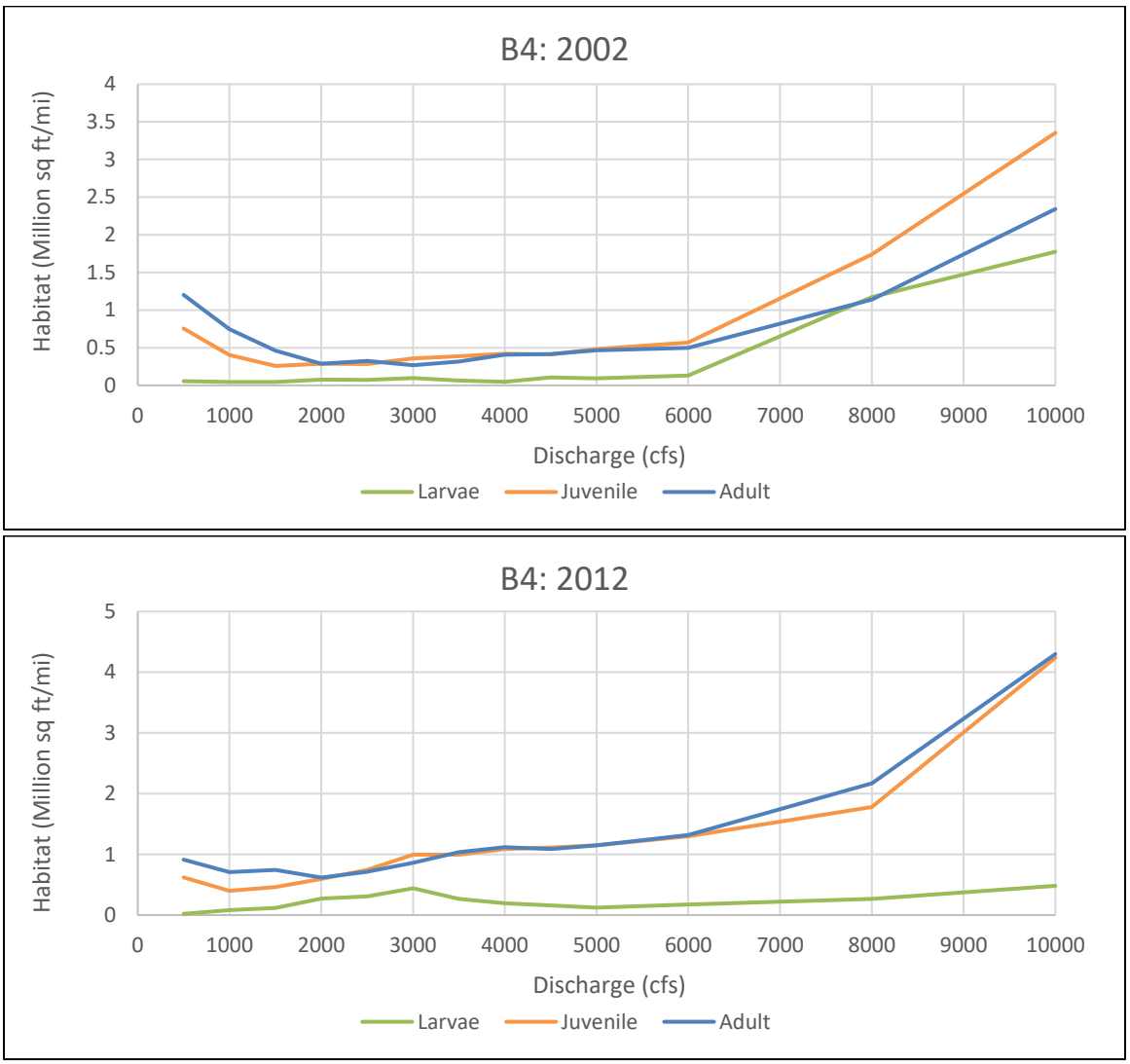

Figure D-13 Life stage habitat curves for Bernalillo Subreach B4 for the years 1962 to 2012.

Appendix E

Maps of Hydraulically Suitable Habitat for the Rio Grande Silvery Minnow

(1,500 cfs, 3,000 cfs, and 5,000 cfs Flow Events)

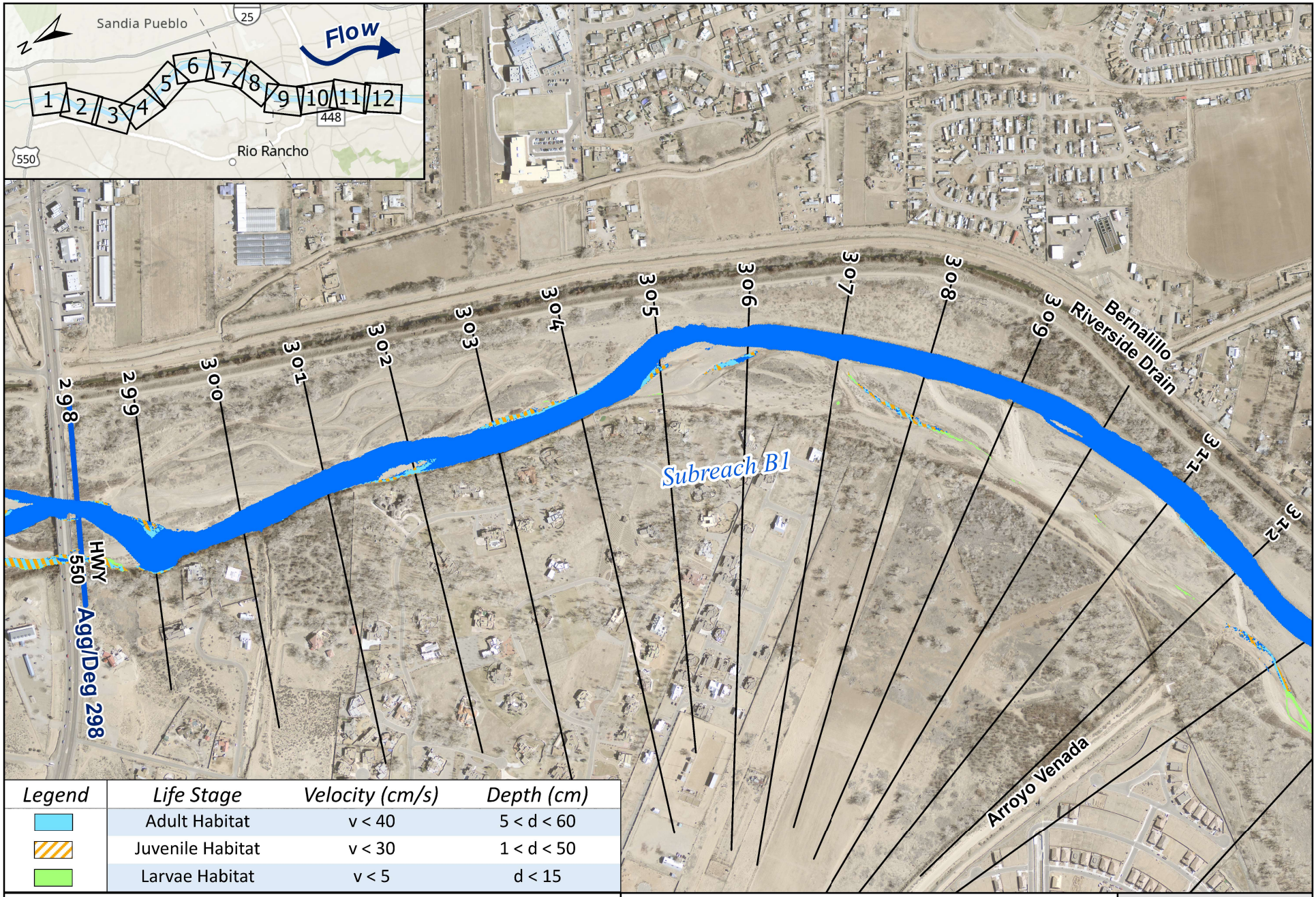

Legend	Life Stage	Velocity (cm/s)	Depth (cm)
	Adult Habitat	v < 40	5 < d < 60
	Juvenile Habitat	v < 30	1 < d < 50
	Larvae Habitat	v < 5	d < 15

1,000 500 0 1,000 Feet

Rio Grande Habitat Map at 1,500 cfs
Bernalillo to Montano

Legend	Life Stage	Velocity (cm/s)	Depth (cm)
	Adult Habitat	v < 40	5 < d < 60
	Juvenile Habitat	v < 30	1 < d < 50
	Larvae Habitat	v < 5	d < 15

1,000 500 0 1,000 Feet

Rio Grande Habitat Map at 1,500 cfs
Bernalillo to Montano

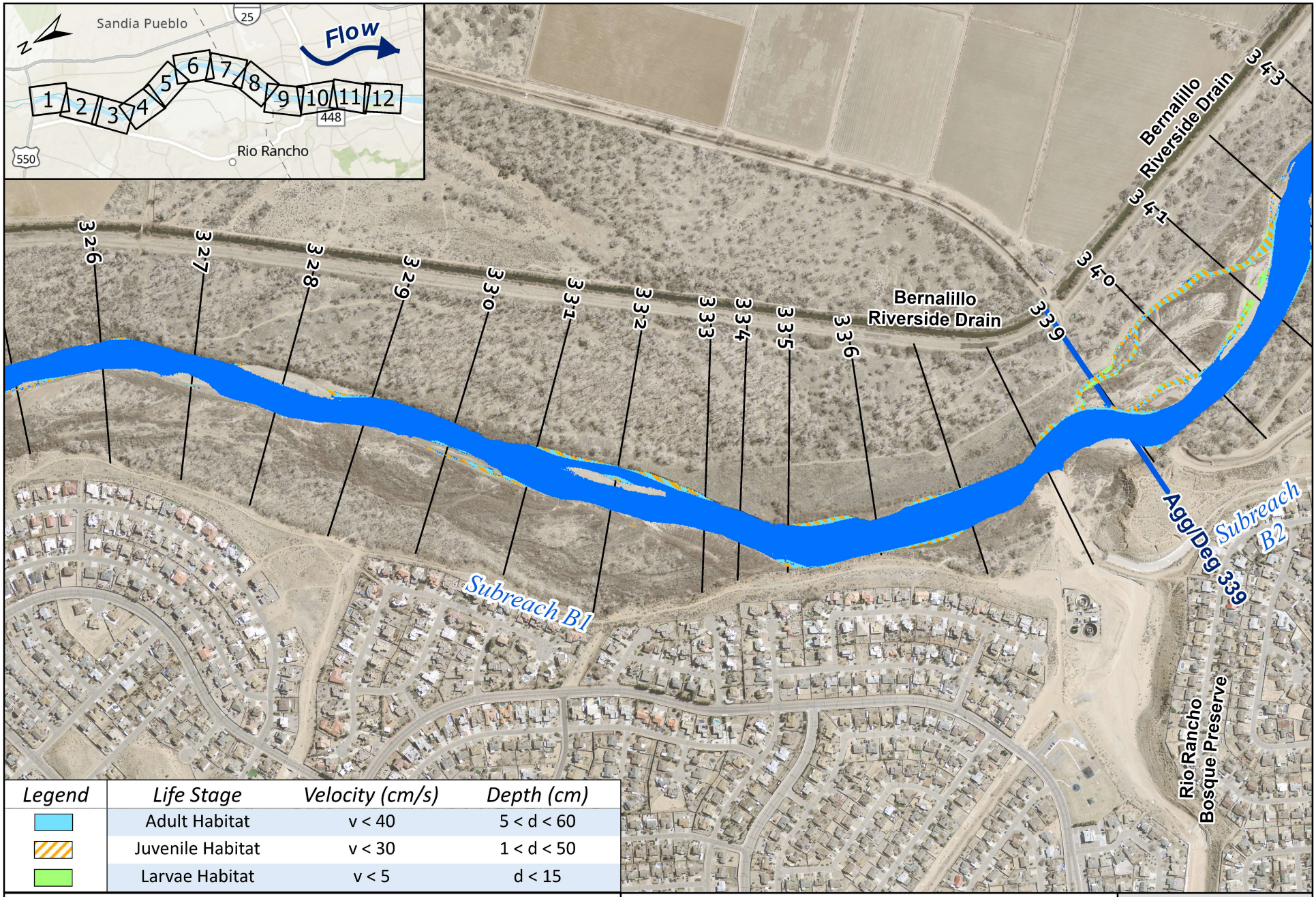

Legend	Life Stage	Velocity (cm/s)	Depth (cm)
	Adult Habitat	v < 40	5 < d < 60
	Juvenile Habitat	v < 30	1 < d < 50
	Larvae Habitat	v < 5	d < 15

1,000 500 0 1,000 Feet

Rio Grande Habitat Map at 1,500 cfs
Bernalillo to Montano

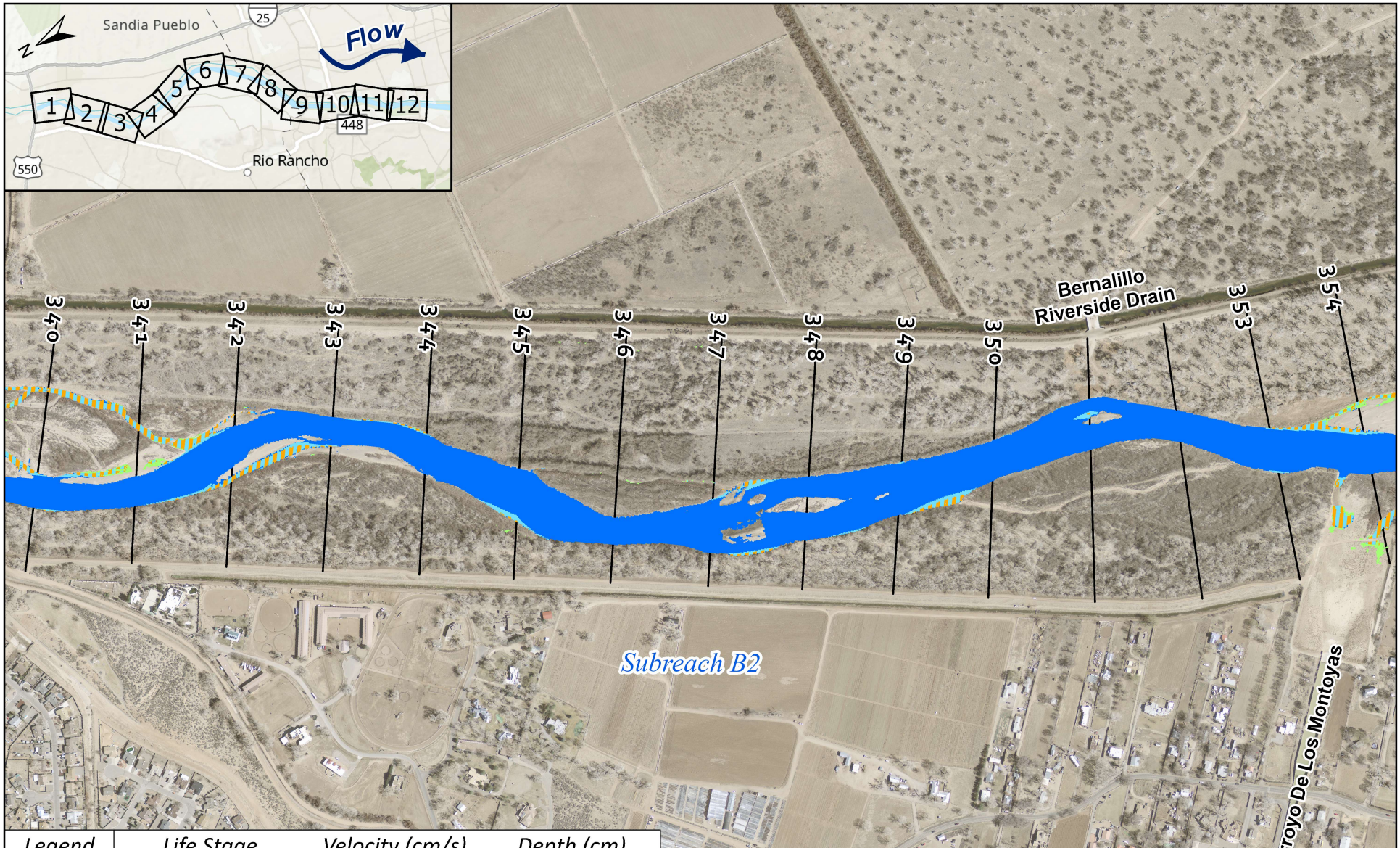

Legend	Life Stage	Velocity (cm/s)	Depth (cm)
	Adult Habitat	v < 40	5 < d < 60
	Juvenile Habitat	v < 30	1 < d < 50
	Larvae Habitat	v < 5	d < 15

N

1,000 500 0 1,000 Feet

Rio Grande Habitat Map at 1,500 cfs
Bernalillo to Montano

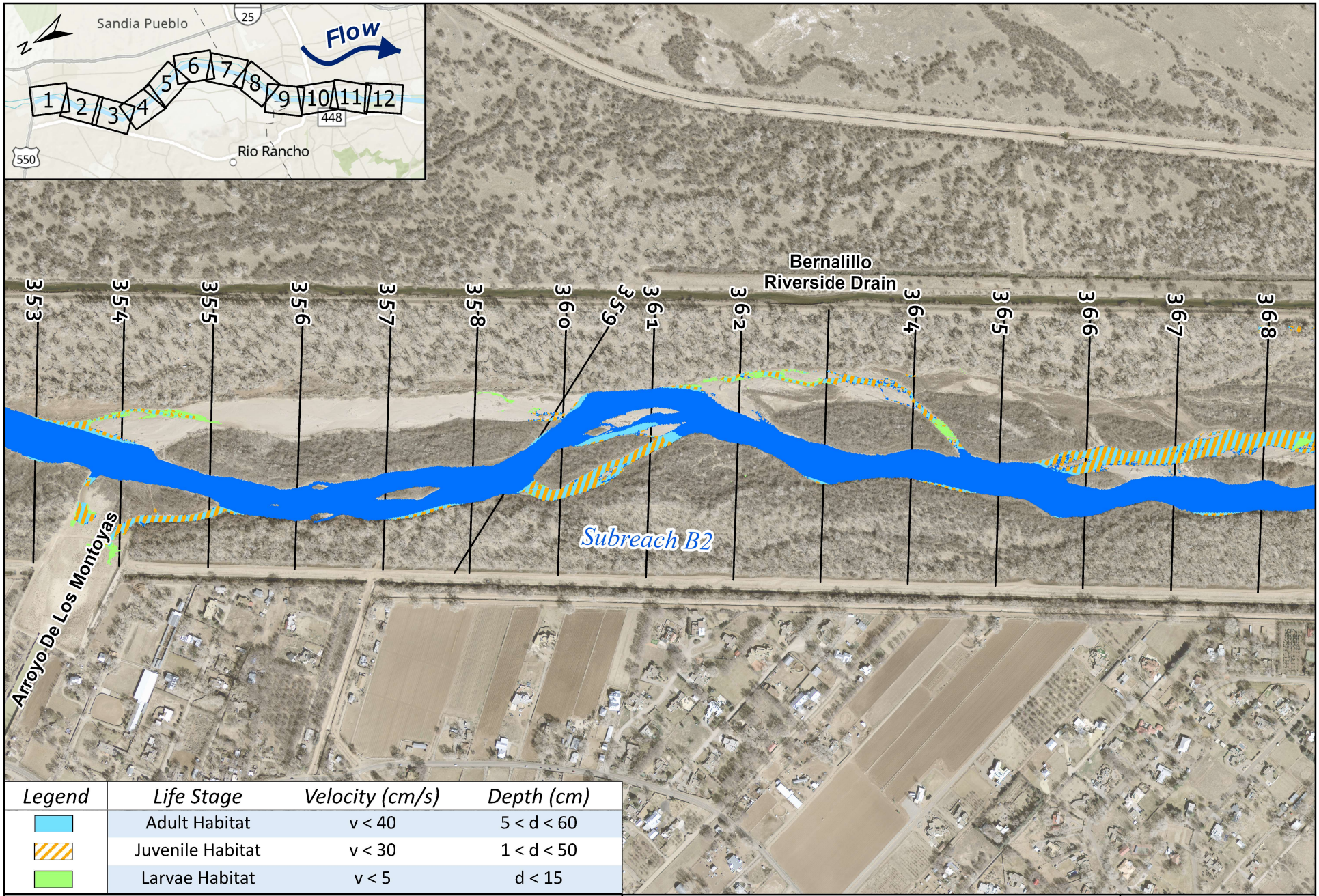

Legend	Life Stage	Velocity (cm/s)	Depth (cm)
	Adult Habitat	v < 40	5 < d < 60
	Juvenile Habitat	v < 30	1 < d < 50
	Larvae Habitat	v < 5	d < 15

N

1,000 500 0 1,000 Feet

Rio Grande Habitat Map at 1,500 cfs
Bernalillo to Montano

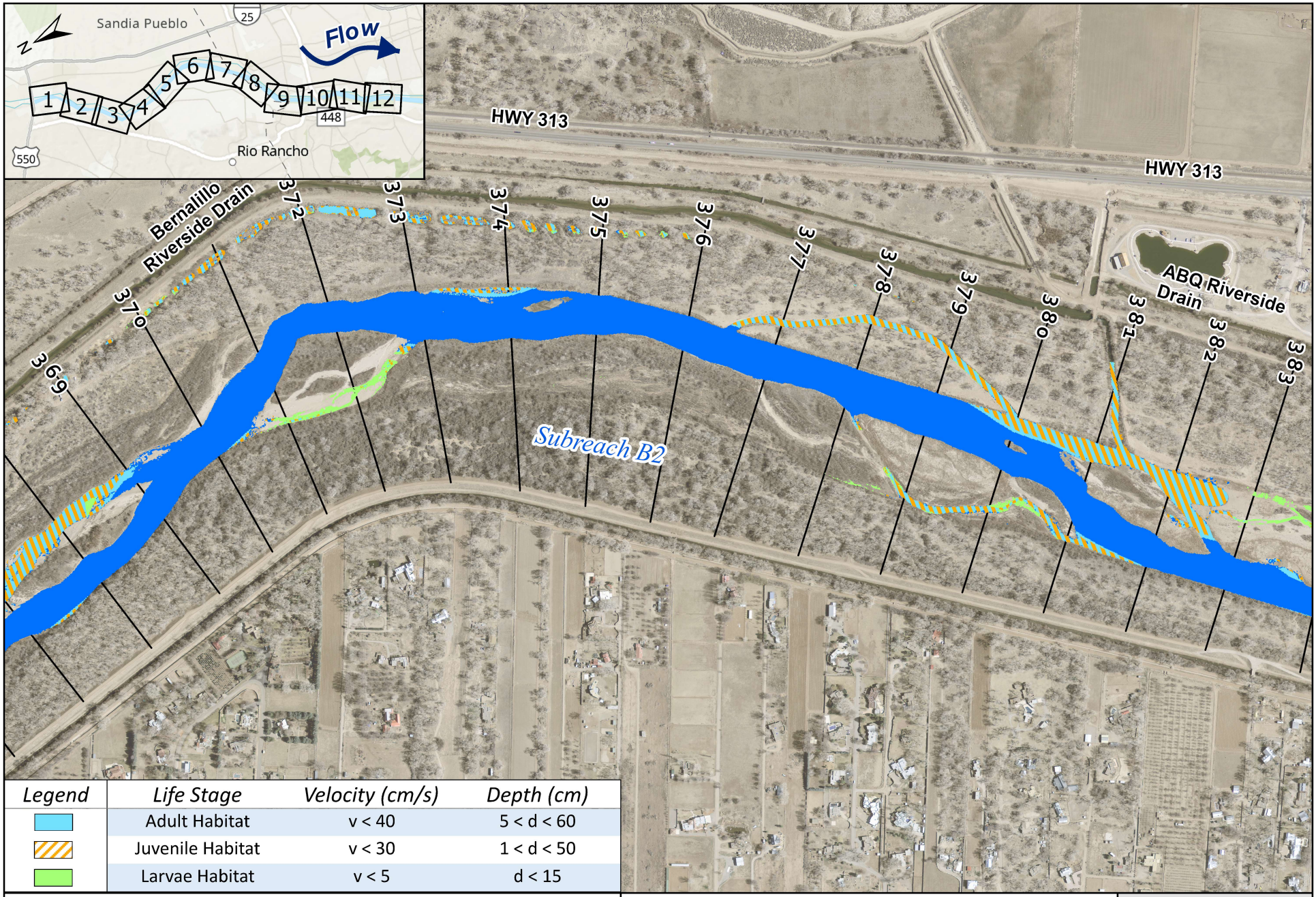

Legend	Life Stage	Velocity (cm/s)	Depth (cm)
	Adult Habitat	v < 40	5 < d < 60
	Juvenile Habitat	v < 30	1 < d < 50
	Larvae Habitat	v < 5	d < 15

1,000 500 0 1,000 Feet

Rio Grande Habitat Map at 1,500 cfs
Bernalillo to Montano

Legend	Life Stage	Velocity (cm/s)	Depth (cm)
	Adult Habitat	v < 40	5 < d < 60
	Juvenile Habitat	v < 30	1 < d < 50
	Larvae Habitat	v < 5	d < 15

1,000 500 0 1,000 Feet

Rio Grande Habitat Map at 1,500 cfs
Bernalillo to Montano

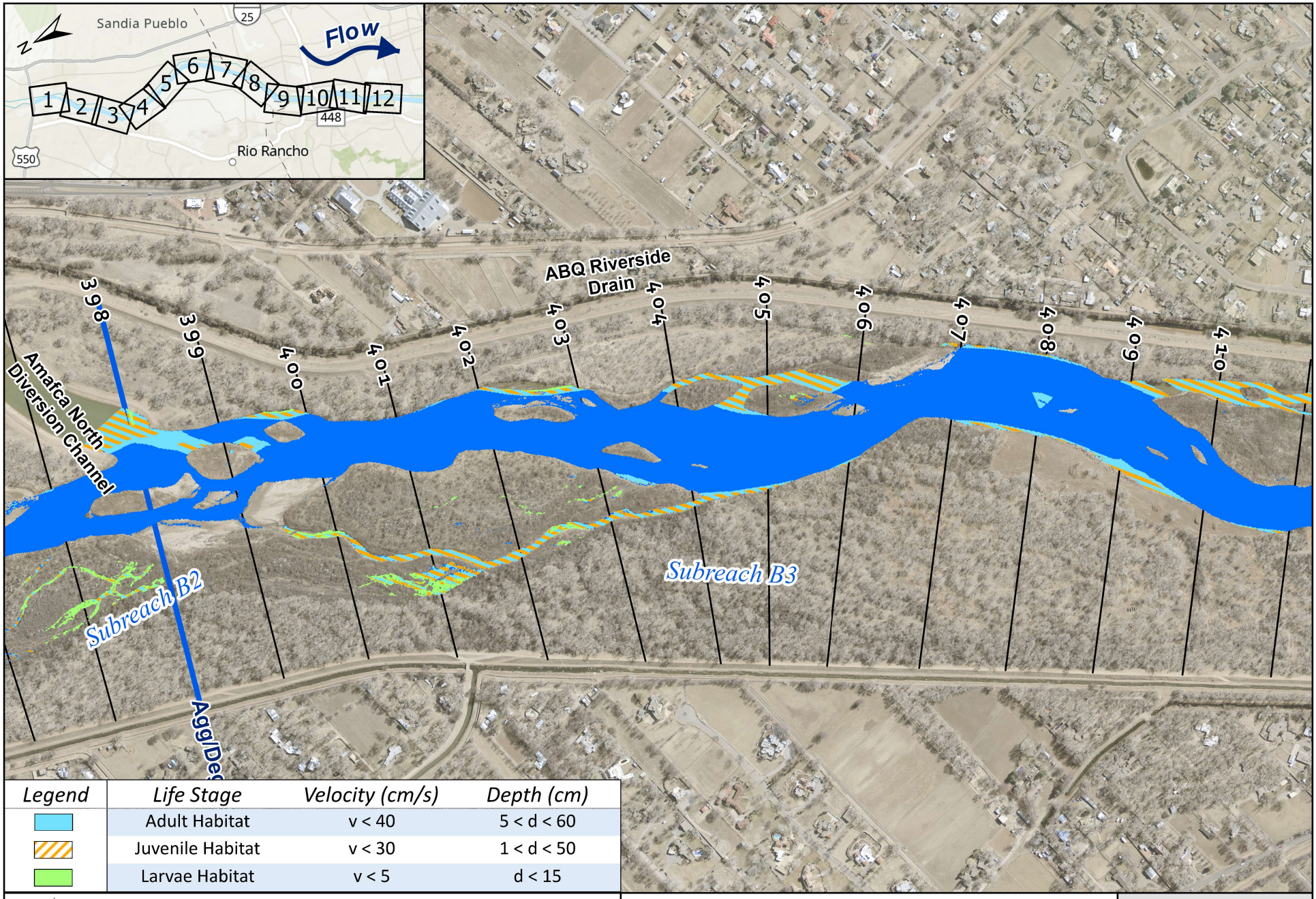

Legend	Life Stage	Velocity (cm/s)	Depth (cm)
	Adult Habitat	v < 40	5 < d < 60
	Juvenile Habitat	v < 30	1 < d < 50
	Larvae Habitat	v < 5	d < 15

N

1,000 500 0 1,000 Feet

Rio Grande Habitat Map at 1,500 cfs
Bernalillo to Montano

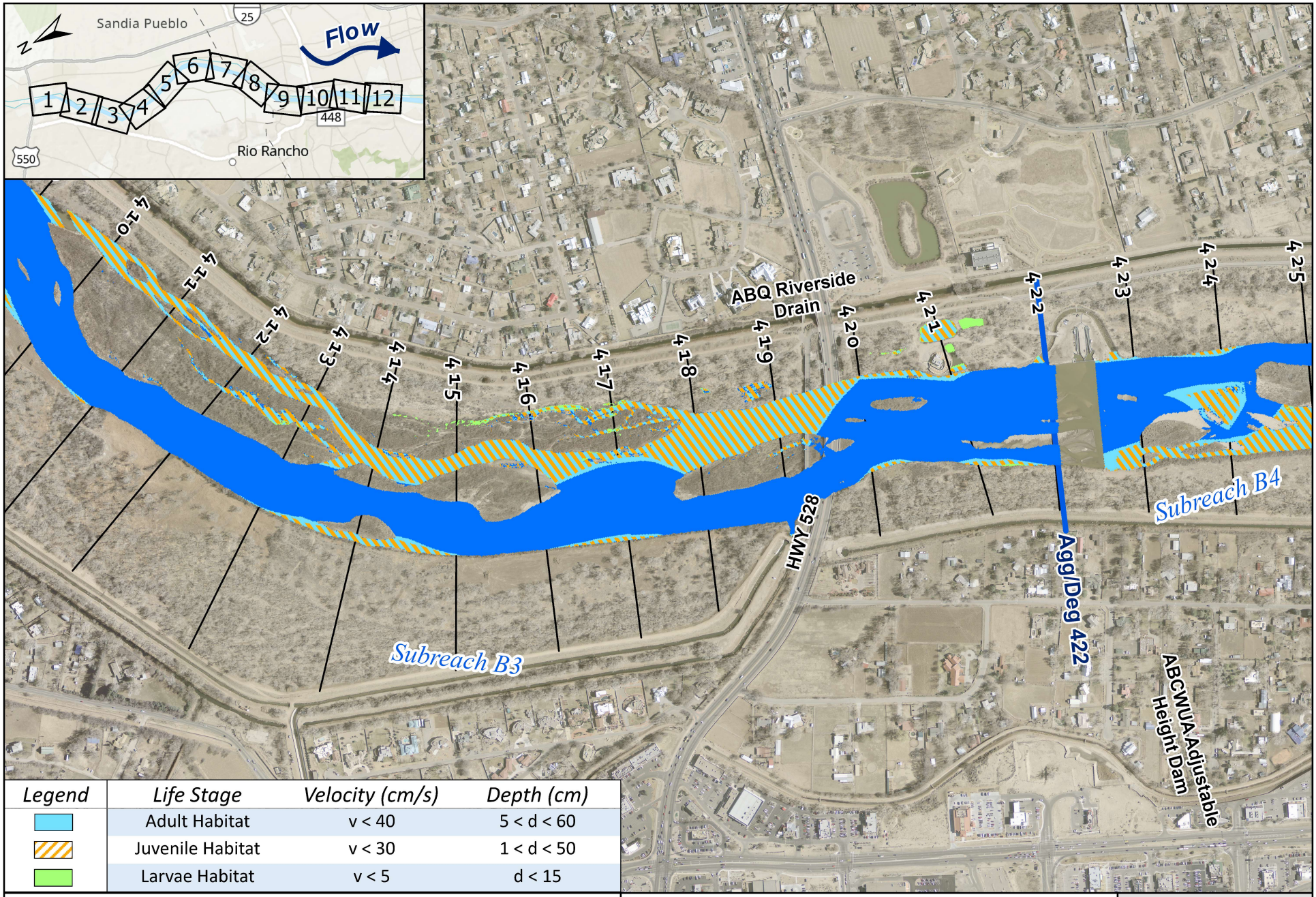

Legend	Life Stage	Velocity (cm/s)	Depth (cm)
	Adult Habitat	v < 40	5 < d < 60
	Juvenile Habitat	v < 30	1 < d < 50
	Larvae Habitat	v < 5	d < 15

1,000 500 0 1,000 Feet

Rio Grande Habitat Map at 1,500 cfs
Bernalillo to Montano

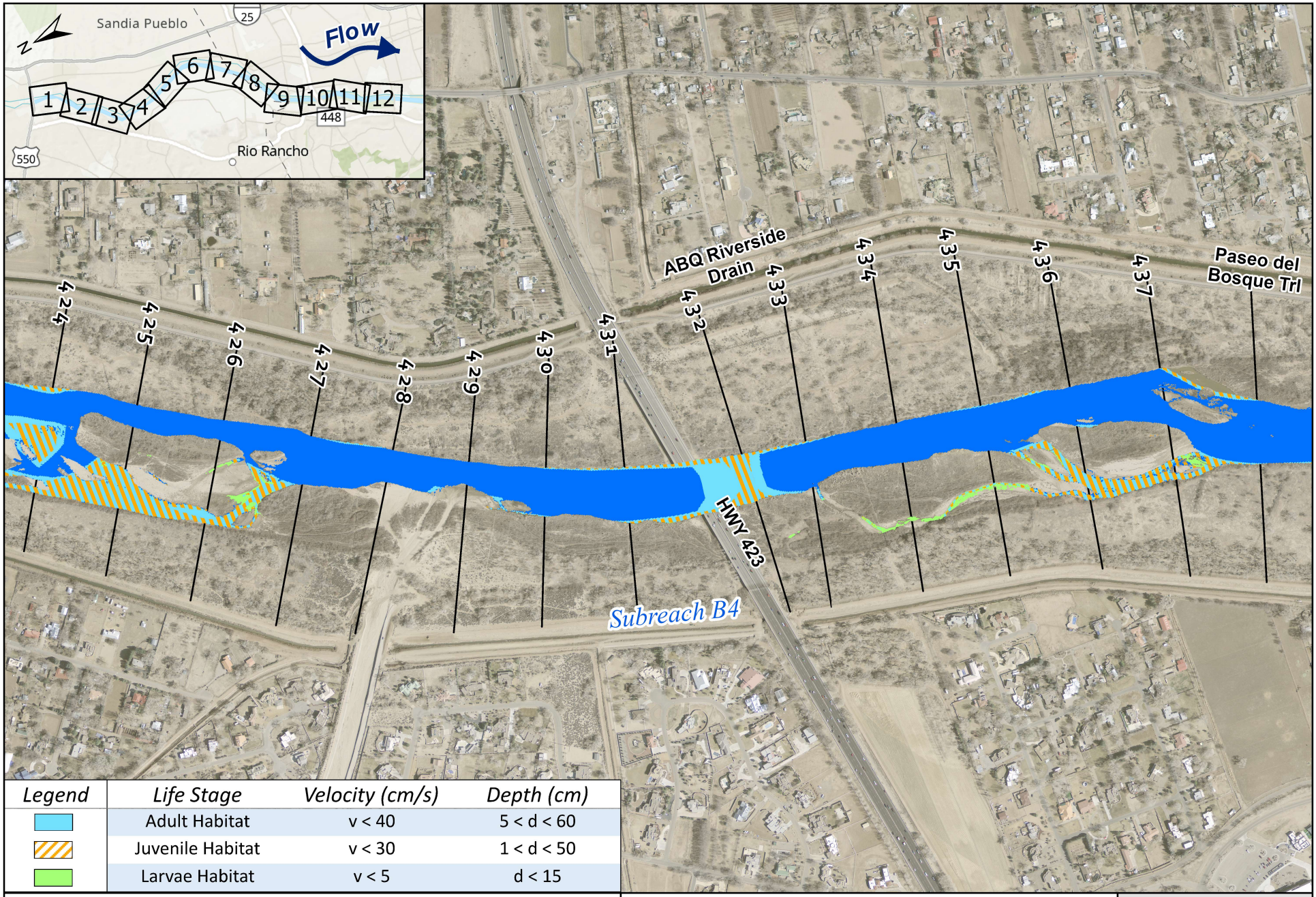

Legend	Life Stage	Velocity (cm/s)	Depth (cm)
	Adult Habitat	v < 40	5 < d < 60
	Juvenile Habitat	v < 30	1 < d < 50
	Larvae Habitat	v < 5	d < 15

1,000 500 0 1,000 Feet

Rio Grande Habitat Map at 1,500 cfs
Bernalillo to Montano

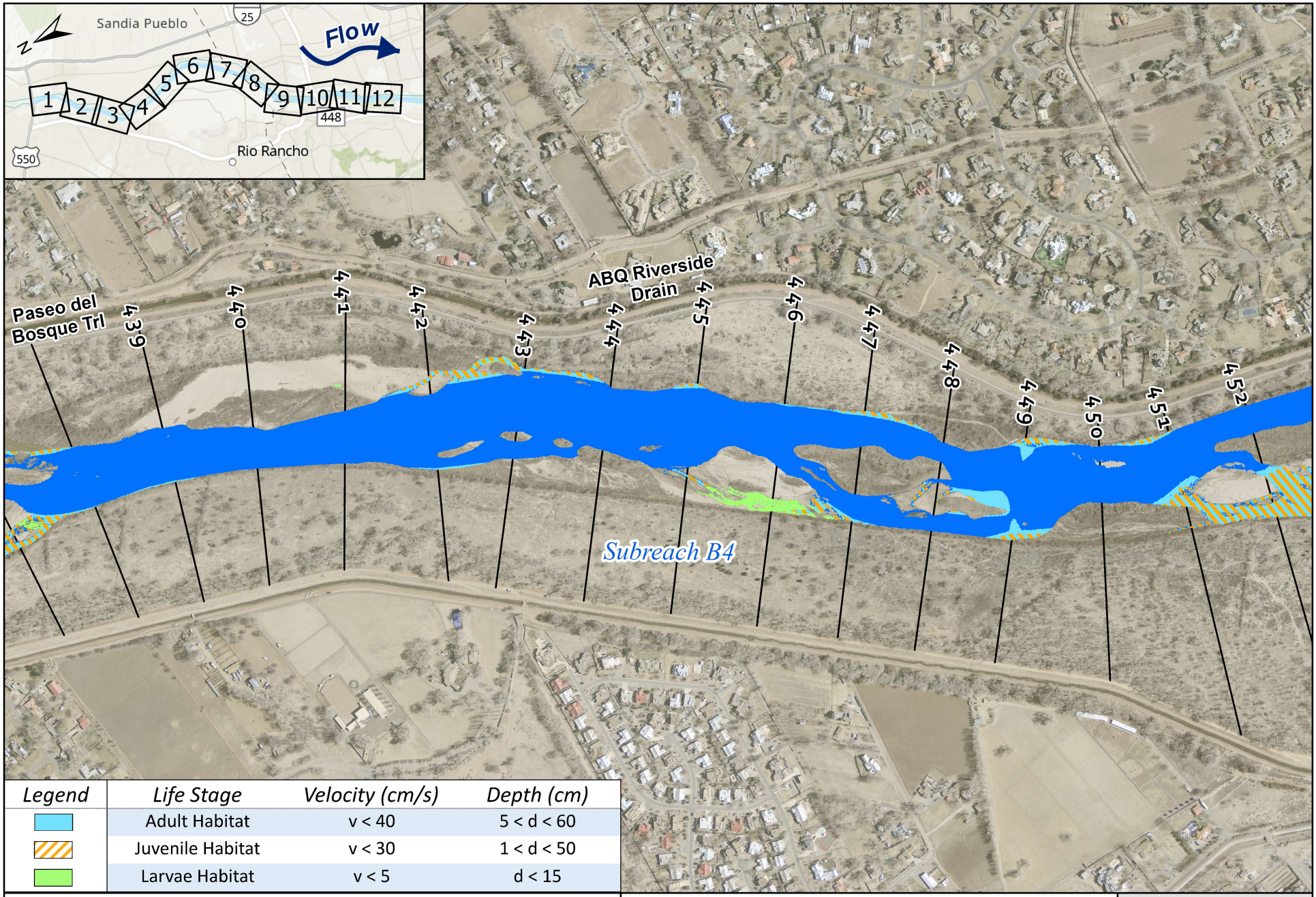

Legend	Life Stage	Velocity (cm/s)	Depth (cm)
	Adult Habitat	v < 40	5 < d < 60
	Juvenile Habitat	v < 30	1 < d < 50
	Larvae Habitat	v < 5	d < 15

1,000 500 0 1,000 Feet

Rio Grande Habitat Map at 1,500 cfs
Bernalillo to Montano

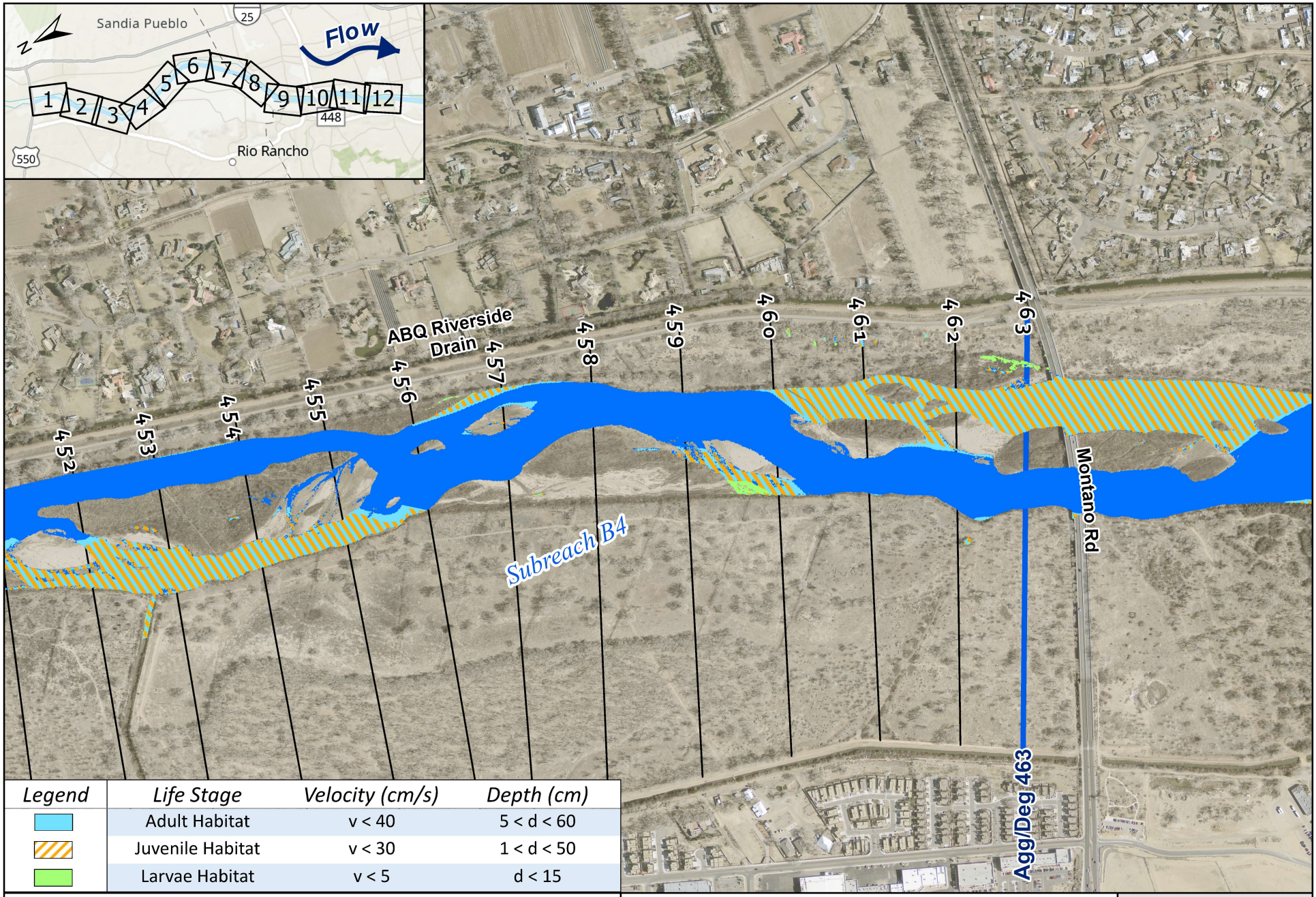

Legend	Life Stage	Velocity (cm/s)	Depth (cm)
	Adult Habitat	v < 40	5 < d < 60
	Juvenile Habitat	v < 30	1 < d < 50
	Larvae Habitat	v < 5	d < 15

1,000 500 0 1,000 Feet

Rio Grande Habitat Map at 1,500 cfs
Bernalillo to Montano

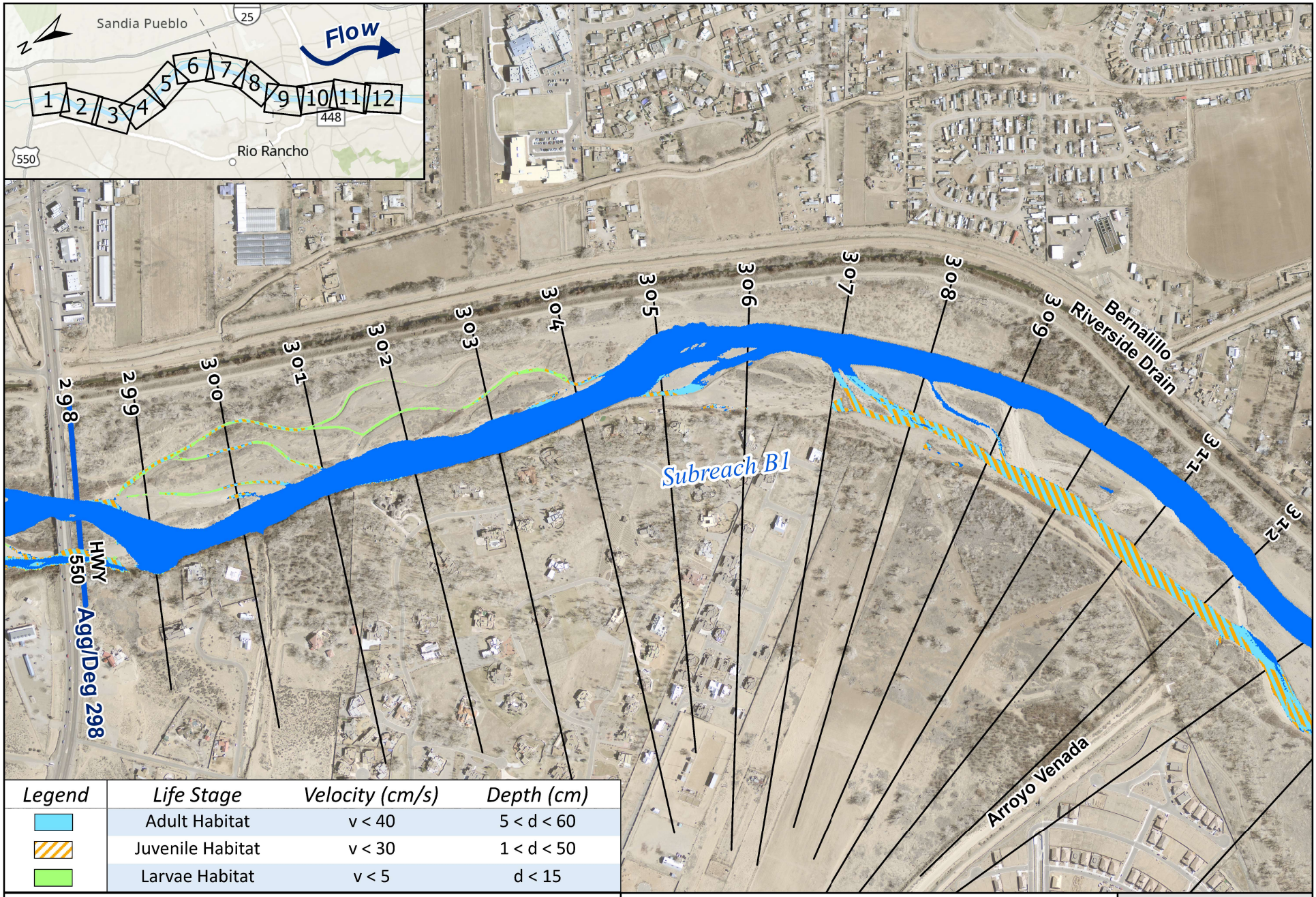

Legend	Life Stage	Velocity (cm/s)	Depth (cm)
	Adult Habitat	v < 40	5 < d < 60
	Juvenile Habitat	v < 30	1 < d < 50
	Larvae Habitat	v < 5	d < 15

1,000 500 0 1,000 Feet

Rio Grande Habitat Map at 3,000 cfs
Bernalillo to Montano

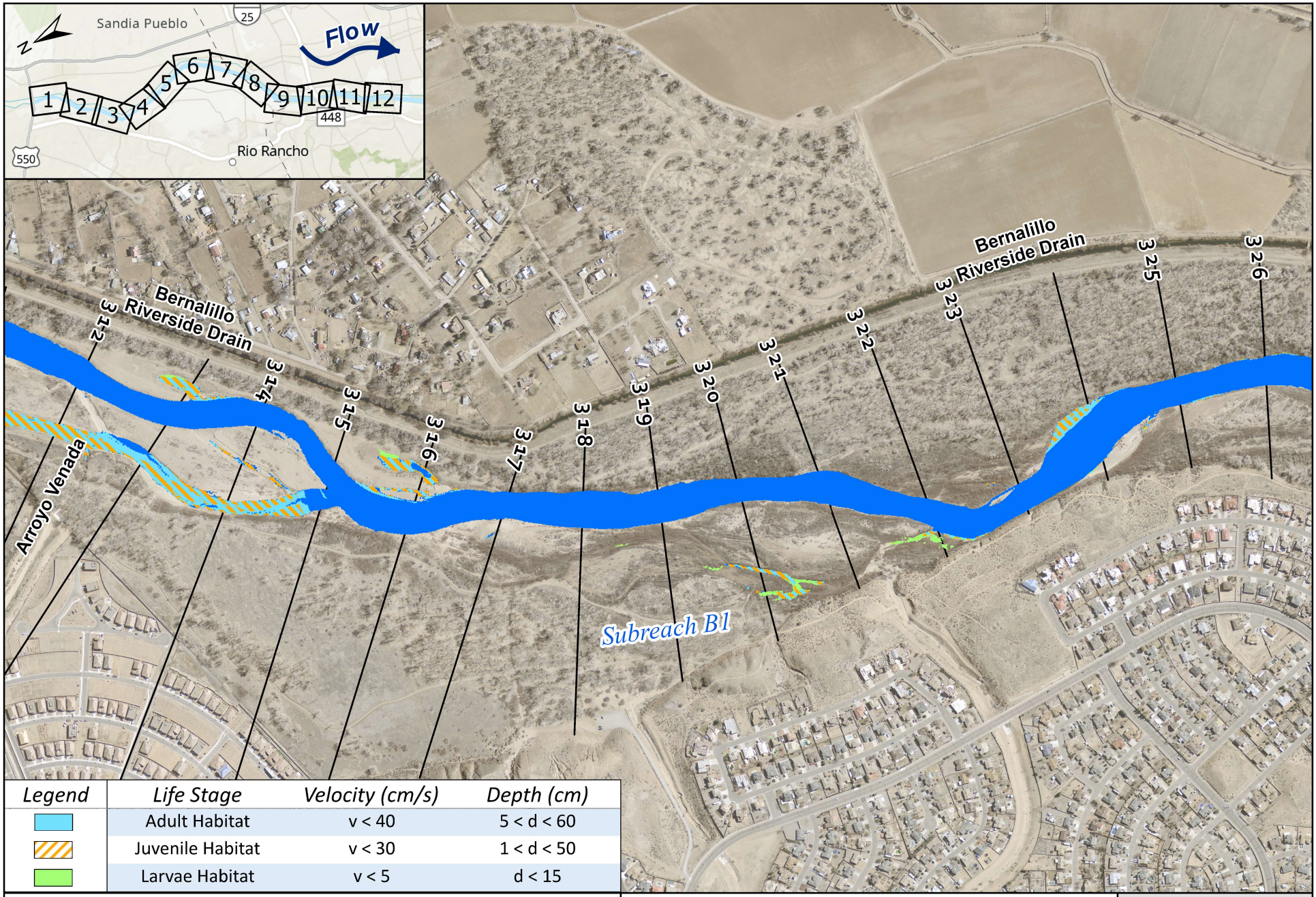

Legend	Life Stage	Velocity (cm/s)	Depth (cm)
	Adult Habitat	v < 40	5 < d < 60
	Juvenile Habitat	v < 30	1 < d < 50
	Larvae Habitat	v < 5	d < 15

1,000 500 0 1,000 Feet

Rio Grande Habitat Map at 3,000 cfs
Bernalillo to Montano

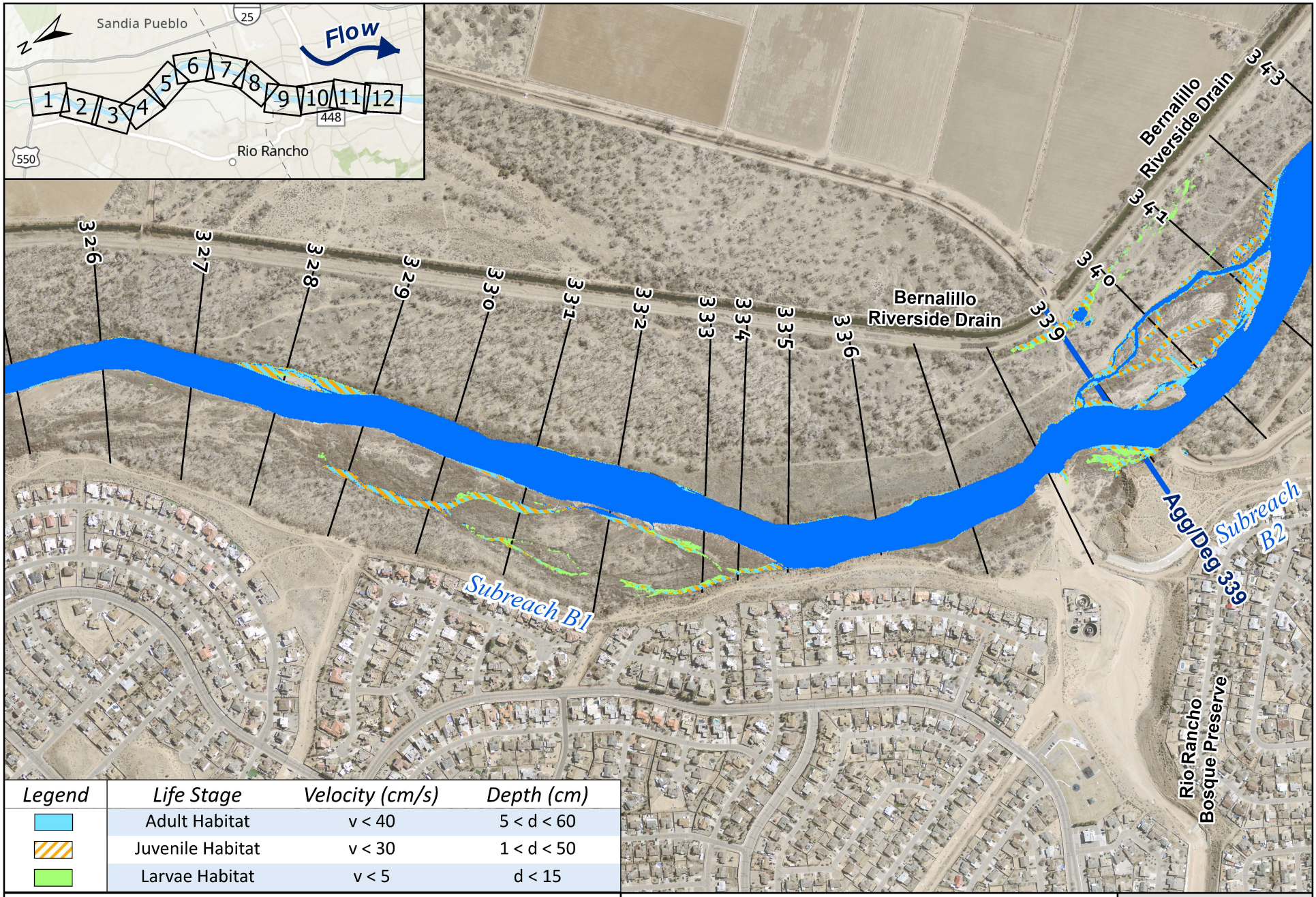

Legend	Life Stage	Velocity (cm/s)	Depth (cm)
	Adult Habitat	v < 40	5 < d < 60
	Juvenile Habitat	v < 30	1 < d < 50
	Larvae Habitat	v < 5	d < 15

N

1,000 500 0 1,000 Feet

Rio Grande Habitat Map at 3,000 cfs
Bernalillo to Montano

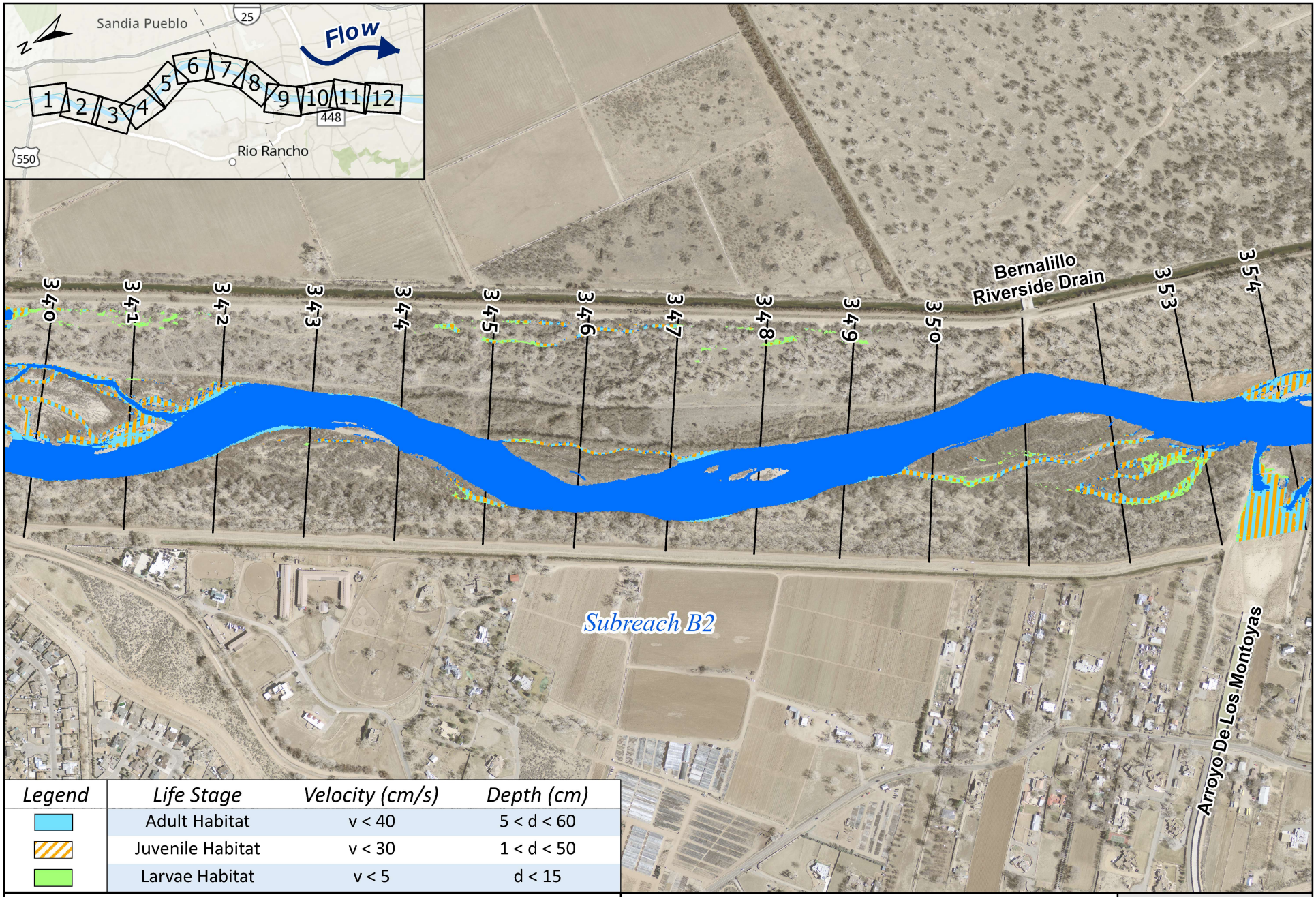

Legend	Life Stage	Velocity (cm/s)	Depth (cm)
	Adult Habitat	v < 40	5 < d < 60
	Juvenile Habitat	v < 30	1 < d < 50
	Larvae Habitat	v < 5	d < 15

N

1,000 500 0 1,000 Feet

Rio Grande Habitat Map at 3,000 cfs
Bernalillo to Montano

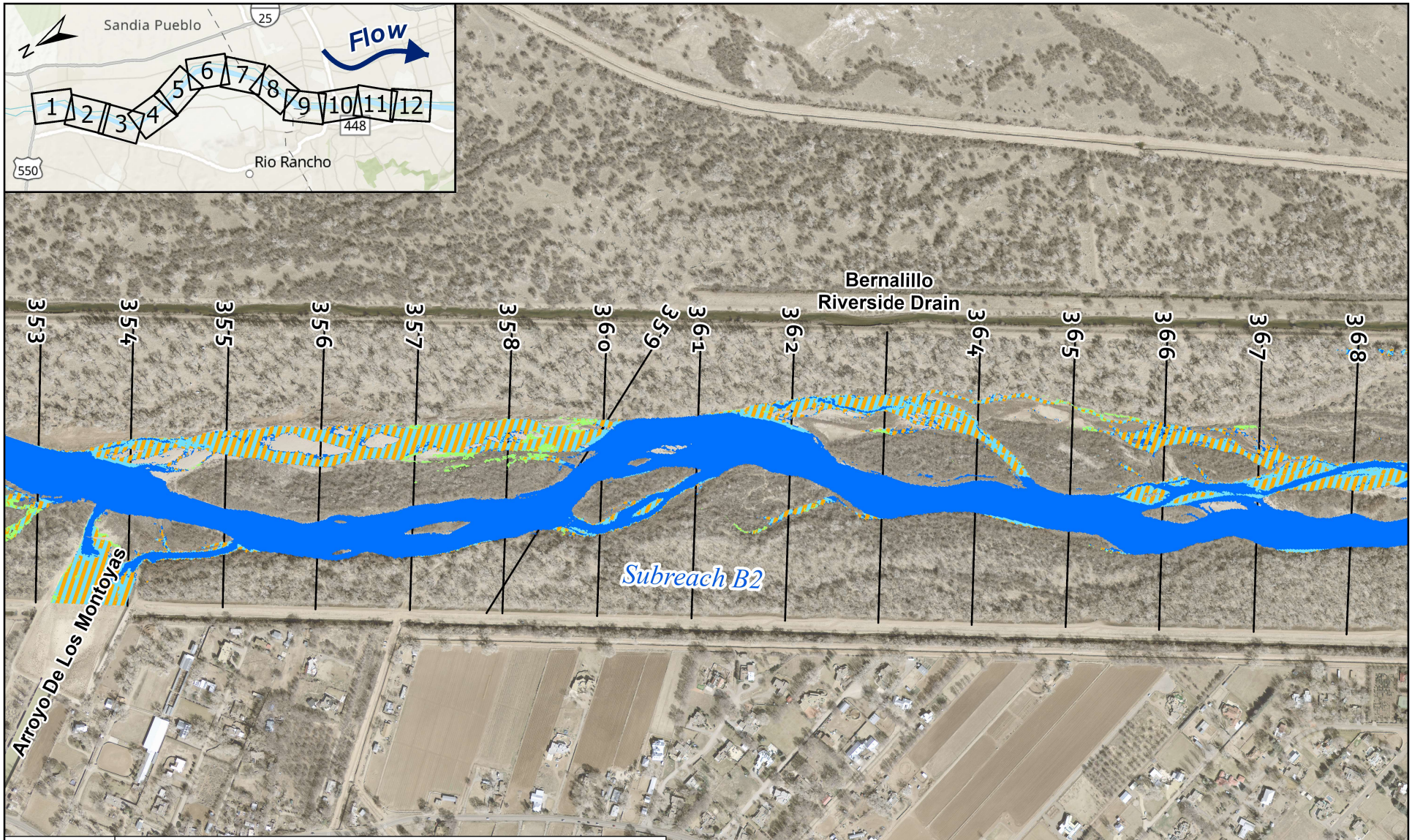

Legend	Life Stage	Velocity (cm/s)	Depth (cm)
	Adult Habitat	v < 40	5 < d < 60
	Juvenile Habitat	v < 30	1 < d < 50
	Larvae Habitat	v < 5	d < 15

N

1,000 500 0 1,000 Feet

Rio Grande Habitat Map at 3,000 cfs
Bernalillo to Montano

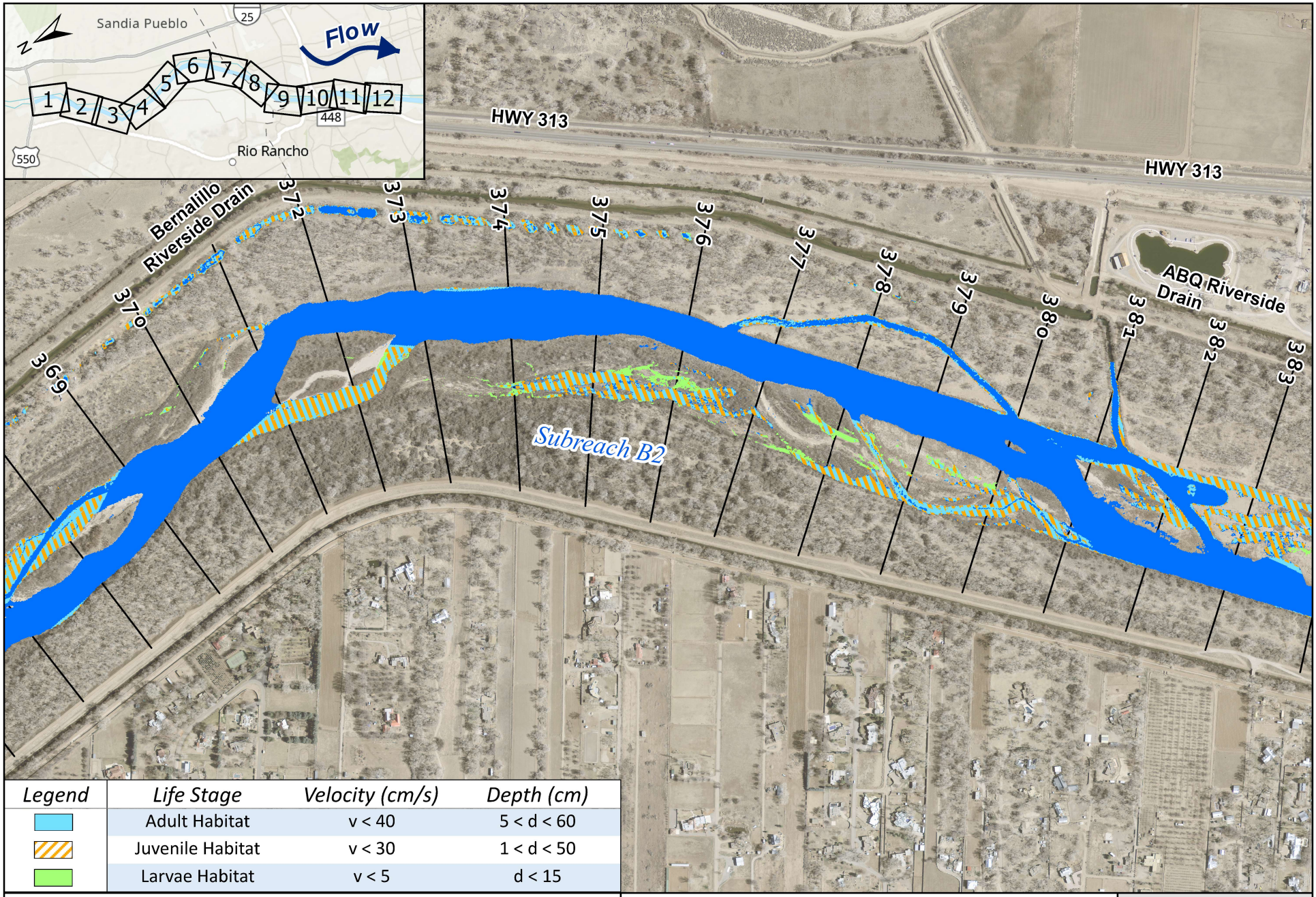

Legend	Life Stage	Velocity (cm/s)	Depth (cm)
	Adult Habitat	v < 40	5 < d < 60
	Juvenile Habitat	v < 30	1 < d < 50
	Larvae Habitat	v < 5	d < 15

1,000 500 0 1,000 Feet

Rio Grande Habitat Map at 3,000 cfs
Bernalillo to Montano

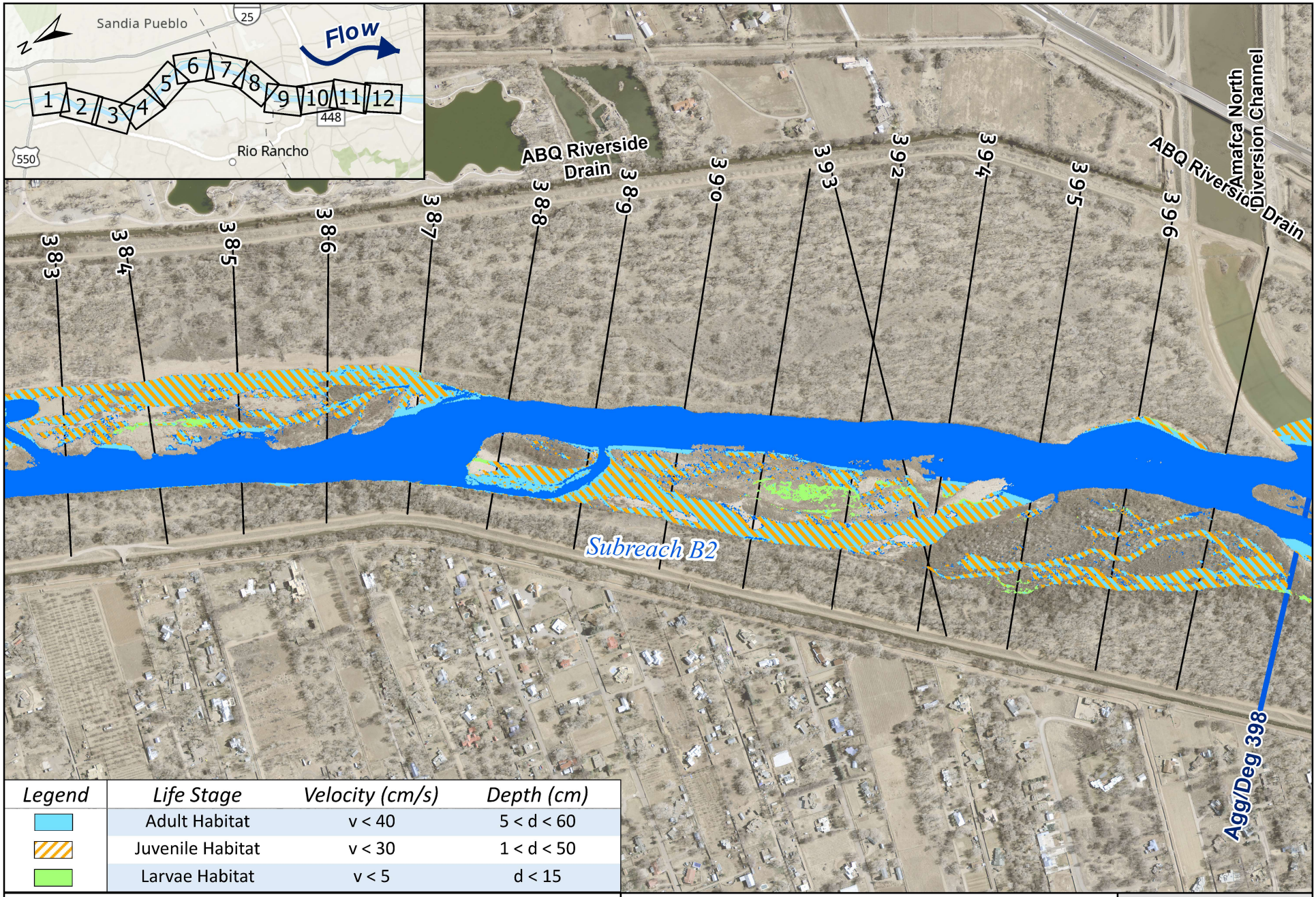

Legend	Life Stage	Velocity (cm/s)	Depth (cm)
	Adult Habitat	v < 40	5 < d < 60
	Juvenile Habitat	v < 30	1 < d < 50
	Larvae Habitat	v < 5	d < 15

1,000 500 0 1,000 Feet

Rio Grande Habitat Map at 3,000 cfs
Bernalillo to Montano

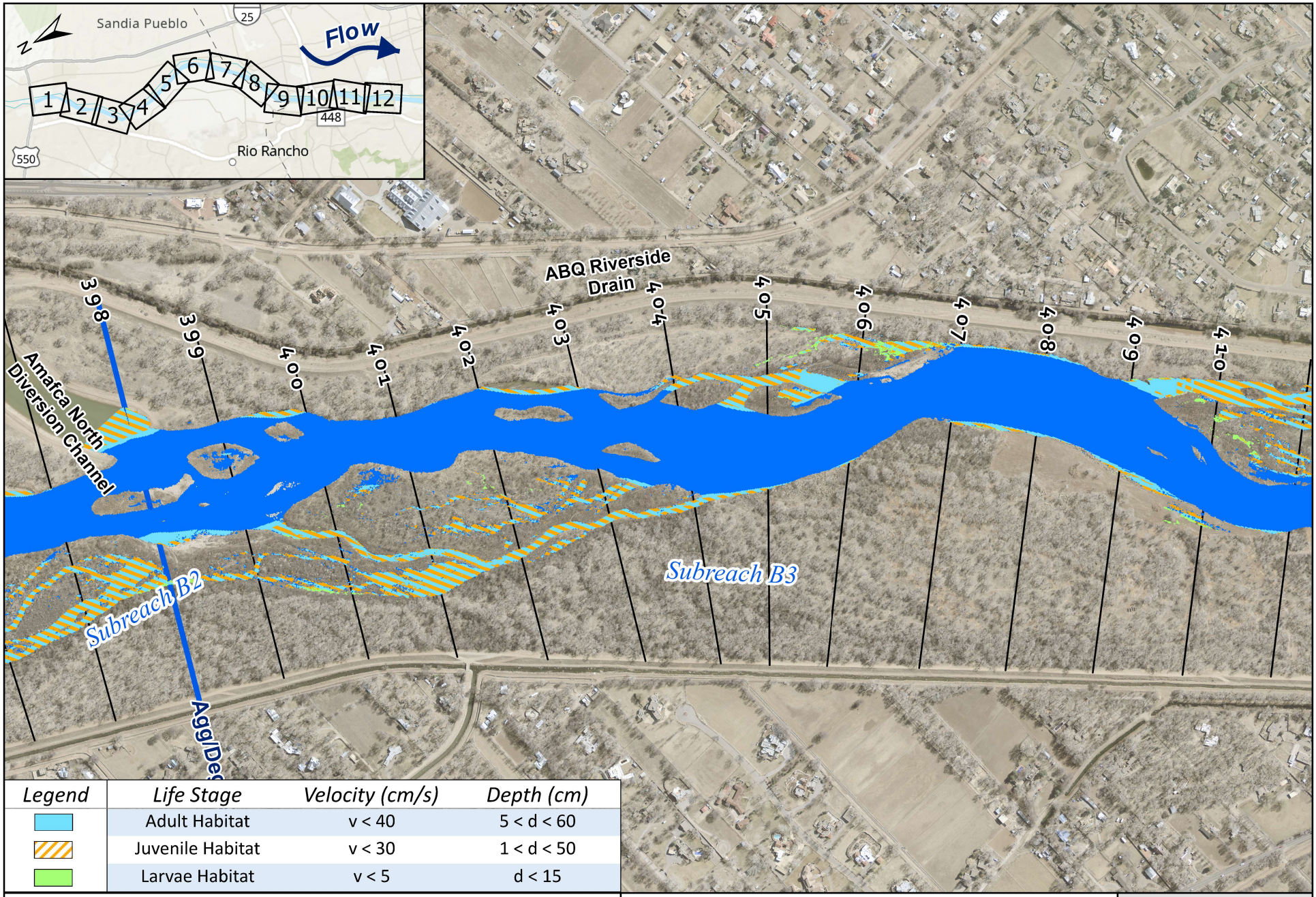

Legend	Life Stage	Velocity (cm/s)	Depth (cm)
	Adult Habitat	v < 40	5 < d < 60
	Juvenile Habitat	v < 30	1 < d < 50
	Larvae Habitat	v < 5	d < 15

N

1,000 500 0 1,000 Feet

Rio Grande Habitat Map at 3,000 cfs
Bernalillo to Montano

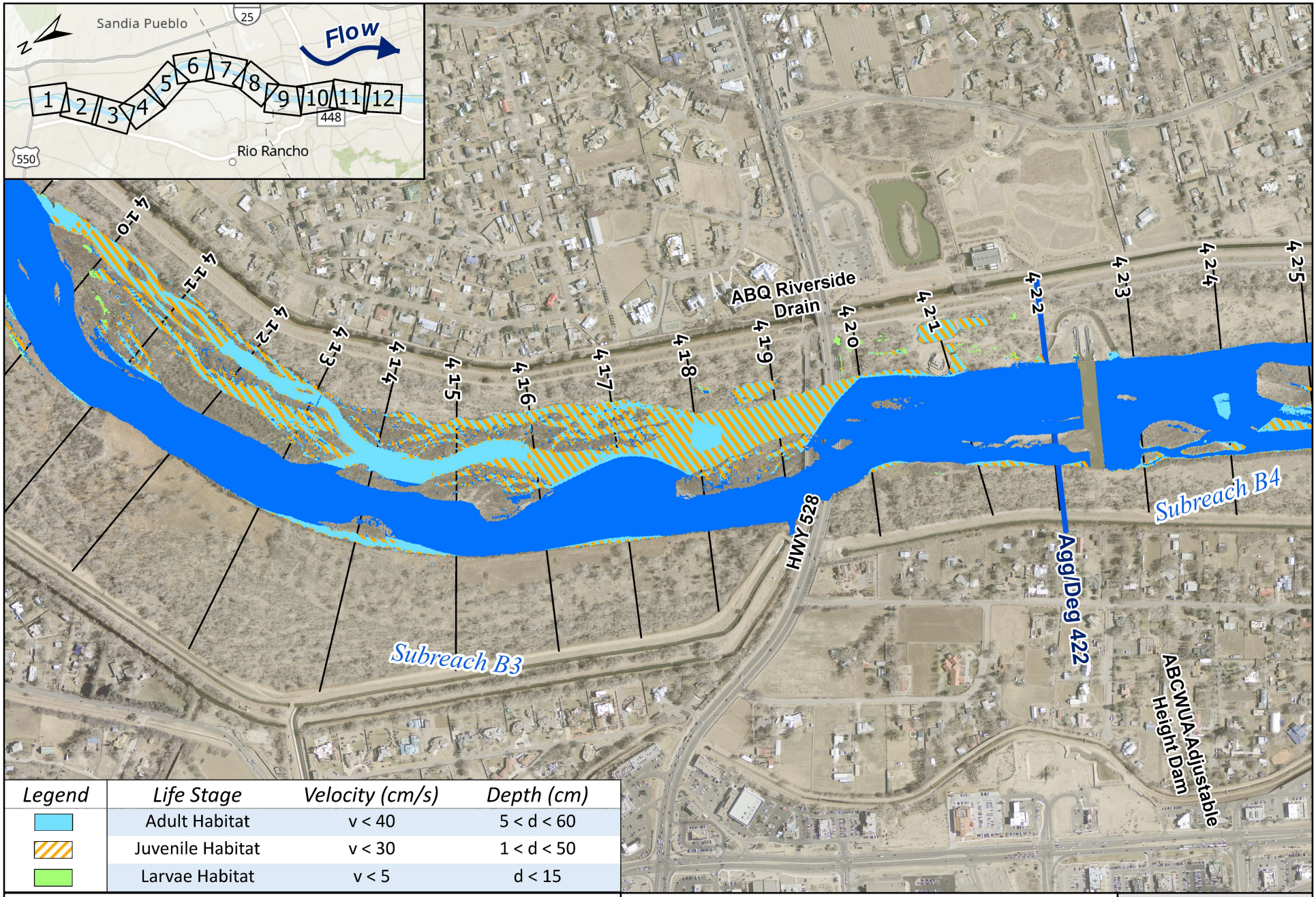

Legend	Life Stage	Velocity (cm/s)	Depth (cm)
	Adult Habitat	v < 40	5 < d < 60
	Juvenile Habitat	v < 30	1 < d < 50
	Larvae Habitat	v < 5	d < 15

1,000 500 0 1,000 Feet

Rio Grande Habitat Map at 3,000 cfs
Bernalillo to Montano

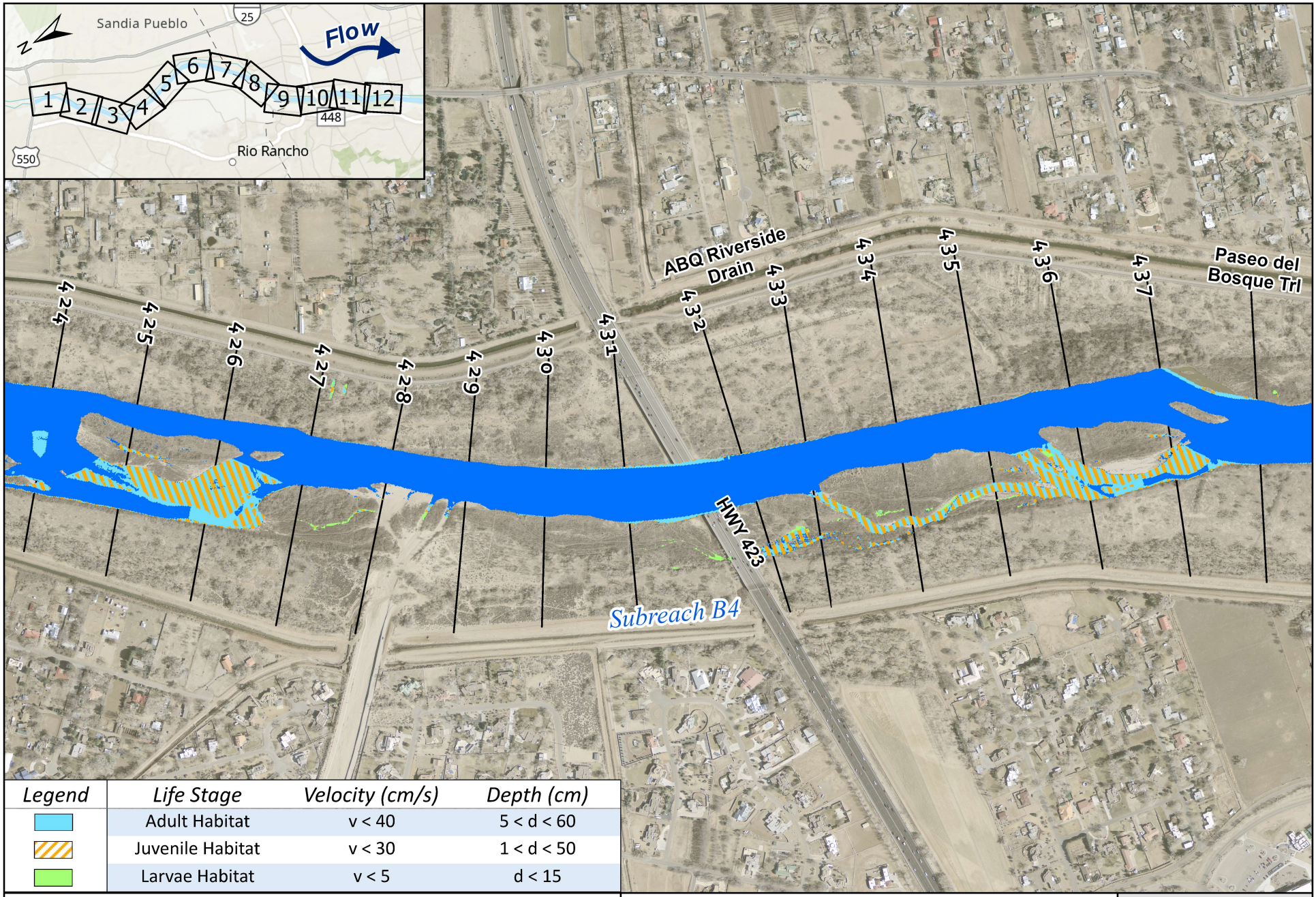

Legend	Life Stage	Velocity (cm/s)	Depth (cm)
	Adult Habitat	v < 40	5 < d < 60
	Juvenile Habitat	v < 30	1 < d < 50
	Larvae Habitat	v < 5	d < 15

1,000 500 0 1,000 Feet

Rio Grande Habitat Map at 3,000 cfs
Bernalillo to Montano

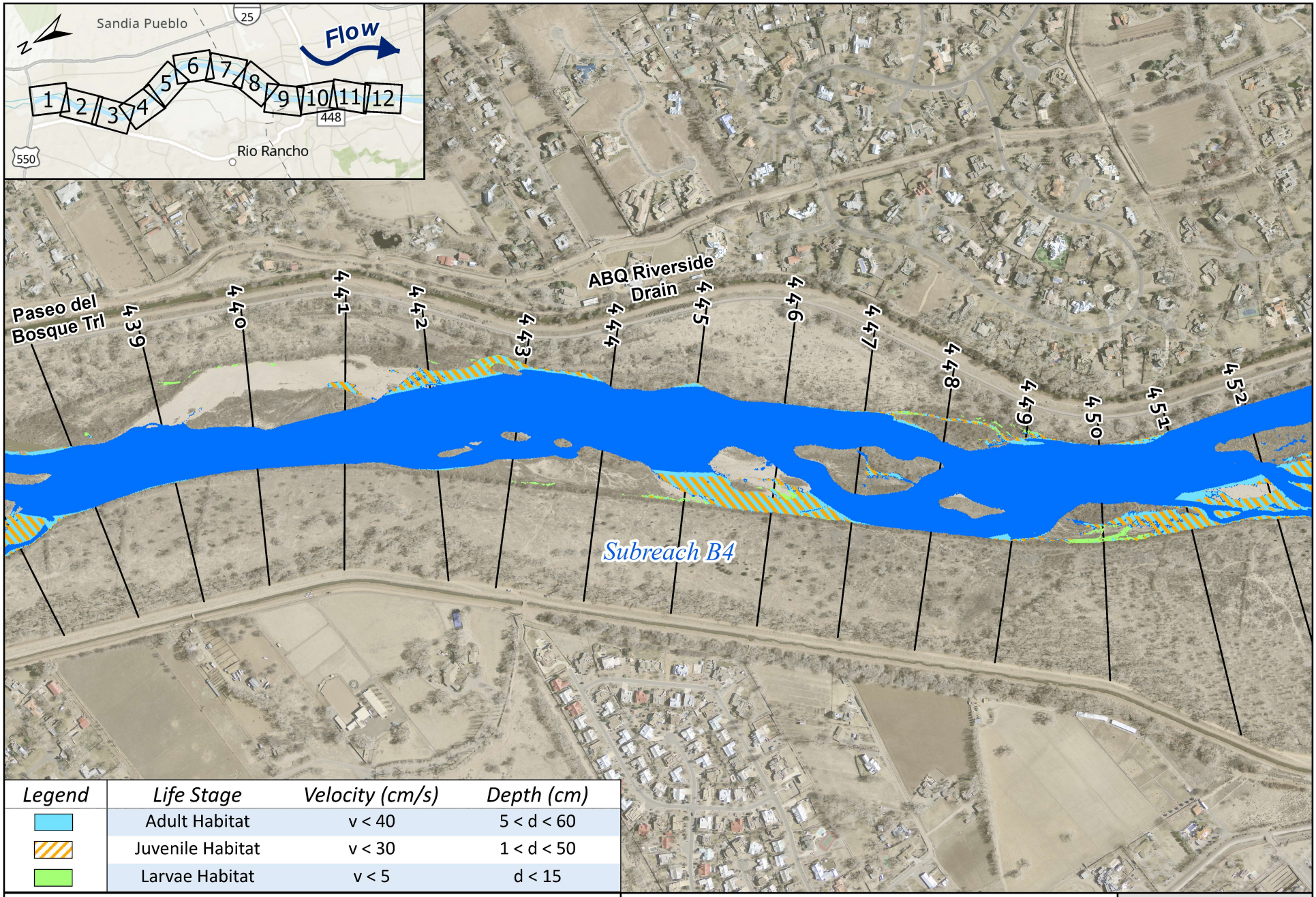

Legend	Life Stage	Velocity (cm/s)	Depth (cm)
	Adult Habitat	v < 40	5 < d < 60
	Juvenile Habitat	v < 30	1 < d < 50
	Larvae Habitat	v < 5	d < 15

1,000 500 0 1,000 Feet

Rio Grande Habitat Map at 3,000 cfs
Bernalillo to Montano

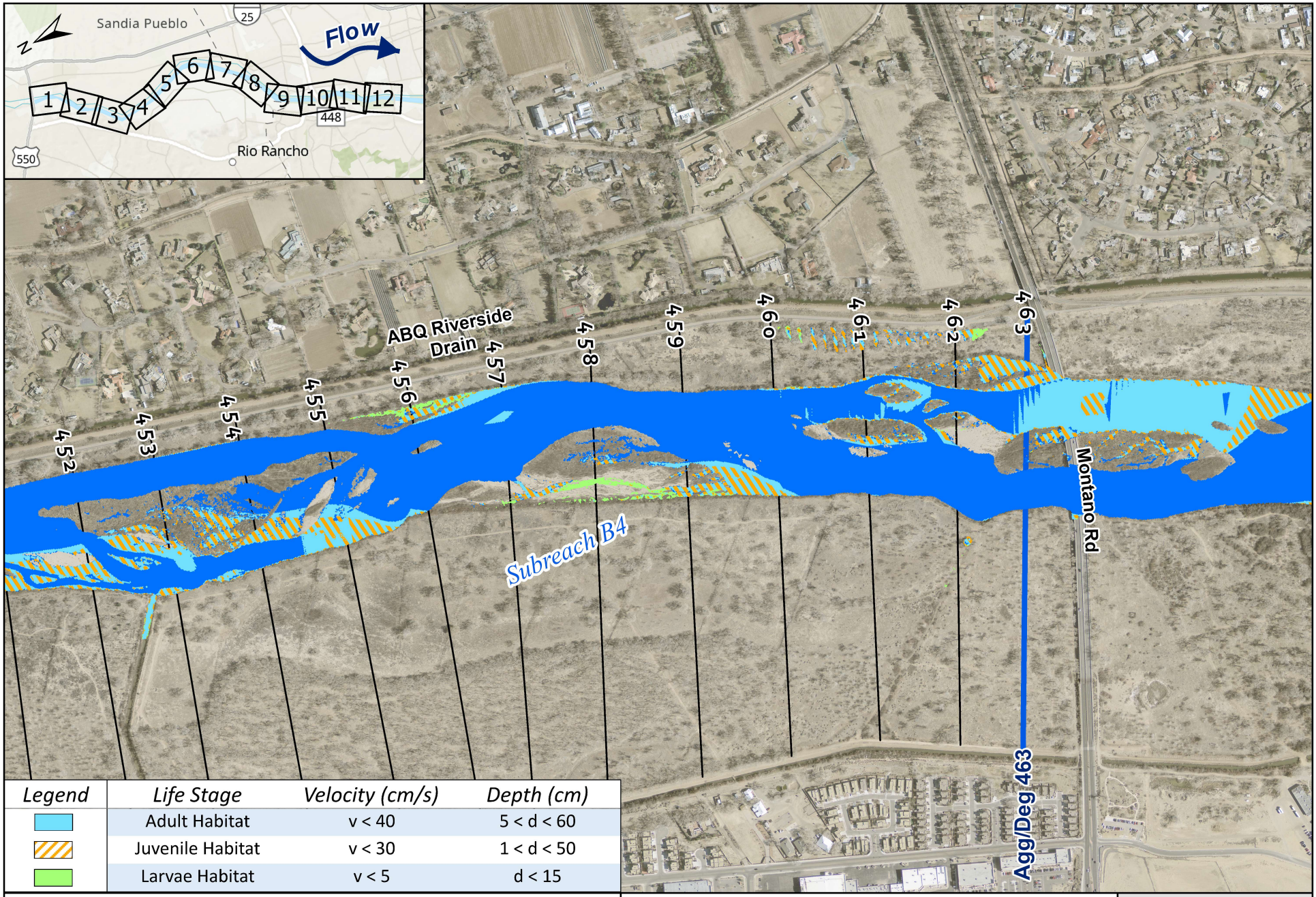

Legend	Life Stage	Velocity (cm/s)	Depth (cm)
	Adult Habitat	v < 40	5 < d < 60
	Juvenile Habitat	v < 30	1 < d < 50
	Larvae Habitat	v < 5	d < 15

1,000 500 0 1,000 Feet

Rio Grande Habitat Map at 3,000 cfs
Bernalillo to Montano

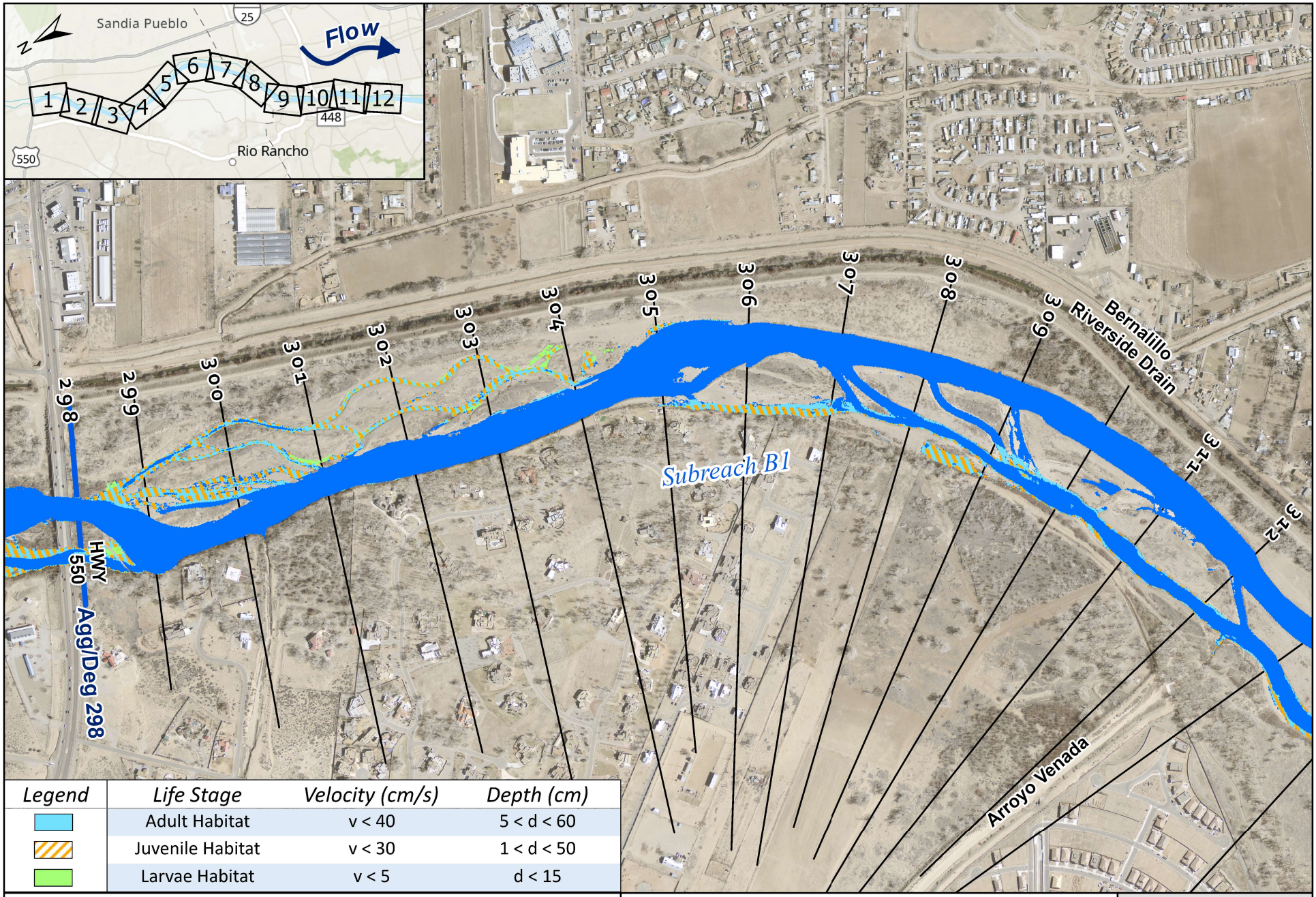

Legend	Life Stage	Velocity (cm/s)	Depth (cm)
	Adult Habitat	v < 40	5 < d < 60
	Juvenile Habitat	v < 30	1 < d < 50
	Larvae Habitat	v < 5	d < 15

1,000 500 0 1,000 Feet

Rio Grande Habitat Map at 5,000 cfs
Bernalillo to Montano

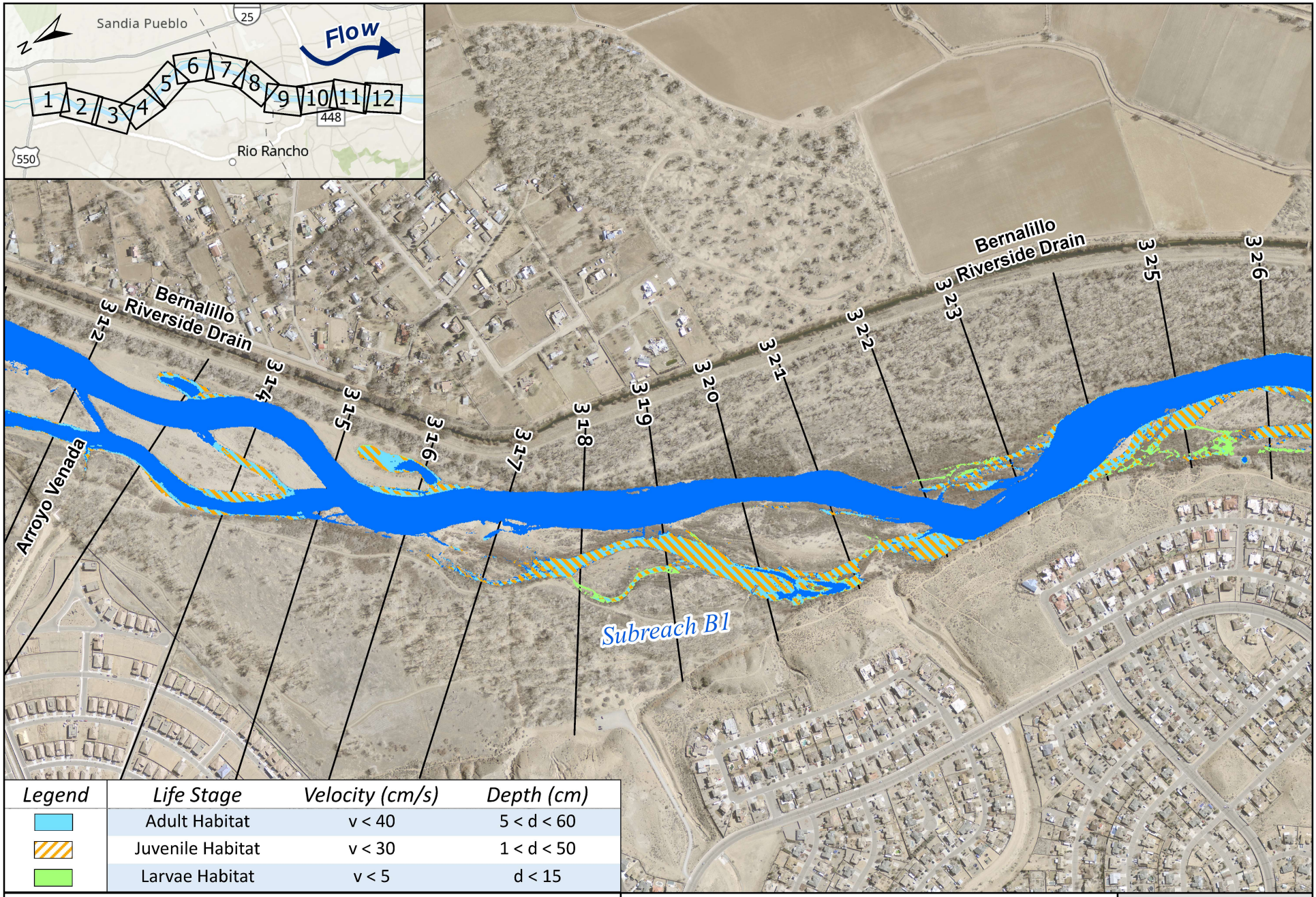

Legend	Life Stage	Velocity (cm/s)	Depth (cm)
	Adult Habitat	v < 40	5 < d < 60
	Juvenile Habitat	v < 30	1 < d < 50
	Larvae Habitat	v < 5	d < 15

1,000 500 0 1,000 Feet

Rio Grande Habitat Map at 5,000 cfs
Bernalillo to Montano

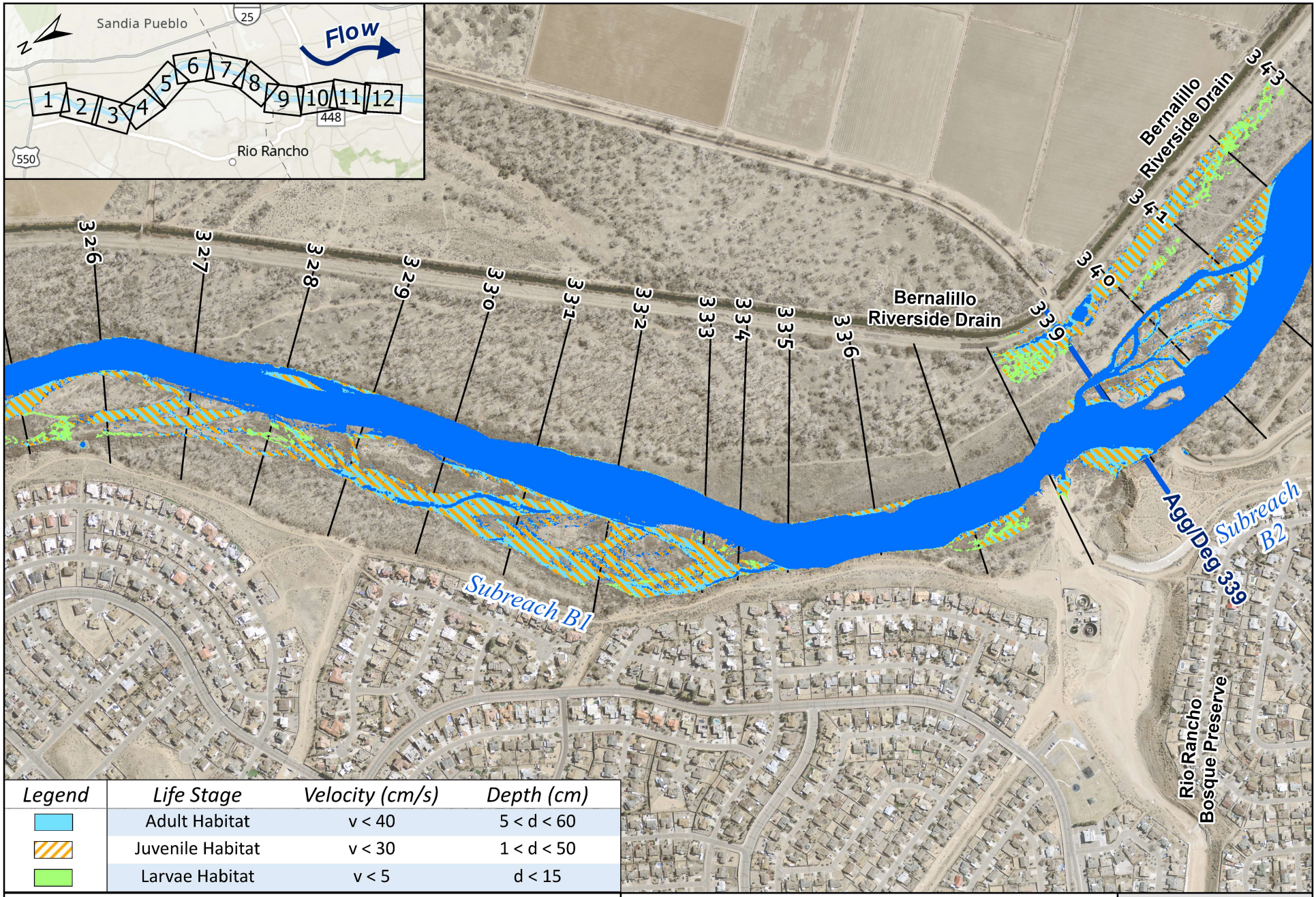

Legend	Life Stage	Velocity (cm/s)	Depth (cm)
	Adult Habitat	v < 40	5 < d < 60
	Juvenile Habitat	v < 30	1 < d < 50
	Larvae Habitat	v < 5	d < 15

1,000 500 0 1,000 Feet

Rio Grande Habitat Map at 5,000 cfs
Bernalillo to Montano

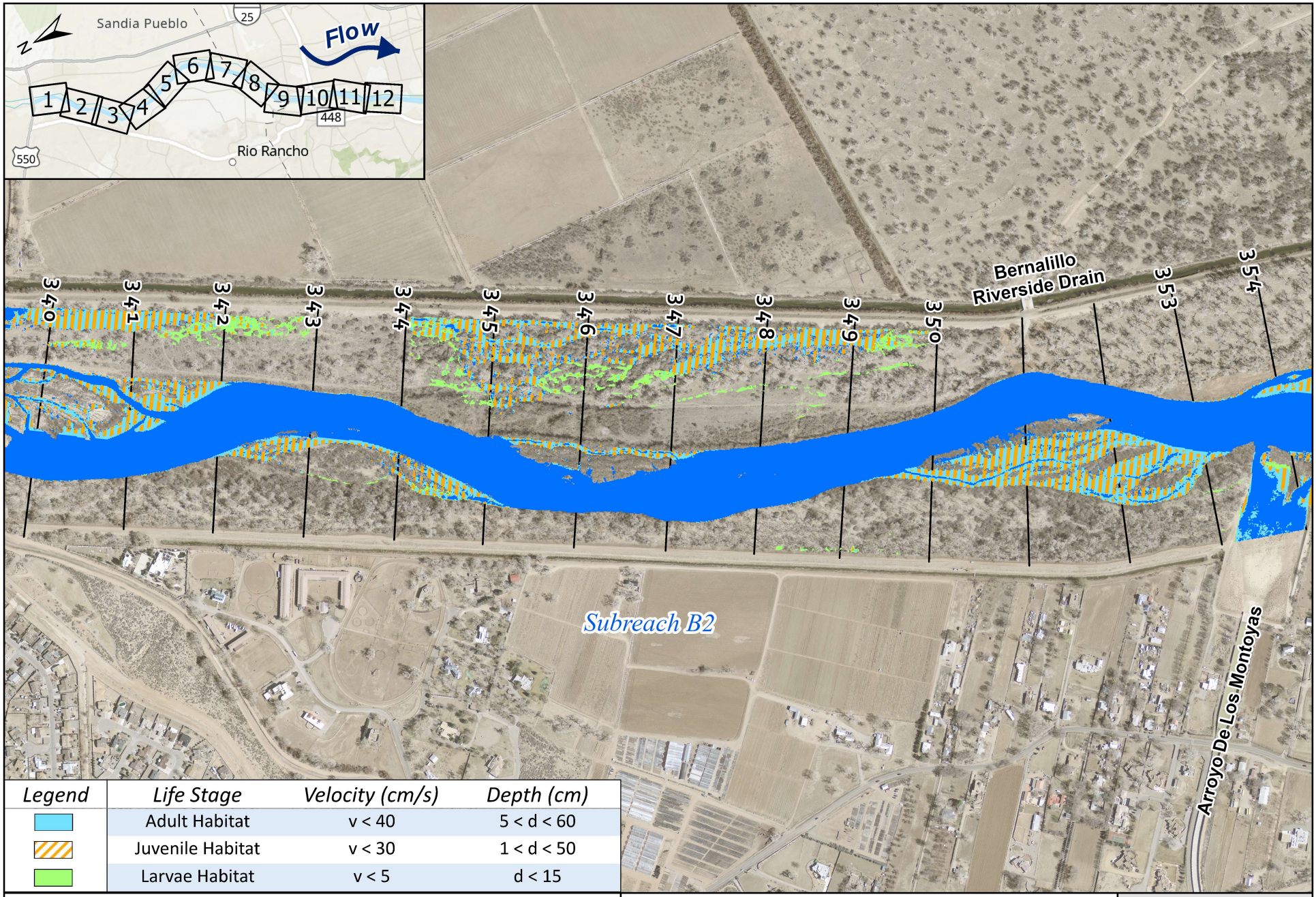

Legend	Life Stage	Velocity (cm/s)	Depth (cm)
	Adult Habitat	v < 40	5 < d < 60
	Juvenile Habitat	v < 30	1 < d < 50
	Larvae Habitat	v < 5	d < 15

1,000 500 0 1,000 Feet

Rio Grande Habitat Map at 5,000 cfs
Bernalillo to Montano

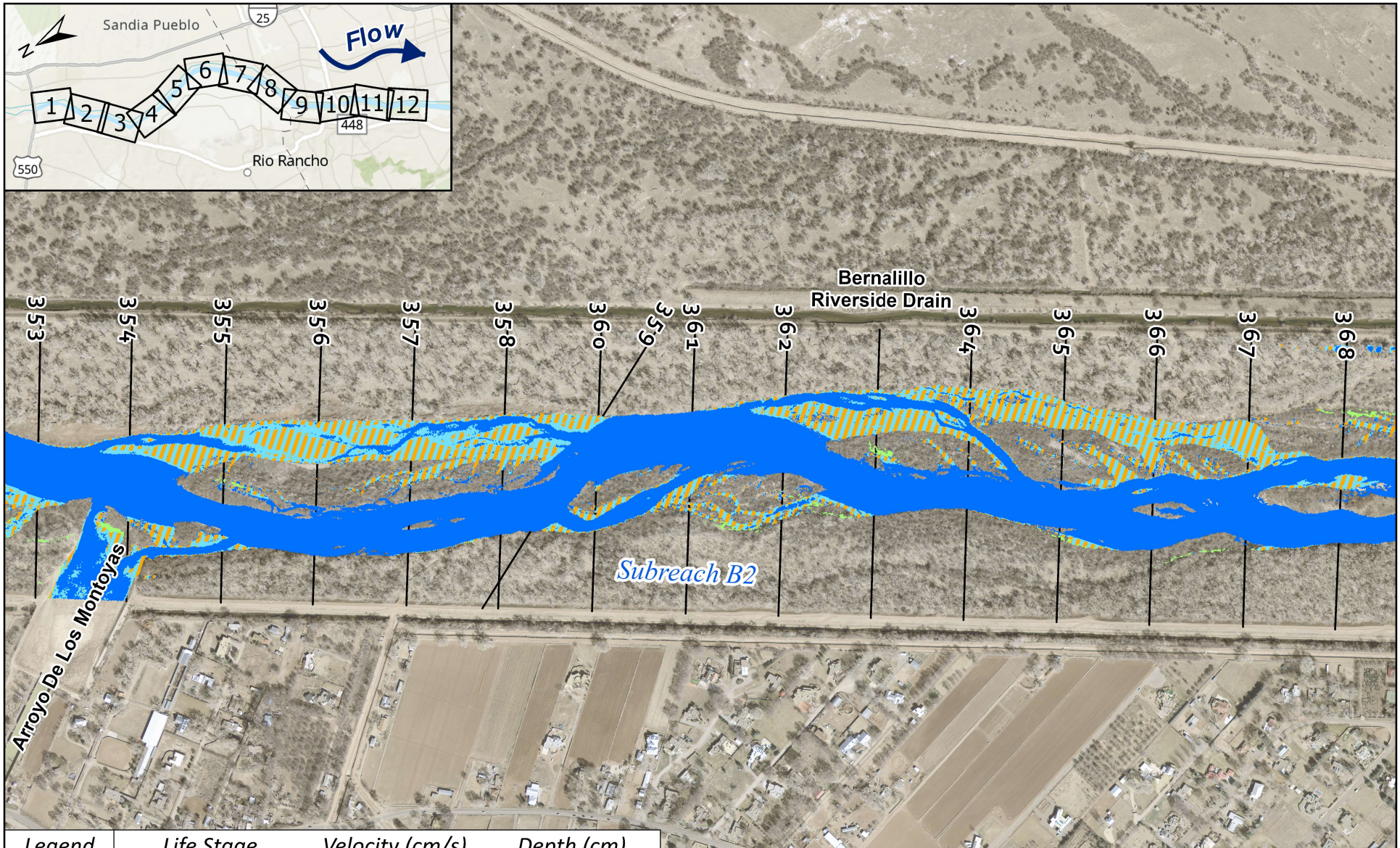

Legend	Life Stage	Velocity (cm/s)	Depth (cm)
	Adult Habitat	v < 40	5 < d < 60
	Juvenile Habitat	v < 30	1 < d < 50
	Larvae Habitat	v < 5	d < 15

N

1,000 500 0 1,000 Feet

Rio Grande Habitat Map at 5,000 cfs
Bernalillo to Montano

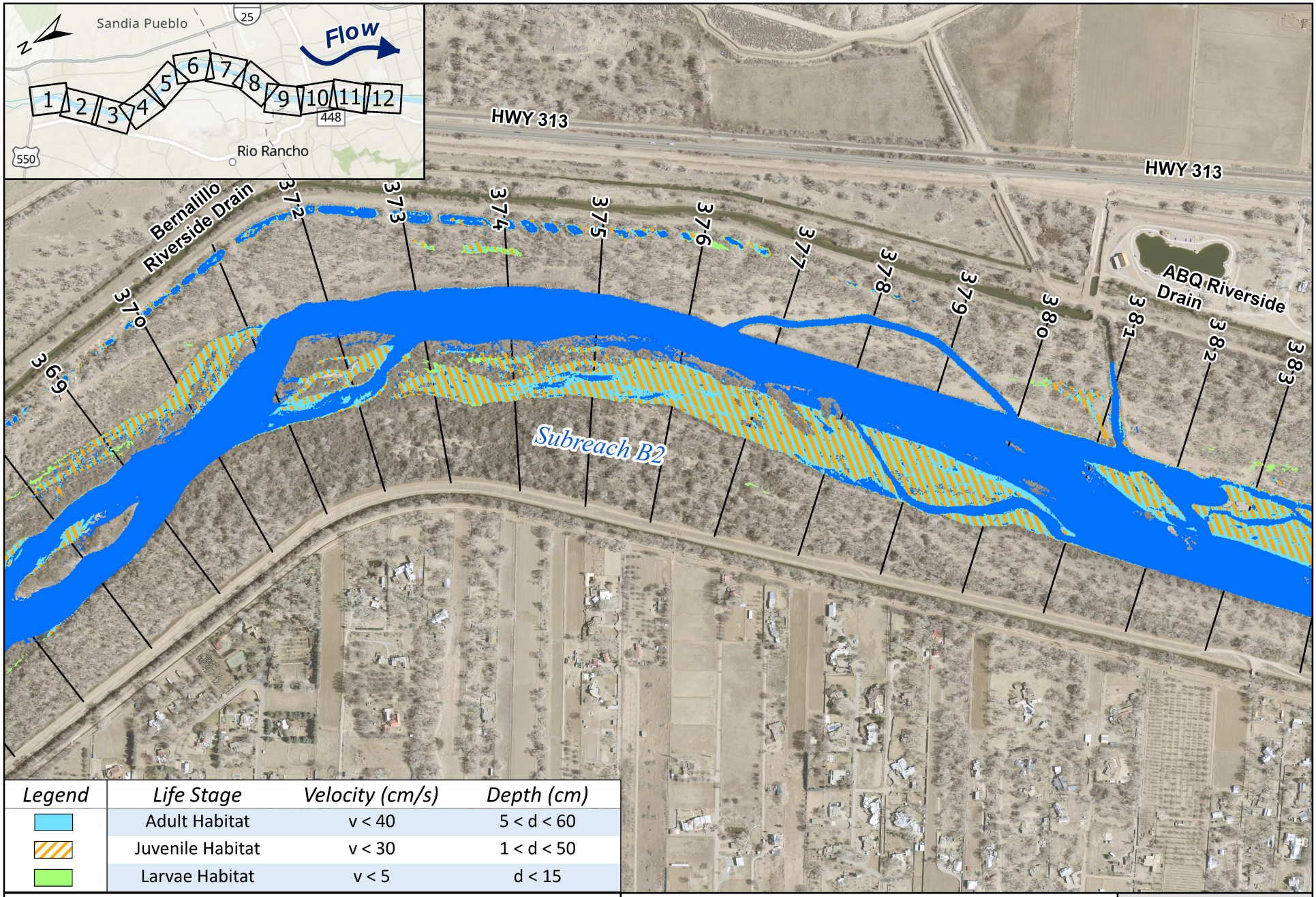

Legend	Life Stage	Velocity (cm/s)	Depth (cm)
	Adult Habitat	v < 40	5 < d < 60
	Juvenile Habitat	v < 30	1 < d < 50
	Larvae Habitat	v < 5	d < 15

1,000 500 0 1,000 Feet

Rio Grande Habitat Map at 5,000 cfs
Bernalillo to Montano

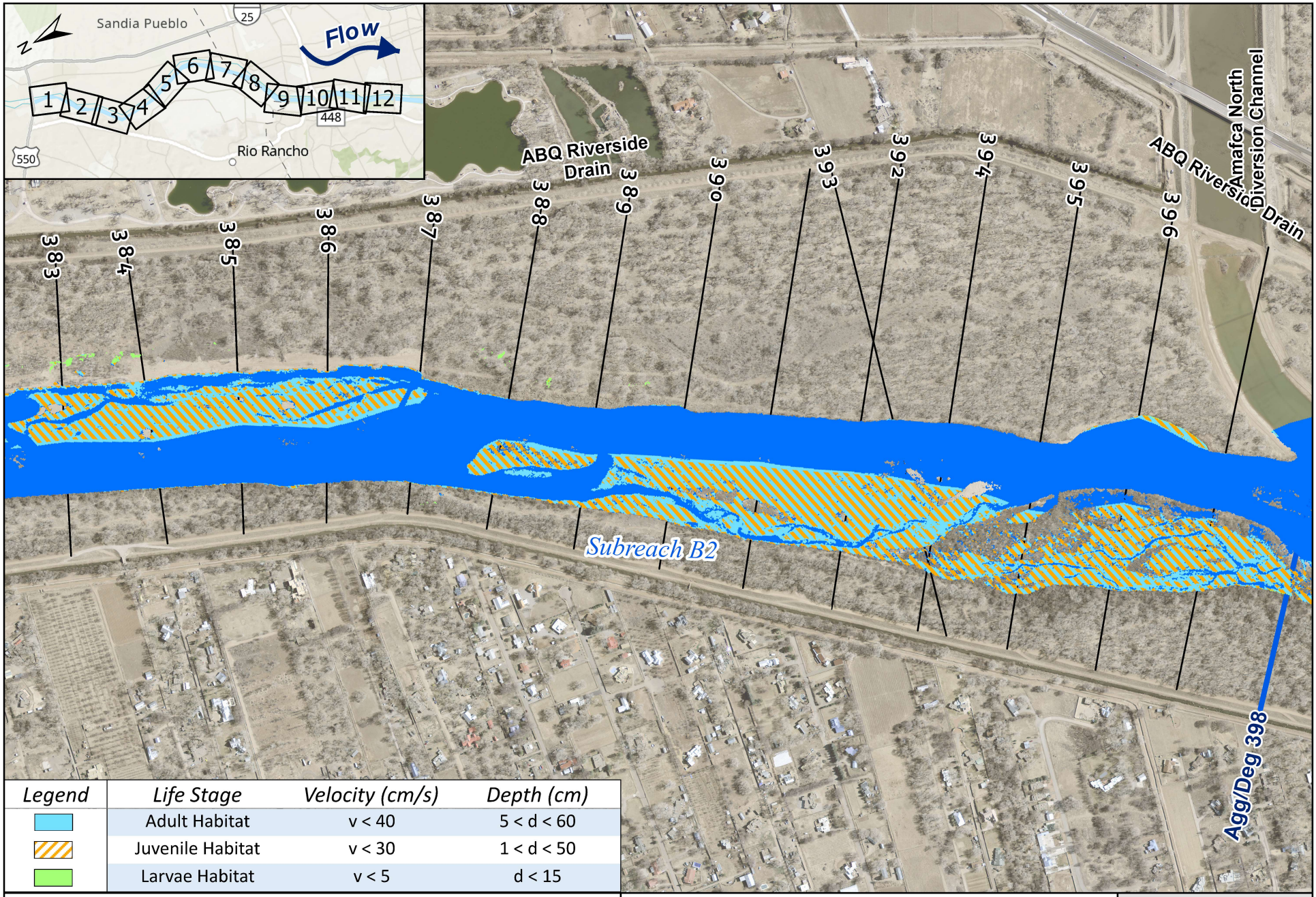

Legend	Life Stage	Velocity (cm/s)	Depth (cm)
	Adult Habitat	v < 40	5 < d < 60
	Juvenile Habitat	v < 30	1 < d < 50
	Larvae Habitat	v < 5	d < 15

1,000 500 0 1,000 Feet

Rio Grande Habitat Map at 5,000 cfs
Bernalillo to Montano

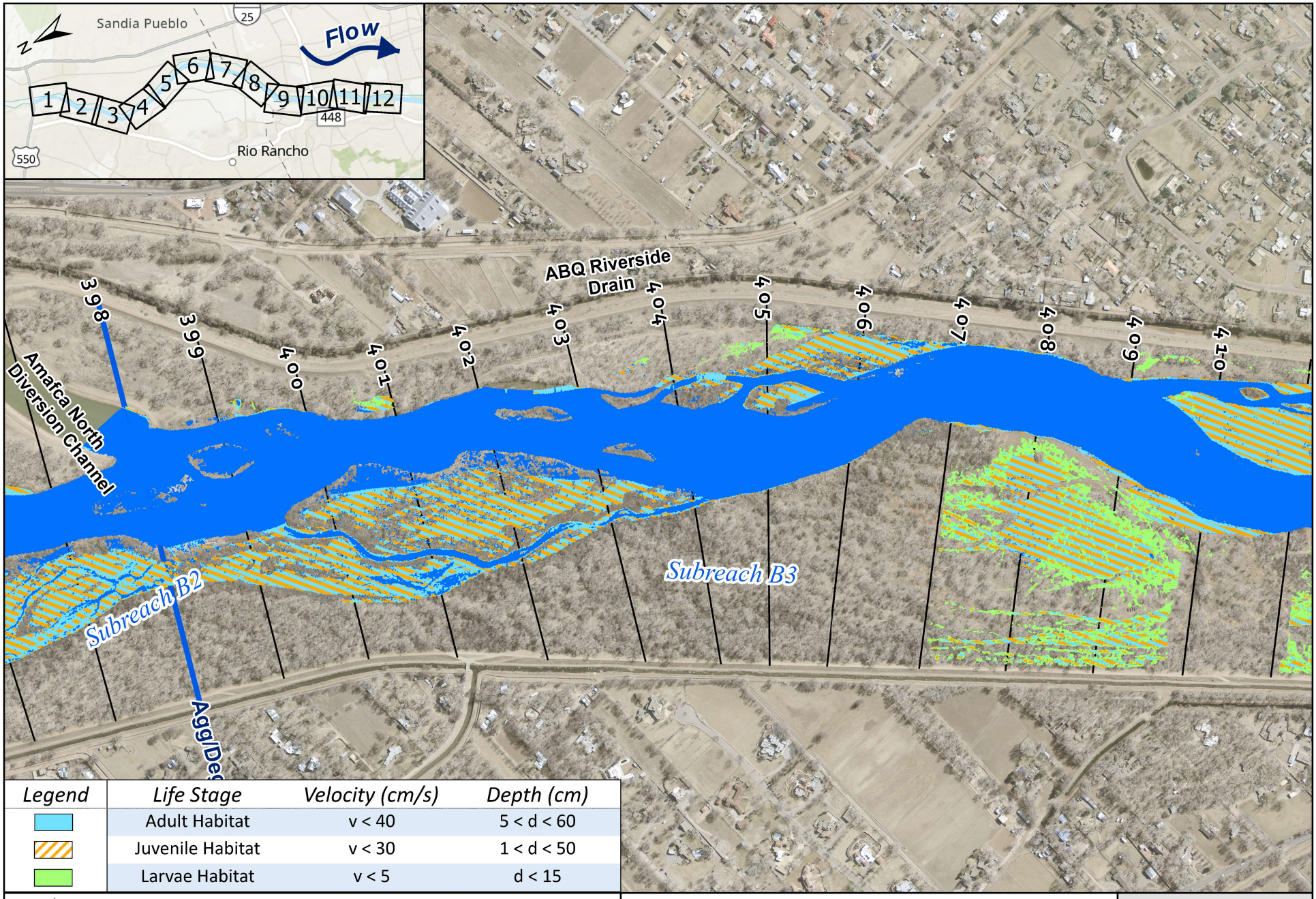

Legend	Life Stage	Velocity (cm/s)	Depth (cm)
	Adult Habitat	v < 40	5 < d < 60
	Juvenile Habitat	v < 30	1 < d < 50
	Larvae Habitat	v < 5	d < 15

N

1,000 500 0 1,000 Feet

Rio Grande Habitat Map at 5,000 cfs
Bernalillo to Montano

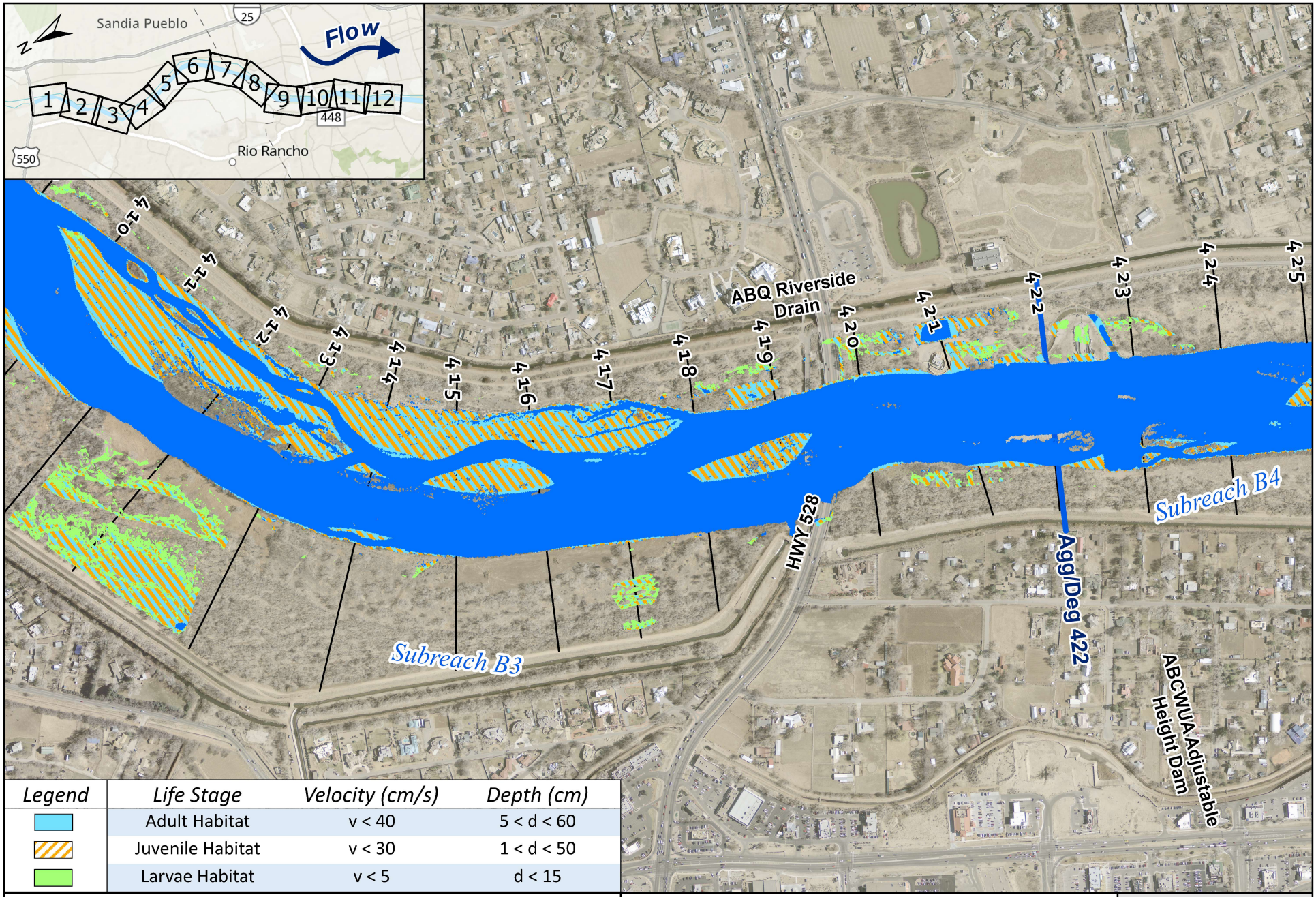

Legend	Life Stage	Velocity (cm/s)	Depth (cm)
	Adult Habitat	v < 40	5 < d < 60
	Juvenile Habitat	v < 30	1 < d < 50
	Larvae Habitat	v < 5	d < 15

1,000 500 0 1,000 Feet

Rio Grande Habitat Map at 5,000 cfs
Bernalillo to Montano

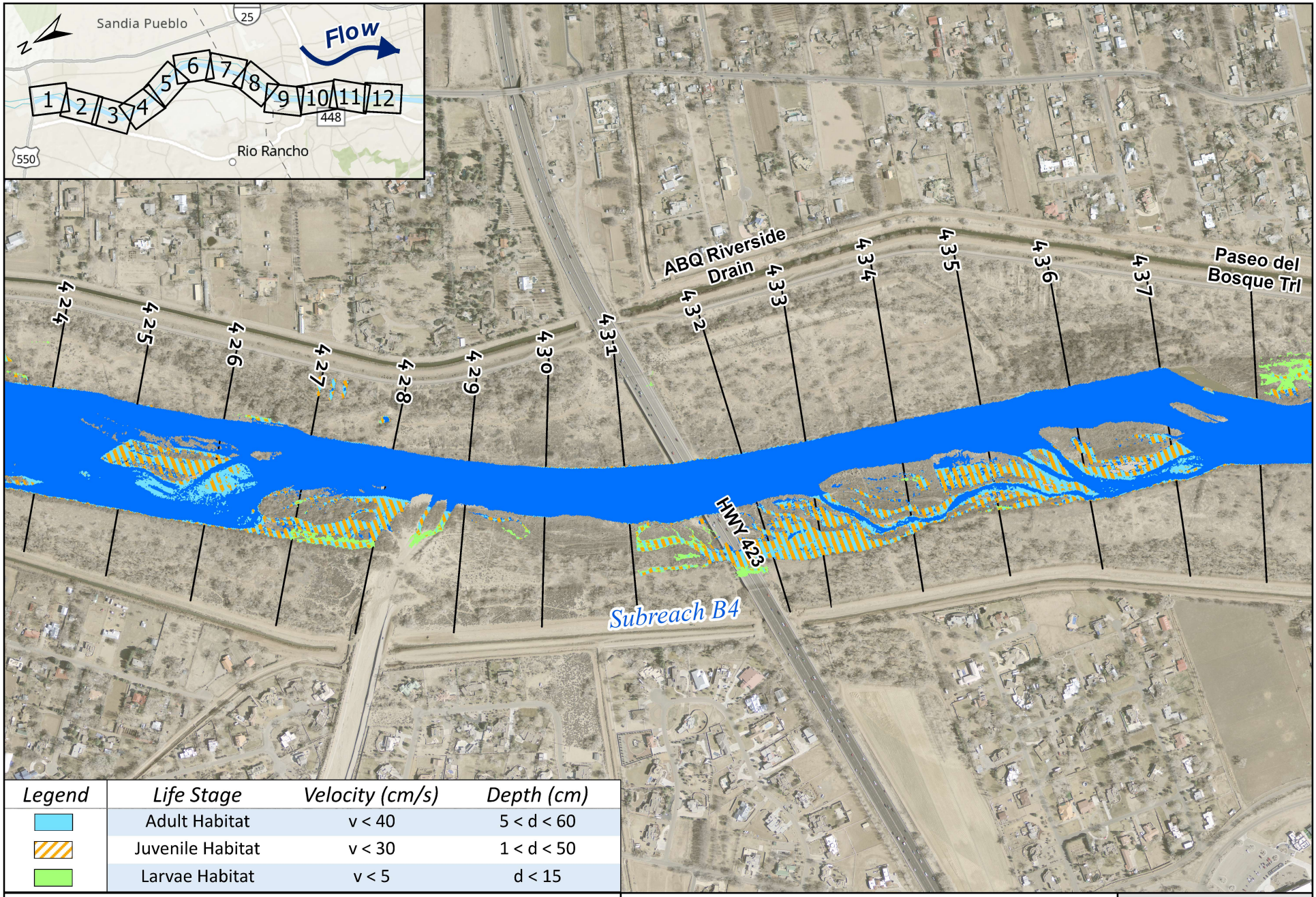

Legend	Life Stage	Velocity (cm/s)	Depth (cm)
	Adult Habitat	v < 40	5 < d < 60
	Juvenile Habitat	v < 30	1 < d < 50
	Larvae Habitat	v < 5	d < 15

1,000 500 0 1,000 Feet

Rio Grande Habitat Map at 5,000 cfs
Bernalillo to Montano

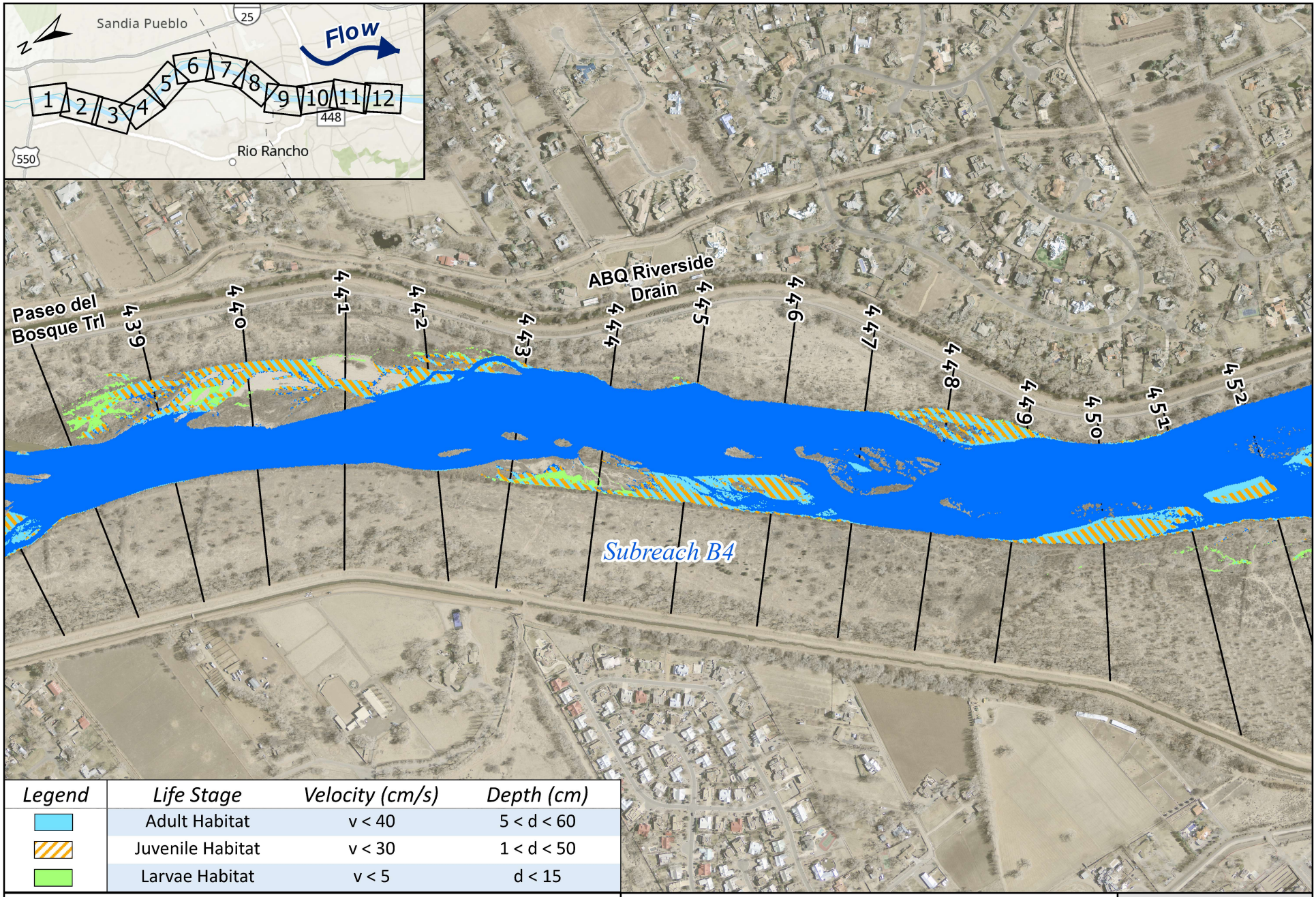

Legend	Life Stage	Velocity (cm/s)	Depth (cm)
	Adult Habitat	v < 40	5 < d < 60
	Juvenile Habitat	v < 30	1 < d < 50
	Larvae Habitat	v < 5	d < 15

1,000 500 0 1,000 Feet

Rio Grande Habitat Map at 5,000 cfs
Bernalillo to Montano

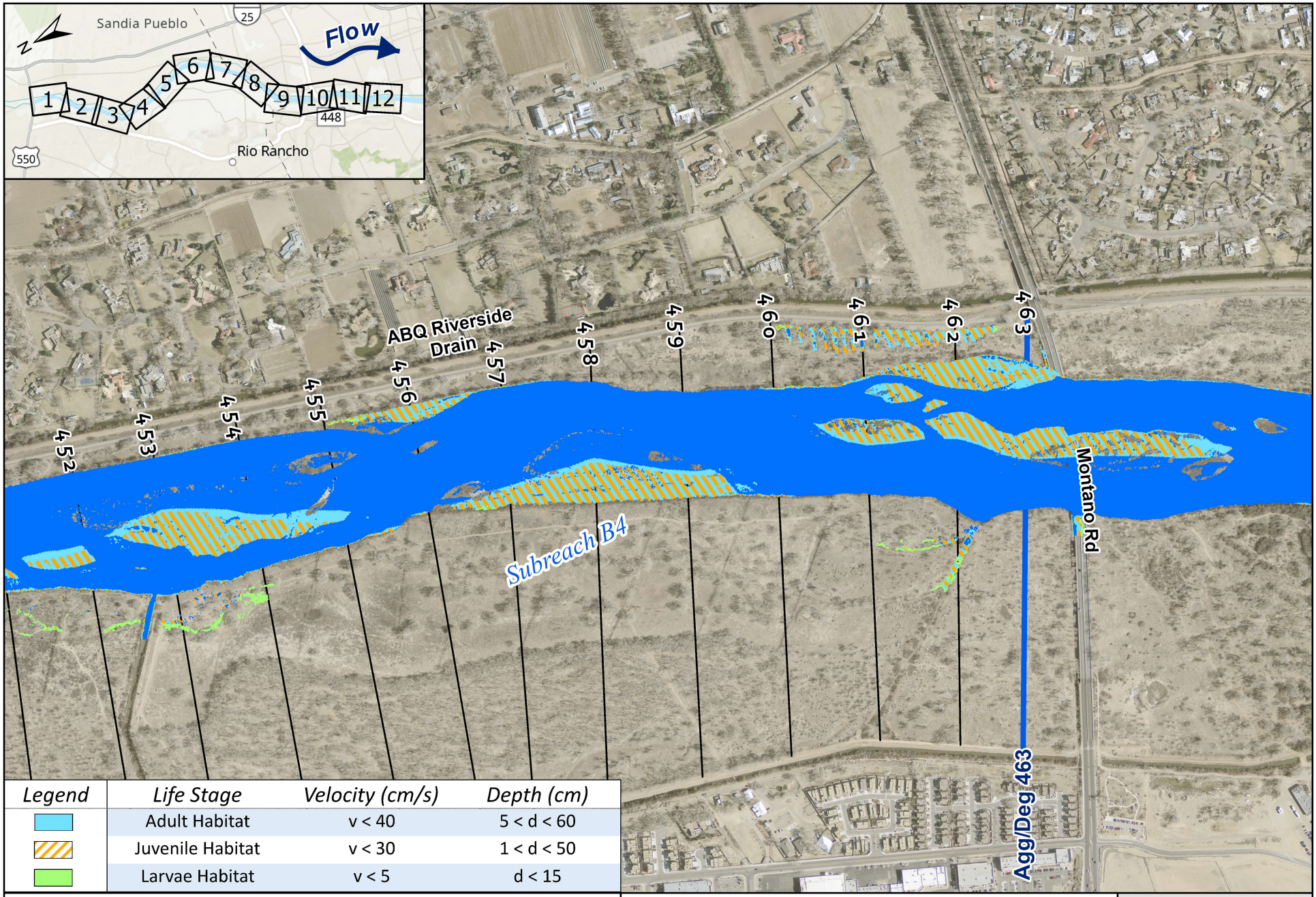

Legend	Life Stage	Velocity (cm/s)	Depth (cm)
	Adult Habitat	v < 40	5 < d < 60
	Juvenile Habitat	v < 30	1 < d < 50
	Larvae Habitat	v < 5	d < 15

1,000 500 0 1,000 Feet

Rio Grande Habitat Map at 5,000 cfs
Bernalillo to Montano

Appendix F

Geomorphology/Habitat Connection Figures for Process Linkage Report

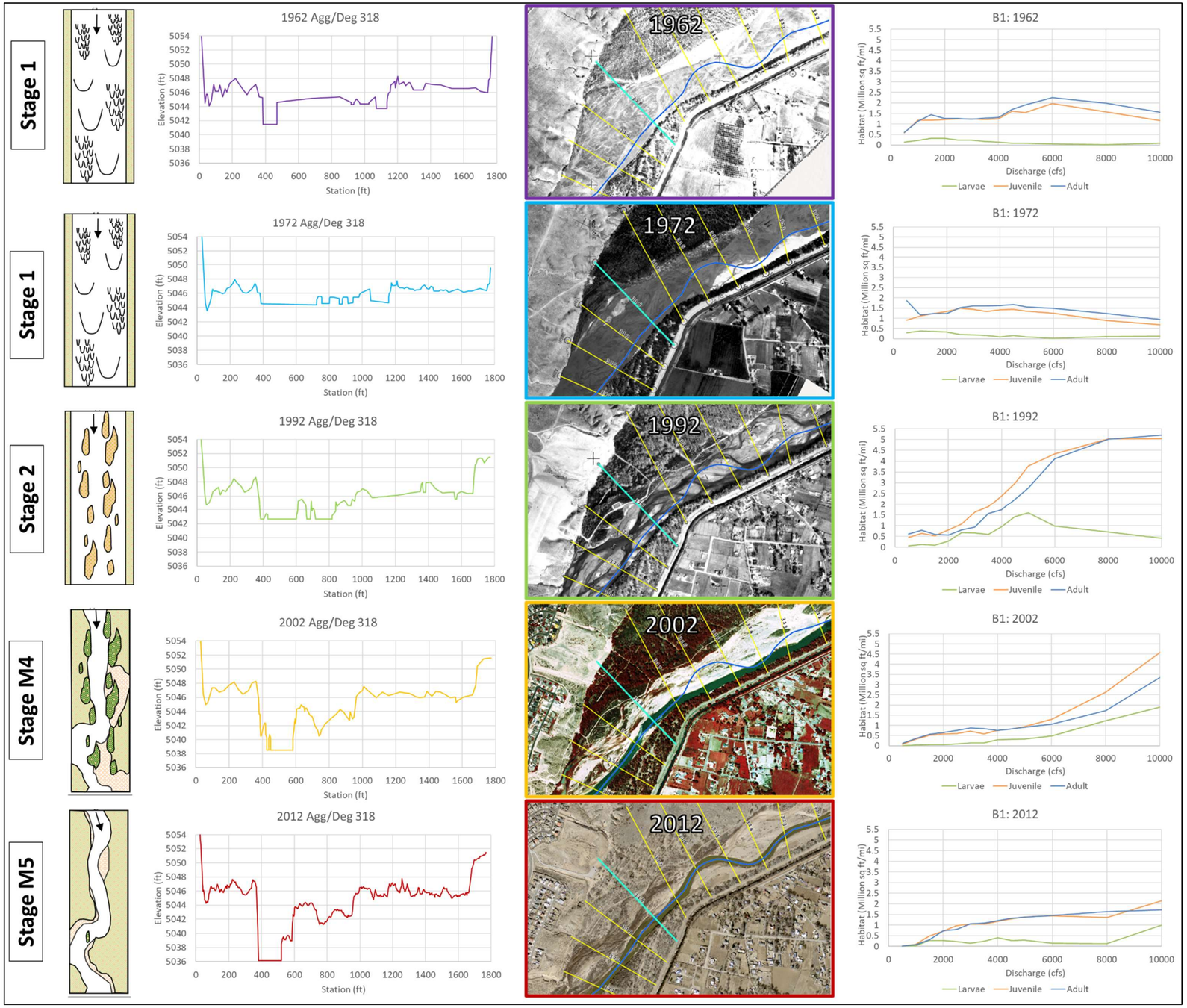
Stage 1
1962 Agg/Deg 318
Elevation (ft)
Station (ft)
1962
B1: 1962
Habitat (Million sq ft/mi)
Discharge (cfs)
Larvae Juvenile Adult
Stage 1
1972 Agg/Deg 318
1972
B1: 1972
Stage 2
1992 Agg/Deg 318
1992
B1: 1992
Stage M4
2002 Agg/Deg 318
2002
B1: 2002
Stage M5
2012 Agg/Deg 318
2012
B1: 2012

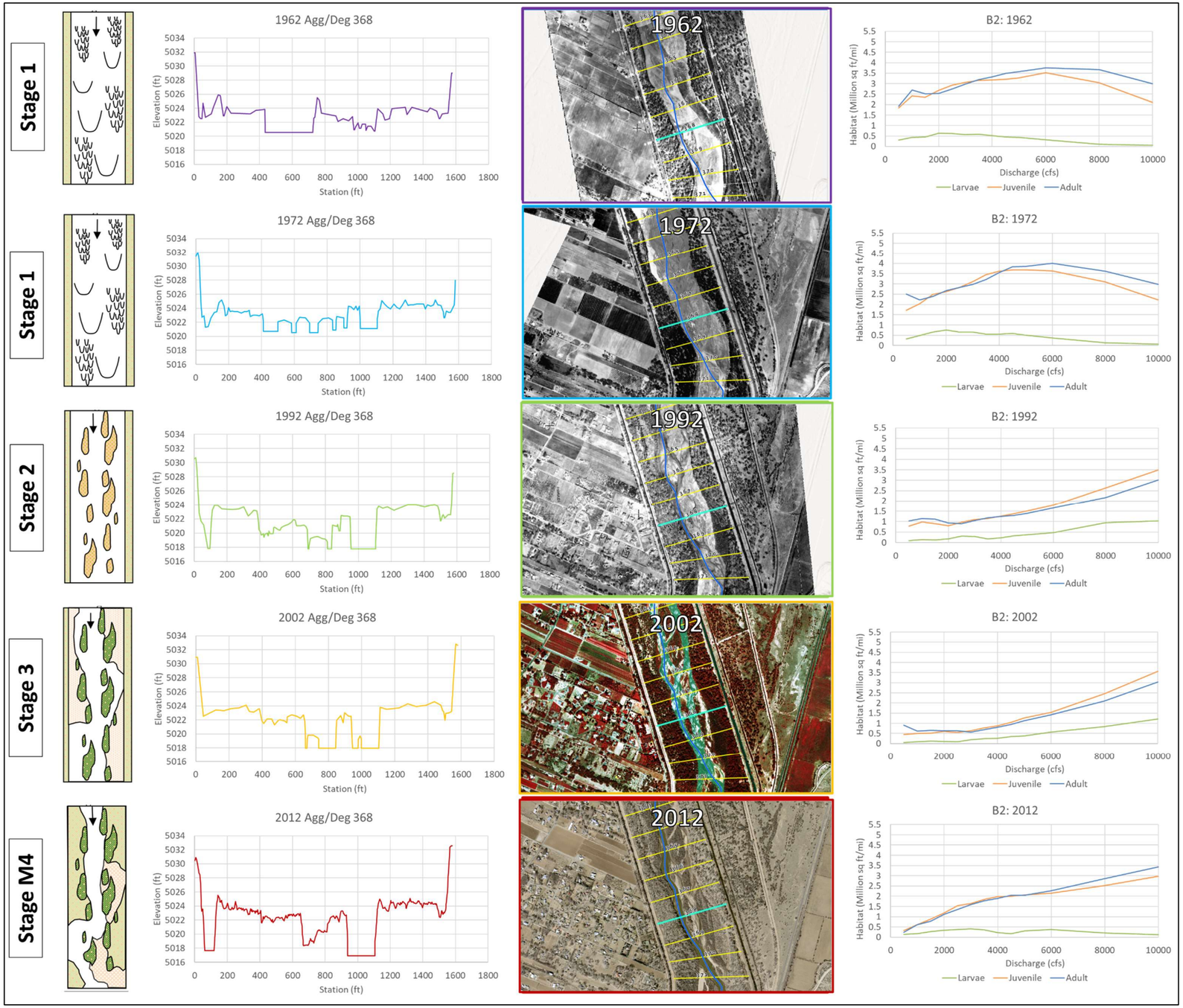
Stage 1
1962 Agg/Deg 368
Elevation (ft)
Station (ft)
1962
B2: 1962
Habitat (Million sq ft/mi)
Discharge (cfs)
Larvae
Juvenile
Adult
Stage 1
1972 Agg/Deg 368
1972
B2: 1972
Stage 2
1992 Agg/Deg 368
1992
B2: 1992
Stage 3
2002 Agg/Deg 368
2002
B2: 2002
Stage M4
2012 Agg/Deg 368
2012
B2: 2012

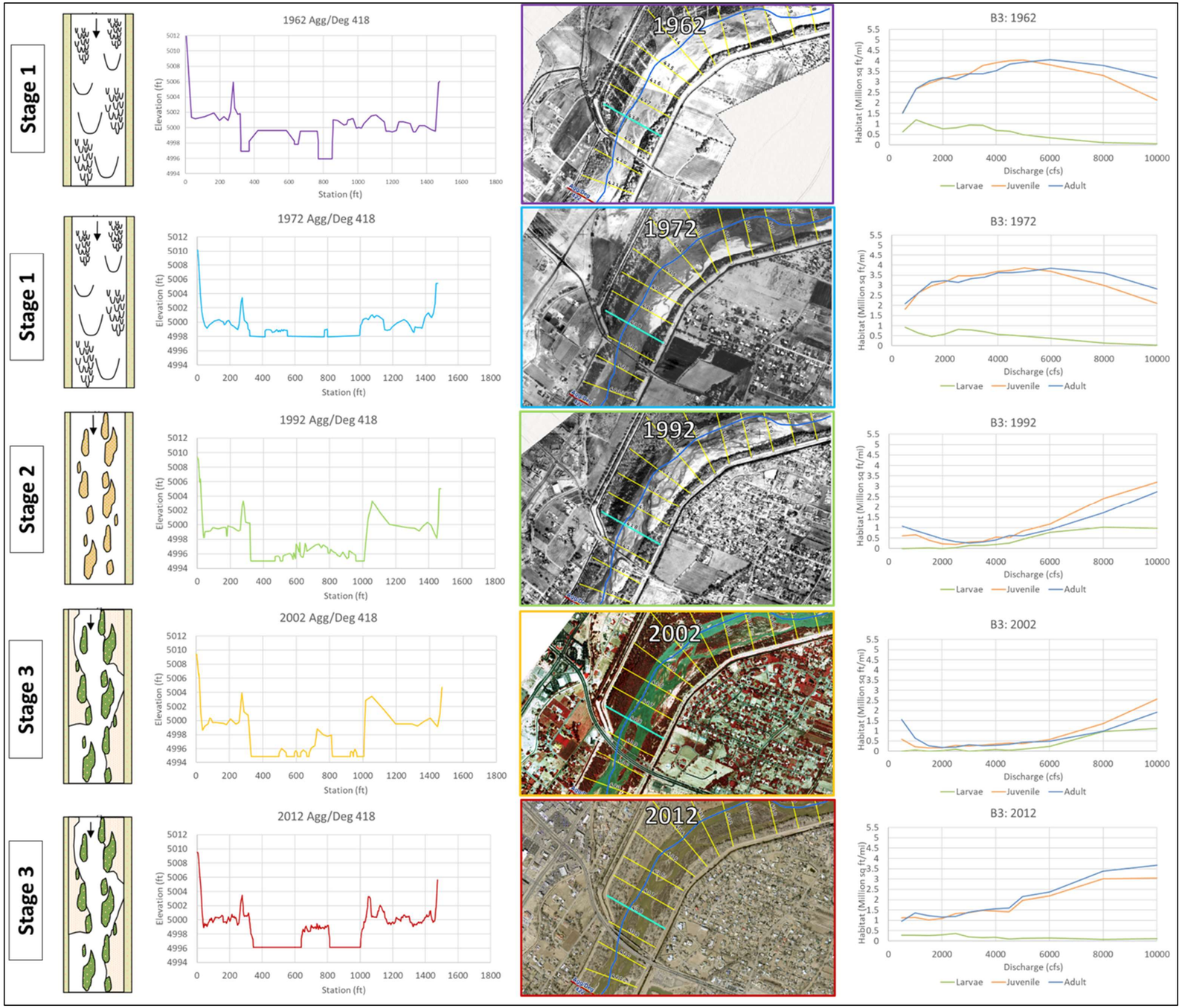
Stage 1
1962 Agg/Deg 418
Elevation (ft)
Station (ft)
1962
B3: 1962
Habitat (Million sq ft/mi)
Discharge (cfs)
Larvae
Juvenile
Adult
Stage 1
1972 Agg/Deg 418
1972
B3: 1972
Stage 2
1992 Agg/Deg 418
1992
B3: 1992
Stage 3
2002 Agg/Deg 418
2002
B3: 2002
Stage 3
2012 Agg/Deg 418
2012
B3: 2012

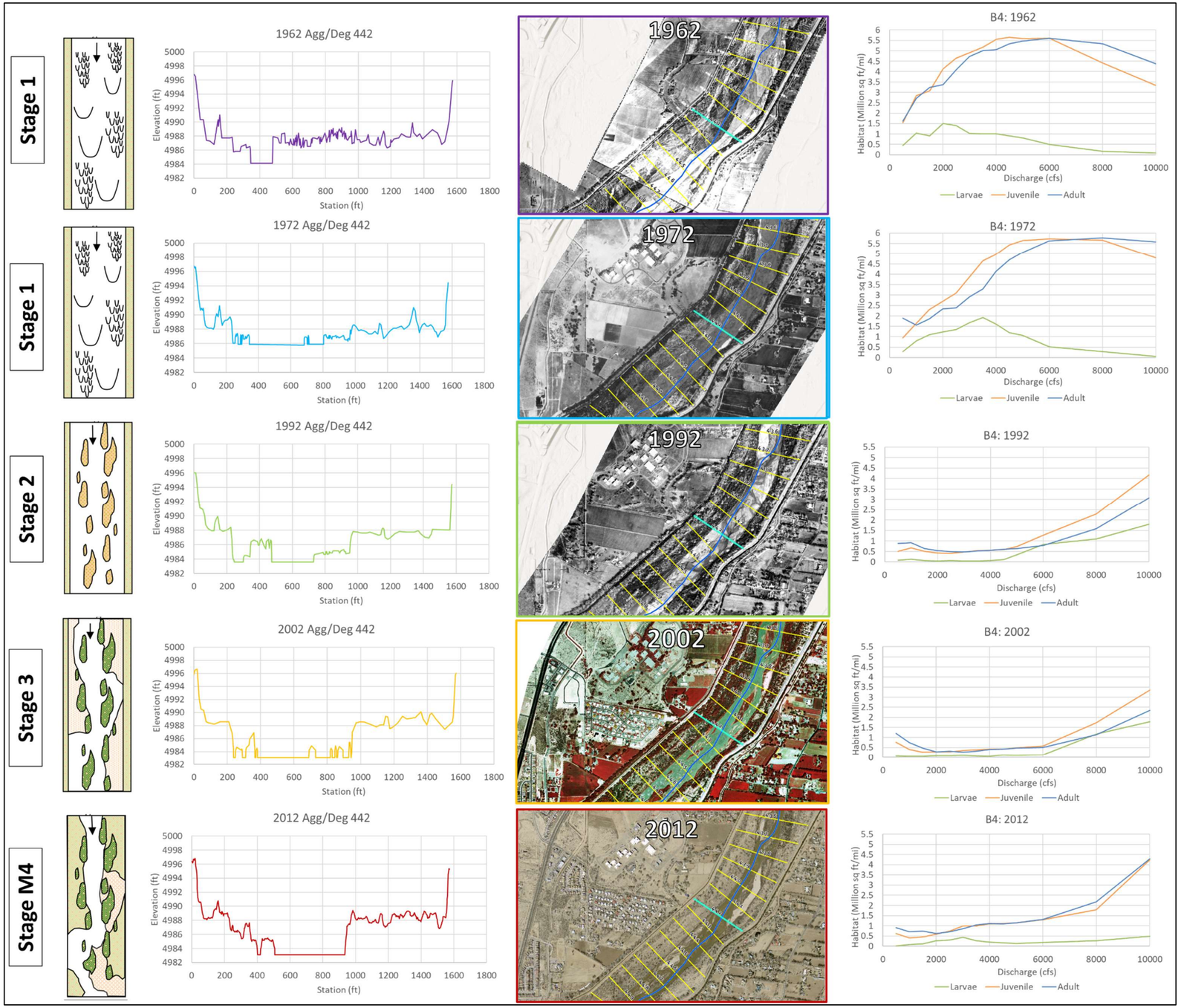
Stage 1
1962 Agg/Deg 442
Elevation (ft)
Station (ft)
1962
B4: 1962
Habitat (Million sq ft/mi)
Discharge (cfs)
Larvae Juvenile Adult
Stage 1
1972 Agg/Deg 442
1972
B4: 1972
Stage 2
1992 Agg/Deg 442
1992
B4: 1992
Stage 3
2002 Agg/Deg 442
2002
B4: 2002
Stage M4
2012 Agg/Deg 442
2012
B4: 2012

Appendix G

HEC-RAS Model File Log

The HEC-RAS model files used for the analyses are shown in **Table G-1**. Most of the files for a given type (geometry, flow, etc.) contain identical conditions. For conciseness, these commonalities are:

- All **Flow files** contain thirteen discharge (cfs) profiles: 500, 1000, 1500, 2000, 2500, 3000, 3500, 4000, 4500, 5000, 6000, 8000, and 10000.
- **Downstream (DS) normal depth boundary conditions** were found from modeling the entire MRG at the specified discharges (DS normal depth boundary condition: 0.0007). The energy grade line slope at 5 cross sections DS of the Bernalillo DS boundary at each discharge became the DS boundary condition for the Bernalillo reach flow files. The boundary conditions range from 0.0007 to 0.0009 depending on the discharge.
- The **Manning's roughness** is n = 0.025 in the main channel and n = 0.1 elsewhere.
- **Flow distribution locations** were set at 10/25/10 for the LOB, Channel, and ROB for plans used to quantify habitat availability.
- **Geometry files** contain 5 cross-sections upstream and 5 cross-sections downstream of the Bernalillo Boundaries

See **Table G-2** for the full list of HEC-RAS files.

Table G-1 HEC-RAS files used during analyses

Project Name		
Extension	***Name***	***Description***
.prj	Bernalillo_reach	Surveyed cross sections in years: 1962,1972, 1992, and 2002. LiDAR in 2012 along the Bernalillo reach of the MRG.
Geometry Files		
Extension	***Name***	***Description***
.g14	1962_modlevee	Existing conditions with some levees in B1 and B2.
.g13	1972_modllevee	Existing conditions with some levees in B1 and B2.
.g11	1992_nolevee	Existing conditions with no flow constraints.
.g12	2002_nolevee	Existing conditions with no flow constraints.
.g08	2012_nolevee	Existing conditions with ineffective flow constraints.
Steady Flow Files		
Extension	***Name***	***Description***
.f02	Bernalillo_2012	DS Boundary condition: Normal Depth 0.0007-0.0009
.f03	Bernalillo_1962-2002	
Steady Plan Files		
Extension	***Name***	***Description (geometry file & flow file)***
.p13	Bernalillo_1972_modLevee	.g14 and .f03
.p12	Bernalillo_1972_modLevee	.g13 and .f03
.p10	Bernalillo_1992_noLevee	.g11 and .f03
.p11	Bernalillo_2002_noLevee	.g12 and .f03
.p08	Bernalillo_2012_noLevee	.g08 and .f02

Steady Plan Files		
Extension	***Name***	***Description (geometry & flow)***
.p01	Full_River	.g07 and .f01
.p02	Bernalillo_2012	.g06 and .f02
.p03	Bernalillo_2002	.g05 and .f03
.p04	Bernalillo_1992	.g04 and .f03
.p05	Bernalillo_1972	.g03 and .f03
.p06	Bernalillo_1962	.g01 and .f03
.p07	Bernalillo_1962_noLevee	.g09 and .f03
.p08	Bernalillo_2012_noLevee	.g08 and .f02
.p09	Bernalillo_1972_noLevee	.g10 and .f03
.p10	Bernalillo_1992_noLevee	.g11 and .f03
.p11	Bernalillo_2002_noLevee	.g11 and .f03
.p12	Bernalillo_1972_modLevee	.g13 and .f03
.p13	Bernalillo_1962_modLevee	.g14 and .f03

Table G-2 Full list of HEC-RAS files

Project Name		
Extension	***Name***	***Description***
.prj	Bernalillo_reach	Surveyed cross sections in years: 1962,1972, 1992, and 2002. LiDAR in 2012 along the Bernalillo reach of the MRG.
Geometry Files		
Extension	***Name***	***Description***
.g01	1962	1962 unmodified Bernalillo reach survey cross sections, as received
.g03	1972	1972 unmodified Bernalillo reach survey cross sections, as received
.g04	1992	1992 unmodified Bernalillo reach survey cross sections, as received
.g05	2002	2002 unmodified Bernalillo reach survey cross sections, as received
.g06	2012	2012 unmodified Bernalillo reach survey cross sections, as received
.g07	Full_2012	Entire MRG 2012 geometry (Agg/Deg: 17 – EB 63), as received
.g08	2012_nolevee	2012 Bernalillo reach survey cross section with original levees removed and ineffective flow areas added
.g09	1962_nolevee	1962 Bernalillo reach survey cross section with original levees removed
.g10	1972_nolevee	1972 Bernalillo reach survey cross section with original levees removed
.g11	1992_nolevee	1992 Bernalillo reach survey cross section with original levees removed
.g12	2002_nolevee	2002 Bernalillo reach survey cross section with original levees removed
.g13	1972_modlevee	1972 Bernalillo reach survey cross section with original levees removed and new levees placed in B1 and B2
.g14	1962_modlevee	1962 Bernalillo reach survey cross section with original levees removed and new levees placed in B1 and B2
Steady Flow Files		
Extension	***Name***	***Description***
.f01	Full_Flows	DS Boundary condition: Normal Depth 0.0007
.f02	Bernalillo_2012	DS Boundary condition: Normal Depth 0.0007-0.0009
.f03	Bernalillo_1962-2002	DS Boundary condition: Normal Depth 0.0007-0.0009